Functional characterisation of the *Cercospora zeina crp1* gene in pathogenesis

by

Johan Liversage

Submitted in partial fulfilment of the requirements for the degree

Magister Scientiae

In the Faculty of Natural and Agricultural Sciences

Department of Plant Science

University of Pretoria

July 2015

Under the supervision of Dr. Bridget G. Crampton and

Co-supervision of Prof. Dave K. Berger

TABLE OF CONTENTS

DECLARATION

I, **Johan Liversage**, declare that the dissertation, which I hereby submit for the degree *Magister Scientiae* at the University of Pretoria, contains my own independent work and has not been submitted by me for a degree at this or any other tertiary institution.

Johan Liversage

July 2015

PREFACE

The research presented in this dissertation was conducted in the Cereal Foliar Pathogen Research (CFPR) group at the University of Pretoria, South Africa. Each chapter of the dissertation is written as independent sections, and thus some degree of repetition is to be expected between the sections.

Maize is an economically important food crop in South Africa. Annually farmers experience devastating losses due to biotic and abiotic stresses. The maize foliar disease grey leaf spot (GLS) is of particular importance to the CFPR group. As a research group we rely on the farmers to identify emerging diseases, which enables us to study the disease spread and causal agent at a molecular level. The foliar pathogen responsible for GLS on maize in South Africa is *Cercospora zeina*.

All organisms depend on light as an environmental cue to synchronise their internal rhythms or circadian clocks to adapt to changing environments accordingly. The broad aim of this study was to functionally characterise a blue light photoreceptor in *C. zeina,* and determine if pathogenesis of the fungus is affected in the absence of the gene and to what level. During the course of the project I was intrigued by the idea that fungi might synchronise their circadian rhythms to that of their hosts to cause disease. This led me to conduct a bioinformatics study on the conservation of blue light perception in fungi and plants and the origin of the sensory domain within the blue light photoreceptor.

Chapter 1 is a review of the literature on blue light perception in fungi, in which the cellular and metabolic processes influenced by blue light photoreceptor were identified. The chapter begins with background information of maize production in Southern Africa followed by how annual yield is influenced by grey leaf spot disease. *Cercospora zeina*, the causal agent of GLS on maize, is introduced followed by circadian rhythms in fungi. All the published research on

blue light perception and related functions in fungi is summarised, and connections made between metabolic processes and the pathogen's ability to cause disease.

Chapter 2 discusses the bioinformatic approaches used to identify and deduce relationships between blue light photoreceptors in fungi. The chapter discusses the conservation of blue light perception across Ascomycota, Basidiomycota and Zygomyocta phyla followed by inferring the relationship between the sensory domains of the blue light photoreceptors from fungi and plants. The chapter concludes with the identification fungal circadian clock proteins and the identification of a previously unknown putative blue light photoreceptor in *C. zeina*.

Chapter 3 of this dissertation discusses the application of the split marker approach to study the function of the CRP1 blue light photoreceptor in *C. zeina*. The generation and screening of putative blue light photoreceptor knock-outs is discussed followed by the phenotypic characterisation of the putative *Δcrp1* knock-outs. The chapter concludes with a discussion how the *crp1* knock-outs were screened, and possible obstacles and solutions in studying gene function in *C. zeina*. The broad aim of the project is discussed based on the phenotype of the *Δcrp1* knock-outs in relation to fungal pathogenesis.

Chapter 4 is a general discussion of the project and future prospects of managing grey leaf spot disease in maize. Based on methods used and results obtained in this project, a workflow is suggested for studying gene function in *Cercospora zeina*. The chapter is concluded with a discussion on how blue light perception in fungi can be used to the advantage of the plant for durable host resistance.

Listed below are the research outputs obtained from this dissertation to date:

Liversage J., Malefo, M.B.L., Visser, A.E., Berger, D.K., Crampton, B.G., 2013. A functional genomics toolbox for *Cercospora zeina*. Genomics Research Institute (GRI), A University of

Pretoria Institutional Research Theme, Seminar Day. November 14. University of Pretoria, South Africa. (Poster presentation)

Liversage, J., Berger, D.K., Crampton, B.G., 2014. Functional characterisation of the *Cercospora zeina crp1* gene as a putative pathogenesis regulation factor. DuPont-Pioneer Plant Breeding Symposium. November 6. University of Pretoria, South Africa. (Oral presentation)

Liversage, J., Berger, D.K., Crampton, B.G., 2015. Functional characterisation of the *Cercospora zeina crp1* gene as a putative pathogenesis regulation factor. 49th Congress of the Southern African Society for Plant Pathology. January 18-21. Bains Lodge, Bloemfontein, South Africa. (Oral presentation)

ACKNOWLEDGEMENTS

I would like to express my full gratitude to the following people and institutions for their support whom without this dissertation would not have been possible:

Firstly, I am grateful to The National Research Foundation (NRF) of South Africa and the Genomic Research Institute (GRI) at the University of Pretoria for the financial support needed to complete this project.

The members of the Forestry and Agricultural Institute (FABI) for support and guidance. The Laboratory for Microscopy and Microanalysis, especially Mr. Alan Hall, for all the guidance and endless patience with the confocal microscopy.

I am extremely blessed to have received all the encouragement, support and assistance from the members of the Molecular Plant Pathogen Interaction (MPPI) and Cereal Foliar Pathogen Research (CFPRG) groups, who became my friends and comrades in the host-pathogen arms race.

Dr. Bridget Crampton, my mentor, for all her patience, encouragement, guidance and keeping me grounded throughout the project. Providing me with the freedom to experiment and the opportunity to learn from my own mistakes. Prof. Dave Berger for providing a valuable insight into the project and asking the questions no one else wants to in order to force us to think outside of the cubicle.

For keeping me emotionally and mentally stable through all the difficult times and trying times, I would like to thank my parents, sister and family for their continued support, encouragement and for believing in me. Thank you to Elsabé, for all her love, standing by me and motivating me throughout the writing of this dissertation.

Lastly, I want to give praise to my heavenly father whom without I would not have had the strength to complete this project.

"I can do all things through him who strengthens me."

Phil 4:13

List of Abbreviations

°C	degrees Celsius
µg	microgram
µl	microliter
µM	micromolar
%	percentage
aa	amino acid
Avr	avirulence gene
BCIP	5-bromo-4-chloro-3-indolyl-phosphate
BIC	Bayesian information criterion
bp	base pair
BLAST	basic local Alignment Search Tool
BSA	bovine serum albumin
$CaCl_2$	Calcium chloride
CFPRG	Cereal Foliar Pathogen Research Group
CK	casein kinase
CM	complete media
CPD	cyclobutane-pyrimidine dimer
CRP1	Cercospora regulator of pathogenesis
CRY	cryptochrome
CTAB	cetyltrimethylammonium bromide
DIG	digoxigenin
dNTP	deoxynucleotide triphosphate
DNA	deoxyribonucleic acid
DMSO	dimethylsulphoxide
dpi	days post inoculation
dH_20	distilled water
dsRNA	double stranded RNA

EDTA	ethylenediamine tetraacetic acid
EtBr	Ethidium Bromide
FAD	flavin adenine dinucleotide
FLO	frequency-less oscillator
FMN	flavin mononucleotide
FRH	frequency-interacting RNA helicase
FRQ	frequency
FWO	frequency/White Collar-based circadian oscillator
GFP	green fluorescent protein
GLS	Grey leaf spot
HIGS	host induced silencing
Hyg^R	Hygromycin resistance gene
IAA	indole-3-acetic acid
IDP	intrinsically disordered protein
IDT	Integrative DNA technologies
kb	kilo base
kW	kilowatt
LB	luria bertani
LCR	low complexity regions
LOV	light, oxygen and voltage
MAFFT	multiple alignment using fast fourier transform
MAP	mitogen activated protein
MAT	mating type
$MgCl_2$	Magnesium chloride
mRNA	messenger ribonucleic acid
MSA	multiple sequence alignment
MTHF	methyl tertahydrofolate
mM	millimolar
M	molar

NBT	nitro blue tetrazolium
nM	nanomolar
ng	nanogram
NCBI	National Centre for Biotechnology Information
PAC	PER-ARNT-SIM-associated C-terminal domain
PAS	PER-ARNT-SIM
PCR	polymerase chain reaction
Phot	phototropin
PHR	photolyase related
PKS	polyketide synthase
PSI-BLAST	Position-Specific Iterated BLAST
RNA	ribonucleic acid
RNAi	RNA interference
ROS	reactive oxygen species
rpm	revolutions per minute
RT-PCR	reverse transcription polymerase chain reaction
SA	South Africa
SCD	scytalone dehydratase
SDS	sodium dodecyl sulfate
siRNA	small interfering RNA
SOEing	synthesis by Overlap Extension
SSC	saline-sodium citrate
TAE	tris acetate ethylenediamine tetraacetic acid
TE	tris ethylene diamine tetraacetic acid
trpC	tryptophan synthase gene
USA	United States of America
UV	ultra violet
U/µl	units per microlitre
VVD	Vivid

WC-1	White Collar-1
WC-2	White Collar-2
WCC	White Collar Complex
ZnF	Zinc-finger
ZTL	zeitlupe

LIST OF TABLES

CHAPTER 1

CHAPTER 3

LIST OF FIGURES

CHAPTER 1

CHAPTER 2

CHAPTER 3

Literature Review

Chapter 1

Fungal blue light regulated processes involved in growth, development and host-pathogen interactions

1.1. Introduction

Maize is an important staple crop in Africa that is used in human and animal feed. South Africa is the main maize producing country in Africa, and produces between 10 and 12 million tons of maize annually (Du Plessis, 2011). Locally 4.8 million tons of maize is consumed each year. In 2013, the population size in South Africa alone was to be about 53 million and growing by 1.2% annually (Statistics SA, 2013). The pressure that is put on the farming system each year is thus increasing. Huang et al. (2002) suggested that this pressure can be in part alleviated by reducing the yield gap. The yield gap is the variation that occurs between yields using the best seeds and agronomic management practices, and the yields that are actually achieved on the farms. The gap is mainly caused by damage to the crops by pests and diseases that impair the physiological development of the crops. One of the plant diseases that cause substantial economic losses each year is grey leaf spot (Ward et al., 1999), which is described in more detail in the following sections.

1.1.1. Grey leaf spot disease of maize

Grey leaf spot (GLS) in maize (*Zea mays*) is a severe fungal foliar disease. The disease was first reported in the U.S.A. in 1925 (Tehon and Daniels, 1925), whereas in South Africa the first known report was in 1988, where it was initially identified in KwaZulu-Natal (Gevers et al., 1994). The distribution of the disease shows a northern migration into the rest of the country and neighbouring countries (Ward et al., 1997).

This foliar disease can reduce the maize yield by 50 to 65% (Ward et al., 1999) and the degree of reduction is dependent upon the level of resistance of the specific maize hybrid. The disease usually progresses from the lower leaves of the plant as a result of the primary inoculum that remains behind in the plant debris from infected maize from the previous season. The disease cycle of grey leaf spot is outlined in Figure 1. In spring, or early summer, conidia are produced and dispersed either by the wind or through splashes of water onto the bottom leaves of the new maize plants. The secondary inoculum is produced from the sporulating lesions on the lower leaves, which aids in the disease progression to the aerial

parts of the plant and neighbouring plants. In one season multiple cycles of secondary infection can occur if the environmental conditions are favourable.

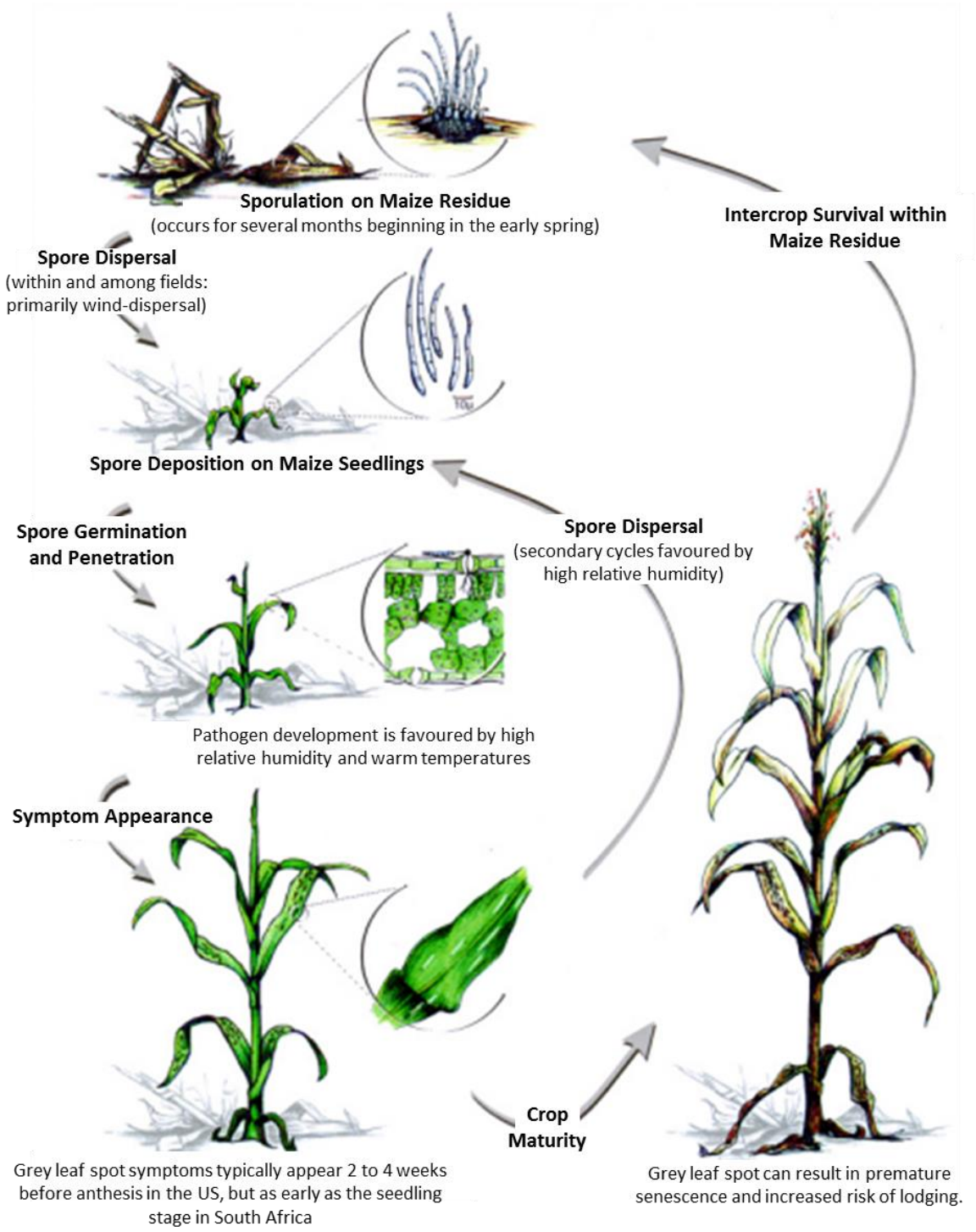

Figure 1. Grey leaf spot disease cycle in maize. (Ward et al., 1999)

GLS is characterised by lesions that form small spots on the leaves that develop into rectangular shape lesions that are confined by the veins of the leaves. The disease stays in the latent phase for up to 28 days after the initial infection after which conidiation is initiated by the humid environmental conditions (Ward et al., 1999). The conidiation within the lesions gives rise to the characteristic grey colouration, which is associated with the disease. The formed lesions may coalesce over time and result in severe blighting of the leaves as can be seen in Figure 2. Blighting ultimately reduces the available photosynthetic area leading to yield losses.

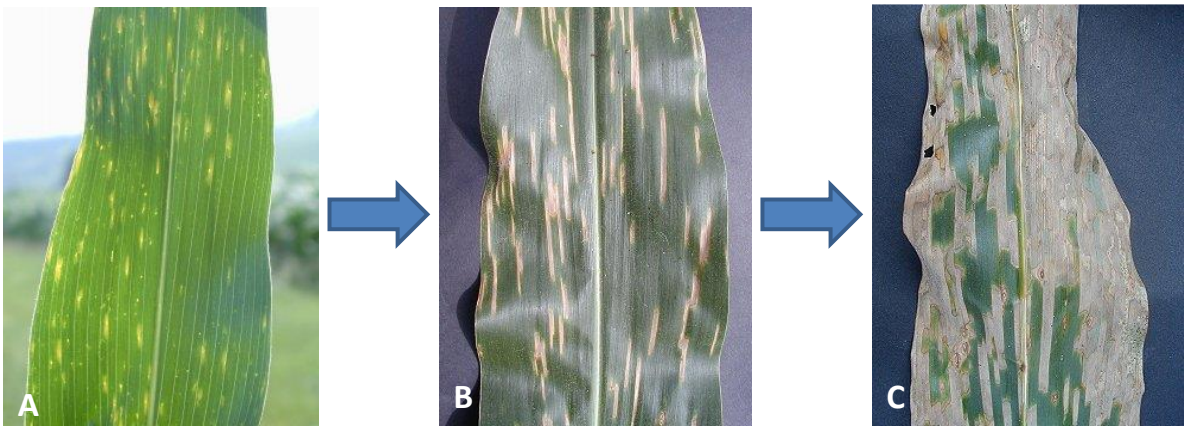

Figure 2. Disease progression of Grey leaf spot in maize. (A) Early signs of infection. (B) Clear rectangular lesions formed, confined by leaf veins. (C) Coalescence of lesions – wilting of the leaf. *(http://agriculture.kzntl.gov.za)*

The most common method to control the spread of the pathogen is to use plant resistant hybrids, however this strategy was found to have its limitations (Dunkle and Levy, 2000). In different regions the resistant hybrids show varying degrees of susceptibility to the pathogen. This observation is believed to be as a result of the interaction between the maize genotypes and the regional environment as well as the physiological diversity of the pathogen in different areas (Dunkle and Carson, 1998).

1.1.2. Causative pathogen of Grey Leaf Spot disease

There are two pathogens associated with grey leaf spot in maize that belong to the fungal genus *Cercospora*: *Cercospora zeae-maydis* and *Cercospora zeina*. It was previously believed that only *C. zeae-maydis* was responsible for grey leaf spot in maize. *C. zeae-maydis* was subdivided into group I and group II based on the genotypic and phenotypic differences between them (Wang et al., 1998). Group I was found to be dominant in the Midwestern U.S.A. and Group II is found in Eastern U.S.A. and Africa (Wang et al., 1998). Group II showed characteristic differences from group I. Group II isolates were incapable of producing cercosporin in culture and had a slower growth rate. In recent years, however, group II was found to be a distinct species (*C. zeina*). Group I, *C. zeae-maydis*, does not seem to be present in Africa (Meisel et al., 2009).

There are three hypotheses regarding the origin of *C. zeina* in Africa (Dunkle and Levy, 2000). In the one scenario Dunkle and Levy (2000) hypothesised that *C. zeina* was introduced from the U.S.A into Africa or, secondly, that the source of inoculum came from Africa. The latter scenario is believed to be more plausible since there is a greater genetic diversity of the pathogen in Africa (Dunkle and Levy, 2000). A third hypothesis is that neither of the two continents may be the point of origin of the pathogen and that the inoculum may have been introduced on a host other than maize. In general the second hypothesis is accepted (Dunkle and Levy, 2000). Africa is believed to be the point of origin for the pathogen, but that the original host was probably another indigenous crop species. Meisel et al. confirmed in 2009 that *C. zeina* is present in commercial maize plantations in South Africa and not *C. zeae-maydis.*

The global distribution of GLS on maize is shown in Figure 3 based on the disease reports from literature. Grey leaf spot caused by *C. zeae-maydis* is prevalent North (Crous and Braun, 2003) and South America (Poza et al., 2009) as well as China (Dunkle and Levy, 2000). *Cercospora zeae-maydis* is not present in Africa (Meisel et al., 2009). The other maize GLS causing pathogen, *C. zeina,* has only been reported in Eastern USA, Africa and more recently in China (Liu and Xu, 2013).

Figure 3. Global distribution of Grey leaf spot on maize based on reports from literature.

The infection strategy of *C. zeina* has been shown, by the Cereal Foliar Pathogen Research (CFPR) group of the University of Pretoria, to be similar to that of *C. zeae-maydis* (A.E. Visser, personal communication). The described strategy of infection by *C. zeae-maydis* is via the stomata of the maize leaves (Ward et al., 1999). The germinated spores form elongating germ tubes, which are able to sense the stomata. Once the germ tube reaches the stomata, it differentiates into an appressorial structure that enters into the stomata. Infectious hyphae then move between the mesophyll tissues.

The maize GLS fungal pathogens, *C. zeina* and *C. zeae-maydis*, are hemibiotrophs that enter a latent period after colonisation before switching to a necrotropic lifestyle. During the necrotrophic growth phase the lesion formation is observed. In *C. zeae-maydis* disease progression is achieved by the production of cercosporin, which is a phytotoxin (Wang et al., 1998). Cercosporin is a photosensitising perylenequinone that is able to generate toxic reactive oxygen species (ROS) that induce necrosis through the disruption of the membranes of the host-cells (Lynch and Geoghegan, 1979). The pathogen is then able to colonise the tissue followed by the formation of conidia. The true infection mechanism of *C. zeina* has not

yet been elucidated, but is believed to be similar to that of *C. zeae-maydis*, although no cercosporin production has been observed *in vitro* by *C. zeina*. Growth and development of fungi is regulated by an internal endogenous rhythm (Dunlap and Loros, 2006).

1.2. Circadian rhythms of fungal pathogens

The Earth's rotation around the sun creates daily fluctuations in temperature as well as in light. Living organisms have evolved in such a way to be able to adapt to these daily changes. Adaptation to light signals gave the organisms ability to anticipate changes in their environment through biological clocks. Biological clocks are responsible for creating a circadian rhythm in all the cells of the organism. The circadian clock allows the organism to entrain its biological clock to that of the external environmental time cues (Hunt *et al.,* 2010). Organisms are thus able to ensure that certain developmental and behavioural processes are executed at the optimal time of day, when they will have the greatest survival advantage.

In filamentous fungi the circadian clock is responsible for the regulation of primary metabolism, growth and development (Jerebzoff, 1965). Furthermore, the circadian rhythms generated regulate positive and negative phototropism, pigment biosynthesis and the development of sexual and asexual structures (Loros and Dunlap, 2001).

There are three characteristics to which a biological rhythm needs to conform to in order to be described as a circadian rhythm (Dunlap and Loros, 2006). The first characteristic states that the rhythm needs to have a period of 24 hours. Secondly the rhythm needs to be conditioned by a certain stimulus, such as light, and once the rhythm is entrained, the external input should no longer be needed. The third characteristic is that the rhythm needs to be buffered against external environmental cues. The circadian rhythms are under the control of positive and negative elements, which form the core of the physiological oscillator. The basic process of such biological oscillators is that the positive elements in the system activate the transcription of the negative elements, which in turn suppress their own transcriptional activation (He et al., 2002). The whole system forms an interwoven network, as will be

described later, which activates downstream cellular events, includes post-transcription and post-translational modifications and the production and degradation of the circadian clock elements (Schafmeier et al., 2005).

1.3. Blue light photoreception by fungi

A well described rhythm is that which is mediated by blue light (~410 – 520 nm) (Linden, 1997). Photoreceptors are proteins, which are able to harvest the light and generate a signal that is then transported into the nucleus to activate the transcription of light-responsive genes. The co-factors, chromophores for these photoreceptors, are able to absorb the light and bind to the receptor thus activating the light dependent signalling pathway (Froehlich et al., 2005). This system has been best studied in *Neurospora crassa*, which is used as the model organism in eukaryotes to study photoperiodism, and thus provides us with a basis from which to view biological clocks in other fungi (Olmedo et al., 2013).

Two main protein components of the circadian clock are White Collar-1 (WC-1) and White collar-2 (WC-2) (Ballario and Macino, 1997; Linden, 1997). This was experimentally proven through mutation studies where an absence of either or both of the proteins in *N. crassa* resulted in the fungus being unable to sense light. These two proteins interact through dimerization to form the active White Collar Complex (WCC), which acts as a transcription factor that drives the expression of light responsive genes, in particular the expression of the frequency gene (*frq*) (Froehlich et al., 2002; Malzahn et al., 2010). The protein encoded by the *frq* gene acts as a negative element in the circadian clock, which inhibits the function of the main clock components (Denault et al., 2001).

The WC-1 protein contains three PAS (Per-Arnt-Sim) domains, named after the three proteins in which these elements were originally discovered, viz. the period circadian protein, aryl hydrocarbon receptor nuclear translocator protein and the single-minded protein (Ballario et al., 1996). The WC-1 protein gained the status of a photoreceptor due to the presence of a LOV domain situated at its N-terminal. Light, Oxygen or Voltage (LOV) domains are specialised PAS domains that are able to bind flavin chromophores, and are differentiated from other PAS domains by the presence of the GXNCRFLQG motif with conserved photoreactive cysteine

residue (Krauss et al., 2009). Aside from these three domains, the WC-1 also has a GATA-zinc-finger DNA binding domain (Figure 4), which allows it to act as a transcription factor. The WC-2 protein lacks a specialised PAS domain (LOV domain) (Linden and Macino, 1997). The 3D model shown in Figure 4 is the *C. zeina* WC-1 orthologue generated using I-TASSER (Ambrish et al., 2010), which is based on the *N. crassa* WC-1 protein used as a template (Liversage, 2012).

The FAD (Flavin-adenine dinucleotide) chromophore harvests the light and transfers the energy to the WC-1 protein by covalently binding to the cysteinine in the LOV domain. Binding of the chromophore activates the WC-1 protein (He et al., 2002). The activated WC-1 protein is translocated to the nucleus, where it is able to form a heterodimer with the WC-2 protein through interaction of their PAS domains (Linden and Macino, 1997). The activated WCC is then able to bind to the promoter regions of light responsive genes and induce their transcription through chromatin remodelling events (Linden and Macino, 1997).

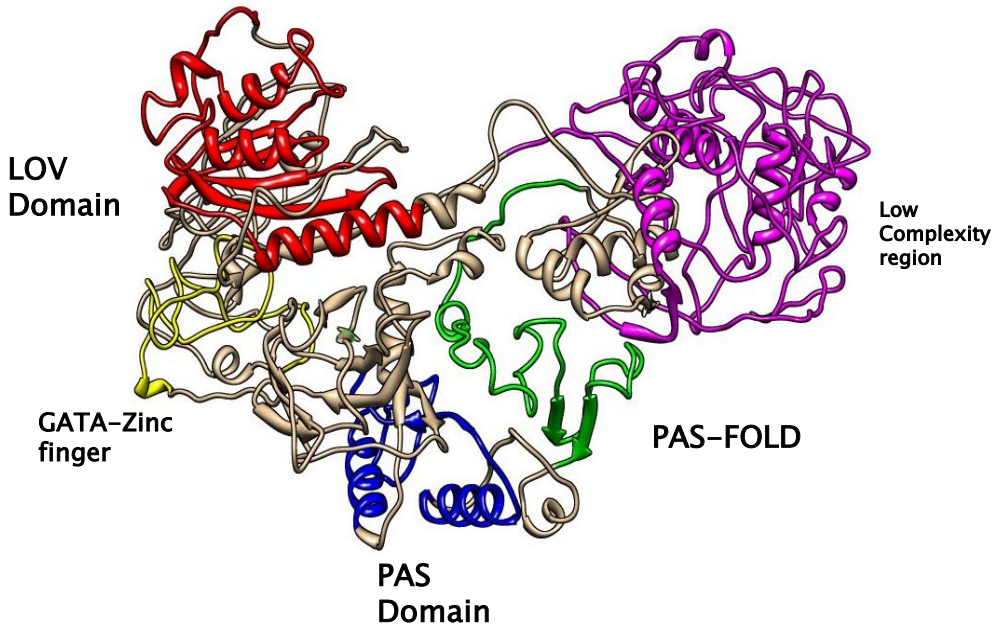

Figure 4. *Cercospora zeina* White Collar-1 orthologue (CRP1) 3D model. The 3D model of the CRP1 protein (*C. zeina* White Collar-1 homologue) indicates the various different domains of the protein. The N-terminal LOV domain can be seen in red. The PAS-Fold is indicated by green and the C-terminal PAS domain by blue. The N-terminal Low complexity regions are indicated by purple and the C-terminal GATA zinc-finger by yellow. (Liversage, 2012)

The central regulatory component of the circadian clock is the FRQ protein, which forms the core of the physiological oscillator (Querfurth et al., 2011). Early in the morning, when light is sensed by the fungus and WCC is formed, transcription of the *frq* gene is activated through the binding of WCC to its promoter region. Within a few hours FRQ proteins are synthesised and form homodimers. The dimerised form of FRQ is then able to interact with the RNA helicase FRH. The FRH protein is a homologue of the yeast Mtr4p, which is a component of the TAMP complex that is involved in pathways for maturation and quality control of the mRNA transcripts (Hurley et al., 2013). The FRQ-FRH complex then enters the nucleus, where it interacts with the activated WCC, inactivating it. It is through this interaction that the FRQ-FRH complex may alter the phosphorylation status of the WCC complex, reducing its affinity for the *frq* promoter region (Castro-Longoria et al., 2010).

The activity of the WCC reaches its lowest level by mid-day, which in turn results in a lower expression level of *frq* transcripts (Salichos and Rokas, 2009). The FRQ protein synthesis declines as its transcript levels are reduced by the end of the day. The FRQ protein is phosphorylated by several kinase enzymes as soon as it is synthesised in the morning. As the day passes the FRQ protein is progressively phosphorylated, which affects its stability. The hyperphosphorylated state of the FRQ protein increases the affinity of the SCE (Skp1-Cull-F-box) type ubiquiting ligase FWD-1 protein (Ping Cheng et al., 2003). By night the FRQ protein is tagged by the FWD-1 protein for degradation. In this manner, the inhibition of the WCC is reversed through the degradation of the FRQ protein, which results in activation of its transcription. The rate of phosphorylation of the FRQ is important as it determines the length of the rhythmic period of the organism (Salichos and Rokas, 2009). The overall circadian oscillator can be seen in Figure 5.

Despite the negative impact on WCC, FRQ has a positive effect on the level of WC-1 present in the cell (Crosthwaite et al., 1995). The activated form of the WC-1, which is able to bind to the DNA, is unstable and thus is degraded as part of the natural cell cycle. As described above, the WCC is phosphorylated due to the activity of the FRQ protein. The inactive phosphorylated state of the WCC complex is not able to bind to the DNA and thus results in stabilisation of the WC-1 protein and an accumulation of the protein in the cell overnight.

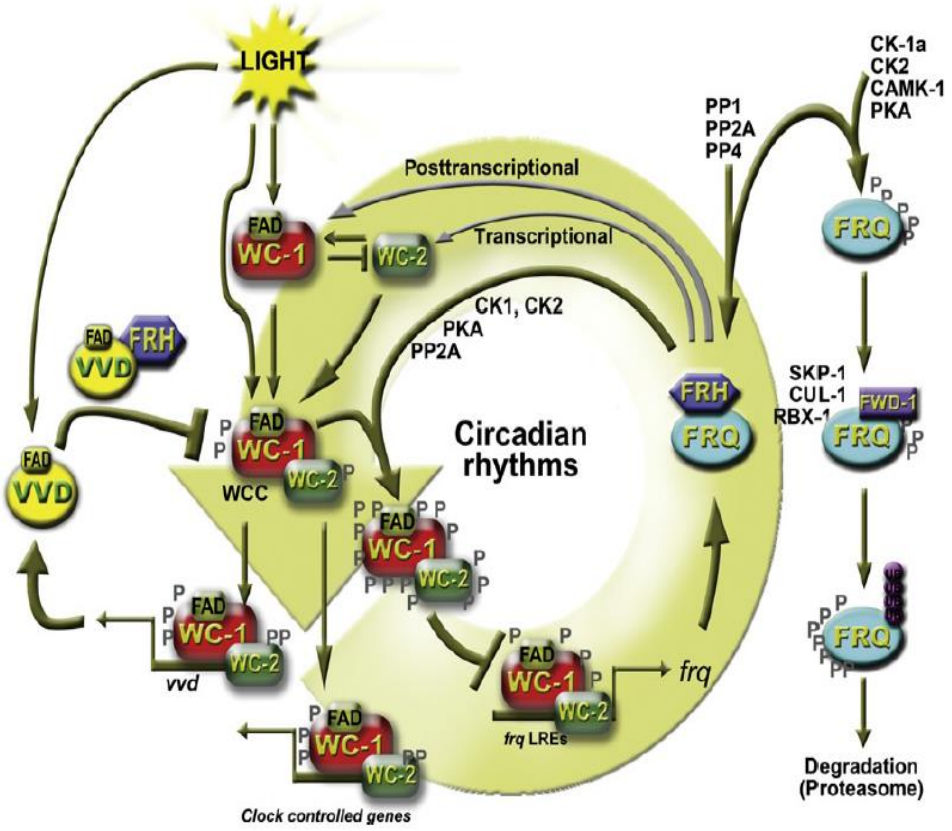

Figure 5. Schematic diagram of the fungal circadian clock. The two photoreceptor proteins (WC-1 and WC-2) form the WCC when WC-1 is activated through the binding of the FAD chromophore. The WCC forms a GATA type zinc finger transcription factor, activating the transcription of light responsive genes including the *frq* gene. The expressed FRQ protein acts through a negative feedback loop to inactivate the WCC and in turn its own expression. The VVD protein, another light activated protein, also acts as a suppressor of the WCC to regulate photoadaptation. CK-1a and CKII – casein kinases, CAMK-1 – calmodulin kinase. PKA – cAMP dependent protein kinase A. Check point kinases PP1, PP2a and PP4. SCF (Skp1-Cull-F-box protein) type ubiquiting ligase FWD-1 protein (Schmoll, 2011)

The importance of the five clock proteins, WC-1, WC-2, FRQ, FRH and FWD-1, has been functionally shown in the FRQ/WC-based circadian oscillator (FWO) of *N. crassa* (Loros and Dunlap, 2001). Additional studies on the FRQ protein have shown that there are rhythmic events observed in *Δfrq* knock-outs suggesting the presence of another oscillator that is dependent on the WC proteins only, termed the FRQ-less oscillator (WC-FLO) (Liu and Bell-Pedersen, 2006). Recently a third oscillator was identified in *N. crassa* that does not require a functional WC-1 or WC-2 proteins nor the FRQ protein, termed FRQ/WC-independent FLO (Liu and Bell-Pedersen, 2006). All three of the mentioned oscillators are present in the *N. crassa* system, but little is known about the molecular components of the last two. The FWO oscillator is the only one of the three tested in other fungal species thus far (Salichos and Rokas, 2009).

In *N. crassa* it has been shown that WC-1 is the limiting factor in the WCC, and overexpression of WC-1 was shown to activate most, but not all clock-associated genes, and is not able to activate all the light responsive genes. The WC-1 protein cannot sufficiently activate all aspects of the light transduction pathway (Lewis et al., 2002). It is known that three percent of the *N. crassa* genome responds to blue light, which is an indication of the important role light plays in the growth and development of the fungus (Lewis et al., 2002). In a microarray study in *Arabidopsis thaliana,* it was found that 34% of the genes are responsive to light (Ma et al., 2001). In both these studies the transcription of the light responsive genes was transiently increased after which a stable state was reached after a period of time. This pattern of regulation is indicative of an underlying photoadaptation event that allows the cells to adapt to increasing illumination. Furthermore, WC-1 has been experimentally shown to not only be involved in the regulation of the circadian clock genes, but is also involved in other non-rhythmic light responses (Lewis et al., 2002). This phenomena that WC-1 can regulate two different classes of genes, is attributed to the phosphorylation status of the WCC complex.

1.4. Fungal circadian photoadaptation

In addition to sensing the presence of light, fungi can also interpret and adapt to different light intensities. Adaptation to light is mediated by the photoreceptor, VIVID (VVD) (Malzahn et al., 2010). The expression of VVD is dependent on the light activation of the WCC. The light sensitive LOV domain present in WC-1, as seen in Figure 6, is also found in the VVD protein, which allows for rapid expression VVD in the presence of light. The WCC is inhibited by the VVD protein, in a light-dependent manner through physically interacting with the WC-1 protein (Olmedo et al., 2013). The VVD proteins are able to form heterodimers with the WCC through their associated LOV domains (Peter et al., 2012). Initially the WCC activates the transcription of the light-responsive genes, which includes *frq* and *vvd*. This raises the level of VVD proteins in the cell, which are able to bind to and inactivate WCC, and as a result, inhibit the expression of light responsive genes (Olmedo et al., 2013). The presence of the VVD protein in the cell declines as the night approaches. However, the level of VVD accumulated during the day is sufficient to inactivate any light induced WCC that may be activated by low levels of light during the night such as the moon rays (Malzahn et al., 2010).

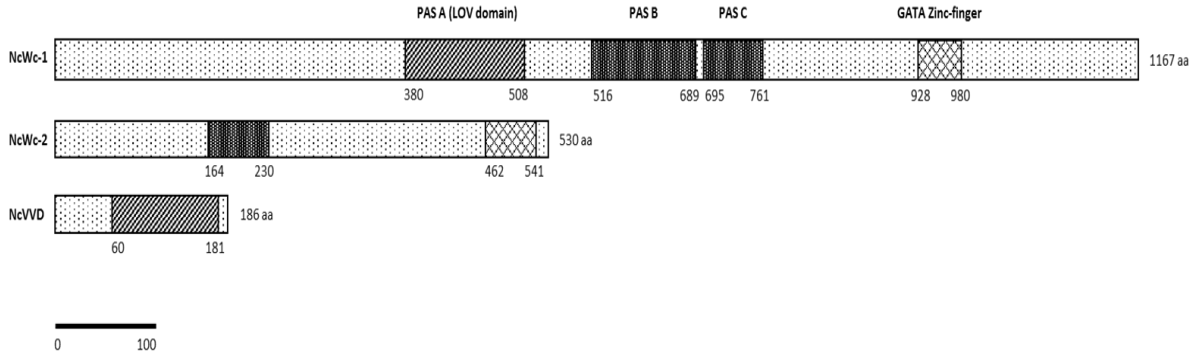

Figure 6. Domain architecture of characterised *Neursopora crassa* clock proteins. The three depictions of the proteins in the figure were downloaded from the Uniprot database (www.uniprot.org) and the SMART online program (www.smart.embl-heidelberg.de) was used to identify the functional domains in the proteins. These proteins include the White Collar-1 protein (WC-1, Q01371), White Collar-2 (WC-2, P78714) and the Vivid protein (VVD, Q9C376).The WC-1 protein contains three PAS domains (one of which is a LOV domain) and a GATA Zinc-finger. The WC-2 protein contains only a single PAS domain and a GATA Zinc-finger. The Vivid protein contains only one modified PAS domain (LOV domain). The standard abbreviations for the three proteins and their accession numbers are placed in the brackets in the legend following their respective names.

In yeast another photoadaptation mechanism, the Tup1-Ssn6 co-repressor complex, has been identified (Schafmeier and Diernfellner, 2011). The function of this co-repressor complex is conserved in *N. crassa*. The homologues of the two repressor components, RCO-1 and RCM-1, were identified and shown to play a role in the repression of the transcription of light dependent genes (Olmedo, 2010). This co-repressor complex is believed to indirectly influence the WCC by modifying the chromatin structure to release the WCC from the promoter regions after light induction (Sancar et al., 2011). This is different from the VVD protein that physically interacts with the WC-1 protein to desensitise the WCC complex (Cheng et al., 2003). Until now no homologue of the vivid gene has been found in the genomes of *Aspergillus* sp. and *Phycomyces* sp., which is an indication that photoadaptation might occur through another unknown mechanism (Herrera-Estrella and Horwitz, 2007). Photoadaptation is a complex process which hasn't been extensively studied in fungi, and from the experimental data generated in *N. crassa,* it is clear that this response is important for the growth and development of the fungus and ultimately its survival (Olmedo et al., 2013).

1.5. Conservation of blue light photoreception

The ability of blue light photoreceptors to perceive light is due to the presence of a chromophore binding domain, LOV domain, at the N – terminal of the protein (He et al., 2002). Plants are also able to sense blue light through phototropins, which function as light regulated protein kinases (Salomon et al., 2004). These phototropins contain two LOV domains, each of which are able to non-covalently bind a chromophore molecule.

Biochemical analysis has shown that plant phototropins use flavin mononucleotide (FMN) as a chromophore, whereas fungi exclusively use flavin adenine dinucleotide (Cheng et al., 2003). The difference of the chromophore binding capabilities between the two kingdoms is due to the presence of a larger loop connecting the alpha-helices in the fungal LOV domains as one can see in the alignment below in Figure 7. The increased length in the connecting loop within the active site of the domain could account for its ability to bind the larger FAD co-factor (Cheng et al., 2003).

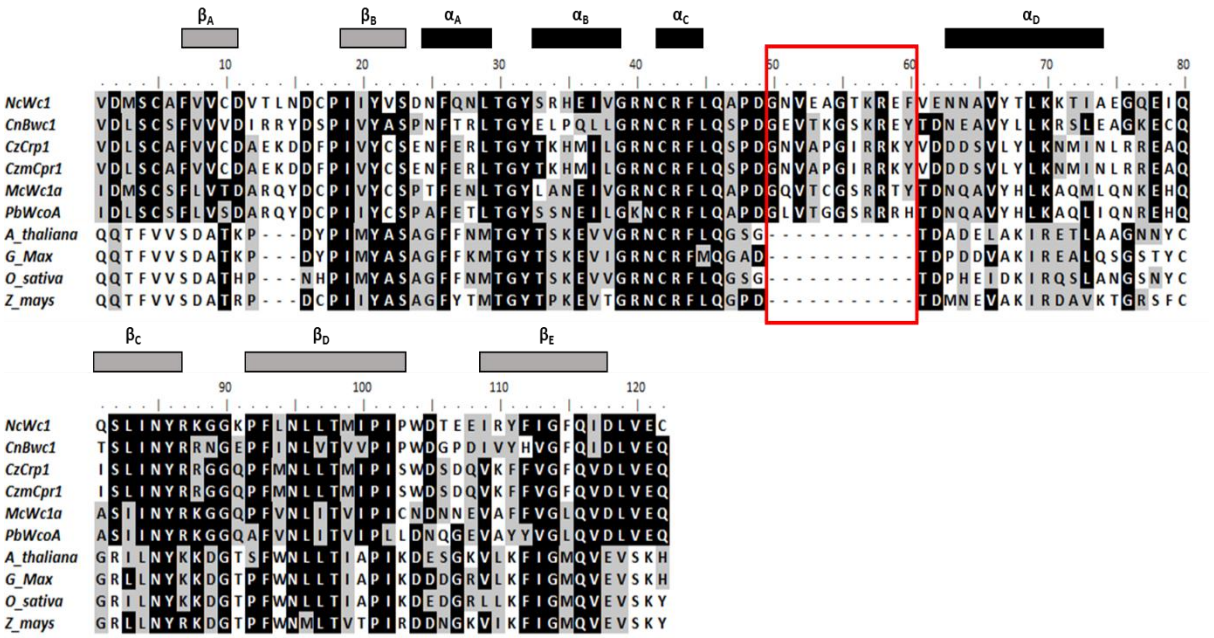

Figure 7. LOV domains of plant and fungal species. A section from the extracted LOV domains from the various WC-1 fungal orthologues and from plant phytotropins were aligned with the conserved motifs shaded (Liversage, 2012). The longer connecting loop present in the fungal LOV domains and absent from plants is indicated by the red box. NcWC1, *Neurospora crassa*; CnBwc1, *Cryptococcus neoformans*; CzCrp1, *Cercospora zeina*; CzmCrp1, *Cercospora zeae-maydis*; McWc1a, *Mucor circinelloides*; PbWcoA, *Phycomyces blakesleeanus*.

In *N. crassa* it was experimentally determined that the fungus is able to respond to light at a molecular level (He et al., 2002). The mRNA transcripts of white collar-1 were present in the dark grown cultures and up-regulated when exposed to light (He et al., 2002). The counter part of WC-1, White Collar-2, showed a constitutive expression upon light exposure. Similar light induction patterns has been observed in other fungal species and are summarised in Table 1.

In Basidiomycetes, *Cryptococcus neoformans* expressed white collar-1 transcripts at very low levels and showed a reverse photoinduction process to that seen in *N. crassa* (Lu et al., 2005). The *bwc-1* transcripts are constitutively expressed while the *bwc-2* transcripts are induced by light. However, the absence of *bwc-1* indicated that the expression of *bwc-2* is dependent on the expression of *bwc-1* (Idnurm and Heitman, 2005). The expression pattern in another Basidiomycete, *Lentinula edodes*, showed that both the white collar transcripts are induced by light (Sano et al., 2009, 2007). Both Basidiomycete species showed an increase in the *wc-2*-like transcripts. It could be that the *bwc-1* transcript level is under strict control of another protein that plays a role in photoadaptation, keeping the expression of the gene constant.

The *wc-1* like transcripts of two Ascomycete fungi, *Trichoderma atroviride* and *Tuber borchii*, showed constitutive expression when cultures grown in the dark were exposed to light (Ambra et al., 2004; Casas-Flores et al., 2004). Their corresponding *wc-2* like transcripts were induced upon irradiation. Whether this increase in transcription is due to activation or de-repression is not known. The other Ascomycete fungal species in which light induced expression of the white collar genes have been observed are shown in Table 1.

The *wc-1* like transcripts of *Magnaporthe oryzae*, *Ophiocordyceps sinensis*, *Aspergillus fumigatus* and *Botrytis cinerea* were rapidly increased upon light exposure (Canessa et al., 2013; Fuller et al., 2013; Kim et al., 2011; Yang et al., 2014). The transcripts were increased within five minutes and only reached a steady state after 30 minutes in most of the species. In *B. cinerea*, *bcwcl-2* was not light induced, but its transcript levels and that of *bcwcl-1* were reduced after 30 minutes of constant light exposure as the expression of the *vvd* gene

homologue increased (Canessa et al., 2013). This is a clear indication of the photoadaption role of the VVD protein. The *Fusarium* species, *Fusarium fujikuroi* and *Fusarium verticilliodes*, showed no photoinduction of either the two white collar transcripts (Bodor et al., 2013; Estrada and Avalos, 2008).

The White Collar Complex plays an important role not only in the entrainment of the fungal circadian clock, but the complex also acts as a transcription factor that binds to and activates the expression of light responsive genes. Overexpression of the white collar genes in *Trichoderma atroviride* resulted in no significant changes in the expression of light responsive genes (Esquivel-Naranjo and Herrera-Estrella, 2007). The same phenomenon was observed in the *Botrytis cinerea* white collar mutant, where the transcription of light responsive genes was still detected (Canessa et al., 2013). This observation could be due to a tightly regulated photoadaptation process as in the case of *T. atroviride* or due to the function of other unidentified photoreceptors.

The white collar genes have been shown to be present as single copies in all the characterised Ascomycete and Basidiomycete fungi to date. Multiple copies of both the white collar genes have been identified in Zygomycetes (Corrochano and Garre, 2010). In *Phycomyces blakesleeanus*, a Zygomycete, the expression of the *wc-1* homologues *wcoA* and *wcB* were rapidly increased upon light exposure (Corrochano et al., 2006). The other *wc-1* homologue, *madA*, was not induced by light, but its transcript level is reduced in light. The same light dependent decrease in transcript level was seen for the *wc-2* homologue, *madB*. These two proteins, MadA and MadB, form the WC complex (Sanz et al., 2009). This complex is present in the dark and is needed to activate the expression of the other two wc-1 homologues (*wcoA* and *wcB*). The MadA/MadB complex might function through inhibiting the expression of the other two wc-1 homologues (*wcoA* and *wcB*) in the dark. Upon light exposure this inhibition is removed and expression is activated. Another Zygomycete, *Pilobolus crystallinus*, has three copies of the *wc-1* homologue. The transcription of the one copy, *pcmadA1*, is suppressed by light, whereas the other copy's transcription, *pcmadA3*, is induced upon light exposure (Kubo, 2009).

Table 1. Fungal blue light photoreceptors.

Fungal Phyla	Species	Wc-1 homologue	Wc-2 homologue	Light Induced	Reference
Basidiomycota	*Cryptococcus neoformans*	*Bwc1*		No	(Lu et al., 2005)
			Bwc2	Yes	(Lu et al., 2005)
	Lentinula edodes	*Le.phrA*		Yes	(Sano et al., 2007)
			Le.phrB	Yes	(Sano et al., 2009)
Ascomycota	*Aspergillus fumigatus*	*LreA*		Yes	(Fuller et al., 2013)
	Botrytis cinerea	*BcWcl1*		Yes	(Canessa et al., 2013)
			BcWcl2	No	
	Fusarium fujikuroi	*WcoA*		No	(Estrada and Avalos, 2008)
	Fusarium verticilloides	*FvWc1*		No	(Bodor et al., 2013)
			FvWc2	No	
	Magnaporthe oryzae	*MgWc1*		Yes	(S. Kim et al., 2011)
	Neurospora crassa	*Wc-1*		Yes	(Ballario et al., 1996)
			Wc-2	No	(Macino, 1997)
	Ophiocordyceps sinensis	*OsWc1*		Yes	(Yang et al., 2014)
	Tricoderma atroviride	*blr1*		No	(Casas-Flores et al., 2004)
			blr2	Yes	(Esquivel-Naranjo and Herrera-Estrella, 2007)
	Tuber borchii	*Tbwc1*		Yes	(Ambra et al., 2004)
Zygomycota	*Pilobolus crystallinus*	*PcmadA1*		No	(Kubo, 2009)
		PcmadA3		Yes	(Kubo, 2009)
	Phycomyces blakesleeanus	*MadA*		No	(Corrochano et al., 2006)
			MadB	No	(Sanz et al., 2009)
		WcoA		Yes	(Corrochano et al., 2006)
	Mucor circineloides	*mcwc1a*		No	(Silva et al., 2006)
		mcwc1b		Yes	
		mcwc1c		Yes	

The Zygomycete, *Mucor circinelloides* also has three copies of the *wc-1* homologue. Blue light dependent transcription of *mcwc1b* and *mcwc1c* was demonstrated, whereas the expression of *mcwc1a* remains unaffected (Silva et al., 2006). Similar to the other two Zygomycetes described, the expression of *mcwc1c* is dependent on the expression of *mcwc1a*. The expression of the WC-1 protein in *N. crassa* is auto-regulated by its own *wc-1* transcripts. It is clear that in Zygomycetes that auto-regulation does not play a role and that the expression of the one photoreceptor regulates the expression of another (Kubo, 2009). The exact function of this type of regulation is not yet known, but it might play a similar role in photoadaptation as the VVD protein in *N. crassa*.

In summary, fungal photoreception is mostly conserved across the phyla. The WC-1 protein appears to be the limiting factor in the regulation of the light dependent genes (Cheng et al., 2001). The expression of the WC-2 protein is dependent on the expression of the WC-1 protein. The WC complex is able to regulate most, but not all, light responsive genes (Lewis et al., 2002). This phenomena stands to reason that there are possibly other photoreceptors, that remain to be identified, that activate the transcription of light dependent genes. In the dark the *wc-1* transcript is present at a basal level and only increase slightly (or not at all in some cases) upon exposure to light before returning to the basal state. This maintenance of a basal level of both the white collar transcripts (*wc-1* and *wc-2*) is a clear indication that the fungus is able to adapt to different light intensities. In Basidiomycota and Ascomycota the WC-1 protein regulates its own expression through the *wc-1* transcripts. The expression of the WC-1 homologous photoreceptors in Zygomycota is regulated by the other copies of the photoreceptor that might function in a similar fashion to the VVD protein for photoadaption (Kubo, 2009).

1.6. Characterised functions of the blue light photoreceptors

Blue light plays an important role in the fungus' ability to survive and adapt to changing environments. Many of the responses to light have been shown in the wild type species, whereas the molecular pathways responsible for these light-dependent phenotypes remain unknown. The identification and characterisation of the WC complex, in particular the WC-1 protein, through gene disruption experiments have shown the important role played by the expression of this gene in light-dependent pathways of *N. crassa*. Subsequently gene disruption experiments of either or both the white collar genes were conducted in various other fungal species. The characterised blue light dependent function of both white collar genes indicated that this light response is partially conserved across fungal species and will be discussed in more detail in this section. A summary of blue light responses in various fungal species is shown in Table 2.

1.6.1. Secondary metabolism

The various secondary metabolic pathways that the WC-1 protein plays a role in and the genes involved are summarised in Table 3.

1.6.1.1. Carotenoid biosynthesis

Certain fungal species are able to produce and accumulate a photoprotective pigment upon exposure to light. The production of carotenoid pigments is the most extensively studied light response in *N. crassa,* and acts to protect the fungus from high light intensities (Ballario et al., 1996). Carotenoids are terpenoid pigments that play an important role in protecting the fungus against UV damage (Lewis et al., 2002). Carotenoids accumulate in light exposed mycelia of the wild type strains as yellow/orange pigments.

The carotenoid, β-carotene, is synthesised from the colourless phytoene precursor during a series of dehydrogenase reactions (Avalos and Estrada, 2010). Fungal species have only a single dehydrogenase enzyme that is responsible for the consecutive dehydrogenase reactions. The expression of two carotenoid biosynthesis genes, *carb* and *carRA*, are upregulated in *F. fujikuroi* in light exposed mycelia (Estrada and Avalos, 2008). These genes

encode for a phytoene dehydrogenase and phytoene synthase respectively. Disruption of the *carb* gene results in phytoene accumulation, whereas the *carRA* null mutants are unable to produce phytoene. The production of carotenoid pigments relies on the expression of both the *carb* and the *carRA* gene, which forms part of the *F. fujikuroi* carotenoid gene cluster (Linnemannstöns et al., 2002).

The role of blue light in the expression of carotenoid biosynthetic genes was tested through *wc-1* mutational studies. In *Δwc-1* knock-out strains the expression of the carotenoid gene cluster (*carb* and *carRA*) was reduced in *F. fujikuroi*, *F. oxysporum* and *F. graminearum* compared to the wild type strains (Estrada and Avalos, 2008; Kim et al., 2013; Ruiz-Roldán et al., 2008). The disruption of the one *wc-1* gene copy, *mcwc1-c*, in the Zygomycete, *M. circinelloides*, showed a similar expression pattern of the two carotenoid biosynthesis genes as observed in *Fusarium* species (Silva et al., 2006). It is believed that the same reduction will be observed in the disruption of *pcmadA3* in *P. crystallinus* based on the similarity in sequence of these two copies of the *wc-1* gene (Kubo, 2009). These two carotenoid biosynthesis genes are closely linked and form part of the same gene cluster in *Fusarium* species and *M. cirinelloides* (Ávalos et al., 2007).

The homologues of *carb* and *carRA* in *N. crassa* are *al-1* and *al-2* (Schmidhauser and Lauter, 1994, 1990). These two genes are present on the same chromosome but separated by other genes. In *Δwc-1* knock-out strains, the same reduction in the carotenoid biosynthesis genes were observed as seen in the *Fusarium* species, which is an indication that the light activation of the carotenoid biosynthetic pathway in fungi is not dependent on the expression of WC-1. (Ballario et al., 1996). The WC-1 independent expression of carotenoid biosynthetic genes opens the possibility of other blue light regulators involved in the carotenoid biosynthesis pathway that remains to be experimentally tested.

1.6.1.2. Melanin biosynthesis

In addition to carotenoids, fungi often produce melanin when exposed to light, which has a role other than protecting the hyphal cells from high light intensities. Melanin protects the fungus against UV damage and aids in penetration of plant cells during appressoria formation. Fungal hyphae are protected *in planta* from plant hydrolytic enzymes through melanin cross-linking in the cell wall (Bluhm et al., 2010). A phytotoxic effect is also produced by secreting melanin precursors.

Fungal melanin can be generated by either of two pathways (Eisenman and Casadevall, 2012). The first pathway produce melanin through the polymerisation of 1,8-dihydroxynaphtalene (DHN) subunits (Langfelder et al., 2003). The first step in the DHN pathway is the formation of 1,3,6,8-tetrahydroxynaphtalene (1,3,6,8-THN), which is catalysed by polyketide synthase (PKS) (Eisenman and Casadevall, 2012). The scytalone and 1,8-dihydroxynaphtalene (DHN) intermediates are then generated through consecutive reduction and dehydration steps (Butler and Day, 2011). The other less common pathway utilises L-dopa or tyrosine as a precursor. This pathway, which resembles the melanin production in mammals, is exclusively used by *C. neoformans* (Pukkila-Worley et al., 2005).

Light has been shown to induce the expression of three important genes encoding key enzymes in the fungal DHN melanin biosynthetic pathway (Kihara et al., 2004a, 2004b, 2001). The three genes, which have been characterised in *B. oryzae*, are, *pks1*, *scd1* and *thrd*, encoding polyketide synthase (PKS), scytalone dehydratase (SCD) and hydroxynaphtalene reductase (THR) respectively. In *A. alternata* the expression of *pksA*, encoding polyketide synthase, is up-regulated in response to blue light, but not when the *LreA* (*wc-1*) gene is disrupted (Pruss et al., 2014). Melanin pigmentation was also lost in *A. fumigatus,* when the *wc-1* homologue was disrupted suggesting a WC-1 blue light dependent activation of melanin synthesis (Fuller et al., 2013). The expression of the three above mentioned melanin biosynthetic genes were differentially expressed in *M. oryzae* between the dark and light grown wild type strains (Kim et al., 2011).

Table 2. Characterised functions of blue light photoreceptors. The blue light functions of the fungal species have been characterised through mutations in the *wc-1* homologues, except for *Tuber borchii* and *Pilobolus crystallinus*. (Only the nine most common functions mentioned in literature are shown)

	Characterised functions of Blue light in fungi								
	Photo-reactivation	Sexual development	Photo - morphogenesis	Asexual reproduction	Secondary metabolism	Hydro - phobicity	Oxidative stress	Phototropism	Reference
Basidiomycota									
Coprinus cinereus			x						(Terashima et al., 2005)
Cryptococcus neoformans	X	X							(Lu et al., 2005)
Schizophyllum commune	X		x						(Ohm et al., 2013)
Ascomycota									
Alternaria alternata				X	x				(Pruss et al., 2014)
Aspergillus fumigatus	X				x		X		(Fuller et al., 2013)
Aspergillus nidulans		X		X	x				(Ruger-Herreros et al., 2011)
Bipolaris oryzae	X			X					(Kihara et al., 2007)
Botrytis cinerea		X					X		(Canessa et al., 2013)
Cercospora zeae-maydis	X			x	x				(H. Kim et al., 2011)
Fusarium fujikuroi				x	x	X			(Estrada and Avalos, 2008)
Fusarium graminearum	X	X		x	x				(Kim et al., 2013)
Fusarium oxysporum	X				x	X			(Ruiz-Roldán et al., 2008)
Fusarium verticilloides		X				X			(Bodor et al., 2013)
Magnaporthe oryzae				x	x				(S. Kim et al., 2011)
Neurospora crassa		X	x	x	x				(Ballario et al., 1996)
Tricoderma atroviride	X			x					(Casas-Flores et al., 2004)
Tuber borchii			x						(Ambra et al., 2004)
Zygomycota									
Mucor circineloides					x			x	(Silva et al., 2006)
Pilobolus crystallinus								x	(Kubo, 2009)
Phycomyces blakesleeanus								x	(Corrochano et al., 2006)

However, the expression of these genes remained unaffected, when exposed to blue light, in the *Δwc-1* mutant background of *B. oryzae* (Kihara et al., 2007). This is an indication that other photoreceptors play a role in the regulation of the three melanin biosynthetic genes. Thus, the fungal melanin biosynthetic pathway is regulated by blue light, which in part, is due to the positive regulation of the WC-1 blue light photoreceptor. The positive regulation played by WC-1 on the expression of *pks1*, *scd1* and *thrd*, which are the melanin biosynthetic genes, could be due to the entrainment of the circadian clock by blue light. The regulation of hyphal melanisation in *Cercospora kikuchii* has been shown to be a result of the entrainment of the underlying circadian rhythm, which is similar to what is seen in *N. crassa* (Bluhm et al., 2010).

1.6.1.3. Phytotoxin biosynthesis

Fusarium species produce a wide range of secondary metabolites that act as mycotoxins, which are synthesised in response to blue light (Avalos and Estrada, 2010). It has been established that blue light plays a role in synthesis of gibberellins, bikaverin and fusarins in *F. fujikuroi* (Estrada and Avalos, 2008). Gibberellin and bikaverin are two secondary metabolites that are produced in the wild type strains under nitrogen starved conditions. Although gibberellin is not a phytotoxin, it is a plant growth regulator hormone that aids in the pathogenicity of *Fusarium* species. The limiting gene in the cluster for the gibberellin biosynthesis is the copalyl diphosphate synthase gene, *gibB*, which encodes for a bifunctional terpene cyclase (Ávalos et al., 2007). The other secondary metabolite under nitrogen-dependent regulation is bikaverin. This metabolite accumulates as a red pigment, and is synthesised though the activation of the *bik1* gene, which encodes a polyketide synthase (Estrada and Avalos, 2008). In the *ΔwcoA* (*wc-1*) mutant background the concentration of both of these secondary metabolites, gibberellin and bikaverin, are reduced compared to the wild type strains, suggesting a light dependent role of WcoA in nitrogen regulation (Estrada and Avalos, 2008).

The White Collar-1 protein has been shown to be a negative regulator of secondary metabolism in fungi (Kim et al., 2013). Aurofusarin and rubrofusarin, produced by *F. graminearum*, accumulated in all wild type strains as a red pigment when grown in constant

light, but no pigment production was observed in the dark (Kim et al., 2013). Gene disruption of *wc-1* resulted in pigment production in both dark and light grown cultures in *F. graminearum*. This effect was confirmed to be due to the absence of expression of *Gip1* and *pks12* (polyketide synthase genes) in the wild type strains grown in dark, while the knock-out strains showed expression of both genes. Similarly, *Alternaria alternata* showed constitutive expression of *pksJ* (polyketide synthase gene in alternariol biosynthesis) in the *ΔLreA* (*wc-1*) background, whereas the wild type strains only showed expression in the light (Pruss et al., 2014).

Table 3. Genes involved in blue light regulated secondary metabolite biosynthesis in fungi.

Metabolic pathways	Secondary metabolite	Enzymes	Gene[a]	Species	Reference[c]
Terpenoid biosynthesis	Carotenoid	Phytonene dehydrogenase	*carb*	*Fusarium spp*[b]*; Mucor circinelloides; Neurospora crassa; Pilobolus crystallinus*	(Linnemannstöns et al., 2002)
		Phytoene synthase	*carRA*		
	Gibberlins	Copalyl diphosphate synthase	*gibB*	*F. fujikuroi*	(Tudzynski and Hölter, 1998)
	Trichothecene	Trichodiene synthase	*tr15*	*F. fujikuroi*	(Brown et al., 2004)
Polyketide biosynthesis	Alternariol	Polyketide synthase	*pksJ*	*Alternaria alternata*	(Kimura and Tsuge, 1993)
	Bikaverin	Polyketide synthase	*bik1*	*F. fujikuroi*	(Wiemann et al., 2009)
	Aurofusarin	Polyketide synthase	*pks12*	*F. graminearum*	(Malz et al., 2005)
		laccase gene	*gip1*		
	Cercosporin	Polyketide synthase	*ctb1*	*Cercospora zeae-maydis*	(Chen et al., 2007)
	Melanin	Polyketide synthase	*pks1*	*A. alternata; Aspergillus fumigatus; Bipolaris oryzae; Magnaporthe oryzae*	(Kimura and Tsuge, 1993)
		Scytalone dehydratase	*scd1*		
		Hydroxynapthalene reductase	*Thrd*		

a - Gene shown to play important role in metabolic pathway; b – *F. fujikuroi, F. gramineraum, F. oxysporum*; c – Publication of metabolic gene cluster

Cercosporin, produced by *C. zeae-maydis*, is another phytotoxin produced through the polyketide pathway that shows a similar production pattern as the above two fungal species (Kim et al., 2011). The red pigment is accumulated within 72 hours in wild type hyphae grown under constant light. The disruption of *crp1* (*wc-1*) resulted in a delayed accumulation of cercosporin production. In *Cercospora nicotiana*, gene disruption experiments indicated that the *ctb1* gene, encoding a polyketide synthase, is the limiting gene in the cluster for cercosporin biosynthesis (Choquer et al., 2005). It would be interesting to see whether or not this gene shows the same expression pattern in the *crp1* mutant background as seen in *F. graminearum* and *A. alternata.* The White collar-1 protein acts as a negative regulator of the polyketide biosynthetic pathway by inhibiting the expression of polyketide synthase genes in the dark.

1.6.2. Phototoxicity

In addition to the blue light dependent production of secondary metabolites in order to protect fungi from UV damage, fungi also possess the ability to reverse the UV damage done to their DNA (Kihara et al., 2007). The wild type *B. oryzae* culture expresses a photolyase gene, *phr1* when grown in light after UV irradiation (Kihara et al., 2007). The enzyme encoded by this gene is able to split the pyrimidine dimer in DNA, caused by UV irradiation, by absorbing the blue light as energy. Absence of the WC-1 protein results in no light dependent transcriptional activation of the photolyase enzyme (Kihara et al., 2007).

Photoreactivation is a process by which the DNA damage caused by UV light is reversed, and is regulated by blue light. The lethal effect UV light has on spore production was observed in *F. oxysporum* wild type and *Δwc-1* knock-out strains, which showed a drastic reduction in spore formation (Ruiz-Roldán et al., 2008). The survival advantage is that the wild type *F. oxysporum* and *F. graminearum* are able to repair UV damage through a process that is known as photoreactivation (Kim et al., 2013; Ruiz-Roldán et al., 2008). This process has been shown to be conserved in *T. atroviride* and *A. fumigatus,* where the *Δwc-1* knock-out was unable to repair the UV damage, demonstrating light enhanced resistance to UV damage in wild type strains (Casas-Flores et al., 2004; Fuller et al., 2013). In C. *zeae-maydis*, the WC-1 protein was

shown to regulate the activation of an additional gene that functions in photoreactivation. In *Δwc-1* knock-out strains, the genes encoding photolyase, *phr1*, and a cyclobutane pyrimidine photolyase (*cdp1*) showed a reduced expression compared to the wild type strains (Kim et al., 2011). In *C. neoformans* the *wc-1* knock-outs showed increased sensitivity to UV light, which was restored to wild type levels of tolerance in *wc-1* complemented strains (Lu et al., 2005). The genome of *C. neoformans* indicated no evidence of a photolyase (Lu et al., 2005). However, the expression of the *hem15* gene, encoding a ferrochelatase, was reduced in *Δwc-1* knock-out cultures of *C. neoformans* and *N. crassa* compared to the wild type strains. This enzyme catalyses the final step in the haem biosynthetic pathway from phototoxic porphyrins, which accumulate in the presence of light (Idnurm and Heitman, 2010). This WC-1 light dependent mechanism against phototoxicity was shown to be conserved in another basidiomycete, *S. commune* (Ohm et al., 2013).

1.6.3. Photomorphogenesis

The effect of light on growth and development of fungal species has been well characterised (Linden, 1997). The role that WC-1 plays in development has been shown in *N. crassa Δwc-1* knock-out strains (Linden, 1997). The wild type strains showed the positive effect that light had on apical growth. Extensive hyphal branching took place under light irradiation resulting in a compact growth compared to the *Δwc-1* knock-outs that showed no light dependent phenotype. The most prominent photomorphogenic effect on growth is observed in Basidiomycota. The transcription of *dst1* (*wc-1*) is higher in the fruiting body primordia compared to the vegetative mycelia as shown in wild strains of *Coprinopsis cinerea* (Terashima et al., 2005). White Collar-1 plays a role in the development and maturation of fungal structures.

The main role of WC-1 in *C. cinerea* and *S. commune* is in the development of mature fruiting bodies (Ohm et al., 2013; Terashima et al., 2005). Light activation of the development of the primordium is seen in *Δwc-1* knock-outs, but no mature fruiting bodies were formed. The White collar 1 protein is the limiting factor in fruiting body maturation, whereas the activation of primordium development is possibly regulated by other blue light photoreceptors. The

growth rate of the wild type strain of *C. cinerea* is reduced under constant light, whereas *Δdst1* knock-out strains have the same growth rate regardless of the light conditions they were subjected to (Kuratani et al., 2010). The WC-1 protein is thus thought to act as a repressor of fungal growth under constant light.

1.6.4. Hydrophobicity

The White Collar-1 protein has been implicated in the alteration of the hydrophobicity of the fungal hyphae. In *F. verticilloides* water droplets were placed on the surface of the wild type cultures and *Δwc-1* knock-out strains (Bodor et al., 2013). The water droplets rapidly soaked into the surface of knock-out strains, whereas they still remained on the surface of wild type strains after twenty hours. It was suggested that in *F. fujikuroi* that hydrophobicity is the result of changes in the accumulation of hydrophobins (Estrada and Avalos, 2008). Putative hydrophobin genes, were identified in *F. oxysporum*. Differential expression of *hyd1* was observed between dark and light grown wild type cultures. The gene in the wild type strain was not expressed in the dark grown mycelia and was supressed in the light compared to the *Δwc-1* knock-out strains. In the wild type and *wc-1* complemented (*Δwc1+wc1*) strains, incomplete splicing of the *hyd1* transcripts resulted in the generation of different transcript sizes (Ruiz-Roldán et al., 2008). Complete splicing of the transcript was only present in the *Δwc-1* knock-out strains. The White collar-1 protein is thus believed to play a role in the light-independent regulation of the *hyd1* gene expression as well as mRNA processing (Ruiz-Roldán et al., 2008).

1.6.5. Sexual development

Sexual reproduction in fungi is influenced by the presence of blue light. The basidiomycete, *C. neoformans*, uses BWC1 (WC-1) to regulate the inhibition of light dependent mating (Idnurm and Heitman, 2005). The *Δwc-1* knock-out strains are insensitive to light. Bilateral crosses, where both the parents carried the disrupted version of the *wc-1* gene, resulted in mating responsive filament production regardless of the lighting conditions. The mating of the wild type strains in bilateral crosses was reduced in constant light. A reduction in filament

production was seen in constant light in unilateral crosses, which used a knock-out and a wild type strain.

The White Collar-1 protein was shown to play an important role in female fertility in *F. verticilloides* (Bodor et al., 2013). Crosses using the knock-out strain as the female to mating type strain, FGSC7600, inhibited the formation of perithecia and thus female sterility. The maturation of perithecia was shown to be positively regulated by the WC-1 protein in *F. graminearum* (Kim et al., 2013). An interesting observation was made that the expression of both *F. verticilloides* white collar genes (*wc-1* and *wc-2*) were down regulated in the mutant mating type gene (*mat1-2-1*) strains (Bodor et al., 2013). This observation suggests the positive regulation of the white collar genes by the *mat1-2-1* product. A similar observation was made for the positive regulation of the carotenoid biosynthetic pathway by MAT1-2-1 (Bodor et al., 2013).

1.6.6. Asexual reproduction

Light provides an environmental cue for the fungus to produce spores in conditions that are favourable to its survival. The activation of conidia formation in light has been reported in *N. crassa*, *T. atroviride* and *B. oryzae* (Casas-Flores et al., 2004; Kihara et al., 2007; Sargent and Briggs, 1967). Disruption of the *wc-1* gene resulted in suppression of light induced conidia formation in all three fungi, which suggests that WC-1 plays a positive role in photoconidiation. In *A. nidulans* the disruption of *LreA* (*wc-1*) had no effect on light activation of conidia (Röhrig et al., 2013). A light induced conidiation gene, *blrA*, was identified and shown to be under the regulation of *LreA* (*wc-2*) and the phytochrome, *FphA* (Ruger-Herreros et al., 2011).

Conidiation was increased in *F. graminearum Δwc-1* knock-out strains when grown in complete media (CM) that inhibits conidiation in the wild type strains (Kim et al., 2013). The White Collar-1 protein thus plays a role in repressing conidiation in the light. The same repression mechanism of WC-1 was seen in *C. zeae-maydis,* where large amounts of conidia

were produced in the *Δcrp1* (*wc-1*) knock-out strains, and none in the wild type strains, when both cultures were grown in constant light (Kim et al., 2011). The repression mechanisms of conidia in light grown cultures is conserved in *B. cinerea* and *A. alternate* and *M. oryzae* (Canessa et al., 2013; S. Kim et al., 2011; Pruss et al., 2014).

It is clear that WC-1 functions as either a positive regulator of conidia formation as seen in *N. crassa*, *T. atroviride* and *B. oryzae* or a negative regulator as observed in *B. cinerea* and *A. alternate*, *M. oryzae* and *C. zeae-maydis.* It still remains to be shown which other photoreceptors are responsible for regulating the formation of conidia. In *A. nidulans* it was shown that the red light photoreceptor, phytochrome, regulates the expression of the *blrA* conidiation gene. However, photoregulation of conidia has been shown to be dispensable in *F. verticilloides* and *A. fumigatus* (Bodor et al., 2013; Fuller et al., 2013).

1.6.7. Phototropism

The directional growth of fungi toward light and subsequent spore dispersal is a well described process in Zygomycota, and is important for their survival (Corrochano and Garre, 2010). The underlying molecular mechanisms involved in this process are still largely unknown. The phototropism observed in *P. blakesleeanus* involves the bending of the fruiting body, the sporangiophore, towards the light (Corrochano and Garre, 2010). This process has been proposed to be under the regulation of the MAD complex (WC complex). The expression of the individual *madA* and *madB* genes forming the complex are not induced by light (Corrochano et al., 2006). The complex is thought to be present in an inactive form in the dark and available to respond to light and activate the genes needed for phototropism (Sanz et al., 2009).

There are three copies of the *wc-1* gene present in the genome sequences of the fungal phyla Zygomycota (Silva et al., 2006). In *M. circinelloides* positive phototropism is regulated by the product of one of the *wc-1* orthologues, the *mcwc1a* gene. The disruption of the other two *wc-1* copies (*mcwc1b* and *mcwc1c*) resulted in the same phenotype as the wild type strain

(Silva et al., 2006). The strains with the mutant form of *mcwc1a* gene produced sporangiophores that grew in random orientations, showing no indication of light dependent directional growth. Positive phototropism is believed to be similar in *P. crystallinus* since the structure of the *mcwc1a* gene is the same as the identified *Pcmad1* gene, but experimental evidence is still lacking (Kubo, 2009).

1.6.8. Oxidative stress

Excessive light has been shown to cause the overproduction of reactive oxygen species (ROS) (Schmoll, 2011). The production of ROS leads to oxidative damage which in turn leads to the cell death. In *B. cinerea* the presence of the White Collar Complex (WCC) has been shown to be necessary in order for the fungus to detoxify the cell (Kuratani et al., 2010). The growth of the wild type *B. cinerea* strains and *Δbcwcl1* + *Δbcwcl2* knock-out strains grown in constant light and in the presence of an exogenous source of ROS (hydrogen peroxide) has indicated that the WCC is involved in targeting the activation of genes involved in the detoxification of ROS. A similar light response has been characterised in *A. fumigatus* (Fuller et al., 2013). A synergistic affect between the blue light photoreceptor (LreA) and the red light receptor (FpA) is needed for detoxification of the fungal cell (Fuller et al., 2013). The blue light photoreceptor, WC-1, plays a role in the detoxification of ROS in order for the fungus to cope with this environmental stress.

1.7. Plant-pathogen interactions and light perception

Fungi have been shown to be able to sense light and thus the time of day, and orientate their pathogenesis related pathways accordingly to aid in disease development. The attachment of conidia and subsequent infection of host leaves by *B. oryzae* and *M. oryzae* was shown to occur only in a dark period (Kihara et al., 2007). It is thus believed that the timing linked to the formation and release of the conidia is important for colonising the host tissue. Kihara et al. (2007) suggested that both of the above mentioned fungi use blue light to sense the optimal time period to initiate attachment of conidia and subsequent infection of the host during the dark phase. Light experiments in *M. oryzae* indicated that illumination during the early stages of rice infection with the wild type strain resulted in reduced disease

development. This light dependent disease suppression in *M. oryzae* was shown to be compromised when rice is infected with *Δmgwc1* (*wc-1*) knock-out strains (Kim et al., 2011). The knock-out strains were able to cause disease regardless of the light conditions they were subjected to. This result suggests that the WC-1 protein is important for light dependent disease suppression by inhibiting the formation of conidia in light conditions.

Blue light dependent disease development through WC-1 was shown to be dispensable in plants by *F. graminearum*, *F. verticilloides* and *F. oxysporum* (Bodor et al., 2013; Kim et al., 2013; Ruiz-Roldán et al., 2008). However, the WC-1 protein of *F. oxysporum* was shown to play a role in the virulence of the fungus in immunocompromised mice. A five-fold reduction in mortality rates of was observed in the mice infected with the *Δwc-1* knock-out strain compared to the mice infected with the wild type strains (Ruiz-Roldán et al., 2008).

The detoxification of ROS is dependent on the activation of the WC-1 protein by blue light (Fuller et al., 2013; Kuratani et al., 2010) This function of the WC-1 was shown to play a role in *B. cinerea* during the colonisation of the host plant. The WC-1 protein (BCWC1) is required for full virulence on *A. thaliana* as a host for *B. cinerea* under light grown conditions when ROS are typically produced by the host plant (Canessa et al., 2013). Furthermore, there was a light dependent reduction in lesion formation in *Phaseolus vulgaris* (French bean) plants infected with the *B. cinerea Δbcwc1* knock-out strains. The WC-1 protein is needed to detoxify ROS produced by the plants (in the form of an oxidative burst) as part of the host's immune response to the invading fungus. The ability of the fungus to colonise the host tissue is reduced as a result of the ROS produced by the plant. The host plant is known to produce elevated amounts of hydrogen peroxide when exposed to increasing light intensities (Luna et al., 2011).

The WC-1 dependent ROS detoxification mechanism was confirmed by the identification of a downstream blue light regulated gene. The light induced virulence gene, BcLTF1 was identified in *B. cinerea*, through random mutagenesis (Schumacher et al., 2014). The

expression of the BcLTF1 (*B. cinerea* light responsive transcription factor) is believed to be regulated by BcWC1 and is needed to achieve an equilibrium between the production and detoxifying of ROS by the fungus. Knock-out strains (*Δbcltf1*) showed reduced virulence on *P. vulgaris* as a host plant. This reduction in virulence is attributed to the fungus' impaired ability to detoxify the ROS generated by the host plant and thus results in a delayed colonisation (Schumacher et al., 2014).

In *C. zeae-maydis* various light dependent processes have been identified that are regulated, at least in part, by the CRP1 (WC-1) protein. Maize plants infected with *C. zeae-maydis* knock-out strains (*Δcrp1*) only exhibited chlorotic flecks, whereas the plants infected with wild type strains developed mature lesions as the disease progressed (Kim et al., 2011). The WC-1 protein is thus required to induce the necrotic phase of the disease. *Cercospora zeae-maydis Δcrp1* knock-outs lost their ability to sense the opening of the stomata in order to re-orientate their growth for subsequent plant infiltration. This was possibly due to a ten-fold reduction in the formation of appressoria. These three WC-1 light dependent processes suggest that the *C. zeae-maydis* uses this environmental cue to synchronise pathogenesis related pathways to certain light dependent processes in the host plant.

1.8. Concluding remarks

The important roles the white collar proteins play in the growth and development of fungi are conserved across species. However, the mechanism by which White Collar-1 and White Collar-2 regulate light responsive genes is not conserved in all fungal species. The examples of blue light dependent functions from the *Fusarium* species clearly showed that the genetic mechanism underlying these functions are not conserved in closely related species, which was shown by the different processes regulated by the WC-1 protein. Very little is known about the plant infection process at a molecular level of both *C. zeae-maydis* and in particular *C. zeina*. Elucidating the role WC-1 (CRP1) plays in the early stages of maize infection will aid in a better understanding of how *C. zeina* colonises the host plant tissue, which will in turn enable us to develop appropriate measures to control the disease in the field.

1.9. References

Ambra, R., Grimaldi, B., Zamboni, S., Filetici, P., Macino, G., Ballario, P., 2004. Photomorphogenesis in the hypogeous fungus *Tuber borchii:* isolation and characterization of Tbwc-1, the homologue of the blue-light photoreceptor of *Neurospora crassa*. *Fungal Genet. Biol.* **41**, 688–97.

Ávalos, J., Cerdá-olmedo, E., Reyes, F., Barrero, A.F., 2007. Gibberellins and Other Metabolites of Fusarium fujikuroi and Related Fungi. *Current Organ. Chem.* **11**, 721–37

Avalos, J., Estrada, A.F., 2010. Regulation by light in *Fusarium*. *Fungal Genet. Biol*. **47**, 930–8.

Ballario, P., Macino, G., 1997. White collar proteins: PASsing the light signal in *Neurospora crassa*. *Trends Microbiol. 5*, 458–62.

Ballario, P., Vittorioso, P., Magrelli, A., Talora, C., Cabibbo, A., Macino, G., Sapienza, L., 1996. White collar-1 , a central regulator of blue light responses in *Neurospora* , is a zinc finger protein. *EMBO J.* **15**, 1650–57.

Bluhm, B.H., Burnham, a M., Dunkle, L.D., 2010. A circadian rhythm regulating hyphal melanization in *Cercospora kikuchii*. *Mycologia*. **102**, 1221–8.

Bodor, Á.M., Stubnya, V., Ádám, a. L., Láday, M., Hornok, L., 2013. The white collar complex is essential for sexual reproduction but dispensable for conidiation and invasive growth in *Fusarium verticillioides*. *Acta Phytopathol. Entomol. Hungarica. 48*, 1–18.

Brown, D.W., Dyer, R.B., McCormick, S.P., Kendra, D.F., Plattner, R.D., 2004. Functional demarcation of the *Fusarium* core trichothecene gene cluster. *Fungal Genet. Biol.* **41**, 454–62.

Butler, M.J., Day, A.W., 2011. Fungal melanins: a review.*Canadian Journ. of Micro*. **44**, 1115-36.

Canessa, P., Schumacher, J., Hevia, M. a, Tudzynski, P., Larrondo, L.F., 2013. Assessing the effects of light on differentiation and virulence of the plant pathogen *Botrytis cinerea*: characterization of the White Collar Complex. *PLoS One. 8*, e84223.

Casas-Flores, S., Rios-Momberg, M., Bibbins, M., Ponce-Noyola, P., Herrera-Estrella, A., 2004. BLR-1 and BLR-2, key regulatory elements of photoconidiation and mycelial growth in *Trichoderma atroviride*. *Microbiology.* **150**, 3561–9.

Castro-Longoria, E., Ferry, M., Bartnicki-Garcia, S., Hasty, J., Brody, S., 2010. Circadian rhythms in *Neurospora crassa*: dynamics of the clock component frequency visualized using a fluorescent reporter. *Fungal Genet. Biol.* **47**, 332–41.

Chen, H., Lee, M.-H., Daub, M.E., Chung, K.-R., 2007. Molecular analysis of the cercosporin biosynthetic gene cluster in *Cercospora nicotianae*. *Mol. Microbiol.* **64**, 755–70.

Cheng, P., He, Q., Yang, Y., Wang, L., Liu, Y., 2003. Functional conservation of light, oxygen, or voltage domains in light sensing. *Proc. Natl. Acad. Sci. U.S.A*. **100**, 5938–43.

Cheng, P., Yang, Y., Liu, Y., 2001. Interlocked feedback loops contribute to the robustness of the *Neurospora circadian* clock. *Proc. Natl. Acad. Sci. U.S.A*. **98**, 7408–13.

Cheng, P., Yang, Y., Wang, L., He, Q., Liu, Y., 2003. White Collar-1, a multifunctional *Neurospora* protein Involved in the circadian feedback loops, light sensing, and transcription repression of wc-2. J. *Biol. Chem.* **278**, 3801-08.

Choquer, M., Dekkers, K.L., Chen, H., Cao, L., Ueng, P.P., Daub, M.E., Chung, K., 2005. The *ctb1* gene encoding a fungal polyketide synthase is required for cercosporin biosynthesis and fungal virulence of *Cercospora nicotianae. Mol. Plant Microbe Interact.* **18**, 468–76.

Corrochano, L.M., Garre, V., 2010. Photobiology in the Zygomycota: multiple photoreceptor genes for complex responses to light. *Fungal Genet. Bio*l. **47**, 893–9.

Corrochano, L.M., Sanz, C., Iturriaga, E.A., Idnurm, A., Rodrı, J., Eslava, A.P., Heitman, J., 2006. The Phycomyces madA gene encodes a blue-light photoreceptor for phototropism and other light responses. *Proc. Natl. Acad. Sci. U.S.A.* **103**, 4546-51.

Crosthwaite, S.K., Loros, J.J., Dunlap, J.C., 1995. Light-induced resetting of a circadian clock is mediated by a rapid increase in frequency transcript. *Cell.* **81**, 1003–12.

Dunkle, L.D., Levy, M., 2000. Genetic Relatedness of African and United States Populations of *Cercospora zeae-maydis. Phytopathology.* **90**, 486–90.

Dunlap, J.C., Loros, J.J., 2006. How fungi keep time: circadian system in *Neurospora* and other fungi. *Curr. Opin. Microbiol.* **9**, 579–87.

Edgar, R.C., 2004. MUSCLE: multiple sequence alignment with high accuracy and high throughput. *Nucleic Acids Res*. **32**, 1792–7.

Eisenman, H.C., Casadevall, A., 2012. Synthesis and assembly of fungal melanin. *Appl. Microbiol. Biotechnol.* **93**, 931–40.

Esquivel-Naranjo, E.U., Herrera-Estrella, A, 2007. Enhanced responsiveness and sensitivity to blue light by *blr-2* overexpression in *Trichoderma atroviride*. *Microbiology*. **153**, 3909–22.

Estrada, A.F., Avalos, J., 2008. The White Collar protein WcoA of *Fusarium fujikuroi* is not essential for photocarotenogenesis, but is involved in the regulation of secondary metabolism and conidiation. *Fungal Genet. Biol.* **45**, 705–18.

Froehlich, A.C., Liu, Y., Loros, J.J., Dunlap, J.C., 2002. White Collar-1, a circadian blue light photoreceptor, binding to the frequency promoter. *Science*. **297**, 815–9.

Froehlich, A.C., Noh, B., Vierstra, R.D., Loros, J., Dunlap, J.C., 2005. Genetic and molecular analysis of phytochromes from the filamentous fungus *Neurospora crassa*. *Eukaryot. Cell.* **4**, 2140–52.

Fuller, K.K., Ringelberg, C.S., Loros, J.J., Dunlap, C., 2013. The fungal pathogen *Aspergillus fumigatus* regulates growth , metabolism , and stress resistance in response to light. *mBio.* **4**, 11–13.

Gevers, H., Lake, J., Hohls, T., 1994. Diallel cross analysis of resistance to gray leaf spot in maize. *Plant Dis.* **78**, 379-83.

He, Q., Cheng, P., Yang, Y., Wang, L., Gardner, K.H., Liu, Y., 2002. White collar-1, a DNA binding transcription factor and a light sensor. *Science*. **297**, 840–3.

Herrera-Estrella, A., Horwitz, B. a, 2007. Looking through the eyes of fungi: molecular genetics of photoreception. *Mol. Microbiol*. **64**, 5–15.

Idnurm, A., Heitman, J., 2005. Light controls growth and development via a conserved pathway in the fungal kingdom. *PLoS Biol*. **3**, e95.

Idnurm, A., Heitman, J., 2010. Ferrochelatase is a conserved downstream target of the blue light-sensing White collar complex in fungi. *Microbiology*. **156**, 2393–407.

Kihara, J., Moriwaki, A., Ito, M., Arase, S., Honda, Y., 2004a. Expression of THR1, a 1,3,8-Trihydroxynaphthalene reductase gene involved in melanin biosynthesis in the phytopathogenic fungus *Bipolaris oryzae*, is enhanced by near-ultraviolet radiation. *Pigment Cell Res.* **17**, 15–23.

Kihara, J., Moriwaki, A., Tanaka, N., Ueno, M., Arase, S., 2007. Characterization of the BLR1 gene encoding a putative blue-light regulator in the phytopathogenic fungus *Bipolaris oryzae*. *FEMS Microbiol. Lett.* **266**, 110–8.

Kihara, J., Moriwaki, A., Ueno, M., Tokunaga, T., Arase, S., Honda, Y., 2004b. Cloning, functional analysis and expression of a scytalone dehydratase gene (*scd1*) involved in melanin biosynthesis of the phytopathogenic fungus *Bipolaris oryzae*. *Curr. Genet*. **45**, 197–204.

Kihara, J., Sato, A., Okajima, S., Kumagai, T., 2001. Molecular cloning, sequence analysis and expression of a novel gene induced by near-UV light in *Bipolaris oryzae*. *Mol. Genet. Genomics.* **266**, 64–71.

Kim, H., Ridenour, J.B., Dunkle, L.D., Bluhm, B.H., 2011. Regulation of stomatal tropism and infection by light in *Cercospora zeae-maydis*: evidence for coordinated host/pathogen responses to photoperiod? *PLoS Pathog*. **7**, e1002113.

Kim, H., Son, H., Lee, Y.-W., 2013. Effects of light on secondary metabolism and fungal development of *Fusarium graminearum. J. Appl. Microbiol.* **116**, 380-9.

Kim, S., Singh, P., Park, J., Park, S., Friedman, A., Zheng, T., Lee, Y.H., Lee, K., 2011. Genetic and molecular characterization of a blue light photoreceptor MGWC-1 in *Magnaporthe oryzae*. *Fungal Genet. Biol.* **48**, 400–7.

Kimura, N., Tsuge, T., 1993. Gene cluster involved in melanin biosynthesis of the filamentous fungus *Alternaria alternata*. *J. Bacteriol.* **175**, 4427–35.

Krauss, U., Minh, B.Q., Losi, A., Gärtner, W., Eggert, T., von Haeseler, A., Jaeger, K.E., 2009. Distribution and phylogeny of light-oxygen-voltage-blue-light-signaling proteins in the three kingdoms of life. *J. Bacteriol*. **191**, 7234–42.

Kubo, H., 2009. Isolation of madA homologs in *Pilobolus crystallinus*. *Mycoscience*. **50**, 400–6.

Kuratani, M., Tanaka, K., Terashima, K., Muraguchi, H., Nakazawa, T., Nakahori, K., Kamada, T., 2010. The *dst2* gene essential for photomorphogenesis of *Coprinopsis cinerea* encodes a protein with a putative FAD-binding-4 domain. *Fungal Genet. Biol.* **47**, 152–8.

Langfelder, K., Streibel, M., Jahn, B., 2003. Biosynthesis of fungal melanins and their importance for human pathogenic fungi. *Fungal Genet. Biol.* **38**, 143-58.

Lewis, Z. a., Correa, a., Schwerdtfeger, C., Link, K.L., Xie, X., Gomer, R.H., Thomas, T., Ebbole, D.J., Bell-Pedersen, D., 2002. Overexpression of White Collar-1 (WC-1) activates circadian clock-associated genes, but is not sufficient to induce most light-regulated gene expression in *Neurospora crassa*. *Mol. Microbiol.* **45**, 917–31.

Linden, H., 1997. Blue Light Regulation in *Neurospora crassa. Fungal Genet. Biol.* **22**, 141–50.

Linden, H., Macino, G., 1997. White collar 2 , a partner in blue-light signal transduction , controlling expression of light-regulated genes in *Neurospora crassa. EMBO J.* **16**, 98–109.

Linnemannstöns, P., Prado, M.M., Fernández-Martín, R., Tudzynski, B., Avalos, J., 2002. A carotenoid biosynthesis gene cluster in *Fusarium fujikuroi*: the genes carB and carRA. *Mol. Genet. Genomics*. **267**, 593–602.

Liu, K.J., Xu, X.-D., 2013. First report of gray leaf spot of maize caused by *Cercospora zeina* in China. *Plant Dis*. **97**, 1656–1656.

Liversage, J., 2012. Functional characterisation of the *Cercospora zeina crp1* gene as a putative pathogensis regulation factor. Unpublished BSc (Hons) Dissertation, University of Pretoria.

Lu, Y.K., Sun, K.H., Shen, W.-C., 2005. Blue light negatively regulates the sexual filamentation via the Cwc1 and Cwc2 proteins in *Cryptococcus neoformans*. *Mol. Microbiol.* **56**, 480–91.

Luna, E., Pastor, V., Robert, J., Flors, V., Mauch-Mani, B., Ton, J., 2011. Callose deposition: a multifaceted plant defense response. *Mol. Plant. Microbe. Interact.* **24**, 183–93.

Lynch, F.J., Geoghegan, M.J., 1979. Regulation of growth and cercosporin photo-induction in *Cercospora beticola*. *Trans. Br. Mycol. Soc.* **73**, 311–327.

Macino, H.L.M.R.G., 1997. Mutants of *Neurospora crassa* defective in regulation of blue light perception. *Mol. Gen. Genet*. **26**, 111–8.

Malz, S., Grell, M.N., Thrane, C., Maier, F.J., Rosager, P., Felk, A., Albertsen, K.S., Salomon, S., Bohn, L., Schäfer, W., Giese, H., 2005. Identification of a gene cluster responsible for the biosynthesis of aurofusarin in the *Fusarium graminearum* species complex. *Fungal Genet. Biol.* **42**, 420–33.

Malzahn, E., Ciprianidis, S., Káldi, K., Schafmeier, T., Brunner, M., 2010. Photoadaptation in *Neurospora* by competitive interaction of activating and inhibitory LOV domains. *Cell*. **142**, 762–72.

Meisel, B., Korsman, J., Kloppers, F.J., Berger, D.K., 2009. *Cercospora zeina* is the causal agent of grey leaf spot disease of maize in southern Africa. *Eur. J. Plant Pathol.* **124**, 577–583. doi:10.1007/s10658-009-9443-1

Ohm, R. a, Aerts, D., Wösten, H. a B., Lugones, L.G., 2013. The blue light receptor complex WC-1/2 of *Schizophyllum commune* is involved in mushroom formation and protection against phototoxicity. *Environ. Microbiol.* **15**, 943–55.

Olmedo, M., 2010. A role in the regulation of transcription by light for RCO-1 and RCM-1, the *Neurospora* homologs of the yeast Tup1–Ssn6 repressor. *Fungal Genet. Biol.* **47,** 939-52.

Olmedo, M., Ruger-Herreros, C., Luque, E.M., Corrochano, L.M., 2013. Regulation of transcription by light in *Neurospora crassa*: A model for fungal photobiology? *Fungal Biol. Rev.* **27**, 10–18.

Peter, E., Dick, B., Baeurle, S.A., 2012. Illuminating the early signaling pathway of a fungal light-oxygen-voltage photoreceptor. *Proteins.* **80**, 471–81.

Pruss, S., Fetzner, R., Seither, K., Herr, A., Pfeiffer, E., Metzler, M., Lawrence, C.B., Fischer, R., 2014. Role of the Alternaria alternata blue-light receptor LreA (white-collar 1) in spore formation and secondary metabolism. *Appl. Environ. Microbiol.* **80**, 2582–91.

Pukkila-Worley, R., Gerrald, Q., Kraus, P., 2005. Transcriptional network of multiple capsule and melanin genes governed by the *Cryptococcus neoformans* cyclic AMP cascade. *Eukaryot. Cell.* **4**, 190-201.

Querfurth, C., Diernfellner, A.C.R., Gin, E., Malzahn, E., Höfer, T., Brunner, M., 2011. Circadian conformational change of the *Neurospora* clock protein FREQUENCY triggered by clustered hyperphosphorylation of a basic domain. *Mol. Cell.* **43**, 713–22.

Röhrig, J., Kastner, C., Fischer, R., 2013. Light inhibits spore germination through phytochrome in *Aspergillus nidulans*. *Curr. Genet.* **59**, 55–62.

Ruger-Herreros, C., Rodríguez-Romero, J., Fernández-Barranco, R., Olmedo, M., Fischer, R., Corrochano, L.M., Canovas, D., 2011. Regulation of conidiation by light in *Aspergillus nidulans*. *Genetics*. **188**, 809–22.

Ruiz-Roldán, M.C., Garre, V., Guarro, J., Mariné, M., Roncero, M.I.G., 2008. Role of the white collar 1 photoreceptor in carotenogenesis, UV resistance, hydrophobicity, and virulence of *Fusarium oxysporum*. *Eukaryot. Cell.* **7**, 1227–30.

Salichos, L., Rokas, a., 2009. The diversity and evolution of circadian clock proteins in fungi. *Mycologia*. **102**, 269–278.

Salomon, M., Lempert, U., Rüdiger, W., 2004. Dimerization of the plant photoreceptor phototropin is probably mediated by the LOV1 domain. *FEBS Lett*. **572**, 8–10.

Sancar, G., Sancar, C., Brügger, B., 2011. A global circadian repressor controls antiphasic expression of metabolic genes in *Neurospora*. *Mol. Cell.* **44**, 684-97.

Sano, H., Kaneko, S., Sakamoto, Y., Sato, T., Shishido, K., 2009. The basidiomycetous mushroom *Lentinula edodes* white collar-2 homolog PHRB, a partner of putative blue-light photoreceptor PHRA, binds to a specific site in the promoter region of the *L. edodes* tyrosinase gene. *Fungal Genet. Biol.* **46**, 333–41.

Sano, H., Narikiyo, T., Kaneko, S., 2007. Sequence analysis and expression of a blue-light photoreceptor gene, Le. phrA from the basidiomycetous mushroom *Lentinula edodes*. *Biosci. Biotechnol. Biochem.* **71**, 2206-13.

Sanz, C., Rodríguez-romero, J., Idnurm, A., Christie, J.M., Heitman, J., Corrochano, L.M., Eslava, A.P., 2009. Phycomyces MADB interacts with MADA to form the primary photoreceptor complex for fungal phototropism. *Proc. Natl. Acad. Sci. U.S.A.* **106**, 7095-100.

Sargent, M.L., Briggs, W.R., 1967. The effects of light on a circadian rhythm of conidiation in *Neurospora*. *Plant Physiol.* **42**, 1504–10.

Schafmeier, T., Diernfellner, A.C.R., 2011. Light input and processing in the circadian clock of *Neurospora*. *FEBS Lett.* **585**, 1467–73.

Schafmeier, T., Haase, A., Káldi, K., Scholz, J., Fuchs, M., Brunner, M., 2005. Transcriptional feedback of *Neurospora* circadian clock gene by phosphorylation-dependent inactivation of its transcription factor. *Cell.* **122**, 235–46.

Schmidhauser, T., Lauter, F., 1990. Cloning, sequence, and photoregulation of al-1, a carotenoid biosynthetic gene of *Neurospora crassa*. *Mol. Cell.* **10**, 5064-70.

Schmidhauser, T., Lauter, F., 1994. Characterization of al-2, the phytoene synthase gene of *Neurospora crassa*. Cloning, sequence analysis, and photoregulation. *J. Biol. Chem.* **22**, 12060-6.

Schmoll, M., 2011. Assessing the relevance of light for fungi: Implications and insights into the network of signal transmission. *Adv. Appl. Microbiol*. **76**, 27–78.

Schumacher, J., Simon, A., Cohrs, K.C., Viaud, M., Tudzynski, P., 2014. The transcription factor BcLTF1 regulates virulence and light responses in the necrotrophic plant pathogen *Botrytis cinerea*. *PLoS Genet.* **10**, e1004040.

Silva, F., Torres-Martínez, S., Garre, V., 2006. Distinct white collar-1 genes control specific light responses in *Mucor circinelloides*. *Mol. Microbiol.* **61**, 1023–37.

Tehon, L.R., Daniels, E., 1925. Notes on the parasitic fungi of Illinois: II. *Mycologia.* **17**, 240–49.

Terashima, K., Yuki, K., Muraguchi, H., Akiyama, M., Kamada, T., 2005. The *dst1* gene involved in mushroom photomorphogenesis of *Coprinus cinereus* encodes a putative photoreceptor for blue light. *Genetics.* **171**, 101–8.

Tudzynski, B., Hölter, K., 1998. Gibberellin biosynthetic pathway in *Gibberella fujikuroi*: evidence for a gene cluster. *Fungal Genet. Biol*. **25**, 157–70.

Wang, J., Levy, M., Dunkle, L.D., 1998. Sibling species of *Cercospora* associated with gray leaf spot of maize. *Phytopathology.* **88**, 1269–75.

Ward, J.M.J., Laing, M.D., Nowelf, D.C., 1997. Chemical control of maize grey leaf spot. *Crop. Protec.* **16**, 265–71.

Ward, J.M.J., Stromberg, E.L., Nowell, D.C., 1999. Gray leaf spot: A disease of global importance in maize production. *Plant Disease.* **83**, 884-95.

Wiemann, P., Willmann, A., Straeten, M., Kleigrewe, K., Beyer, M., Humpf, H.-U., Tudzynski, B., 2009. Biosynthesis of the red pigment bikaverin in *Fusarium fujikuroi*: genes, their function and regulation. *Mol. Microbiol.* **72**, 931–46.

Yang, T., Xiong, W., Dong, C., 2014. Cloning and analysis of the *oswc-1* gene encoding a putative blue light photoreceptor from *Ophiocordyceps sinensis*. *Mycoscience.* **55**, 241–45.

Zhang, Y., 2008. I-TASSER server for protein 3D structure prediction. *BMC Bioinformatics*. **9**, 40.

Bioinformatics

Chapter 2

Evolutionary relationships and conservation of photoreceptors and clock proteins in *Cercospora zeina* and *Cercospora zeae-maydis*

2.1. Abstract

Blue light photoreception in fungal and plant species plays a central role in the entrainment of the circadian clock and regulates growth and development of these organisms for enhanced fitness in varying environments. The White Collar 1 (WC-1) protein, first identified and characterised in *Neurospora crassa*, lead to the identification of these blue light photoreceptors in other fungal species. In this study, a local database containing homologous WC-1 protein sequences was constructed based on literature reports. The evolutionary relationships between the WC-1 orthologues across three fungal phyla were analysed using a Maximum likelihood approach in Mega6. The phylogeny of LOV domains, the sensory domains in blue light receptors, was studied across plant, bacterial and fungal species, which suggested independent convergent evolution of fungal LOV domains to regulate similar functions to that of plant LOV domains. The interconnected feedback loops of the circadian oscillator in *N. crassa* are based on the function of WC-1, WC-2 and the negative regulator, Frequency (FRQ). This FRQ/WC oscillator is conserved in and between the *Cercospora* species causing grey leaf spot (GLS) in maize. Three known classes of cryptochromes, a putative alternative blue light receptor protein family, are present in the genome sequences of *Cercospora zeina* and *Cercospora zeae-maydis*. The photolyase type cryptochromes, 6-4 photolyase and cyclobutane-pyrimidine-dimer class I photolyase (CPDI), have been previously characterised in *C. zeae-maydis*. This study provides the first report of the CRY-DASH cryptochrome in *Cercospora* species, which remains to be functionally characterised and its role elucidated in the circadian clock. A molecular model for the interaction between the circadian oscillator and blue light photoreceptors in *C. zeina* is proposed based on the conservation of these role players in literature.

2.2. Introduction

All living organisms have an internal clock that is entrained by external stimuli, which is referred to as a circadian clock. Organisms use their circadian clocks to sense changes in their environment and to interact with their surroundings. Light acts as an important external environmental signal, which is able to regulate fungal growth and development. Furthermore, light is responsible for the entrainment of the circadian oscillator that ensures a phase relationship is generated between the oscillator and the external environment. Entrainment ensures that certain biological pathways are activated at the time of day when they are of the highest adaptive advantage to the organism.

2.2.1. Fungal circadian oscillator.

The circadian oscillator of *Neurospora crassa*, which has been extensively studied, has three core proteins that regulates a complex network of light dependent transcriptional and translational feedback loops (Loros and Dunlap, 2003). The White Collar-1 (WC-1) and White Collar-2 (WC-2) proteins form the White Collar Complex (WCC), which is localised in the nucleus (He et al., 2002; Linden and Macino, 1997). The WCC is a transcription factor that activates the transcription of light responsive genes, in particular the expression of its negative regulator, frequency (*frq*) (Froehlich et al., 2002; He et al., 2002). These core proteins in the oscillator are regulated by post-transcriptional and post-translational modifications. The phosphorylation status of the WCC influences its affinity to the promoter regions of the *frq* gene. In turn, the FRQ protein interacts with the FRQ-interacting RNA helicase (FRH) in the nucleus (Cheng et al., 2001). The FRQ-FRH complex (FFC) inhibits the functioning of the WCC by increasing its phosphorylation status. The FRQ protein is also progressively phosphorylated, which labels it for degradation through binding of the FWD-1 protein (Cheng et al., 2003; He et al., 2003). The FWD-1 protein is an F-box SCF-type ubiquitin ligase complex that labels proteins for degradation by the proteome system (He et al., 2003). As the level of the FRQ protein decreases the inhibition of the WCC is lifted, which results in the circadian clock being reset.

2.2.2. Domain architecture of White Collar-1. The WC-1 protein consists of four functional domains (He et al., 2002). The first functional domain found close to the N-terminal is the PAS_A domain followed by PAS_B, PAS_C and a C-terminal Zinc-Finger (ZnF). The N-terminal functional domain forms part of a special sensory PAS subclass called Light-Oxygen-Light (LOV domain) (Cheng et al., 2003). The most important functional domain of WC-1 is the LOV domain, which is present in most, but not all, sensory proteins from bacteria, animals and plants. Signal transduction occurs through the N-terminal PAS (LOV) domain, whereas the other two PAS domains play a role in forming protein complexes with the other clock associated proteins. The WC-1 protein acts as a transcription factor through the C-terminal Zinc finger (Cheng et al., 2003).

2.2.3. PAS domain evolution. The evolution of PAS domains in eukaryotic genes has been described by Mei and Dvornyk (2014). Briefly, these PAS domains are present in all signal proteins that generally function as a sensor for a diverse range of environmental stimuli. Based on phylogenetic inference, proteins containing a PAS protein are clustered into two main groups. The proteins in the one cluster play a role in protein-protein interactions (PAS domains), whereas the proteins in the other cluster are more light/sensor (LOV domain) related proteins, and include plant and fungal blue light sensory proteins (Mei and Dvornyk, 2014).

2.2.4. Phototropin movement LOV proteins. The photo movements of all green and flowering plants, which includes green algae, are regulated by blue light receptors called phototropins (phot). Phototropins were first characterised in *Arabidopsis thaliana* (Briggs and Christie, 2002). Two N-terminal LOV domains and a single serine/threonine kinase C-terminal end are present in phototropins. The two LOV domains are each able to form a non-covalent interaction with the co-factor FMN upon exposure to blue light. Activation of the phototropins leads to a conformational change, which enhances the kinase activity of the protein. The first N-terminal LOV domain (LOV1) plays no role in signal transduction but acts as a dimerization domain (Salomon et al., 2004). The dimerization domains are necessary to form a heterodimer consisting of phot1 and phot2 (Nakasako et al., 2008). This interaction is

similar to the heterodimer that forms between the WC-1 and WC-2 proteins through their individual PAS domains. The exact function of LOV1, however is still not characterised and thus the biological role remains unknown (Demarsy and Fankhauser, 2009). The other phototropin LOV domain (LOV2) is essential in signal transduction upon blue light activation (Christie, 2007). In the dark the LOV2 domain interacts with the linker region between LOV1 and LOV2. Blue light activates the phototropin and allows the LOV2 domains to dissociate from the linker region in order to regulate the activity of the C-terminal kinase (Kong et al., 2007). Stomatal opening is regulated through the phosphorylation of four sites in the linker region upon blue light exposure (Christie, 2007). Blue light-dependent functions, other than stomatal opening, include phototropism, chloroplast relocation and photo morphogenesis (Christie, 2007).

2.2.5. Plant circadian Zeitlupe proteins.

All terrestrial plants contain another blue light photoreceptor that contains a functional LOV domain. Zeitlupe (ZTL) was found to modulate the circadian clock in *A. thaliana* (Suetsugu and Wada, 2013). The ZTL protein has an N-terminal LOV domain followed by an F-box and six Kelch repeats (Suetsugu and Wada, 2013). The LOV domain also binds the FMN chromophore in a similar manner to phototropin through the conserved cysteine residue (Imaizumi et al., 2005). The blue light-dependent responses of ZTL have been found to regulate non-reversible light responses.

Another important photo response mediated by the ZTL protein is the flowering pathway (Suetsugu and Wada, 2013). The ZTL protein functions through light dependent protein degradation. The F-box contained in ZTL is a component of the SCF-type ubiquitin E3 ligase (Yu et al., 2008). In fungi the F-box and blue light photoreceptor domains are split across two proteins, FWD-1 and WC-1, whereas in plants both are present on a single protein. The circadian clock is regulated by ZTL in plants through the degradation of key clock proteins (Lechner et al., 2006).

2.2.6. Blue light induced DNA repair. Organisms are able to use blue light to repair DNA damage caused by ultraviolet A (UV-A) light through the action of photolyases (Thompson and Sancar, 2002). Photolyases have two chromophores, the one is catalytic, which binds FAD, whereas the other one is able to harvest light using methyl tetrahydrofolate (MTHF) (Thompson and Sancar, 2002). Excitation of the flavin chromophore results in the activation of a process known as photoreactivation. Two types of photolesions are produced upon UV-A exposure: cyclobutane-pyrimidine-dimers (CPD) and 6-4 pyrimidine pyrimidine photoproducts (Sinha and Häder, 2002).

2.2.7. Alternative blue light photoreceptor. Cryptochromes, which are believed to have evolved from photolyases, are able to sense blue/UV-A light, but have reduced DNA repair capabilities (Lin and Shalitin, 2003; Selby and Sancar, 2006). These photolyase-like proteins, cryptochromes, have an N-terminal photolyase related domain (PHR) and an additional carboxy-terminal tail, cryptochrome C-terminus (CCT) (Lin and Shalitin, 2003). The C-terminal extension is involved in light signalling by acting as a repressor or as a dimerization element for interacting partners. The exact mode of action and the process behind signal transduction is not yet known.

Based on phylogenetic analysis, the cryptochrome family can be divided into five distinct classes: cyclobutane pyrimidine dimer photolyase class 1 (CPD I), CPD class II, plant cryptochrome (CRY), animal 6-4 photolyase-like cryptochrome and CRY-DASH (Drosophila, Arabidopsis, Synechocystis, Homo) (Daiyasu et al., 2004; Kim et al., 2014). The CRY-DASH class first described in 2003, has no C-terminal extension and only binds single stranded DNA and RNA (Brudler et al., 2003). Cryptochromes have been shown to play a role in the entrainment of the circadian clock (Thompson and Sancar, 2002). In *A. thaliana*, three cryptochromes were identified. *Cry1* and *cry2* are required for circadian clock entrainment, whereas *cry3* showed photolyase activity specific to single stranded DNA (Kleine et al., 2003). *Drosophila* cryptochromes exhibited a similar response to *A. thaliana* by resetting the circadian clock by mediating the degradation of a key clock protein, timeless (TIM) (Brudler et al., 2003). Overall, cryptochromes have been found to play a role in the growth and development of the

organisms possibly through controlling daily and physiological rhythms by regulating the circadian clock.

2.2.8. *Cercospora zeina* and *Cercospora zeae-maydis* blue light perception.

Grey leaf spot on maize was believed to be caused by a single *Cercospora* species, *Cercospora zeae-maydis* (Wang et al., 1998). It is now clear that GLS on maize in Africa is caused by *C. zeina,* whereas the predominant species in USA is *C. zeae-maydis* (Meisel et al., 2009). These two *Cercospora* species are separated based on genotypic differences (Crous et al., 2006). It would be interesting to discover how these two *Cercospora* species differ at a molecular level and still be able to cause the same disease, which at a phenotypic level is indistinguishable. Molecular research thus far has only focused on *Cercospora zeae-maydis*. The White Collar-1 orthologue was identified and characterised in *C. zeae-maydis* and found to play an important role in pathogenesis through regulating stomatal tropism (Kim et al., 2011). Furthermore, two cryptochrome proteins (CDP and PHL1) were identified and shown to have 6-4 photolyase activity and thus play a role in photoreactivation (Bluhm and Dunkle, 2008). In this chapter we focused on the identification of WC-1 and related clock proteins in both *Cercospora* species as well as the identification of other putative photoreceptors. The broader aim of the chapter was to determine, at a sequence level, the degree of conservation light (in particular blue light) plays in the circadian clock machinery between *C. zeina* and *C. zeae-maydis*.

2.2.9. Aims and hypotheses.

This chapter is divided into three sections. The first section focuses on the evolutionary relationship of homologous WC-1 proteins across three fungal phyla: Ascomycota, Basidiomycota and Zygomycota. In this study genes and proteins in different species are defined as being homologous to each other based on sequence similarity and domain architecture. If these genes or proteins have evolved from a common ancestor, they are defined as being orthologues and thus believed to be similar in function. We aimed to identify how diverse the WC-1 orthologues are in these fungi. The evolution of the LOV domains of blue light photoreceptors across all three Kingdoms (Plantae, Fungi and Animals) has been broadly studied by other authors. In the second section we examined the evolutionary relationship between plant and fungal LOV domains. Following the identification

of the WC-1 orthologue in *Cercospora zeina* (Liversage, 2012), we investigated whether the whole FRQ/WC-1 circadian oscillator is conserved in the *Cercospora* species causing grey leaf spot in maize. Finally, we aimed to see if the other potential blue light photoreceptor, cryptochrome, identified in *N. crassa*, which is known to regulate/influence blue light photo responses, is conserved in *C. zeina* and *C. zeae-maydis*.

2.3. Materials and Methods

2.3.1. Sequence retrieval of circadian clock proteins and photoreceptors

2.2.1.1. Homologous White Collar-1 proteins in fungi. A local database was constructed from homologous White Collar 1 (WC-1) sequences. Originally homologous WC-1 sequences were obtained by performing a protein BLAST with the characterised *Neurospora crassa* WC-1 (Q01371) as a query sequence on the UniProt database (http://www.uniprot.org/blast/). The Universal Protein Resource (UniProt) protein BLAST was performed using the fungal database as a target and an E-value threshold of 0.1 (Altschul, 1997). The expectation value (E-value) threshold is a statistical measure used to determine the number of expected matches in a random database, with the lowest E-value (closest to zero) being the most biologically significant (Altschul, 1997). Furthermore, homologous WC-1 sequences added to the local database were compared to the characterised WC-1 orthologues reported in literature from 1996 to 2014. The WC-1 sequences included in the final local WC-1 database can be seen in Table 1A and 2A in the Appendix, which is comprised of 37 Ascomycota, eleven Basidiomycota and eleven Zygomycota sequences.

2.3.1.2. Clock protein orthologues in *Cercospora zeina* and *Cercospora zeae-maydis*. The characterised circadian clock proteins of *N. crassa* described in literature were downloaded from the Uniprot database. The *N. crassa* White Collar-2 (P78714), Frequency (P19970), FWD-1 (F8MTJ4), FRH (Q873J5) and VVD (Q1K5Y8) were used as query sequences in a tBLASTn (blast protein against translated nucleotide) search against the *Cercospora zeae-maydis* v1.0 sequence using the default parameters. The *Cercospora zeae-maydis* genome sequence is contained on the Joint Genome Institute (JGI) database under MycoCosm, which is a Fungal Genomics Resource (http://genome.jgi.doe.gov). The genome sequence of *Cercospora zeae-maydis* was released in November 2011, and was produced using 454 Roche and Sanger sequencing and velvet assembly of Illumina data.

The identified scaffolds were downloaded and the gene regions predicted with the corresponding amino acid sequences using the web interface of AUGUSTUS (http://augustus.gobics.de/). The organism used as an example for the prediction of intron/exon sites was *Magnaporthe grisea*. The intron/exon boundries predicted using *M. grisea* were tested using the characterised *C. zeae-maydis* CRP1 (HQ646376) and PHL1 (EU443730.1) proteins. The domain architecture of all the protein sequences of the predicted transcripts were identified with the Simple Modular Architecture Research Tool (SMART) (http://smart.embl.de/) and compared to the mentioned *N. crassa* clock proteins. The verified sequences of the *Cercospora zeae-maydis* clock genes were used to perform a nucleotide BLAST against the draft *C. zeina* genome sequence (N.A. Olivier, unpublished). The significant hits were downloaded and annotated for later comparison to the *C. zeae-maydis* and *N. crassa* orthologues.

2.3.1.3. LOV domain containing plant and bacterial proteins**.** The phytozome database v10 (http://phytozome.net) contains the annotated genome sequences of green plants. Sequences homologous to the plant phototropin of *A. thaliana* (NP190164.1) were identified using a protein BLAST against the proteomes of selected green plants. The zeitlupe (ZTL) protein sequence of *A. thaliana* (Q9C9W9) was used to identify homologous proteins using the protein BLAST against the proteomes of selected green plants using default parameters. The *N. crassa* WC-1 protein sequence was used as a query for **a** Position-Specific BLAST (PSI-BLAST) on NCBI (http://www.ncbi.nlm.nih.gov/blast) targeting the cyanobacteria and proteobacteria organisms**.** The Position-Specific BLAST (PSI-BLAST) uses position-specific score matrices or motifs to detect weak relationships between proteins that a normal database search would miss (Altschul, 1997).

2.3.1.4. Cryptochrome orthologues in *Cercospora zeina* and *Cercospora zeae-maydis*. A collection for the cryptochrome family was downloaded. These proteins are sub-divided into five different classes and therefore representatives from each of the cryptochrome classes were downloaded from the dbCRY database (Kim et al., 2014). The cryptochrome database (dbCRY) is a central web-based platform containing collected information about

cryptochromes from various organisms, which allows the user to browse for cryptochrome representatives by class or by species. The individual photoreceptor files were used to perform a tBLASTn against the *Cercospora zeae-maydis* v1.0 on the JGI database. Regions of scaffold sequences were downloaded if the BLAST score was above 200. The resulting scaffold sequences were then analysed with AUGUSTUS as described above. The predicted protein sequences were analysed with SMART 7 to check if all the photoreceptors contained all the functional domains in the correct order observed in characterised orthologues. The final gene sequences of the identified orthologues in *C. zeae-maydis* were used to perform a BLASTn search against the draft genome of *C. zeina*.

2.3.2. Sequence analysis of circadian clock proteins and photoreceptors

2.3.2.1. Functional domain identification. The various functional domains of the homologous WC-1 proteins were identified using the SMART web resource (http://smart.embl.de/). The SMART tool contains manually curated models for over 1200 protein domains, which incorporates annotations from other protein databases (Uniprot, Ensembl and STRING). The identified protein domain regions for PAS_A (LOV domain), PAS_B, PAS_C and the Zinc finger are recorded in Table A3 and A4 in the Appendix. The identified plant phototropin and zeitlupe LOV domains are recorded in Table A5 and A6. The bacterial, cyanobacteria and proteobacteria, LOV domain representatives are recorded in Table A7. Individual domain regions were extracted and saved in their respective domain FASTA files using CLCBio Main Workbench v6.9. A graphical presentation of the proteins and their functional domains was illustrated using IBS 1.0 (Liu et al., 2014) (an illustrator for the presentation and visualisation of biological sequences).

2.3.2.2. Multiple sequence alignment. Multiple sequence alignments (MSA) were performed using the online version of MAFFT v6 (Multiple Alignment using Fast Fourier Transform) (http://mafft.cbrc.jp/alignment/software). The MAFFT alignment program is used for the rapid calculation of a multiple sequence alignment for a large dataset. The basis of this alignment program is a fast group to group alignment based on fast Fourier Transform (FFT) and an approximate distance calculation using *k*-mer approach (Ogdenw and Rosenberg,

2006; Rausch et al., 2008). The *k*-mer is a short continuous word in a subsection of a sequence. The more related sequences are to each other, the more *k*-mers they will have in common (Edgar, 2004). The specific *k*-mer size utilised by MAFFT is a reading frame of six. The MAFFT program selected for the MSA of the homologous WC-1 proteins sequences was the progressive iterative refinement method called E-INS-i. This method evaluates the consistency between a multiple and pairwise alignment. Furthermore, the iterative refinement method assumes that all the sequences have one or more conserved motifs, which are used in generating the final alignment. The default MAFFT settings were used to generate the MSA for the individual domains of the homologous WC-1 proteins, clock proteins and the other photoreceptors. The final multiple sequence alignments were manually edited to include the maximum number of reliably aligned sites for phylogenetic inference.

2.3.2.3. Conservation of amino acid residues. The evolutionary conservation of amino acid positions were calculated using Consurf (http://consurf.tau.ac.il/), which is based on the phylogenetic relationships between homologous sequences in the multiple sequence alignment. Amino acid conservation at every position is dependent on its structural and functional importance in the protein. Variable regions are evolving at a more rapid rate compared to conserved regions, which evolve at a slower rate. The multiple sequence alignment generated using MAFFT was uploaded on Consurf. The evolutionary calculation method chosen was Bayesian with the substitution method based on the Le Gascuel (2008) model. The Consurf results were analysed with UCSF Chimera 1.10.1 (Pettersen and Goddard, 2004), which is a molecular modelling system. The percent identity of all the homologous sequences was determined against *N. crassa* sequences. The graphic representation of all multiple alignments was generated using Bioedit's graphic view (Hall, 1999).

2.3.3. Phylogenetic reconstruction of WC-1, LOV domains and cryptochromes

The phylogenetic reconstruction of homologous WC-1 proteins and LOV domains were performed using protein sequences. The amino acid substitution model that best describes the evolutionary relationships among the sequences was determined using Mega6 (Tamura et al., 2013) based on the Bayesian information criterion (BIC). The model with the lowest BIC score is considered to describe the best substitution pattern. The initial tree was generated using BioNJ from PAUP*using a JTT model (Swofford, 1998). Two phylogenetic algorithms were used to construct the WC-1 and LOV domain phylogenetic trees. The first was maximum likelihood as implemented by Mega6 (Tamura et al., 2013). Bootstrap resampling, with 100 replicates for WC-1 and 1000 replicates for the LOV domain tree, were applied to estimate the statistical support for the individual nodes. The cryptochrome tree was only constructed using BioNJ in order to determine the grouping of the various putative *C. zeina* and *C. zeae-maydis* sequences into the five different classes. The three phylogenetic trees (WC-1, LOV and cryptochrome) were visualised and annotated using FigTree v 1.3.1 (http://tree.bio.ed.ac.uk/software/figtree). Only branch support greater than 70% is shown in the figures.

2.4. Results

2.4.1. Identification of homologous White Collar-1 proteins.

The White Collar Complex plays an important role in the entrainment of the circadian clock as well as the growth and development of the fungus (Olmedo et al., 2010). The WCC consists of the White Collar-1 and White Collar-2 protein (He et al., 2002; Olmedo et al., 2010). Once activated by light, the complex acts as a transcription factor for light responsive genes. The limiting component of the WCC is the WC-1 protein (Cheng et al., 2001). Absence of the WC-1 protein results in abolishment of the circadian rhythms and the transcription of various light responsive genes.

In this section we set out to identify proteins homologous to WC-1 in all three (Ascomycota, Basidiomycota and Zygomycota) of the fungal phyla and to determine how conserved the overall domain architecture is. The identification of the WC-1 orthologue, CRP1, in *Cercospora zeae-maydis* (Kim et al., 2011) led us to question whether or not this gene is conserved in the closely related sister species, *Cercospora zeina*. We have a draft genome sequence available for *C. zeina,* which was used in the identification of a homologous *crp1* gene (Liversage, 2012). Thereafter we performed a BLAST search on Uniprot using the *Neurospora crassa* WC-1 (Q01371) as a query sequence to identify fungal WC-1 homologues. The resulting hits were correlated with the homologous WC-1 sequences characterised in literature and the final selection of WC-1 sequences were made. The final WC-1 orthologue database consisted of 37 Ascomycota (including the CRP1 protein sequences from *C. zeina* and *C. zeae-maydis*), eleven Basidiomycota and eleven Zygomycota sequences (Table A1 and A2 in Appendix).

The well characterised WC-1 *N. crassa* protein consists of three PAS domains and a GATA Zinc-finger (ZnF) (Froehlich et al., 2002). The N-terminal PAS-domain is part of a sub-family called the light-oxygen and voltage (LOV) domain. The LOV domain is composed of the N-terminal PAS domains and the PAC motif. The second PAS domain, PAS-fold, consist of a PAS domain and a PAC motif, whereas the third PAS domain is not associated with a PAC motif. The PAC

motif occurs at the C-terminal end of most PAS domains and its purpose is to aid in the correct folding of the PAS domain.

Domain architecture of the WC-1 orthologues in three fungal phyla was determined. Individual domains were extracted and reported in Table A3 and Table A4 in the Appendix. A subsection of the WC-1 orthologues, representing all three phyla, were selected to visually show the results as seen in Figure 1. The Ascomycota WC-1 orthologues have all the domains in the same order as the *N. crassa* WC-1 protein, except for *Chaetomium globosum*, which lacks the GATA Zinc-finger (ZnF) as seen in Table A3.

None of Basidiomycota WC-1 orthologues have the C-terminal GATA ZnF (Table A4). The ZnF allows the protein to function as a transcription factor by binding to the DNA sequence (A/T)GATA(A/G) within the promoter regions of the light responsive genes (Corrochano, 2007). Furthermore, four of the Basidiomycota WC-1 orthologues (*Agaricus bisporus, Coprinopsis cinerea, Cryptococcus gatti* and *Schizophyllum commune*) do not have the C-terminal PAS domain (Table A4).

In the Zygomycota phylum three homologous WC-1 copies are present, whereas only a single copy is present in the other two phyla (Corrochano and Garre, 2010). The C-terminal ZnF is absent from three of the identified homologous WC-1 proteins, PcMadA2, McWc1 and RoWc1b, in *Pilobolus crystallinus*, *Mucor circinelloides* and *Rhizopus oryzae* respectively. Overall, the domain architecture of the WC-1 orthologues in the three fungal phyla are conserved based on the presence of all the functional domains in the same order as in the characterised WC-1 of *N. crassa*, with the exception being the absence of a ZnF in all the Basidiomycota and the three Zygomycota representatives.

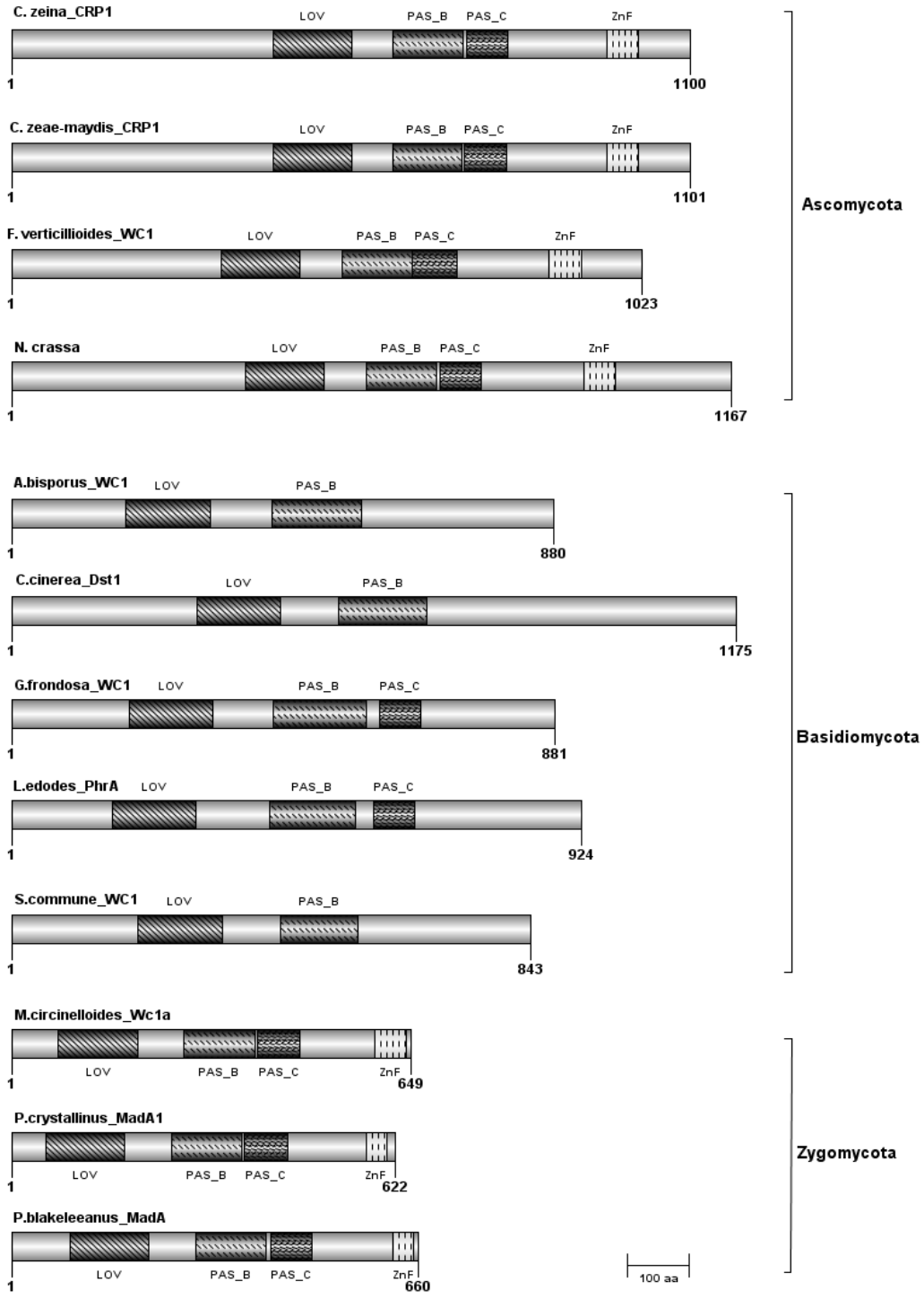

Figure 1. Domain architecture of selected homologous White Collar-1 (WC-1) proteins. The homologous WC-1 proteins in the Ascomycota and the Zygomycota phylum all have a similar domain architecture. The proteins consist of an N-terminal LOV domain followed by PAS_B and PAS_C. The transcriptional Zinc-finger is on the C-terminal end. The WC-1 orthologues of the Basidiomycota phylum have a similar architecture to the other two fungal phyla except for the absence of the transcriptional Zinc finger (ZnF). Refer to Table A1 and A2 in Appendix for names of species and sources of amino acid sequences. Domains are listed in Table A3 and A4.

2.4.2. Conservation of the WC-1 residues across the fungal phyla

The conservation of the domains within the WC-1 orthologues was analysed through sequence alignments. Conservation in this section refers to the presence of a specific functional domain within the homologous WC-1 proteins. The multiple sequence alignment of the all the homologous WC-1 proteins across the fungal phyla collected in this study is shown in Figure 2. The conservation and gap fraction plot were generated with CLCBio Main Workbench v6.9. The average percentage identity of the three phyla was calculated in comparison to the characterised *N. crassa* WC-1 protein sequence. The ten Basidiomycota WC-1 orthologues showed, on average, 23.7% identity to the *N. crassa* WC-1 protein, whereas the eleven Zygomycota homologous WC-1 proteins showed, on average, 34.2% identity. The Ascomycota WC-1 orthologues show, on average, above 40% to *N. crassa* (also an Ascomycete) identity with *C. zeina* and *C. zeae-maydis* showing 37.9% and 37.4% respectively.

The general domain architecture of the WC-1 protein is shown on top of the alignment in Figure 2 in order to explain the conservation plot. The N-terminal end of the WC-1 orthologues is highly variable. Most of the Ascomycota and Basidiomycota sequences contain at least four N-terminal low complexity regions (LCRs). In general, LCRs that fall within the N-terminal region of the protein are important if the protein has more than one interacting partner (Coletta et al., 2010). This is the case with the blue light photoreceptor, WC-1, which interacts with WC-2, VVD and FRQ (Cheng et al., 2003). The variable N-terminal allows this WC-1 protein the flexibility to change conformation for the various protein interactions. The N-terminal end of all the homologous WC-1 proteins from Zygomycota are associated with a Fus3/Kss1 family mitogen-activated protein (MAP) kinase upstream of the WC-1 functional domains (Corrochano and Garre, 2010). The LOV domain region is highly conserved across all three phyla followed by PAS_B and PAS_C.

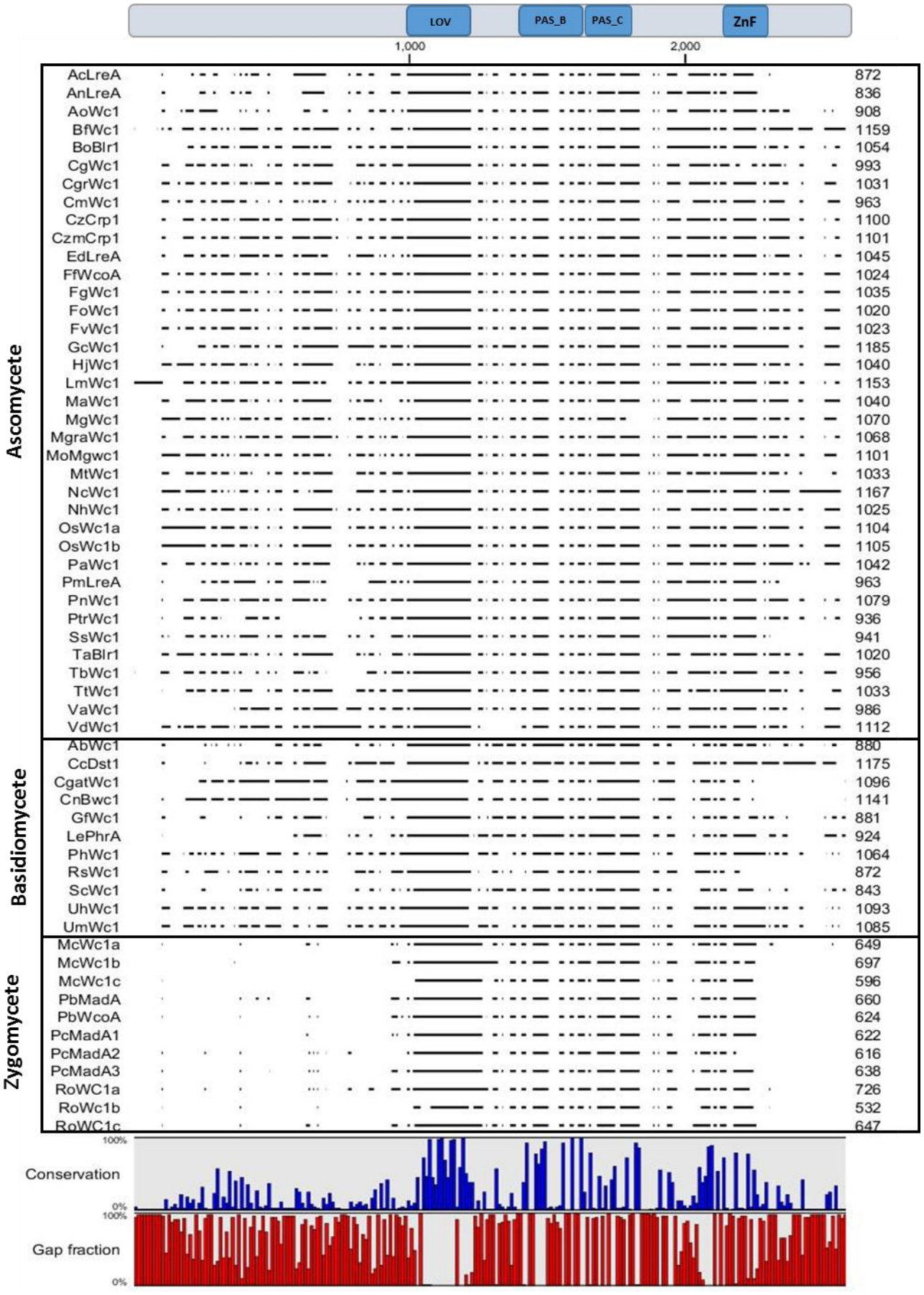

Figure 2. Alignment and conservation of homologous WC-1 proteins across three fungal phyla. The alignment of selected homologous WC-1 proteins was performed using MAFFT (www.mafft.com). Conservation graph (red) and Gap fraction were determined with CLCBio Main Workbench v6.9. The domain regions, as seen on top of the alignment, are conserved across the sequences. The WC-1 N-terminal and C- terminal ends are highly variable. Refer to Table A1 and A2 in the Appendix for names of species.

2.4.3. Phylogenetic analysis of the WC-1 orthologues.

The phylogeny of the WC-1 orthologues was generated using a Maximum likelihood approach. In total, 48 amino acid substitution models were tested. The LG model was selected with a discrete gamma distribution to model the evolutionary rates among sites (Le and Gascuel, 2008). The rate variation model also allowed for some sites (1.0045%) to be evolutionary invariable. The initial tree was generated using BioNJ from PAUP*using a JTT model (Swofford, 1998). The tree with the highest likelihood (-78135.3839) is shown in Figure 3, the value is calculated by multiplying the likelihood at each site based on the evolutionary model selected.

The homologous WC-1 sequences grouped into their separate phyla as expected (Figure 3). All the Dothideomycete WC-1 orthologues grouped together. The Ascomycota and Zygomycota WC-1 orthologues grouped more closely than the Basidiomycota phylum. The WC-1 orthologues of the Basidiomycota phylum indicate that the protein underwent an independent evolution to the other two phyla.

The *Cercospora zeina* WC-1 orthologue forms a monophyletic group with the rest of the Ascomycota sequences. All the representative species from Ascomycota and Basidiomycota had only a single copy of the WC-1 like protein. Members of the Zygomycota phylum all had three copies homologous to the WC-1 protein from *N. crassa*. The three copies grouped together with their other counterparts in the Zygomycota phyla forming three subgroups with the groups containing McWc1a and McWc1c grouping closely together and the group harbouring McWc1b grouped separately to the other two copies. The phylogenetic tree of homologous WC-1 proteins showed incongruence compared to the fungal phylum branch order, which indicates that the fungal subkingdom Dikarya forms a sister group to the early divergent Zygomygota phylum (Wang et al., 2009). The WC-1 phylogenetic tree showed that the fungal subkingdom Dikarya is split across two clusters, where the Zygomycota phyla groups closer to Ascomycota than the Basidiomycota phylum. Based on this result we speculate that WC-1 orthologues from Basidiomycota evolved independently to the other two phyla.

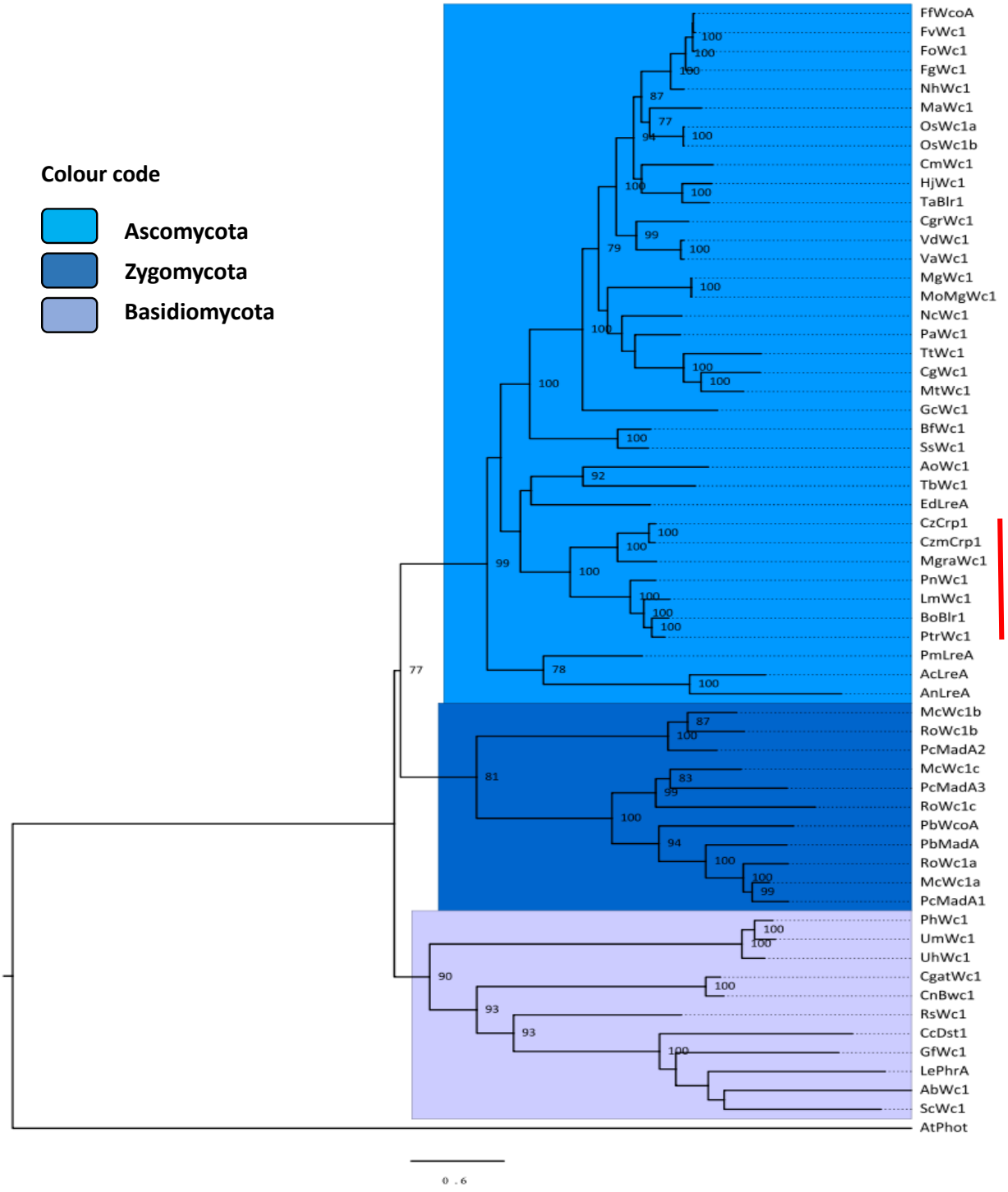

Figure 3. Alignment and conservation of homologous WC-1 proteins across three fungal phyla. The evolutionary history of the WC-1 orthologues was inferred by using the Maximum Likelihood method based on the Le Gascuel (2008) model. The tree with the highest log likelihood (-78135.3839) is shown. The percentage of trees in which the associated taxa clustered together is shown next to the branches. Initial tree(s) for the heuristic search were obtained by applying the BioNJ method to a matrix of pairwise distances estimated using a JTT model. A discrete Gamma distribution was used to model evolutionary rate differences among sites (5 categories (+G, parameter = 1.0272)). The rate variation model allowed for some sites to be evolutionarily invariable ([+I], 1.0045% sites). The analysis involved 60 amino acid sequences. There were a total of 2581 positions in the final dataset. Evolutionary analyses were conducted in MEGA6 (Tamura et al., 2013). The red bar indicates what proteins from species belonging to the Dothideomycete class of the Ascomycota phylum. Refer to Table A1 and A2 in the Appendix for names of species.

2.4.4. White Collar-1 domain analyses

The most important functional domain of the WC-1 blue light receptor is the LOV domain (Cheng et al., 2003). The WC-1 protein is activated upon binding of the flavin co-factor. In order to study conservation of the LOV domains, the identified PAS domains from all fungal WC-1 orthologues (Table A3 and A4 in Appendix) were screened for the presence of the conserved LOV domain motif, GXNCRFLQG (Krauss et al., 2009). The conserved cysteine residue is the most important residue in the motif and is indispensable to the functioning of the LOV domain since it is the photo reactive residue. A multiple sequence alignment of selected fungal LOV domains was generated through MAFFT is shown in Figure 4. The arrows in Figure 4 indicate the eleven FMN interacting residues identified in the crystal structure of a plant phototropin. Cheng et al., (2003) suggested that the LOV domain of the WC-1 protein will adopt a similar binding pattern for the FAD co-factor. Overall the LOV domain sequence is well conserved between the three fungal phyla. The most noticeable difference is the insertion of seven residues in the LOV domain of the five representatives from the Basidiomycota phylum (Figure 4).

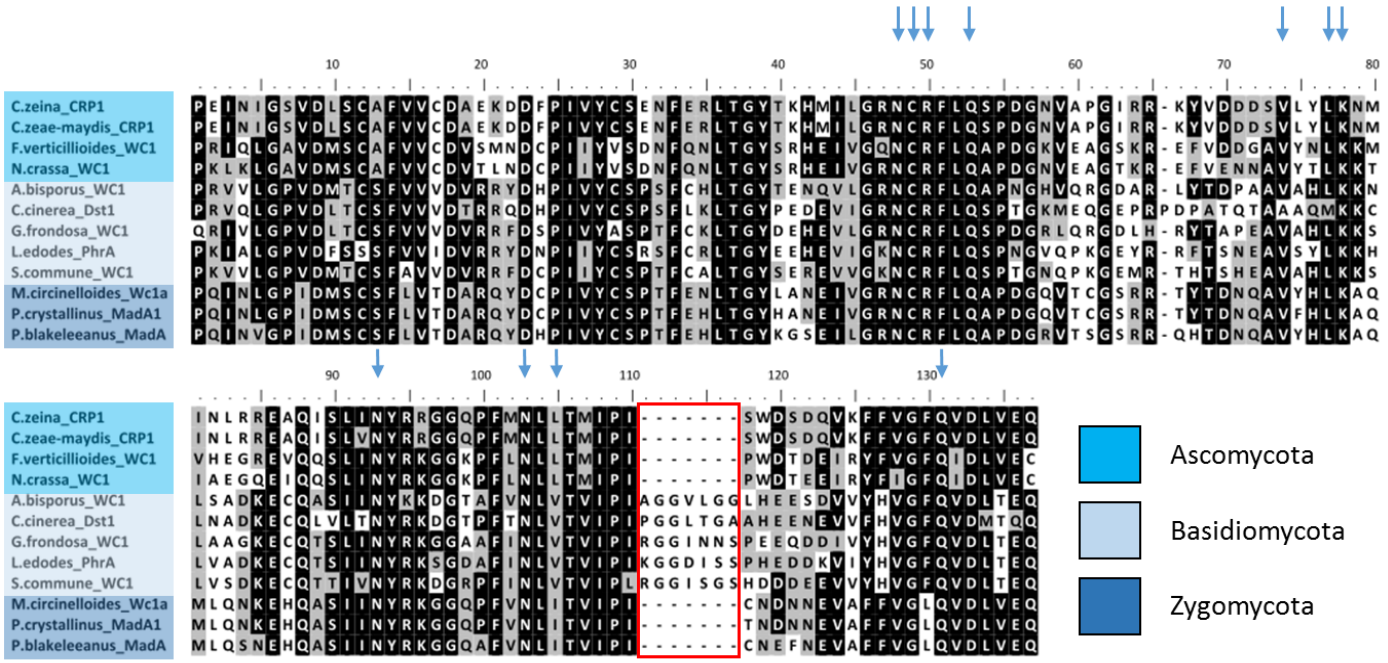

Figure 4. LOV domain alignment of selected WC-1 orthologues representing three fungal phyla. The alignment of selected WC-1 orthologues were aligned using MAFFT (www.mafft.com). The black regions represents identical conserved regions. The light grey regions represents similar amino acid residues. An insertion in the Basidiomycota orthologues is indicated by the red box. For simplicity, the first residue of each LOV domain was numbered as one. The arrows indicate the important residues for flavin binding.

The conservation of the residues in LOV domains across all twelve fungal species representing three phyla was identified by ConSurf. The conservation score ranges from 0 – 9. Conservation refers to slow evolving sites or positions within a multiple sequence alignment when reporting ConSurf results in this section. In total 40 out of the 152 sites of the LOV domains had a conservation score of 9, which means that the conserved sites are shared by all the fungal species analysed. Only 26% of the LOV domain residues are shared by all twelve the species across the three phyla (Figure 4).

The second PAS domain, PAS_B, has no known function in the literature, but the overall sequence is well conserved between the three fungal phyla as seen in Figure 5. The PAS_B domains, as with the LOV domain, consists of a PAS domain followed by a PAC motif. The PAS_B domain is referred to as the PAS-Fold. The PAC motif is present at the C-terminal end of most PAS domains, and aids in the correct folding of the PAS domain. Alignment of the PAS_B domains of selected fungi (Figure 5) again showed that the Basidiomycota WC-1 representatives were more divergent than the other two phyla, with all five Basidiomycota representatives having an insertion in the PAS_B domain of WC-1 orthologues, between residue 80 and 120.

Phylogenetic studies suggest the PAS-Fold (PAS_B) of WC-1, the PAS domain of WC-2 and the PAS domain of animal circadian genes evolved from a common ancestor (Mei and Dvornyk, 2014). Furthermore, Mei and Dvornyk (2014) showed the PAS-Fold of WC-1 is present in a cluster with other protein-protein PAS domains, which suggests that it forms a dimer with another protein. However the interacting partner is not yet known. On average the percent identity of the amino acid sequence compared to the characterised *N. crassa* PAS-fold showed that Zygomyocta representatives share 57.4% identity, whereas the Basidiomyocta share 49.7% identity between the residues. As expected the other Ascomycota species share, on average, 75.4% identical residues to the PAS-fold of *N. crassa*. Based on the conservation analysis of PAS_B by ConSurf only 18 of the 170 residues have a score of nine, which results in 10.6% of the residues being highly conserved (Figure 5).

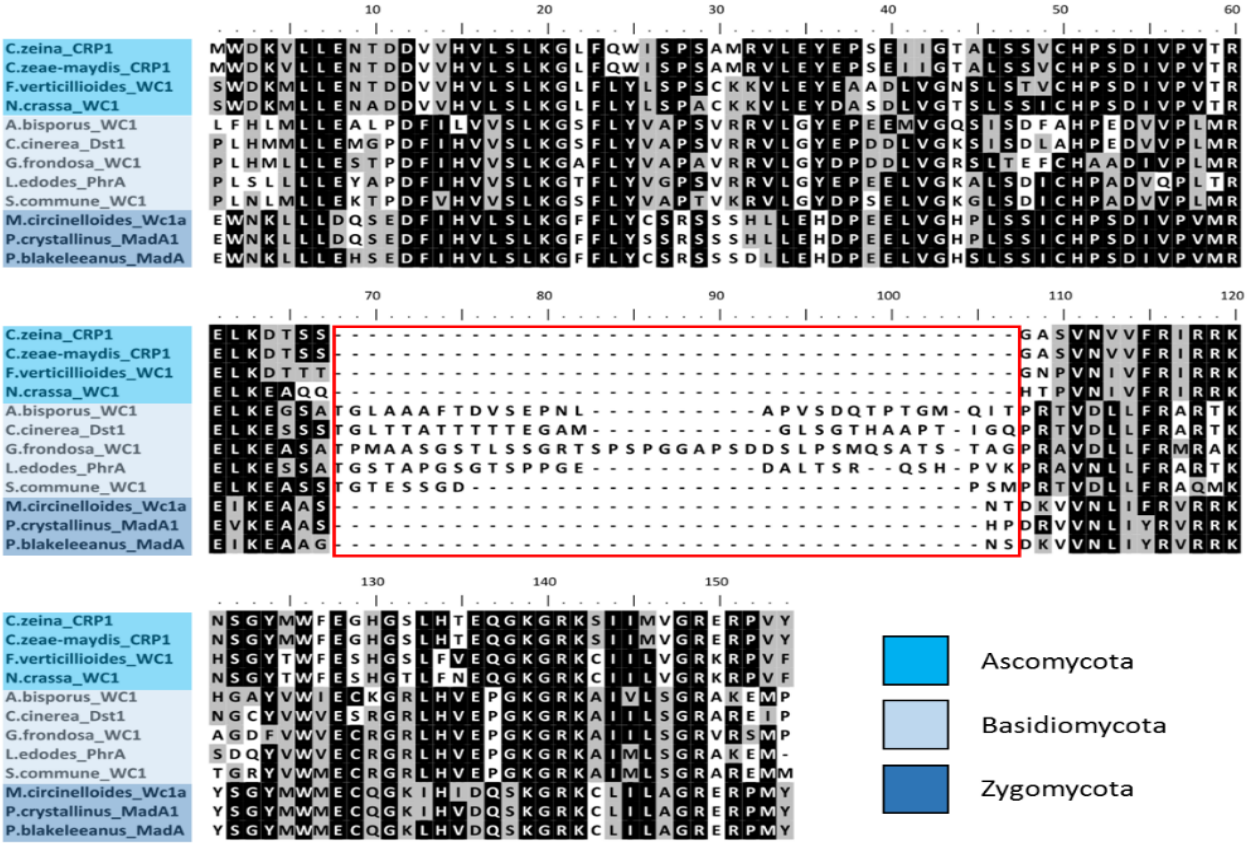

Figure 5. PAS_B domain alignment of selected homologous WC-1 proteins representing three fungal phyla. The alignment of selected homologous WC-1 proteins was performed using MAFFT (www.mafft.com). The black regions represents identical conserved regions. The light grey regions represents similar amino acid residues. An insertion is indicated by the red box in the Basidiomycota orthologues. For simplicity, the first residue of each PAS_B domain was numbered as the first residue.

The third PAS domain, PAS_C, is the most variable PAS domain in the WC-1 protein. The multiple sequence alignment of the PAS_C domain of selected fungi is shown in Figure 6. The N-terminal PAS domain of PAS_C is known to interact with the PAS domain of WC-2 to form the White Collar Complex. PAS_C domains of the Basidiomycota WC-1 orthologues were more divergent than those from the other two phyla, as was the case for the LOV and PAS_B domains. Not all the Basidiomycota species have a PAS_C domain. The two PAS_C domains of Basidiomycota WC-1 orthologues (*Grifola frondosa* and *Lentinula edodes*) have a deletion of two residues at position 15 and 16 in the multiple alignment (Figure 6). Only two of the total of 82 amino acids sites of the PAS_C domain in the multiple alignment have a conservation score of nine (Figure 6), which means that only 2.4% of the sites in PAS_C are conserved across the three fungal phyla.

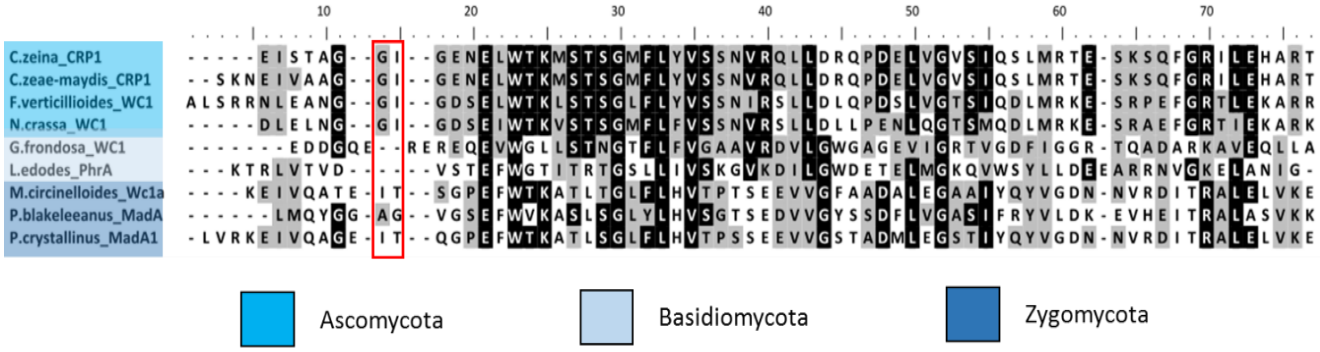

Figure 6. PAS_C domain alignment of selected homologous WC-1 proteins representing three fungal phyla. Selected PAS_C domains of homologous WC-1 proteins were aligned using MAFFT (www.mafft.com). The black regions represents identical conserved residues. The light grey regions represents similar amino acid residues. A deletion present in Basidiomycota orthologues is indicated by the red box. For simplicity, the first residue of each PAS_C domain was numbered as one.

2.4.5. Evolution of the LOV domain across Kingdoms

Putative LOV domains were identified in proteins from the bacterial and plantae kingdoms. The *N. crassa* (Q01371) WC-1 protein sequence was used as a query. The protein-protein BLAST (PSHI-BLAST) database search was targeted towards Cyanobacteria (taxid: 1117) and Proteobacteria (taxid: 1224). Only eight Cyanobacteria sequences were selected from the 122 BLAST hits, which showed a 9 – 10 % coverage of the query sequence and 37 – 42% identity. In total 100 Proteobacteria BLAST hits were obtained and only nine hits were selected, which showed a 9 -11 % coverage of the *N. crassa* WC-1 protein and 37 – 41% identity. The plant phototropin proteins contain two LOV domains. The *A. thaliana* Phot1 (AAC01753) was used as a query sequence using protein-protein BLAST (BLASTp) on the Phytozome v9.1 database targeting the genomes of species listed in Table A5. The other plant blue light receptor, Zeitlupe (ZTL), also contains a LOV domain. The orthologues of the *A. thaliana* ZTL (NP564919.1) were used as a query sequence on the Phytozome v9.1 database using BLASTp (Table A6).

The phylogeny of the LOV domains across the three kingdoms (fungi, bacteria and plants) was generated using a Maximum likelihood approach. The WAG model was selected with a discrete gamma distribution to model the evolutionary rates among sites (Whelan and

Goldman, 2001). The initial tree was generated using BioNJ from PAUP*using a JTT model. The tree with the highest likelihood (-10166.6315) is shown in Figure 7.

All the LOV domains from the three fungal phyla grouped separately to the plant and bacterial LOV domains (Figure 7). A similar branch order was observed in the fungal LOV domain phylogeny (Figure 7) as seen in the WC-1 orthologue tree in Figure 3. The LOV domains extracted from the sensory proteins of Cyanobacteria formed a sister group to the LOV domains from the Zeitlupe (ZTL) plant proteins, which are known to modulate the circadian clock. The plant phototropins have two LOV domains: the N-terminal LOV domain (LOV1) and the C-terminal LOV domain (LOV2) (Christie, 2007). The sensory proteins of the Proteobacteria contain a single LOV domain, which formed a sister group to LOV2 from plant phototropins. The LOV1 domains from phototropins group outside the LOV2/phot cluster.

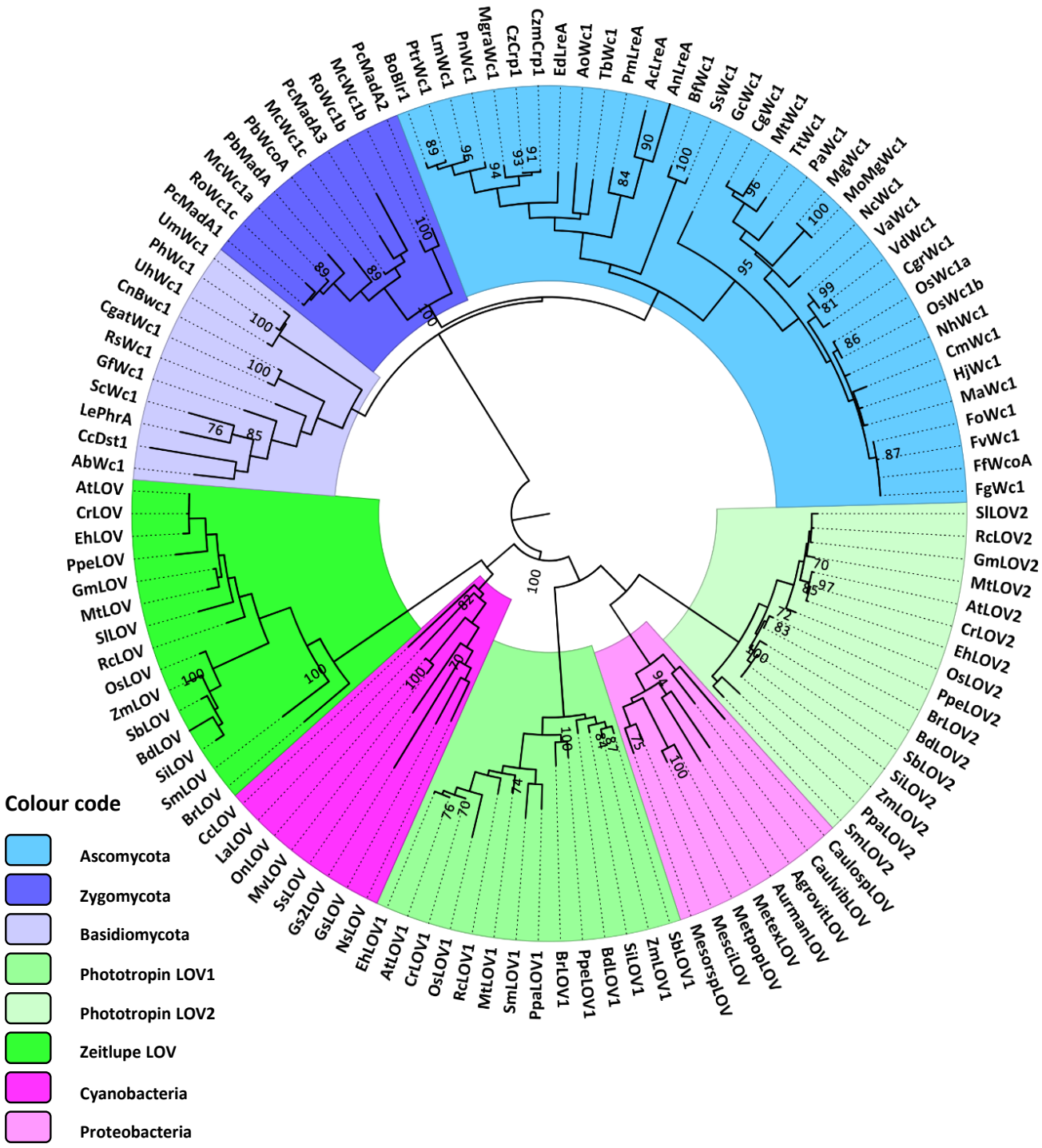

Figure 7. Molecular phylogenetic analysis of LOV domains from three Kingdoms by Maximum Likelihood method. The evolutionary history of LOV domains from plants, fungi and bacteria was inferred by using the Maximum Likelihood method based on the Whelan and Goldman model (Whelan and Goldman, 2001). The tree with the highest log likelihood (-10166.6315) is shown. The percentage of trees in which the associated taxa clustered together is shown next to the branches. Initial tree(s) for the heuristic search were obtained by applying the BioNJ method to a matrix of pairwise distances estimated using a JTT model. A discrete Gamma distribution was used to model evolutionary rate differences among sites (5 categories (+G, parameter = 0.9944)). The tree is drawn to scale, with branch lengths measured in the number of substitutions per site. The analysis involved 118 amino acid sequences. There were a total of 156 positions in the final dataset. Evolutionary analyses were conducted in MEGA6 (Tamura et al., 2013).

The multiple sequence alignment of selected LOV domains generated by MAFFT is shown in Figure 8. In total, only 17 of the 129 amino acid sites (13.2%) are highly conserved between all the selected LOV domains, which includes representatives from plant (phototropin and zeitlupe), bacterial (cyanobacteria and proteobacteria) and fungal (Ascomycota). The ZTL and fungal LOV domains have an insertion between residue 56 and 68. The Zeitlupe LOV domains have an insertion of nine residues, whereas the fungal LOV domains have insertion of eleven residues. This insertion forms a loop between the α_C and α_D helices in the secondary structure. The extended loop (of eleven residues) between the two helices is thought to enable the fungal LOV domains to accommodate the larger FAD chromophore (Cheng et al., 2003).

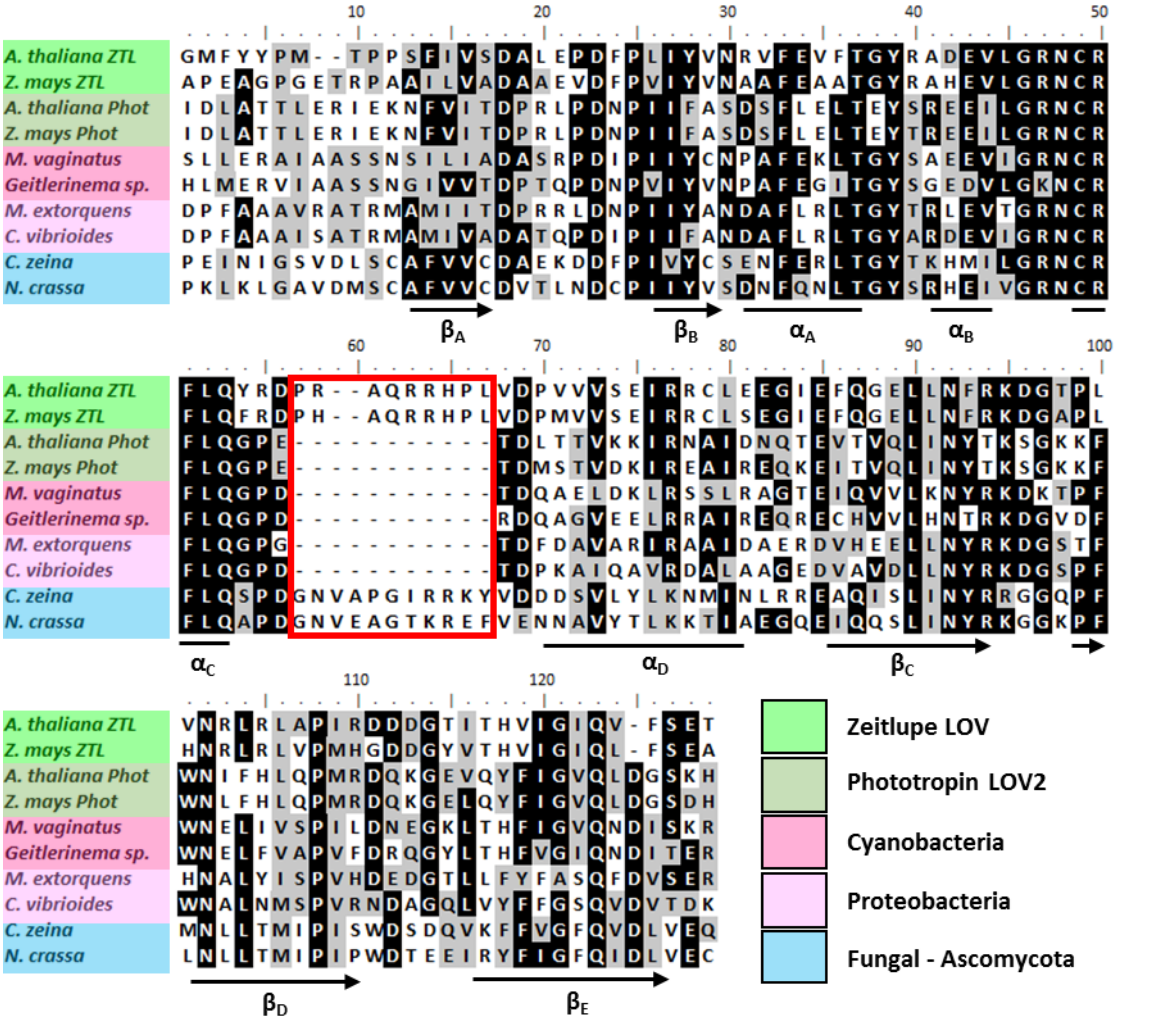

Figure 8. Sequence alignment of selected LOV domains across three kingdoms. LOV domains, representing three kingdoms, were aligned using MAFFT. The secondary structure of the aligned LOV domains is shown below each block. The linker region between α_C and α_D is indicated by the red box.

2.4.6. Conservation of the clock proteins in *C. zeina* and *C. zeae-maydis*

The fungal circadian oscillator and all its associated clock proteins have been well characterised in *N. crassa* (Castro-Longoria et al., 2010). We set out to see how conserved the circadian oscillator is in *C. zeina* and *C. zeae-maydis* by identifying all the clock protein orthologues. It is known that some fungal species function without one or two of the clock proteins though an alternative oscillator (Salichos and Rokas, 2009). Furthermore we aimed to see how similar the clock proteins between *C. zeina* and *C. zeae-maydis* are, as these two closely related species are known to differ at a genetic level, but cause the same disease in maize.

The counter part of the WC-1 protein in the WCC is the WC-2 protein. These two proteins form a heterodimer upon light exposure through their individual PAS domains (Linden and Macino, 1997). The domain architecture of WC-2 and all the other clock proteins can be seen in Figure 14. The WC-2 orthologue was identified in the genome sequence of *C. zeae-maydis* on scaffold four. There are no introns predicted in the 1572 bp *wc-2* gene sequence of *C. zeae-maydis*. The WC-2 orthologue was also identified in the genome sequence of *C. zeina* on scaffold seven (1581 bp) and shares 89.8% identical nucleotides with *C. zeae-maydis*. The *C. zeina wc-2* gene has nine base pair (three amino acid) in-frame deletion compared to *C. zeae-maydis* in the 5' region of the gene as seen in Figure 9. The predicted WC-2 protein sequences of *C. zeina* (526 aa) and *C. zeae-maydis* (523 aa), share 91.8% identity to each other and 45.3% and 45% respectively to the 530 aa protein sequence of *N. crassa* (P78714).

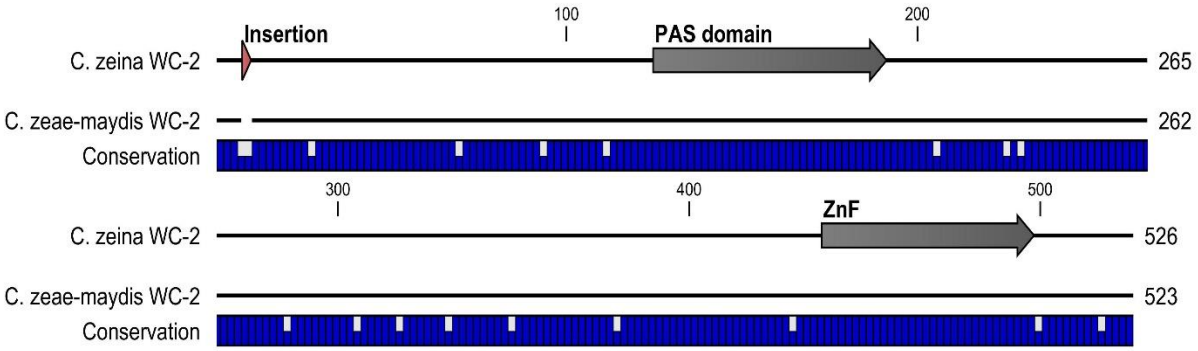

Figure 9. Protein sequence alignment of *C. zeina* and *C. zeae-maydis* WC-2 orthologues. Alignment of the WC-2 orthologues from *C. zeina* and *C. zeae-maydis* shows overall conservation of 91.8% as indicated by the blue graph. An insertion is present in the WC-2 protein in *C. zeina* when compared *C. zeae-maydis* at the N-terminal. The two function domain, PAS domain and the GATA Zinc Finger, are represented by the grey arrows.

The timing of the circadian clock of *N. crassa* is controlled by the negative regulator called Frequency (FRQ) (Schafmeier et al., 2005). The expression of the *frq* transcript is controlled by the WCC, which acts as a light induced transcription factor for the activation of light responsive genes. The orthologue of the FRQ protein was identified in the genome sequence of *C. zeae-maydis* and *C. zeina* on scaffold nine and four respectively. The *C. zeae-maydis frq* gene sequence of 3767 bp is predicted to contain a single intron, whereas the *C. zeina frq* (3003 bp) contains no intron. The amino acid sequence of *C. zeina*, which shares 74.5% identical residues with *C. zeae-maydis*, has one deletion of 210 aa and an insertion of three aa compared to the *C. zeae-maydis* FRQ protein. The predicted FRQ proteins of *C. zeina* and *C. zeae-maydis* share 28.8% and 24.4% identity to the *N. crassa* (P19970) protein.

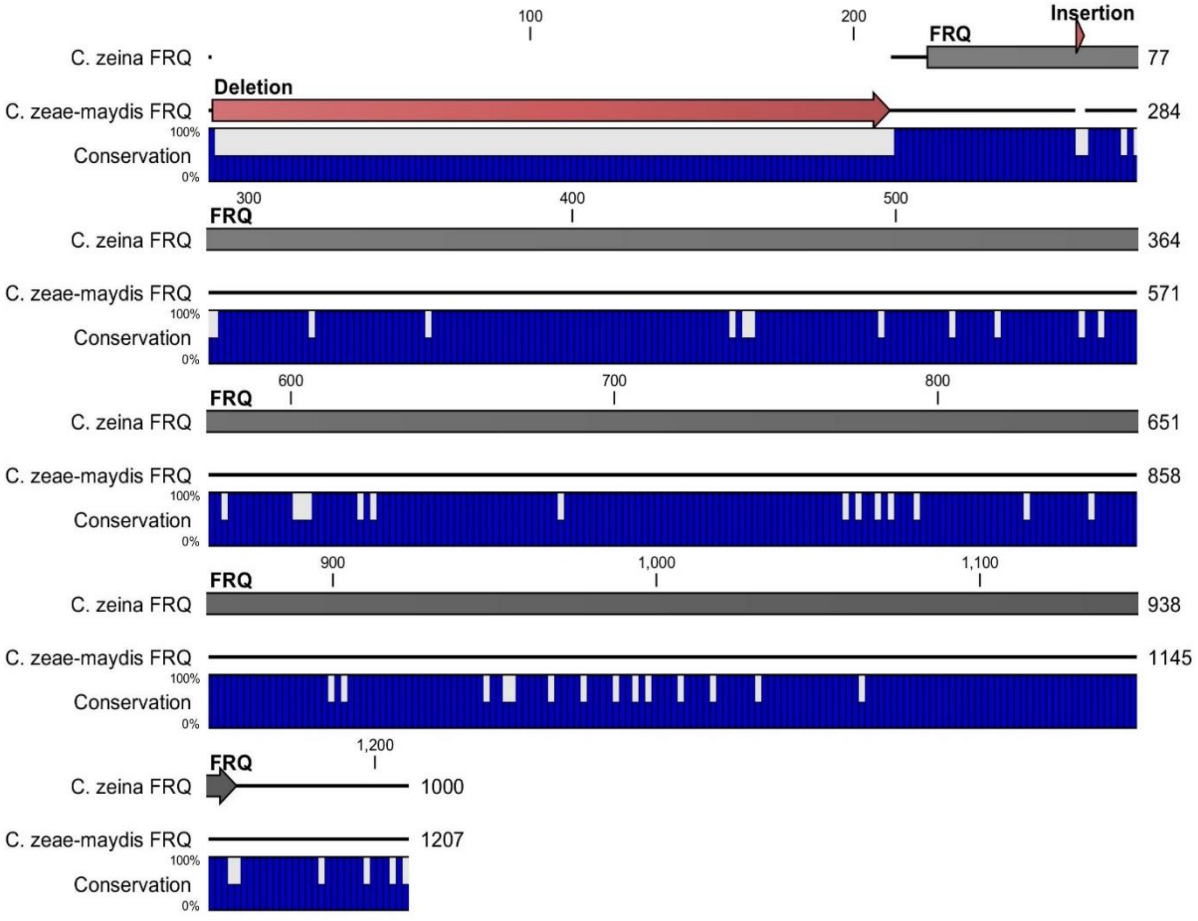

Figure 10. Protein sequence alignment of *C. zeina* and *C. zeae-maydis* FRQ orthologues. The amino acid alignment of the *C. zeina* and *C. zeae-maydis* FRQ proteins have an overall conservation of 74.5%. The *C. zeina* FRQ protein has a large deletion in the N-terminal compared to the *C. zeae-maydis* FRQ protein. The FRQ functional domain is represented by the grey arrow.

The phosphorylation status of the WCC is increased as the day progresses, which influences its ability to bind to and activate the promoter regions of light responsive genes. The Frequency interacting RNA helicase (FRH) forms a complex with FRQ that inhibits the functioning of the WCC by altering its phosphorylation status (Hurley et al., 2013). The genome sequence of *C. zeae-maydis* contains an orthologue of *frh* on scaffold 22, which is predicted to contain a single intron in the 3 563 bp gene. An *frh* orthologue is also present in the genome of *C. zeina* on scaffold seventeen, and has a single intron in the 3 291 bp gene. Comparison between the two *Cercospora* species revealed a deletion in *C. zeina* of 90 amino acids, which shares 85.4% identity to the *C. zeae-maydis frh* orthologue as seen in Figure 11. The *C. zeae-maydis* and *C. zeina* FRH orthologues share 57.8% and 62% identity to the characterised FRH from *N. crassa* respectively. The FRH orthologues in *C. zeina* and *C. zeae-maydis* contain the same functional domains is the same order as *N. crassa* (Q873J5) as predicted by SMART 7.

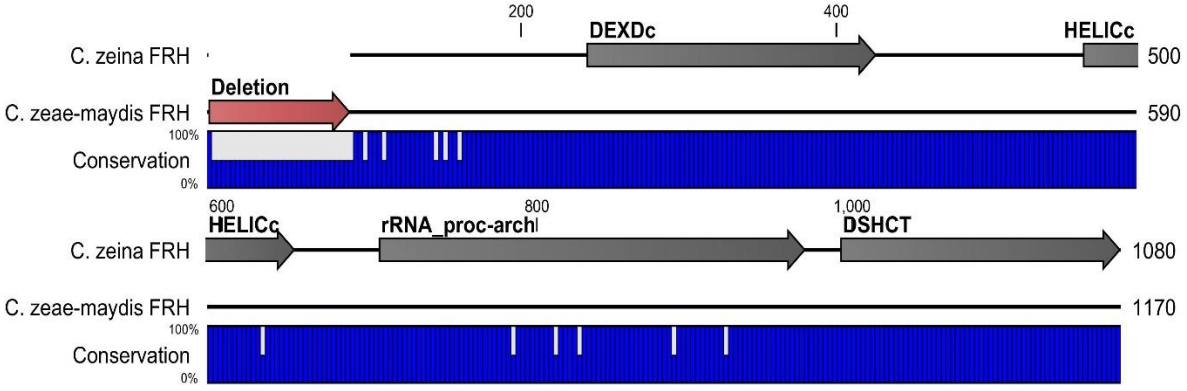

Figure 11. Protein sequence alignment of *C. zeina* and *C. zeae-maydis* FRH orthologues. The putative FRH orthologues of *C. zeina* and *C. zeae-maydis* are well conserved, sharing 85.4% identical residues. The *C. zeina* N-terminal has a deletion compared to the *C. zeae-maydis* FRH orthologue. The grey arrows represents the four functional domains: DEXDc, HELICc, rRNA_proc-archi and DSHCT.

During the day, as the FRQ protein is expressed, the protein is phosphorylated, which labels it for ubiquitylation. The protein, FWD-1, is an F-box/WD40-repeat protein that physically interacts with the phosphorylated form of FRQ (He et al., 2003). It was shown that FWD-1 is the substrate-recruiting unit of an SCF-type ubiquitin ligase, which is responsible for the subsequent degradation of the FRQ protein. The orthologue of the *fwd-1* gene from *N. crassa* was identified on scaffold five in the genome sequence of *C. zeae-maydis* and on scaffold one

in *C. zeina*. The *C. zeae-maydis fwd-1* gene sequence of 3 339 bp is predicted to contain a single intron, whereas the 4987 bp *fwd-1* gene of *C. zeina* is predicted to contain four introns. *Cercospora zeina* and *C. zeae-maydis* species share 62% and 78.2% identical residues at the nucleotide level and the amino acid level respectively. The *N. crassa* FWD-1 protein shares 14.5% and 17% identical amino acid residue positions to *C. zeina* and *C. zeae-maydis* respectively. There is an insertion of 249 amino acids at the N-terminal of *C. zeina* that is predicted to contain a transmembrane domain as seen in Figure 12.

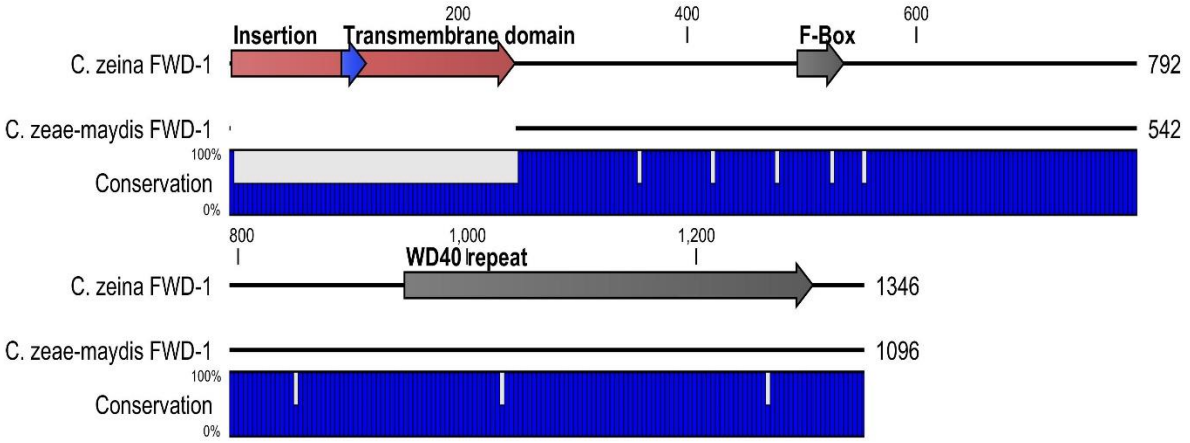

Figure 12. Protein sequence alignment of *C. zeina* and *C. zeae-maydis* FWD-1 orthologues. The amino acid sequence alignment of the FWD-1 *C. zeina* and *C. zeae-maydis* orthologues share 78.2% identical residues. The *C. zeina FWD-1* orthologue has an N-terminal insertion that contains a transmembrane. The two functional domains are shown in the grey arrows, which includes an F-box domain and a WD40 repeat region.

The final protein that forms part of the circadian oscillator is VIVID (VVD), which is responsible for photoadaptation of the circadian clock. The fungus' ability to respond to changes in light intensity is regulated by VVD (Malzahn et al., 2010). The VVD protein acts as a negative regulator of WCC light dependent gene expression and as a positive regulator of photo responsiveness of the circadian clock. A heterodimer, between VVD and WCC is formed through their respective LOV domains. The *N. crassa vvd* orthologue was identified on scaffold seven in the genome sequence of *C. zeae-maydis* and on scaffold three in *C. zeina*. The *vvd* gene sequence of *C. zeae-maydis* (2084 bp) and *C. zeina* (2096 bp) are both predicted to contain a single intron. The predicted VVD protein sequences of *C. zeae-maydis* and *C. zeina* contains a PAS domain followed by a PAC motif, which together forms a PAS-fold, which share

87.2% identical amino acid residues. The LOV motif, GXNCRFLQG, was identified in the PAS-fold sequences and thus is classified as a true LOV domain. *Cercospora zeina* and *C. zeae-maydis* species are predicted to share 9.8% and 10.1% identity to the *N. crassa* VVD protein (Q1K5Y8) respectively. The *C. zeina* protein sequence has six insertions relative to the *C. zeae-maydis* VVD protein. The N-terminal end of the *C. zeina* VVD protein has two insertions and four insertions at the C-terminal end relative to the *C. zeae-maydis* VVD protein as seen in Figure 13.

The comparison of the clock protein domain architecture between *C. zeae-maydis* and *N. crassa* is graphically presented in Figure 14. All five of the clock proteins orthologues contain all the functional domains in the same order as in *N .crassa*.

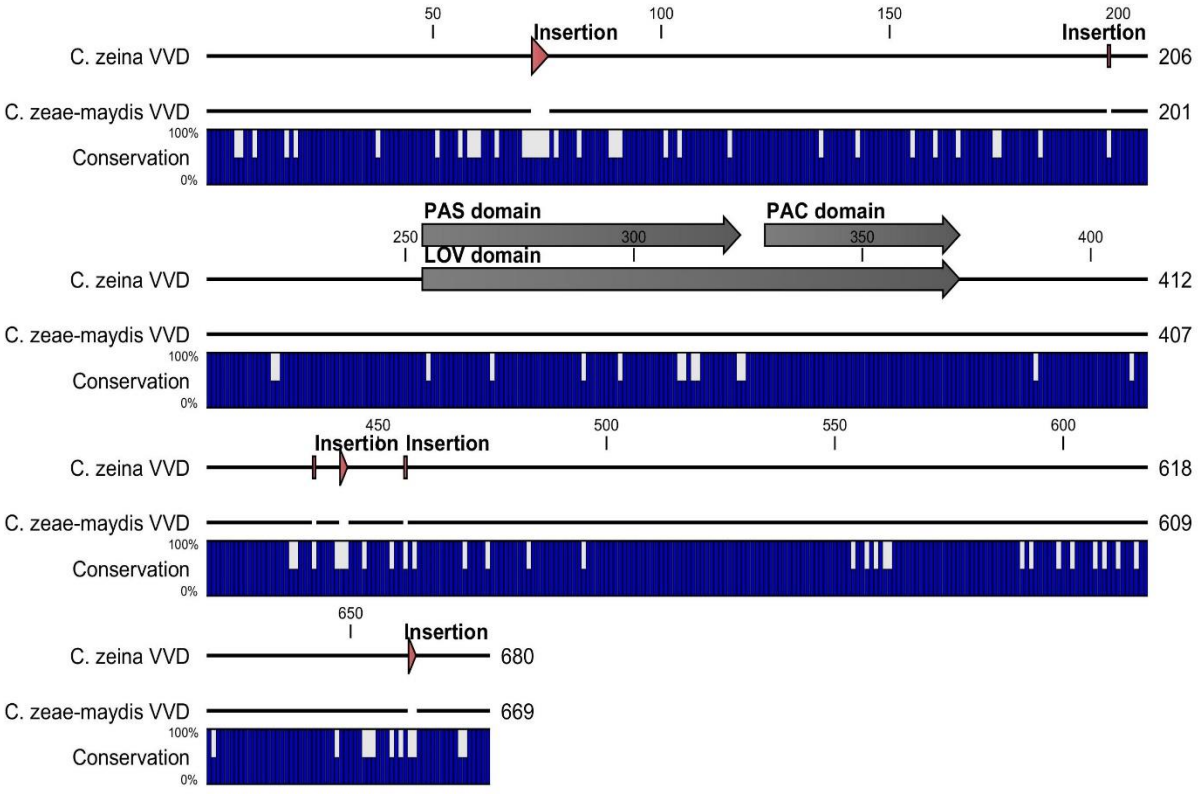

Figure 13. Protein sequence alignment of *C. zeina* and *C. zeae-maydis* VVD orthologues. The protein sequences of the VVD orthologues of *C. zeina* and *C. zeae-maydis* share 87.2% identical residues. The *C. zeina* VVD protein contains six insertions compared to *C. zeae-maydis*. The PAS and PAC domain, which form the LOV domain, are represented by the grey arrows.

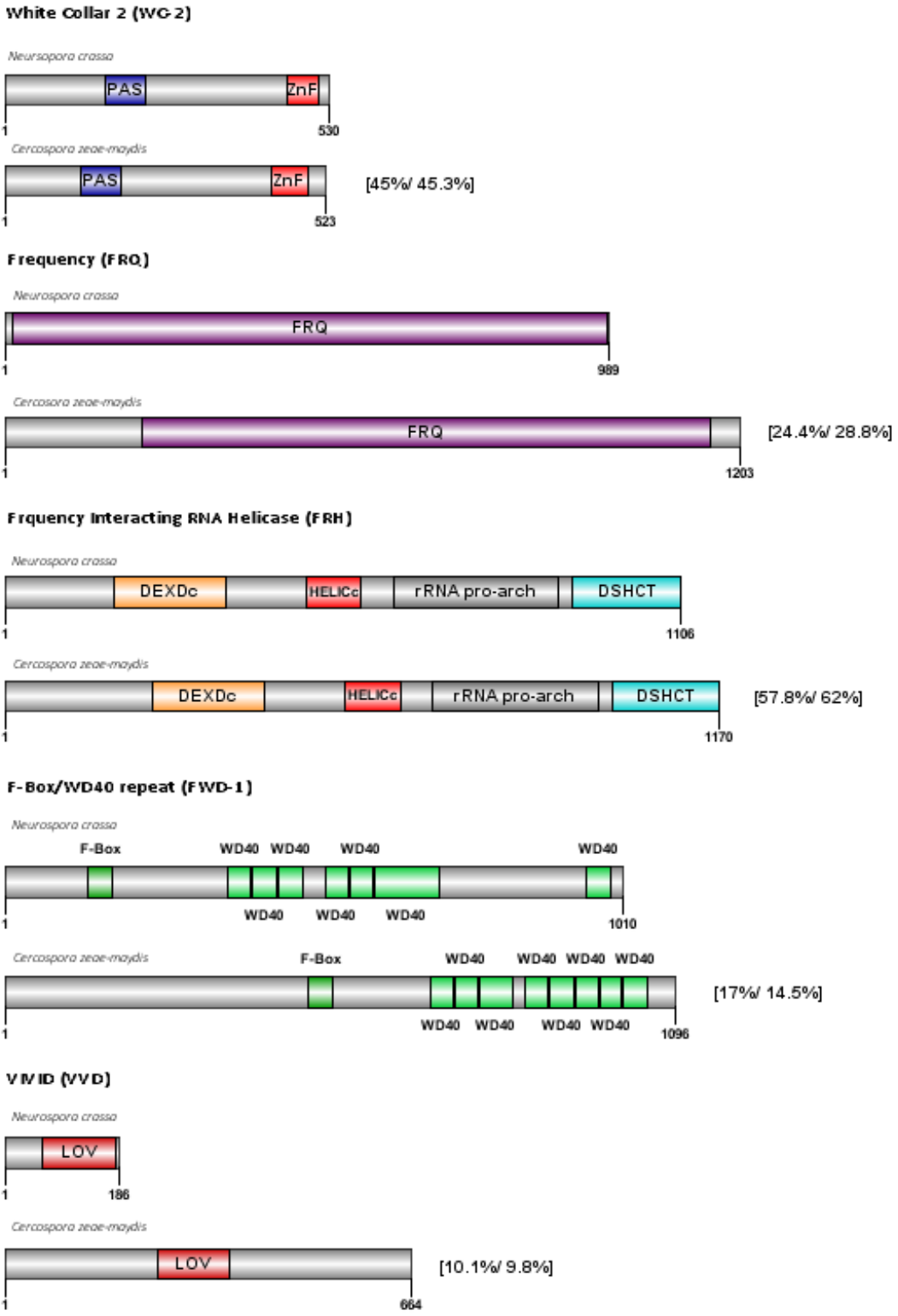

Figure 14. Domain architecture clock protein orthologues in *N. crassa* and *C. zeae-maydis*. The domain architecture of the clock proteins identified in the *Neursopora crassa* circadian oscillator are shown. Orthologues of the clock proteins identified in *Cercospora zeina* and *Cercospora zeae-maydis* are shown below the *N. crassa* proteins. The domain positions and proteins sizes of *C. zeae-maydis* are shown and is similar for *C. zeina*. The percentage amino acid identity of *C. zeae-maydis* and *C. zeina* clock proteins relative to *N. crassa* respectively is indicated next to the *C. zeae-maydis* proteins in brackets.

2.4.7. Identification of other blue light photoreceptors in *C. zeina* and *C. zeae-maydis*

The White Collar-1 protein is considered to be the main photoreceptor for blue light. The involvement of WC-1 in the circadian oscillator has been well studied in *N. crassa* (Salichos and Rokas, 2009). Most of the mutational studies done on WC-1 orthologues showed that some blue light responses are still being detected despite the lack of a functional WC-1 blue light photoreceptor. This observation suggested that another, unknown, blue light photoreceptor might be present in fungi.

The function of the various classes of cryptochromes in fungi are understudied. Based on literature, only seven functional cryptochrome characterisation experiments were performed in fungi. In *Fusarium fujikuroi*, *N. crassa* and *Sclerotinia sclerotiorum* a CRY-DASH type cryptochrome was identified (Castrillo et al., 2013; Froehlich et al., 2010; Veluchamy and Rollins, 2008). A class I CPD cryptochrome was characterised in *Aspergillus nidulans*, *C. zeae-maydis* and *Trichoderma atroviride* (Bayram and Biesemann, 2008; Berrocal-Tito, 2007; Bluhm and Dunkle, 2008). The animal class cryptochrome with 6-4 photolyase activity was only thus far characterised in *Cercospora zeae-maydis* and *Trichoderma reesei* (Bluhm and Dunkle, 2008; Guzmán-Moreno et al., 2014). To date, no plant nor CPD II class cryptochromes have been identified in fungal species. Based on functional analysis cryptochrome proteins are able to function as blue light receptors, although the exact function still remains to be elucidated.

In order to identify additional blue light photoreceptors in *C. zeina* and *C. zeae-maydis* the different type of characterised fungal cryptochromes were downloaded from the dbCry database and used to perform a tBLASTn against the genome sequence of *C. zeae-maydis*. A BLAST alignment score of greater than 200 was found to scaffold two and twelve. Gene regions for these two scaffold were predicted using AUGUSTUS. Scaffold two was predicted to contain a gene with no introns that is 1 779 bp in length. The gene identified on scaffold two will now be referred to as *cry2*. The *cry2* orthologue was identified on scaffold 58 in the genome sequence of *C. zeina* (1 779 bp) and shares 86.9% identical nucleic acid residues to the putative *C. zeae-maydis cry2*. The predicted protein sequences encoded by the identified

C. zeina and *C. zeae-maydis cry2* genes were analysed for the presence of the two conserved cryptochrome domains, PHR and FAD binding as indicated in Figure 15 A. Bluhm and Dunkle (2008) uploaded a partial *cpd1* gene sequence, which they characterised to be a cyclobutane pyrimidine dimer photolyase class 1 (CPD I) in *C. zeae-maydis*. This partial *cpd1* gene sequence aligned to a region on the 3' end of the putative *cry2* identified on scaffold two from *C. zeae-maydis* as seen in Figure 15 B. Based on this observation *cry2* is believed to be the complete sequence of *cpd1* characterised by Bluhm and Dunkle (2008).

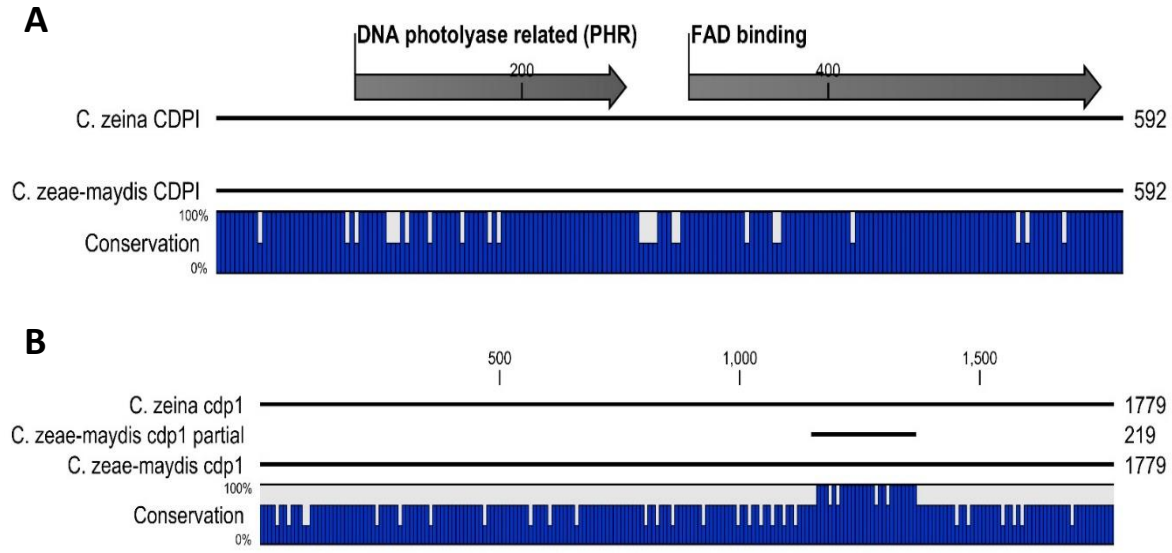

Figure 15. Protein sequence alignment of *C. zeina* and *C. zeae-maydis* CDP1 orthologues. (A) The amino acid sequence alignment of the CPD1 *C. zeina* and *C. zeae-maydis* orthologues shares 86.9% identical residues. The PHR and FAD functional domains are indicated by the grey arrows. (B) The partial *cpd1* sequence identified by Bluhm and Dunkle (2008) align with the two *cdp1* orthologues from *C. zeina* and *C. zeae-maydis*.

The predicted putative *C. zeae-maydis* cryptochrome gene (1798 bp) identified on scaffold twelve, contains two introns (652-705 bp and 1226-1274 bp). The gene identified on scaffold twelve will be referred to as *cry12*. The putative orthologue of *cry12* was identified on scaffold 23 in *C. zeina*, which is predicted to encode a protein that shares 85.7% identical residues. The amino acid alignment of the *C. zeina* and *C. zeae-maydis*, shown in Figure 16, shows multiple arginine-glycine-glycine (RGG) repeats in the C-terminus of CRY12 in *C. zeina*.

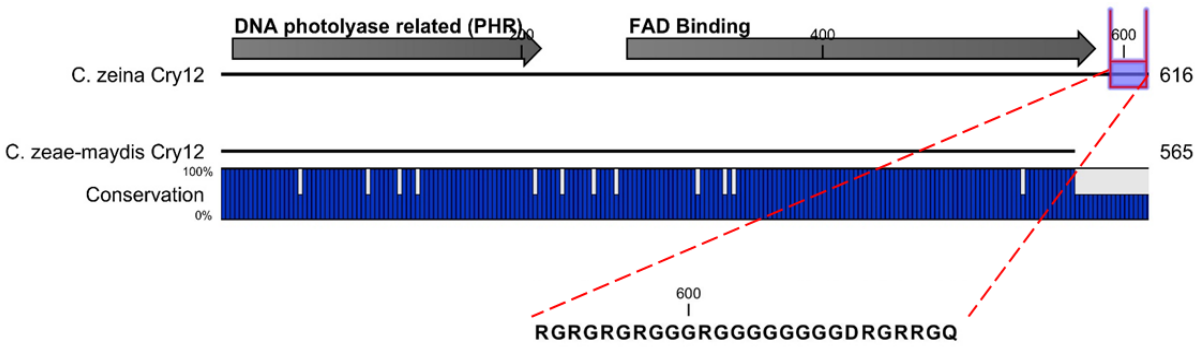

Figure 16. Protein sequence alignment of *C. zeina* and *C. zeae-maydis* CRY12 orthologues. The putative CRY12 *C. zeina* and *C. zeae-maydis* orthologues shares 85.7% identity. The two function domains, PHR and FAD binding, are represented by the grey arrows. An arginine-glycine-glycine (RGG) repeat region is present in the C-terminal of the CRY12 *C. zeina* orthologue.

The complete sequence of the 6-4 photolyase identified and characterised in *C. zeae-maydis*, *phl1*, was downloaded and compared to *cry2* and *cry12*, which are the two putative *C. zeina* and *C. zeae-maydis* cryptochome gene sequences identified in this study. The characterised *phl1* gene did not align to either of the two putative cryptochrome genes identified on scaffold two and twelve. The *phl1* gene was aligned to scaffold twelve, on which the putative *C. zeae-maydis cry12* gene is located, and was found to be present on the 3' end of the scaffold. The putative *cry12* gene is located on the 5' end of the scaffold. Thus, the two genes, *cry12* and *phl1*, are present on scaffold twelve in *C. zeae-maydis*. The same observation was made in *C. zeina*, where the orthologue of *phl1* was also present on scaffold 23, which is the same scaffold on which *cry12* is present. The *C. zeina* PHL1 orthologue, as see in Figure 17, is predicted to contain two insertions at the N-terminal in the PHR domain, and two deletions and an insertion at the C-terminal end. Overall the sequences between the *C. zeina* and *C. zeae-maydis* PHL1 proteins are conserved, with 82.2% identical residues.

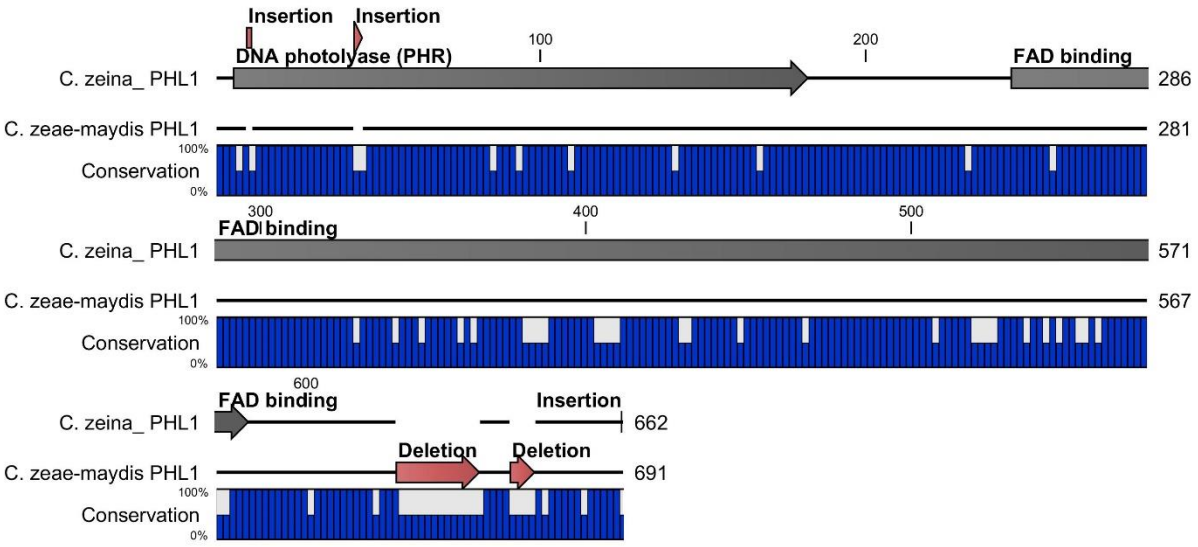

Figure 17. Protein sequence alignment of *C. zeina* and *C. zeae-mayids* PHL1 orthologues. The amino acid alignment of the *C. zeina* and *C. zeae-maydis* PHL1 share 82.2% identity. Two insertions are present in the PHR domain of *C. zeina*. There are two deletions and one insertion at the C-terminal of the *C. zeina* PHL1 orthologue. The FAD binding and PHR domain are indicted by the grey arrows.

Based on sequence similarity alone it is difficult to make a clear distinction between cryptochrome and photolyases as the domain architecture is similar, which makes it challenging to divide the different cryptochromes into the five different functional classes (Krauss et al., 2009; Van der Horst et al., 2007). The dbCRY database contains known and predicted cryptochromes across all kingdoms of life categorised under the five different classes(Kim et al., 2014). Representatives of each class were downloaded and included in a phylogenetic study with the identified cryptochromes from *Cercospora zeae-maydis*. Based on the neighbour joining tree generated by PAUP*, the three CRY proteins from *C. zeina* and *C. zeae-maydis* clustered into three different classes (Figure 18). The PHL1 protein is characterised as a 6-4 photolyase (Bluhm and Dunkle, 2008) and clusters with the Animal cryptochrome class as expected, based on its characterised function. The second cryptochrome protein, characterised as CPD1, clustered with the CPD class I. The final putative cryptochrome protein identified in this study, CRY12, clustered with the other CRY-DASH proteins. The function of this protein is yet to be determined in *C. zeina* and *C. zeae-maydis*.

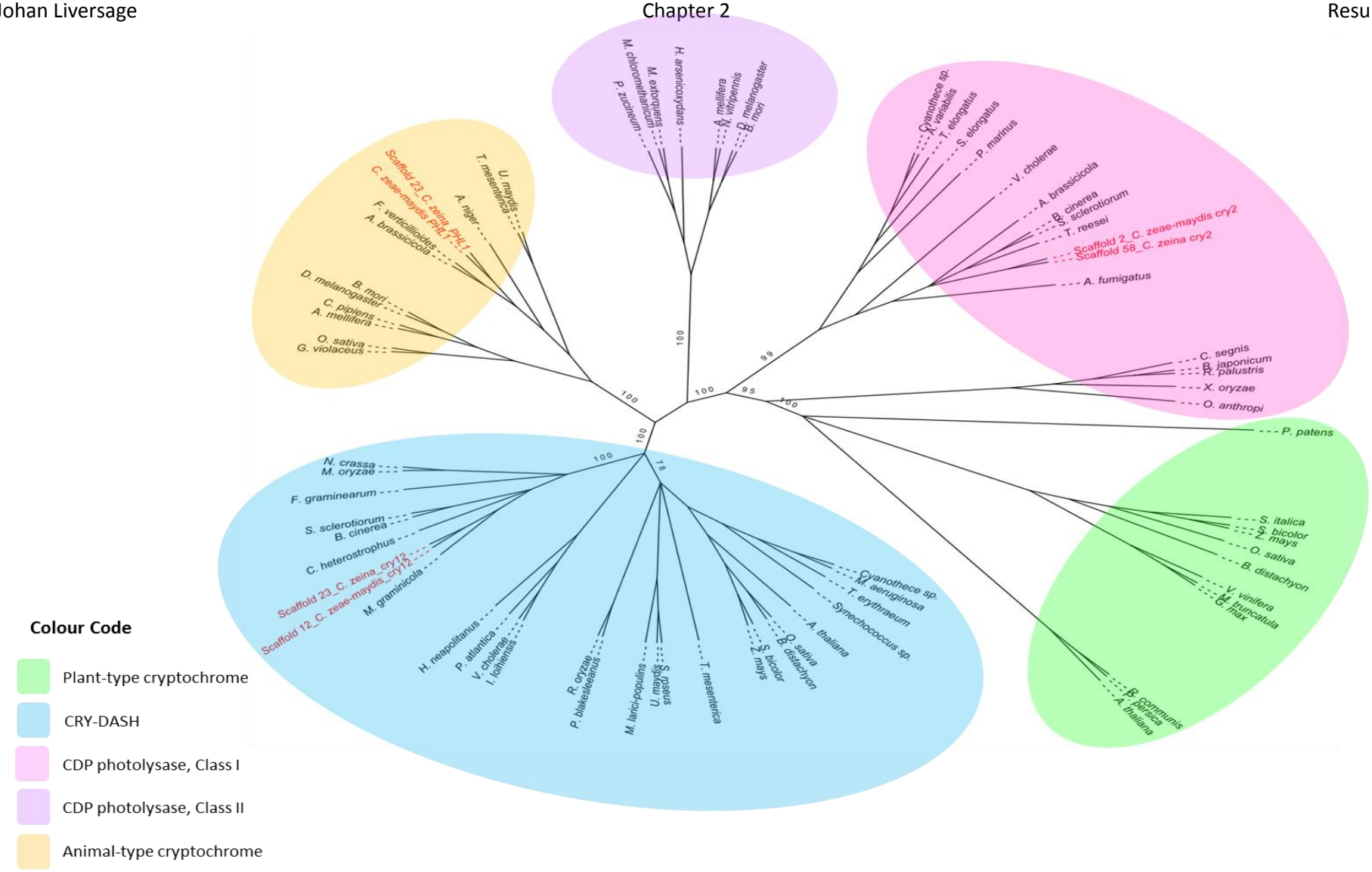

Figure 18. Phylogenetic analysis of putative *C. zeina* and *C. zeae-maydis* cryptochrome proteins. The cryptochrome database (Kim et al., 2014) was used to set up a local database containing representatives of each type of cryptochome. The putative *C. zeina* and *C. zeae-maydis* CRY proteins were included in the alignment. The multiple sequence alignment was performed with MAFFT and the phylogenetic tree constructed with BioNJ from PAUP*. The *C. zeina* and *C. zeae-maydis* sequences are shown in red.

2.5. Discussion

2.5.1. Conservation of homologous WC-1 proteins in fungi

This study showed that blue light photoreception in fungi through WC-1 is conserved. Since the identification of the WC-1 protein in *N. crassa*, orthologues in other fungal species were identified. We wanted to determine the distribution and evolution of the WC-1 protein across the three fungal phyla. The fungal kingdom, Mycota, consists of the early divergent Zygomycota and the subkingdom, Dikarya, which includes Basidiomycota and Ascomycota based on fungal phylogeny (Wang et al., 2009). Single gene phylogeny is used to infer the evolution of a gene and to predict the function of an unknown gene (Eisen and Wu, 2002). A maximum likelihood phylogenetic tree was constructed based on homologous WC-1 proteins from Ascomyocta, Basidiomycota and Zygomycota. The phylogenetic tree showed that all the homologous WC-1 proteins grouped within their respective phyla as expected. The WC-1 orthologues from Ascomycota formed a sister group to Zygomycota WC-1 orthologues, with the Basidiomycota representatives grouping separately. This clustering is incongruent to the fungal species tree, where Zygomycota is the early divergent phyla. Taking a closer look at the Ascomycota phyla, the WC-1 orthologues clustered into the respective classes, which includes Dothideomycetes, Eurotiomycetes, Leotiomycetes and Sadariomycetes (Schoch et al., 2009). Congruency is observed in the Dothideomycete class relating to their lifestyle strategies (Ohm et al., 2012), where the hemibiotrophs, which include *C. zeina* and *C. zeae-maydis*, form a sister group to the necrotrophs. The biological relevance of the WC-1 protein in the respective lifestyle strategies of fungi could be interesting to explore further.

Controversy surrounds the phylogeny of the WC-1 in literature (Bodor et al., 2013; Estrada and Avalos, 2008; Idnurm et al., 2010; Kim et al., 2011; Kubo, 2009). Some studies show phylogeny based on WC-1 was found to resemble that of the fungal speciation tree, whereas in other reports the Zygomycota orthologues form a sister group to Ascomycota. We analysed the individual functional domains of the WC-1 orthologues in an attempt to better explain the phylogeny. The Basidiomycota WC-1 orthologues all contain the LOV domain and at least a single PAS domain. The third PAS domain, PAS_C, is not present in all Basidiomycota WC-1 orthologues. None of the Basidiomycota orthologues contain a C-terminal Zinc-finger, which

enables WC-1 to bind to DNA and act as a transcription factor, however experimental studies have shown that these Basidiomycete orthologues are still able to activate transcription of light responsive genes. Sequence alignments of the functional domains (LOV and PAS_B) indicated how divergent the Basidiomycota WC-1 orthologues are, which showed insertions in both the domains. The phylogeny was tested under different amino acid substitution models and versions of the multiple sequence alignment (the inclusion and exclusion of variable N- and C-terminal as well as gap regions), which all resulted in a similar phylogeny as shown in Figure 3. The insertions in the LOV, PAS_B and the deletion in PAS_C in the WC-1 orthologues from Basidiomycota, clearly provides support for the independent evolution of the homologous WC-1 protein in this phyla seen in Figure 3, where the Zygomycota form a sister group to Ascomycota, which is incongruent to what is stated in other studies.

2.5.2. Evolution of LOV domains across three Kingdoms

Light Oxygen or Voltage (LOV) domains are distributed across three of the kingdoms of life (Krauss et al., 2009). LOV domains are a subclass of PAS domains, which are phylogenetically distinct from other protein-protein interacting PAS domains (Mei and Dvornyk, 2014). In this study we collected LOV domains from three kingdoms in order to see how divergent these domains are between plants, bacteria and fungi. It has been suggested that pathogens are able to synchronise their circadian rhythms to that of the host plant, which enables the pathogen to activate light responsive genes that will aid in its infection strategy (Kim et al., 2011). This suggestion lead us to analyse the LOV domains from the two plant LOV domain containing proteins, Phototropin and Zeitlupe, and bacterial sensory proteins to determine the origin of the blue light sensitive domains. The maximum likelihood tree revealed that the plant ZTL LOV domain in plants forms a monophyletic group with the cyanobacteria clade, and the plant C-terminal LOV domain forms a monophyletic group with the proteobacteria representatives. This grouping was also observed by Krauss et al. (2009), where the phylogeny is in agreement with the endosymbiotic theory. Proteobacteria are believed to be the ancestor of eukaryotic mitochondria, whereas cyanobacteria are said to be the ancestor of chloroplasts (Esser et al., 2007; McFadden, 2001). The eukaryotic LOV domains are now only present in the nuclear genomes and not in the mitochondrial nor the chloroplast genomes,

which occurred through a process called endosymbiotic gene transfer from the organelles to the nucleus (Timmis et al., 2004).

Independent evolution of the LOV domains occurred in the fungal kingdom. The phylogenetic analysis of the LOV domains in this study clearly shows the fungal representatives forming a monophyletic group (Figure 3). Krauss et al. (2009) speculated that the plant and fungal LOV domains might have originated from two different endosymbiotic events, evolving independently to regulate two distinct blue light dependent processes, namely, the entrainment of the circadian clock and light dependent growth and development. The phylogenetic data generated in this study, taken together with the findings in literature, indicates that the fungi and plants have acquired their blue light receptors from unrelated lineages, but convergently evolved to use the same blue light sensitive domain for the control and regulation of similar cellular and metabolic processes.

2.5.3. FRQ/WC – Oscillator conservation in *C. zeina* and *C. zeae-maydis*

The presence of a circadian rhythm has been observed in a few representatives across the fungal phyla. However, the molecular mechanisms behind the observed circadian rhythms are not completely understood nor is there experimental evidence for the roles played by clock proteins in most fungal species. The circadian oscillator of *N. crassa* has been extensively studied, with the important clock proteins identified and their role in the circadian clock characterised (François, 2005). Salichos and Rokas (2010) traced the evolution of the clock proteins identified in *N. crassa* across the fungal kingdom, which enabled them to infer the ancestral origin of the important clock proteins. The circadian rhythm, as characterised in *N. crassa*, is generated by of a negative feedback loop that is produced through the interactions of WC-1, WC-2, FRQ, FRH and the FWD-1 proteins (Cheng et al., 2001).

Prior to this study, it was unknown if the components of the fungal circadian clock were conserved in *C. zeina* and *C. zeae-maydis*. At least two types of circadian oscillators have been identified in *N. crassa*, the first of which is the FRQ/WC-based (FWO) oscillator that requires

a functional WC-1, WC-2, FRQ and FRH protein (Dunlap and Loros, 2006). In contrast to this there is an oscillator that functions in the absence of FRQ (FRQ-less oscillator(FLO)) and the WC proteins (WC-FLO) has been identified (Salichos and Rokas, 2009). In this project we identified all five of the clock proteins (WC-1, WC-2, FRQ, FRH, and FWD-1) forming the circadian oscillator within *C. zeina* and *C. zeae-maydis* genomes, which makes it tempting to suggest that a functional FRQ-WC-based oscillator is present in *C. zeina* and *C. zeae-maydis*. Functional characterisation will require analysis of the expression of the genes encoding the clock proteins.

Based on literature reports on the function of the FRQ/WC-based oscillator, we compiled a model of interaction for all the *C. zeina* and *C. zeae-maydis* clock proteins (Figure 19). The White Collar proteins (WC-1 and WC-2) are well conserved across the three fungal phyla. Based on the phylogenetic study of Salichos and Rokas (2010), the WC-1 and WC-2 protein most likely evolved from a common ancestor of Ascomycetes, Basidiomycetes and Zygomycetes. Orthologues of the WC-1 protein are known to be present in *C. zeina* and *C. zeae-maydis* (Kim et al., 2011; Liversage, 2012). The orthologues of the WC-2 protein were discovered in the genome sequences of the two *Cercospora* species, with the functional domains predicted to be present. The WC-2 protein forms a heterodimer with the activated CRP1 (WC-1) through their respective PAS domains (Figure 19 a - b). The rhythmic period of the clock is influenced by the expression of FRQ (Figure 19 d), which was recently characterised as an intrinsically disordered protein (IDP) that enables it to interact with multiple partners (Hurley et al., 2013). Basidiomycetes and Zygomycetes are believed not to contain an orthologue of FRQ, which is suggested to have originated in Ascomycetes though a common ancestor to Dothideomycetes, Leotiomycetes and Sordariomycetes (Salichos and Rokas, 2009). The conservation of FRQ, however is not conserved within the genomes of Dothideomycetes based on the absence of *frq* in the sequence genome of *Pyrenophora tritcici-repentis* and the presence of an orthologue in the genome of *Mycosphaerella fijiensis*. We identified an orthologue of FRQ in the genome sequences of *C. zeina* and *C. zeae-maydis*, which is predicted to contain the FRQ functional domain.

Two clock proteins, FRH and FWD-1, are not essential for the circadian oscillator to function. All the functional domains of the FRH protein are present in the putative orthologues identified in *C. zeina* and *C. zeae-maydis*. The FRQ protein is very unstable and is degraded as soon as it is transcribed. The FRQ-interacting RNA helicase (FRH) binds non-enzymatically to FRQ (Figure 19 g) in order to stabilise the protein (Hurley et al., 2013), which in turn affects the periodicity of the clock. The FRH protein is an orthologue of the exosome complex that has known RNA helicase activity. The helicase activity of FRH has been shown not to be essential through deletion of the helicase related domains, HELICc and DSHCT. Interaction of FRH and FRQ is through an N-terminal region, which regulates phosphorylation of the FRQ protein (Hurley et al., 2013). The FWD-1 protein regulates the degradation of the FRQ protein (Figure 19 j - k) and is an F-box/WD40 repeat containing protein (He et al., 2003). As the FRQ protein is progressively phosphorylated the FWD-1 protein binds to and labels the FRQ protein for degradation via the ubiquitination pathway. This F-box/WD40 repeat containing protein is conserved in the genome sequences of *C. zeina* and *C. zeae-maydis* with both functional domains predicted to be present. The FWD-1 orthologue of *C. zeina* contains an N-terminal insertion predicted to contain a transmembrane domain. This transmembrane region is also present in the mammalian FBXW7, which is an E3 ubiquitin protein ligase that forms part of the SCF (SKP1-cullin-F-box) complex characterised in *Caenorhabditis elegans*, *D. melanogaster* and *Homo sapiens* (Jin et al., 2004; Yada et al., 2004). The SCF complex functions in the phosphorylation dependent ubiquitination of proteins. The FRH and FWD-1 proteins may not be essential to the circadian clock, but they play an important role in determining the periodic length of the clock through regulating the stability of the FRQ protein.

Photoadaptation is controlled through the inhibition of the WCC by another LOV domain containing clock protein the VVD protein. This protein contains the light sensitive LOV domain that physically interacts with the WC-1 protein (Figure 19 m), which leads to the inhibition of the WCC (Malzahn et al., 2010). The FRH protein interacts with and stabilises the VVD protein, which ultimately suppresses the expression of FRQ (Hurley et al., 2013). The genome sequences of both *C. zeina* and *C. zeae-maydis* contain an orthologue of the *N. crassa* VVD protein. The VVD orthologues are predicted to contain a PAS domain followed by a PAC

domain, which together form the LOV domain. The identity of the LOV domain in *C. zeina* and *C. zeae-maydis* VVD was confirmed through the presence of the highly conserved GXNCRFLQG motif, previously identified and characterised in plant phototropin sequences (Salomon et al., 2000). We believe that the presence of the genes encoding VVD protein in the genomes of *C. zeina* and *C. zeae-maydis* indicates that the mechanism of photoadaptation is conserved. However, the function of photoadaptation through VVD in *C. zeina* and *C. zeae-maydis* remains to be experimentally determined.

2.5.4. Alternative blue light photoreceptors in *C. zeina* and *C. zeae-maydis*

In addition to WC-1 other blue light photoreceptors have been identified and characterised, which play light dependent roles in fungi. The photoreceptors belong to the Cryptochrome/photolyase family of proteins, which are mainly responsible for photoreactivation (CPDI, CPDII, Animal type 6-4 photolyase and plant cryptochromes), with the exception being Cry-DASH, which is believed to act as a blue light photoreceptor as it has limited DNA repair capabilities (Froehlich et al., 2010). In this study, we showed that the genomes of *C. zeina* and *C. zeae-maydis* contain three types of cryptochrome proteins, which are believed to be involved in light- dependent biological functions based on their phylogenetic clustering with the five cryptochrome types (Kim et al., 2014).

The cryptochrome/photolyase 6-4 photolyase subclass is present in *C. zeina* and *C. zeae-maydis*. Functional studies through deletion of the *phl1* gene (6-4 photolyase) in *C. zeae-maydis*, showed the protein to be involved in photoreactivation, which is dependent on the expression of the CRP1 (WC-1 orthologue) (Bluhm and Dunkle, 2008). Furthermore, the PHL1 protein was shown to be the main regulator of photoreactivation by regulating the expression of a CPDI class protein (Figure 19 o - q). This cryptochrome family plays a role in growth and secondary metabolism in *C. zeae-maydis* and *E. turcicum,* but is dispensable for growth in *T. reesei* (Bluhm and Dunkle, 2008; Flaherty and Dunkle, 2005; Guzmán-Moreno et al., 2014). This cryptochrome class is not present in *N. crassa*. An orthologue of the 6-4 photolyase is present in the genome sequence of *C. zeina* and contains the PHR and FAD binding domains,

and is a 6-4 photolyase based on sequence similarity and monophyletic clustering with other characterised 6-4 photolyases.

Cyclobutane pyrimidine dimer photolyase class I (CPDI) is another cryptochrome present in fungi capable of double stranded DNA damage repair. In *C. zeae-maydis*, the expression of *cpd1* is regulated by the expression of the *phl1* gene, which is dependent of the light regulated expression of CRP1 (homologous to WC-1) (Kim et al., 2011). This regulation mechanism of photoreactivation is not conserved in fungi, where in *T. reesei* the expression of c*pd1* is not dependent of the expression of *phr1* (6-4 photolyase) (Guzmán-Moreno et al., 2014). It would be interesting to see if the *C. zeina cpd1* orthologue identified in this study shows the same PHL1 dependent regulation as seen in *C. zeae-maydis* (Figure 19 o – q), and whether or not asexual reproduction is influenced by this cryptochrome, which was an observation made in *T. atroviride* (Berrocal-Tito, 2007).

The function of the most recently identified cryptochrome class, CRY-DASH, is understudied in fungal species. Sequence analysis indicated that the C- terminal extension present in the other cryptochrome classes is absent in CRY-DASH proteins (Müller and Carell, 2009). This cryptochrome class does not function in photoreactivation, and its biological role is largely unknown at this stage. This study is the first report of CRY-DASH proteins present in *Cercospora* species. The genome sequences of both *C. zeina* and *C. zeae-maydis* contain a gene encoding a protein homologous to the CRY-DASH cryptochrome family. The characterised CRY-DASH protein from *N. crassa* showed non-specific binding to single and double stranded DNA and RNA (Froehlich et al., 2010). The ability of the *N. crassa* CRY-DASH protein to bind to RNA was attributed to the presence of arginine-glycine-glycine repeats (RGG) at the carboxyl-terminus (Froehlich et al., 2010). Until now, the presence of these RGG repeats was thought to be unique to *N. crassa*. However, the C-terminal end of the *C. zeina* CRY-DASH protein contains RGG repeating residues, which are believed to be involved in the maturation events of RNA (Godin and Varani, 2007). The disruption of CRY-DASH in *N. crassa* resulted in a phase-delay of the clock and the antiphasic expression of *cry-dash* and *frq* (Froehlich et al., 2010). This observation lead us to speculate that the function of CRY-DASH

in the circadian clock, is to regulate the stability of *frq* transcripts (Figure 19 s). The CRY-DASH cryptochrome is induced by light in a WC-1 dependent manner in *F. fujikuroi* and *N. crassa* (Castrillo et al., 2013; Froehlich et al., 2010), but not in *S. sclerotiorum* (Veluchamy and Rollins, 2008), where the cryptochrome is only induced through the UV-A light (Figure 19 t). The divergent functions of CRY-DASH in fungi open the opportunity to explore the functions of this protein and its role in the circadian clock in *C. zeina* and *C. zeae-maydis*.

2.6. Conclusion

In conclusion, the WC-1 protein is conserved across the fungal kingdom. The WC-1 orthologues from Basidiomycota show an independent evolution to those from Ascomycota and Zygomycota. Orthologues of the WC-1 proteins in Dothideomycetes group according to their respective lifestyle strategies. The LOV domains from WC-1 and plant blue light sensing proteins indicates an independent convergent evolution to control similar cellular processes. The synchronisation of the pathogen circadian rhythm to that of the plant could enhance the fitness of the pathogen during infection.

Cercospora zeina and *C. zeae-maydis* contain all the clock proteins required for the FRQ/WC oscillator. Conservation of the circadian clock proteins in *C. zeina* and *C. zeae-maydis* forming the FRQ/WC oscillator lead us to reason that similar circadian regulation of light responsive genes to that of *N. crassa* occur in these *Cercospora* species.

An alternative putative blue light photoreceptor to WC-1, CRY-DASH, is present in *C. zeina* and *C. zeae-maydis*, which remains to be characterised. Determining the function of this protein might prove to be difficult as WC-1 forms the central blue light photoreception unit. Functional characterisation and comparison of single and double mutants of both the *wc-1* and *cry-dash* orthologues in *C. zeina* might determine the actual role blue light plays in the growth and development of *C. zeina*. As a first step however we aim to characterise the function of the WC-1 orthologue in *C. zeina* followed by that of the CRY-DASH protein.

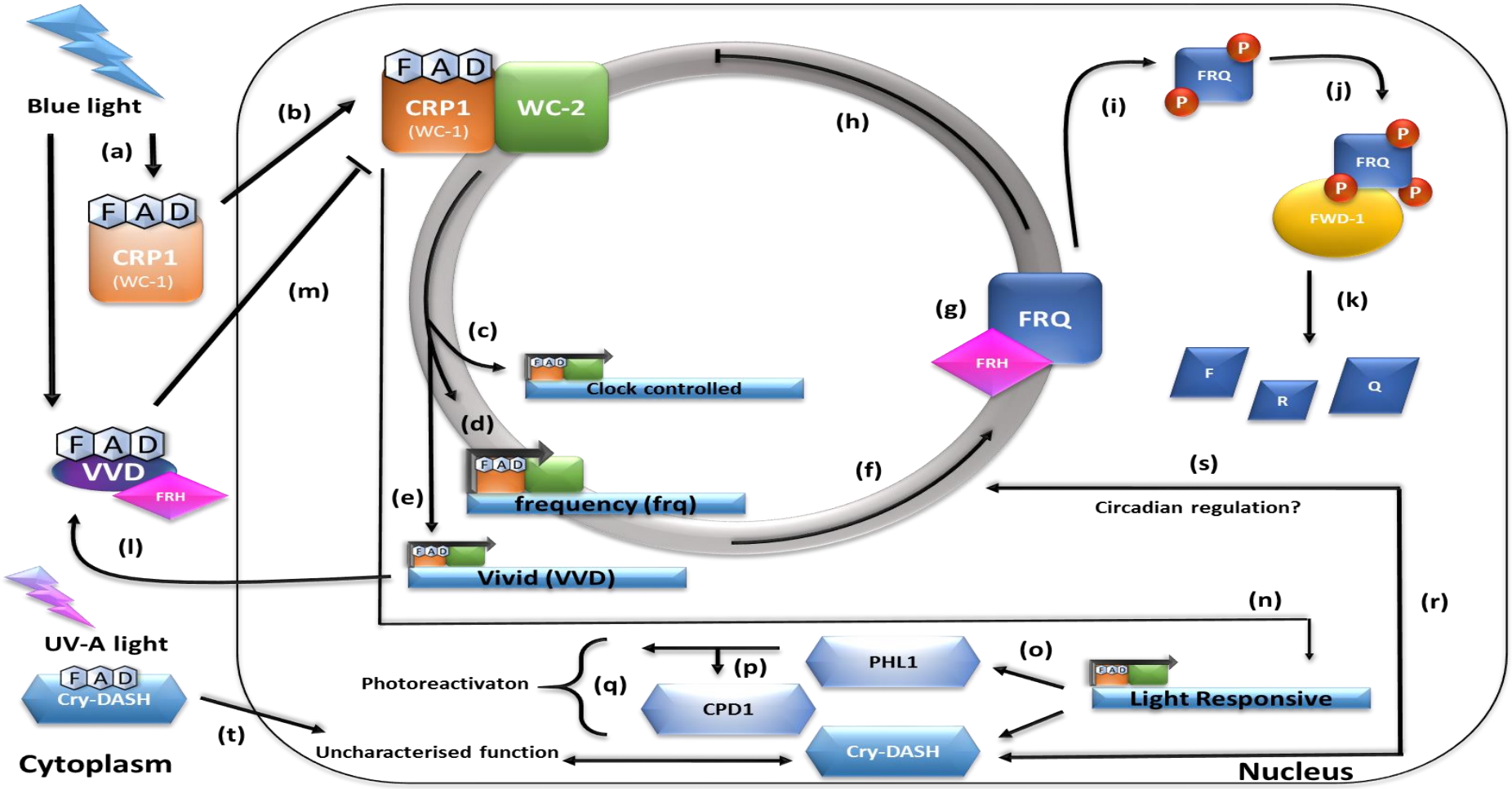

Figure 19. *Cercospora zeina* circadian clock and blue light photoreceptor interaction model. (a) The CRP1 (WC-1) protein is activated by blue light through FAD co-factor binding. (b) The activated CRP1 protein is translocated to the nucleus where it forms the WCC with WC-2. (c) The WCC activates the transcription of clock controlled genes, (d) frequency and (e) the vivid gene. (f) The concentration of FRQ increases during the day, where it interacts with (g) FRH and inhibits the (h) interaction of CRP1 and WC-2. (i) The FRQ-FRH complex is progressively phosphorylated, which (j) attracts binding of FWD-1 and (k) results in FRQ degradation. (l) The VVD protein is activated by light, which (m) inactivates CRP1. (n) Transcription of light responsive genes are activated by CRP1. (o) The cryptochrome PHL1 activates the transcription of the other (p) CPDI cryptochrome, which (q) activates photoreactivation. (r) The Cry-DASH cryptochrome is activated by the WCC, (s) which possibly affects the timing of the circadian clock. (t) The CRY-DASH protein is possibly activated by UV-A light. Circadian clock processes (a) to (m) adapted from Schmoll, 2011.

2.7. References

Altschul, S., 1997. Gapped BLAST and PSI-BLAST: a new generation of protein database search programs. *Nucleic Acids Res.* **25**, 3389–402.

Bayram, Ö., Biesemann, C., 2008. More than a repair enzyme: *Aspergillus nidulans* photolyase-like CryA is a regulator of sexual development. *Mol. Biol. Cell.* **19**, 3254-62.

Berrocal-Tito, G., 2007. *Trichoderma atroviride* PHR1, a fungal photolyase responsible for DNA repair, autoregulates its own photoinduction. *Eukaryot. Cell*. **6**, 1682-92.

Bluhm, B.H., Dunkle, L.D., 2008. PHL1 of *Cercospora zeae-maydis* encodes a member of the photolyase/cryptochrome family involved in UV protection and fungal development. *Fungal Genet. Biol.* **45**, 1364–72.

Bodor, Á.M., Stubnya, V., Ádám, a. L., Láday, M., Hornok, L., 2013. The white collar complex is essential for sexual reproduction but dispensable for conidiation and invasive growth in *Fusarium verticillioides*. *Acta Phytopathol. Entomol. Hungarica.* **48**, 1–18.

Briggs, W.R., Christie, J.M., 2002. Phototropins 1 and 2: versatile plant blue-light receptors. *Trends Plant Sci.* **7**, 204–10.

Brudler, R., Hitomi, K., Daiyasu, H., Toh, H., Kucho, K., Ishiura, M., Kanehisa, M., Roberts, V.A., Todo, T., Tainer, J.A., 2003. Identification of a new cryptochrome class structure, function, and evolution. *Mol. Cell*. **11**, 59–67.

Castrillo, M., García-Martínez, J., Avalos, J., 2013. Light-dependent functions of the *Fusarium fujikuroi* CryD DASH cryptochrome in development and secondary metabolism. *Appl. Environ. Microbiol*. **79**, 2777–88.

Castro-Longoria, E., Ferry, M., Bartnicki-Garcia, S., Hasty, J., Brody, S., 2010. Circadian rhythms in *Neurospora crassa*: dynamics of the clock component frequency visualized using a fluorescent reporter. *Fungal Genet. Biol.* **47**, 332–41.

Cheng, P., He, Q., Yang, Y., Wang, L., Liu, Y., 2003. Functional conservation of light, oxygen, or voltage domains in light sensing. *Proc. Natl. Acad. Sci. U.S.A.* **100**, 5938–43.

Cheng, P., Yang, Y., Liu, Y., 2001. Interlocked feedback loops contribute to the robustness of the *Neurospora* circadian clock. *Proc. Natl. Acad. Sci. U.S.A.* **98**, 7408–13.

Cheng, P., Yang, Y., Wang, L., He, Q., Liu, Y., 2003. White Collar-1, a multifunctional *Neurospora* protein involved in the circadian feedback loops, light sensing, and transcription repression of *wc-2*. *J. Biol. Chem.* **278**, 3801-08.

Christie, J.M., 2007. Phototropin blue-light receptors. *Annu. Rev. Plant Biol.* **58**, 21–45.

Coletta, A., Pinney, J.W., Solís, D.Y.W., Marsh, J., Pettifer, S.R., Attwood, T.K., 2010. Low-complexity regions within protein sequences have position-dependent roles. *BMC Syst. Biol.* **4**, 43.

Corrochano, L.M., 2007. Fungal photoreceptors: sensory molecules for fungal development and behaviour. *Photochem. Photobiol. Sci.* **6**, 725–36.

Corrochano, L.M., Garre, V., 2010. Photobiology in the *Zygomycota*: multiple photoreceptor genes for complex responses to light. *Fungal Genet. Biol.* **47**, 893–9.

Daiyasu, H., Ishikawa, T., Kuma, K., Iwai, S., 2004. Identification of cryptochrome DASH from vertebrates. *Genes to cell*. **9**, 479-95.

Demarsy, E., Fankhauser, C., 2009. Higher plants use LOV to perceive blue light. *Curr. Opin. Plant Biol*. **12**, 69–74.

Dunlap, J.C., Loros, J.J., 2006. How fungi keep time: circadian system in *Neurospora* and other fungi. *Curr. Opin. Microbiol.* **9**, 579–87.

Edgar, R.C., 2004. MUSCLE: multiple sequence alignment with high accuracy and high throughput. *Nucleic Acids Res.* **32**, 1792–7.

Eisen, J.A., Wu, M., 2002. Phylogenetic analysis and gene functional predictions: phylogenomics in action. *Theor. Popul. Biol.* **61**, 481-87.

Esser, C., Martin, W., Dagan, T., 2007. The origin of mitochondria in light of a fluid prokaryotic chromosome model. *Biol. Lett.* **11**, 180-84.

Estrada, A.F., Avalos, J., 2008. The White Collar protein WcoA of *Fusarium fujikuroi* is not essential for photocarotenogenesis, but is involved in the regulation of secondary metabolism and conidiation. *Fungal Genet. Biol.* **45**, 705–18.

Flaherty, J.E., Dunkle, L.D., 2005. Identification and expression analysis of regulatory genes induced during conidiation in *Exserohilum turcicum*. *Fungal Genet. Biol.* **42**, 471–81.

François, P., 2005. A model for the *Neurospora* circadian clock. *Biophys. J.* **88**, 2369–83.

Froehlich, A.C., Chen, C.-H., Belden, W.J., Madeti, C., Roenneberg, T., Merrow, M., Loros, J.J., Dunlap, J.C., 2010. Genetic and molecular characterization of a cryptochrome from the filamentous fungus *Neurospora crassa*. Eukaryot. *Cell.* **9**, 738–50.

Froehlich, A.C., Liu, Y., Loros, J.J., Dunlap, J.C., 2002. White Collar-1, a circadian blue light photoreceptor, binding to the frequency promoter. *Science.* **297**, 815–9.

Godin, K., Varani, G., 2007. How arginine-rich domains coordinate mRNA maturation events. *RNA Biol.* **4**, 69-75.

Guzmán-Moreno, J., Flores-Martínez, A., Brieba, L.G., Herrera-Estrella, A., 2014. The *Trichoderma reesei* Cry1 protein is a member of the cryptochrome/photolyase family with 6-4 photoproduct repair activity. *PLoS One*. **9**, e100625.

Hall, T., 1999. BioEdit: a user-friendly biological sequence alignment editor and analysis program for Windows 95/98/NT. *Nucleic Acids Symp. Ser*. **41**, 95-8.

He, Q., Cheng, P., Yang, Y., 2003. FWD1-mediated degradation of Frequency in *Neurospora* establishes a conserved mechanism for circadian clock regulation. *EMBO J.* **22**, 4421–30.

He, Q., Cheng, P., Yang, Y., Wang, L., Gardner, K.H., Liu, Y., 2002. White collar-1, a DNA binding transcription factor and a light sensor. *Science.* **297**, 840–3.

Hurley, J.M., Larrondo, L.F., Loros, J.J., Dunlap, J.C., 2013. Conserved RNA helicase FRH acts nonenzymatically to support the intrinsically disordered *Neurospora* clock protein FRQ. *Mol. Cell*. **52**, 832–43.

Idnurm, A., Verma, S., Corrochano, L.M., 2010. A glimpse into the basis of vision in the kingdom Mycota. *Fungal Genet. Biol.* **47**, 881–92.

Imaizumi, T., Schultz, T., Harmon, F., Ho, L., Kay, S., 2005. FKF1 F-box protein mediates cyclic degradation of a repressor of Constans in *Arabidopsis*. *Science.* **309**, 293-7

Jin, J., Cardozo, T., Lovering, R.C., Elledge, S.J., Pagano, M., Harper, J.W., 2004. Systematic analysis and nomenclature of mammalian F-box proteins. *Genes Dev.* **18,** 2573–80.

Kim, H., Ridenour, J.B., Dunkle, L.D., Bluhm, B.H., 2011. Regulation of stomatal tropism and infection by light in *Cercospora zeae-maydis*: evidence for coordinated host/pathogen responses to photoperiod. *PLoS Pathog*. **7**, e1002113.

Kim, Y., Choi, J., Lee, H., Lee, G., 2014. dbCRY: a Web-based comparative and evolutionary genomics platform for blue-light receptors. *Database*. doi:10.1093/database/bau037

Kleine, T., Lockhart, P., Batschauer, A., 2003. An *Arabidopsis* protein closely related to *Synechocystis* cryptochrome is targeted to organelles. *Plant J.* **35**, 93–103.

Kong, S.-G., Kinoshita, T., Shimazaki, K.-I., Mochizuki, N., Suzuki, T., Nagatani, A., 2007. The C-terminal kinase fragment of *Arabidopsis* phototropin 2 triggers constitutive phototropin responses. *Plant J.* **51**, 862–73.

Krauss, U., Minh, B.Q., Losi, A., Gärtner, W., Eggert, T., von Haeseler, A., Jaeger, K.-E., 2009. Distribution and phylogeny of light-oxygen-voltage-blue-light-signaling proteins in the three kingdoms of life. *J. Bacteriol.* **191**, 7234–42.

Kubo, H., 2009. Isolation of madA homologs in *Pilobolus crystallinus*. *Mycoscience*. **50**, 400–6.

Le, S., Gascuel, O., 2008. An improved general amino acid replacement matrix. *Mol. Biol. Evol.* **7**, 1307-20.

Lechner, E., Achard, P., Vansiri, A., Potuschak, T., Genschik, P., 2006. F-box proteins everywhere. *Curr. Opin. Plant Biol.* **9**, 631–8.

Lin, C., Shalitin, D., 2003. Cryptochrome structure and signal transduction. *Annu. Rev. Plant Biol.* **54**, 469-96

Linden, H., Macino, G., 1997. White collar 2, a partner in blue-light signal transduction, controlling expression of light-regulated genes in *Neurospora crassa*. *EMBO J.* **16**, 98–109.

Liversage, J., 2012. Functional characterisation of the *Cercospora zeina crp1* gene as a putative pathogensis regulation factor. Unpublished BSc (Hons) Dissertation, University of Pretoria.

Loros, J.J., Dunlap, J.C., 2003. Genetic and molecular analysis of circadian rhythms in *Neurospora*. *Ann. Rev. Physo.* **63**, 757-94.

Malzahn, E., Ciprianidis, S., Káldi, K., Schafmeier, T., Brunner, M., 2010. Photoadaptation in *Neurospora* by competitive interaction of activating and inhibitory LOV domains. *Cell*. **142**, 762–72.

McFadden, G.I., 2001. Chloroplast origin and integration. *Plant Physiol.* **125**, 50–53.

Mei, Q., Dvornyk, V., 2014. Evolution of PAS domains and PAS-containing genes in eukaryotes. *Chromosoma.* **123**, 385–405.

Meisel, B., Korsman, J., Kloppers, F.J., Berger, D.K., 2009. *Cercospora zeina* is the causal agent of grey leaf spot disease of maize in southern Africa. *Eur. J. Plant Pathol.* **124**, 577–83.

Müller, M., Carell, T., 2009. Structural biology of DNA photolyases and cryptochromes. *Curr. Opin. Struct. Biol.* **19**, 277-85.

Nakasako, M., Zikihara, K., Matsuoka, D., Katsura, H., Tokutomi, S., 2008. Structural Basis of the LOV1 Dimerization of *Arabidopsis* Phototropins 1 and 2. *J. Mol. Biol.* **381**, 718–33.

Ogdenw, T.H., Rosenberg, M.S., 2006. Multiple sequence alignment accuracy and phylogenetic inference. *Syst. Biol.* **55**, 314–28.

Ohm, R. a, Feau, N., Henrissat, B., Schoch, C.L., Horwitz, B. a, Barry, K.W., Condon, B.J., Copeland, A.C., Dhillon, B., Glaser, F., Hesse, C.N., Kosti, I., LaButti, K., Lindquist, E. a, Lucas, S., Salamov, A. a, Bradshaw, R.E., Ciuffetti, L., Hamelin, R.C., Kema, G.H.J., Lawrence, C., Scott, J. a, Spatafora, J.W., Turgeon, B.G., de Wit, P.J.G.M., Zhong, S., Goodwin, S.B., Grigoriev, I. V, 2012. Diverse lifestyles and strategies of plant pathogenesis encoded in the genomes of eighteen Dothideomycetes fungi. *PLoS Pathog*. **8**, e1003037.

Olmedo, M., Ruger-Herreros, C., Luque, E.M., Corrochano, L.M., 2010. A complex photoreceptor system mediates the regulation by light of the conidiation genes *con-10* and *con-6* in *Neurospora crassa*. *Fungal Genet. Biol.* **47**, 352–63.

Pettersen, E., Goddard, T., 2004. UCSF Chimera—a visualization system for exploratory research and analysis. *J. Comput. Chem.* **13**, 1605-12.

Rausch, T., Emde, A.-K., Weese, D., Döring, A., Notredame, C., Reinert, K., 2008. Segment-based multiple sequence alignment. *Bioinformatics.* **24**, 187–92.

Salichos, L., Rokas, a., 2009. The diversity and evolution of circadian clock proteins in fungi. *Mycologia.* **102**, 269–78.

Salomon, M., Christie, J.M., Knieb, E., Lempert, U., Briggs, W.R., 2000. Photochemical and mutational analysis of the FMN-binding domains of the plant blue light receptor, Phototropin. *Biochem.* **39**, 9401–10.

Salomon, M., Lempert, U., Rüdiger, W., 2004. Dimerization of the plant photoreceptor phototropin is probably mediated by the LOV1 domain. *FEBS Lett*. **572**, 8–10.

Schafmeier, T., Haase, A., Káldi, K., Scholz, J., Fuchs, M., Brunner, M., 2005. Transcriptional feedback of *Neurospora* circadian clock gene by phosphorylation-dependent inactivation of its transcription factor. *Cell.* **122**, 235–46.

Schoch, C.L., Sung, G.-H., López-Giráldez, F., Townsend, J.P., Miadlikowska, J., Hofstetter, V., Robbertse, B., Matheny, P.B., Kauff, F., Wang, Z., Gueidan, C., Andrie, R.M., Trippe, K., Ciufetti, L.M., Wynns, A., Fraker, E., Hodkinson, B.P., Bonito, G., Groenewald, J.Z., Arzanlou, M., de Hoog, G.S., Crous, P.W., Hewitt, D., Pfister, D.H., Peterson, K., Gryzenhout, M., Wingfield, M.J., Aptroot, A., Suh, S.-O., Blackwell, M., Hillis, D.M., Griffith, G.W., Castlebury, L. a, Rossman, A.Y., Lumbsch, H.T., Lücking, R., Büdel, B., Rauhut, A., Diederich, P., Ertz, D., Geiser, D.M., Hosaka, K., Inderbitzin, P., Kohlmeyer, J., Volkmann-Kohlmeyer, B., Mostert, L., O'Donnell, K., Sipman, H., Rogers, J.D., Shoemaker, R. a, Sugiyama, J., Summerbell, R.C., Untereiner, W., Johnston, P.R., Stenroos, S., Zuccaro, A., Dyer, P.S., Crittenden, P.D., Cole, M.S., Hansen, K., Trappe, J.M., Yahr, R., Lutzoni, F., Spatafora, J.W., 2009. The Ascomycota tree of life: a phylum-wide phylogeny clarifies the origin and evolution of fundamental reproductive and ecological traits. *Syst. Biol. 58*, 224–39.

Selby, C., Sancar, A., 2006. A cryptochrome/photolyase class of enzymes with single-stranded DNA-specific photolyase activity. *Proc. Natl. Acad. Sci. U.S.A.* **103**, 17696-700

Sinha, R., Häder, D., 2002. UV-induced DNA damage and repair: a review. Photochem. *Photobiol. Sci*. **1**, 225-36.

Suetsugu, N., Wada, M., 2013. Evolution of three LOV blue light receptor families in green plants and photosynthetic stramenopiles: phototropin, ZTL/FKF1/LKP2 and aureochrome. *Plant Cell Physiol*. **54**, 8–23.

Swofford, D.L., 1998. PAUP*: Phylogenetic Analysis Using Parsimony (and other methods) 4.0.b5.

Tamura, K., Stecher, G., Peterson, D., 2013. MEGA6: molecular evolutionary genetics analysis version 6.0. *Mol. Biol.* **30**, 2725-29.

Thompson, C., Sancar, A., 2002. Photolyase/cryptochrome blue-light photoreceptors use photon energy to repair DNA and reset the circadian clock. *Oncogene.* **21**, 9043-56.

Timmis, J., Ayliffe, M., Huang, C., Martin, W., 2004. Endosymbiotic gene transfer: organelle genomes forge eukaryotic chromosomes. *Nat. Rev. Genet.* **5**, 123-35.

Van der Horst, M.A., Key, J., Hellingwerf, K.J., 2007. Photosensing in chemotrophic, non-phototrophic bacteria: let there be light sensing too. *Trends Microbiol.* **15**, 554–62.

Veluchamy, S., Rollins, J.A., 2008. A CRY-DASH-type photolyase/cryptochrome from *Sclerotinia sclerotiorum* mediates minor UV-A-specific effects on development. *Fungal Genet. Biol.* **45**, 1265–76.

Wang, H., Xu, Z., Gao, L., Hao, B., 2009. A fungal phylogeny based on 82 complete genomes using the composition vector method. *BMC Evol. Biol*. **9**, 195.

Wang, J., Levy, M., Dunkle, L.D., 1998. Sibling species of *Cercospora* associated with gray leaf spot of maize. *Phytopathology*. **88**, 1269–75.

Whelan, S., Goldman, N., 2001. A general empirical model of protein evolution derived from multiple protein families using a maximum-likelihood approach. *Mol. Biol. Evol.* **18**, 691-9.

Yada, M., Hatakeyama, S., Kamura, T., Nishiyama, M., Tsunematsu, R., Imaki, H., Ishida, N., Okumura, F., Nakayama, K., Nakayama, K.I., 2004. Phosphorylation-dependent degradation of c-Myc is mediated by the F-box protein Fbw7. *EMBO J.* **23**, 2116–25.

Yu, J., Rubio, V., Lee, N., Bai, S., Lee, S., Kim, S., 2008. COP1 and ELF3 control circadian function and photoperiodic flowering by regulating GI stability. *Mol. Cell.* **32**, 617-30.

Functional Genetics

Chapter 3

Functional characterisation of the *Cercospora zeina crp1* gene as a putative pathogenesis regulation factor

3.1. Abstract

Grey leaf spot (GLS) is a devastating maize foliar disease caused by *Cercospora zeina* in South Africa. The fungal circadian clock regulates various aspects of pathogenesis including the fungus' ability to perceive and orientate growth towards the plant's stomata. The limiting component of the circadian clock, as identified in *Neurospora crassa*, is the putative blue-light receptor, White Collar-1 (WC-1). The *Cercospora* Regulator of Pathogenesis (*crp1*) gene from *Cercospora zeae-maydis* encodes a putative blue-light receptor homologous to the WC-1 protein. Functional characterisation of the CRP1 protein in *C. zeina* was performed through gene disruption with split marker constructs, which replaced the *crp1* gene with a hygromycin resistance gene cassette. The generated transformants were cultured and screened for the presence and correct genomic location of the hygromycin resistance gene. The inability of the knockout strains to sense blue light contributed to the fungus forming a higher concentration of conidia in the presence of light, compared to the wild type *C. zeina,* which could only effectively produce conidia in the dark. Additionally, the disrupted gene altered the way melanin was deposited in the *C. zeina crp1* knock-outs. Pathogenesis of the *Δcrp1 C. zeina* cultures was tested through a maize infection trial and subsequent confocal microscopy, which revealed a reduction in infection structure formation compared to the wild type. In conclusion, these experiments suggest that *crp1* plays a role in the pathogenesis of *C. zeina* on maize.

3.2. Introduction

Grey leaf spot is a globally important maize foliar disease, which causes yield losses due to a reduction in the plants photosynthetic capability. The disease is caused by two genetically distinct, but morphologically similar species. *Cercospora zeina* and *Cercospora zeae-maydis* are the main causal agents for GLS in Africa and USA, respectively (Meisel et al., 2009). The two haploid, ascomycete fungal species belongs to the class Dothideomycetes. The pathogens are hemibiotrophs, and first infect and colonise the host tissue during the biotrophic life cycle after which the pathogens cause host cell death during the necrotrophic stage resulting in blighting of the leaves as the disease progresses (Kim et al., 2011).

The spread of GLS throughout maize production areas has increased due to the incorporation of conservation practices, which includes the adoption of minimum to no-tillage farming practices (Latterell and Rossi, 1983; Ward and Stromberg, 1999). The two key factors favouring disease development are relative humidity and temperature (Ward and Stromberg, 1999). It was shown that relative humidity greater than 95% is needed for optimal elongation of the *C. zeina* germ tube from conidia (Thorson and Martinson, 1993). The wetness of the leaf surface was also identified as a factor that aids in the germination and survival of spores (Beckman and Payne, 1983). Currently the disease is managed through combining the use of tolerant hybrids, crop rotation and fungicide applications. Crop rotation reduces the presence of inoculation build up between growing seasons (Bhatia and Munkvold, 2002.; Munkvold et al., 2001; Ward et al., 1999).

3.2.1. Cercosporin as a pathogenesis factor.

Cercospora species are known to produce a phytotoxic compound known as cercosporin. The phytotoxin is a light-activated perylenequinone toxin that is encoded by a cercosporin biosynthetic gene cluster (Chen et al., 2007). Cercosporin is responsible for the production of reactive oxygen species that have been shown to be important pathogenicity factors resulting in plant cell death (Upchurch et al., 1991). *Cercospora zeae-maydis* produces cercosporin, but thus far no evidence exists for the *in vitro* production of cercosporin in *C. zeina*. The expression of the biosynthetic gene

cluster is activated by light, which is an indication that a photoreceptor is needed for the production of cercosporin (Kim et al., 2011). It is believed that the formation of lesions are the result of alternating between invasive growth during the day and colonising of host tissue at night (Kim et al., 2011). Once the pathogen has infiltrated the plant intracellular space, light would activate the production and secretion of cercosporin that would cause host cell death followed by the production of conidia at night (Kim et al., 2011).

3.2.2. Functional characterisation of pathogenicity factors.

Studying the molecular basis of pathogenesis requires the identification and functional characterisation of virulence factors. Only three genes thus far have been functionally characterised in *C. zeae-maydis*. The first characterised gene was *czk3*, which encodes a MAP kinase kinase kinase that is involved in the formation of conidia and cercosporin production (Shim and Dunkle, 2003). A 6-4 photolyase encoded by *phl1* was found to play an important role for photoreactivation, and is able to repair DNA damage following ultra violet (UV) light exposure (Bluhm and Dunkle, 2008). Lastly, the *crp1* gene, which is homologous to the WC-1 *N. crassa* blue light photoreceptor, was functionally characterised through targeted gene disruption (Kim et al., 2011). The CRP1 protein characterisation revealed that multiple aspects of pathogenesis are under the control of blue light. Kim et al. (2011) showed that blue light is responsible for the inhibition of conidia production and partially regulates cercosporin production. Cercosporin production, however, is not solely regulated by blue light, but might involve the interaction of an alternative uncharacterised photoreceptor (Kim et al., 2011). Furthermore, the CRP1 protein was shown to regulate photoreactivation, thorough the expression of the previously characterised *phl1* gene (Kim et al., 2011). The pathogenicity of *C. zeae-maydis* was severely reduced in the absence of a functional *crp1* gene, which indicated that the ability of the pathogen to sense and reorient its growth towards the stomata is regulated by the CRP1 protein (Kim et al., 2011).

3.2.3. Molecular characterisation of pathogenesis.

Forward genetics relies on studying the function of a specific gene under controlled conditions by disrupting the expression of the gene. Falkow's molecular version of Koch's postulates is based on studying pathogenesis at a

molecular level through disruption of a specific gene followed by complementation as proof of pathogenesis (Falkow, 1988). DNA-mediated transformation is used to replace the target gene through homologous recombination. The transformation event results either in abolishing gene expression or a modified strain is produced where a truncated version of the gene is transcribed. Effective analysis of single gene function is achieved through site specific homologous recombination (Kück and Hoff, 2010).

3.2.4. Methods to study gene function.

There are three types of transformation events that result in either a truncated transcript (knock-in), no expression of the target gene (knock-out) or silencing of the targeted gene resulting in reduced gene expression through RNA interference (RNAi). The knock-in approach relies on inserting a foreign DNA sequence into the target gene, whereas a in a knock-out approach the target gene is replaced by a selectable marker gene. Both of these approaches are used when the function of a single copy gene is to be analysed. RNA interference is particularly useful when a multi copy gene is to be studied where the gene is not removed or modified but the transcript level is reduced resulting in varying levels of silencing of the target gene (Kück and Hoff, 2010).

3.2.5. Homologous recombination.

In filamentous fungi homologous recombination events are very rare and occur at frequencies less than 1% (Kück and Hoff, 2010). Typical transformation events based on homologous recombination results in a high frequency of ectopic insertions, which means that a large number of colonies need to be screened to identify true transformants (Pratt and Aramayo, 2002). These problems lead to the development of the split marker transformation approach, which was initially developed for *S. cerevisiae* (Fairhead et al., 1996). The split marker technology requires the transformation of two PCR fragments consisting of overlapping regions of a selectable marker generated by a single overlap extension (SOEing) PCR (Fu et al., 2006). In theory, colonies will only grow on media supplemented with the selection agent if three cross over events (between the flanking and the overlapping selectable marker regions) occurred, which results in the generation of a functional selectable marker gene that displaces the target gene.

3.2.6. Split marker technology.

Gene disruption through the split marker approach generates a high number of specific homologous integration events. Integration events as high as 60% have been reported, but the success of transformation is dependent on the target gene, the strain and species involved as well as the selectable marker used (You et al., 2009). The length of the flanking regions for homologous recombination in filamentous fungi is required to be at least 0.5 kb, with higher transformation frequencies occurring with longer fragments of homologous DNA (Nelson et al., 2003). Split marker technology gives rise to a reduced frequency of ectopic insertions, which means that the approach is less time consuming and requires the screening of fewer transformants (You et al., 2009).

3.2.7. Aims and hypotheses.

The molecular basis of pathogenicity of *C. zeina* is unknown. In this study we aimed to functionally characterise the *C. zeina* orthologue of the CRP1 blue light photoreceptor previously characterised in *C. zeae-maydis*. We hypothesised that the CRP1 protein plays a role in pathogenesis of *C. zeina*. However, characterisation of the blue light photoreceptor orthologue, WC-1, in *Fusarium* species showed that the role played by the protein in growth and development is not conserved in closely related species (Bodor et al., 2013; Estrada and Avalos, 2008). We aimed to test whether the split marker technology could be applied to perform the first reported gene disruption in *C. zeina*. Furthermore, we aimed to elucidate whether or not the CRP1 protein played a role in the growth and development of *C. zeina*.

3.3. Materials and Methods

All chemicals were purchased from Sigma-Aldrich (Aston Manor, South Africa) unless otherwise stated.

3.3.1. Generation of *crp1* split marker constructs

The *Cercospora zeina crp1* gene was disrupted using the split marker approach (Liversage, 2012). Briefly, the 5'- and the 3'-flanking regions of the *crp1* gene were fused to overlapping fragments of the hygromycin cassette containing the hyg^R gene under the control of the *trpC* promoter through a SOEing PCR as outlined in Figure 2. Fungal protoplasts were generated and transformed with the 5'-construct (5'-flank + HY fragment) and the 3'- construct (YG fragment + 3'-flank). A functional hygromycin resistance gene will be formed if three cross over events occurred enabling the transformed colonies to grow on media supplemented with hygromycin B (Figure 2). The transformed protoplasts were regenerated on regeneration media supplemented with increasing concentrations of hygromycin B (0 – 90 µg/ml). The wild type *C. zeina* strain was cultured on V8® media supplemented with increasing concentrations of hygromycin B ranging from 0 – 120 µg/ml in order to determine what antibiotic concentration would inhibit the growth of the wild type strain (M.B.L. Malefo, personal communication). Colonies growing on the media supplemented with 60 µg/ml and 90 µg/ml were transferred to V8® media supplemented with 90 µg/ml (Liversage, 2012).

3.3.2. DNA sequencing of split marker constructs and gene fragments

The split marker DNA fragments used to transform the fungal protoplast were cloned and sequenced to verify their identity. The 5'- and 3'-constructs were cloned into the pJET1.2/blunt vector using the CloneJet™ PCR cloning kit (ThermoFisher Scientific, Waltham, USA) according to the manufacturer's specifications. Competent *Escherichia coli* cells, DH5α strain (Taylor et al., 1993), were prepared using the $CaCl_2$ method (Nishimura et al., 1990). Transformation of competent *E. coli* cells was performed using the heat-shock method (Froger et al., 2007). As a positive transformation control 5.8 ng of the supercoiled pAHC25 plasmid (Christensen and Quail, 1996) was used to transform the competent cells and a negative control to which no DNA was added. The transformation reactions were plated out

in duplicate onto LB agar selective media supplemented with 100 µg/ml ampicillin. Putative transformed *E. coli* colonies were selected and screened in a colony PCR using the pJet 1.2 primer set (CloneJet™ PCR Cloning kit, ThermoFisher Scientific, Waltham, USA). The PCR reactions were set up in a total volume of 10 µl, which consisted of: 1 x KAPA2G Robust HotStart ReadyMix (KapaBiosystems, Wilmington, Massachusetts), 0.5 µm of each primer. The thermal cycler conditions of the BioRAD S100™ for the two primer sets were as follow: 95°C for five minutes, and 25 cycles of 95°C for 20 seconds, 61°C for 30 seconds, and 72°C for 40 seconds, which was followed by a final extension step of 72°C for five minutes.

Plasmid extraction was performed on selected positive PCR screened transformed *E. coli* colonies using the Zippy™ Plasmid Miniprep kit (Zymo Research, Irvine, California, USA) according to the manufacturer's specifications. A restriction digest was performed on the extracted plasmids to confirm the *in silico* assembly of the 5'-HY and 3'-YG construct sequences. The 5'-HY digests were performed by a single BglII digest and BglII+EcoRI, SalI + EcoRI and BglII + BamHI double digests. The 3'-YG digest were performed by a single BglII digest and a BglII + BamHI double digest. All the restriction digests were performed using FastDigest™ restriction enzymes (Life technologies, Carlsbad, USA) according to the manufacturer's specifications with one microgram of plasmid DNA incubated at 37°C. The sequencing reactions were setup using the BigDye® Terminator v3.1 Cycle Sequencing kit (Applied Biosystems, CA, USA) according to the manufacturer's guidelines using 400 ng plasmid DNA per sequencing reaction. The sequencing primers used for the 5'-HY construct were: pJetF, M13F, HYG_F_New, YG-N, HY-N and pJetR. The primers used for the 3'-YG construct were: pJetF, M13R, HYG_R_New, HY-N, YG-N and pJetR. The cycle sequencing conditions were as follows: 95°C for five minutes, followed by 25 cycles of 95°C for 30 seconds, 58°C for 10 seconds and 60°C for four minutes.

The products of the cycle sequencing were purified by filtration through a 20 µm receiver column containing Sephadex® G50 resin, which removes unincorporated dNTPs and primer dimers through size exclusion. The Sephadex® G50 purification columns were prepared by rehydrating three gram Sephadex® G50 resin in 45 ml distilled water through incubation at

room temperature for at least 60 minutes. A 20 µm receiver column was placed into a collection tube. The rehydrated Sephadex® G50 was added to the receiver column and centrifuged at 2000 rpm for two minutes after which the flow-through was discarded. The formed column was subjected to an additional centrifugation step at 2000 rpm for a minute to remove any residual water. The cycle sequencing products were purified using the prepared Sephadex® G50 columns placed into a 1.5 ml microcentrifuge tube. The PCR products were placed onto the middle of the column and centrifuged at 2000 rpm for two minutes followed by an additional centrifugation step at 2000 rpm for a minute. The purified sequencing reactions were sent to the DNA sequencing Facility of the Natural and Agricultural faculty at the University of Pretoria. The trace files were analysed and edited in CLC Bio Main workbench 6.9.

3.3.3. Fungal cultures and growing conditions

The wild type *Cercospora zeina* (Mkushi) strain (Meisel et al., 2009) was cultivated from glycerol stocks prepared from conidia isolated from a previous greenhouse maize infection trial (Velushka Swart, personal communication). The cultures were grown on V8® media (3.5 mg/ml $CaCO_3$, 20 mg/ml Bacteriological agar and 1:5 Campbell's V8® Original juice) in constant darkness at room temperature to induce conidiation. Sub-culturing onto fresh V8® media plates was performed every five to seven days. Glycerol stocks of putative *Δcrp1* knock-out strains were cultured on V8® media, but supplemented with 90 µg/ml HyClone™ Hygromycin B solution (Fisher Scientific, Waltham, MA, USA).

3.3.4. Genomics DNA isolation from *Cercospora zeina* cultures

All centrifugation steps were performed at room temperature for ten minutes unless otherwise stated.

3.3.4.1. Rapid DNA extraction method

Various rapid DNA extraction methods were tested of which a modified rapid fungal DNA isolation protocol was developed which provided the most acceptable quality DNA. Single colonies were picked from the individual cultures and homogenised in a 1.5 ml microcentrifuge tube containing 500 µl urea-lysis buffer (0.42 g/ml urea, 5 M NaCl, 2 M Tris-

HCl, 0.5 M EDTA and 1% SDS), pH 8. The homogenised tissue was mixed and incubated at room temperature for ten minutes. An equal volume of phenol:chloroform:IAA (24:24:1) was added, mixed and centrifuged. The resulting aqueous phase was transferred to a 1.5 ml microcentrifuge tube containing an equal volume of chloroform:IAA (24:1), which was mixed and centrifuged. Contaminating RNA was removed, by treating the aqueous phase with 1 µl of a 10 mg/ml RNAseA solution, which was incubated at 37°C for 30 minutes. The DNA in the solution was precipitated by adding 0.1 volume of 3 M sodium acetate and 2.2 volumes 100% ethanol, which was incubated at -20°C for 30 minutes. The precipitated DNA was pelleted during centrifugation after which the DNA pellet was washed with 70% ethanol and re-suspended in 20 µl 1 x TE Buffer (10 mM Tris-HCl and 1 mM EDTA, pH 8.0).

3.3.4.2. Large scale genomic DNA isolation

The large scale isolation of inhibitor-free DNA proved to be difficult. The best method providing high yields was the CTAB method (Möller and Bahnweg, 1992) with minor modifications. The composition of the CTAB buffer was modified to contain 7 M urea and a phenol:chloroform:IAA clean up step was added. The fungal strains were cultured on cellophane sheets, which separated inhibitors such as melanin from the fungal culture. The best method however to isolate inhibitor free DNA was to use the ZR Fungal/Bacterial DNA Midi™ isolation kit (Zymo Research, Irvine, California, USA) according to the manufacturer's specifications with minor modifications. The fungal tissue was cultured for seven days on cellophane sheets placed on V8® media, which was removed and ground under liquid nitrogen. One gram of the ground fungal tissue was added to a ZR BashingBead™ Lysis/Filtration Tube, which contained six millilitre Fungal/Bacterial DNA Binding Buffer. The samples were processed on a vortex at high speed for 15 minutes to ensure complete homogenisation of the fungal tissue. The DNA was eluted from the column by adding 150 µl of DNA Elution Buffer.

3.3.5. Quality and quantity of nucleic acids

3.3.5.1 Spectrophotometric quantification of nucleic acids

The quality of nucleic acids was analysed on the Thermo Scientific Nanodrop™ 2000 spectrophotometer (ThermoFisher Scientific, Waltham, USA). The spectrophotometer was

calibrated with the same solution used to elute the nucleic acids from silica columns (1x TE buffer) or the dH_20 used to dilute samples. The purity of the nucleic acid solution is shown by the adsorption ratio at 260/280, which should fall within the range of 1.8 and 2.0 for protein free DNA samples (Wilfinger et al., 1997). The adsorption ratio at 260/230 indicates if the sample is free from contamination with phenol and urea if the value is greater than 2.0 (Wilfinger et al., 1997).

3.3.5.2. Agarose gel electrophoresis of nucleic acids

The integrity of the DNA was tested through gel electrophoresis using a 0.8% agarose gel. The volume of agarose needed for the casting tray was calculated by using the following formula:

Agarose volume = gel width (cm) x gel length (cm) x gel thickness (cm)

The size of the gel tray used was 10 cm x 15 cm with a desired gel thickness of 0.5 cm. For a 0.8% agarose gel 0.6 g agarose was weighed out and dissolved in 75 ml 1x TAE buffer (prepared from 50x TAE buffer; 2 M Tris-acetate, 50 mM EDTA, pH 8 at 25°C). After the agarose has been completely dissolved through heating and left to cool to about 60°C, ethidium bromide was added at a final concentration of 0.5 µg/ml and swirled to mix. The agarose was poured into the casting tray with the comb inserted and left to cool for about 20 minutes. The comb was removed and the casting tray placed into the gel tank, which was filled with the appropriate volume of 1 x TAE buffer. A small aliquot of the DNA sample (10 µl) was mixed with 6x loading buffer (30% glycerol, 0.25% bromophenol blue) at a 2:5 ratio. The samples were loaded into the well and ran at 7V per cm of the gel length. The DNA separated on the agarose gel was visualised under ultra-violet (UV) light using the Molecular Imager® Gel Doc™ XR System equipped with the Image Lab™ software (Bio-Rad laboratories, USA).

3.3.6. Genotypic characterisation of putative *Cercospora zeina Δcrp1* knock-outs

The quality of the isolated genomic DNA was tested through the amplification a fragment of the endogenous histone H3 gene using a primer set specific to *C. zeina* (Crous et al., 2006), in Table 1. The presence of the entire inserted hygromycin (*hyg*) cassette, consisting of the hygromycin resistance gene under the control of the tryptophan synthetase gene (*trpC*)

promoter (B.H. Bluhm, personal communication), was screened for by using the M13 primer set and an internal *hyg*^{R} screen (HYG_ScrnF + HYG_ScrnR) primer sets (Velushka Swart, personal communication) (Table 1). The M13 primer set binds outside the *hyg* cassette, whereas the internal *hyg*^{R} primer set binds to the 5'-region of the *trpC* promoter and the 3'-end of the *hyg*^{R} gene (Figure 1).

The PCR reactions were set up in a total volume of 10 µl, which consisted of: 1 x KAPA2G Robust HotStart ReadyMix (KapaBiosystems, Wilmington, Massachusetts), 0.5 µm of each primer. Dimethyl sulfoxide (DMSO) and Bovine Serum Albumin (BSA) were added at 9% and 0.8 µg/µl respectively. The amount of the template DNA added to the PCR reaction was 50 ng.

Table 1. Primer sets used for genomic characterisation of putative *Δcrp1* knock-outs.

Name	Primer sequence (5'-3')	Tm (°C)	Amplicon size (bp)	Gene/region amplified
M13F	GTAAAACGACGGCCAGT	52.6	1549	*Hyg*-cassette
M13R	CAGGAAACAGCTATGAC	47		
CzHist	TCGAGTGGCCCTCACCGT	61.5	284	Histone H3
CYLH3R	AGCTGGATGTCCTTGGACTG	56.9		
HYG_ScrnF	CGCTCGAAGTGTGACTCTTATT	62	1186	*Hyg*-cassette
HYG_ScrnR	GGCGTCGGTTTCCACTATC	62		
HY-N	TAGCGCGTCTGCTGCTCCATACAAG	56	428	Internal *hyg*^{R}
YG-N	ACCGAACTGCCCGCTGTTCTC	61		
Ext5_crp1	CGGTGTTGGACGAGGCATAGA	63	888	5'-genomic screen
Ext5_HY	GCCGCCGCTACTGCTACAA	62		
Ext3_YG	GTCCGAGGGCAAAGGAATAGAGTA	63	1052	3'-genomic screen
Ext3_crp1	CGCACATGGTCACGCCTTGATT	67		
qCrp1_F	CGTCACACCTGAATGGAGAAGA	60	134	3'-*crp1* intron
qCrp1_R	CGCTGTGGACGCTTTGTTG	60		
LOV_crp1_F	ATCGACCATGAGCGGCAAG	64	706	*Crp1* LOV domain
LOV_crp1_R	GATGGATCCGGACCGTTCA	63		
Crp1_frag_F	CATGCTTGCCGAAGAAGTG	61	710	3'-*crp1* fragment
Crp1_frag_R	GAAGTCCGTCTCGCAAATG	60		

The thermal cycler conditions of the BioRAD S100™ (Bio-Rad laboratories, USA) for the genomic characterisation primer sets were as follow: 95°C for five minutes, and 30 cycles of 95°C for 20 seconds, 60°C for 30 seconds, and 72°C for 40 seconds, which was followed by a final extension step of 72°C for five minutes. The annealing temperature for the *hyg*^{R} screening primer set was 62°C. A negative water control was included, which enables one to detect nucleic acid contamination of the PCR reagents. As a positive control the pTA-Hyg plasmid (containing the *hyg*-cassette flanked by M13 regions) served as an indicator for the efficacy of the reaction setup.

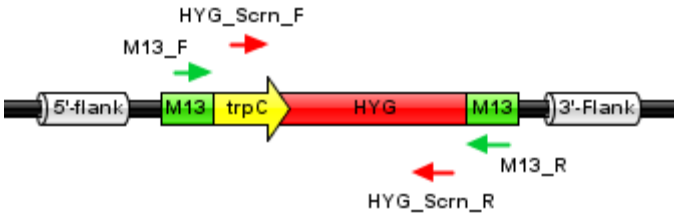

Figure 1. Primer binding sites to the inserted hygromycin resistance gene. The M13 forward and reverse primer set binds to regions on either side of the inserted hygromycin cassette consisting of the hygromycin resistance gene (*hyg*^{R}) under the control of the *trpC* promoter. The second *hyg*^{R} primer set binds to the *trpC* promoter and the 3'-end of the *hyg*^{R} open reading frame.

Following confirmation of the presence of the complete *hyg*-cassette, we determined whether or not the individual constructs (5'-construct and 3'-construct) inserted into the correct genomic location. For this purpose primers were designed to the external regions of the inserted constructs, which bind to the regions up and down stream of the endogenous *crp1* gene. Furthermore, new primers were designed to bind to the 5' and 3' regions of the *hyg*^{R} gene as seen in Figure 2. The primer sets were designed manually, with the compatibility, dimer and hairpin formation, and the stability of the 3' regions of the primer sets tested on NETprimer (http://premierbiosoft.com/netprimer/). The PCR setup and thermal cycler conditions for the external primer sets (Ext5_crp1 + Ext5_HY and Ext3_YG + Ext3_crp1) were the same as for the previous primer sets with an annealing temperature of 62°C.

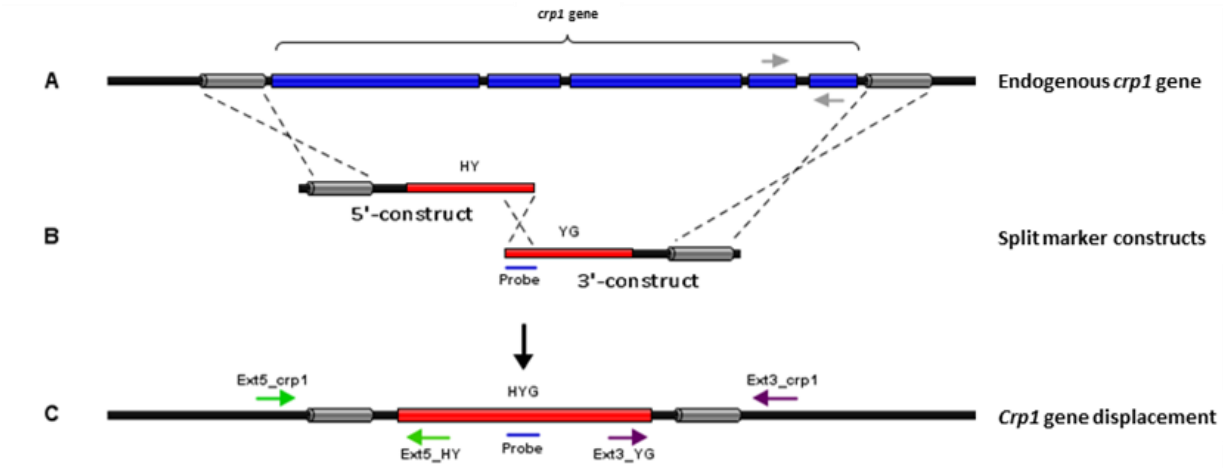

Figure 2. Split marker process overview and characterisation. (A) Representation of the endogenous *crp*1 gene (blue) with its four introns and flanking regions (grey). The primer set (grey) spanning the last intron was used to test the expression of the *crp*1 gene. (B) The two generated split marker constructs (5'-flank + HY and YG + 3'-flank) and their homologous overlapping regions indicated by the dashed lines. (C) The integrated hyg^R gene flanked by the endogenous *crp*1 flanking regions. The external primer pairs for the 5' and 3' regions are Ext5_crp1+Ext5_HY (green) and Ext3_YG+Ext_crp1 (purple). The probe designed to determine the number of copies of the 5' and 3'-constructs integrated is indicated by the blue line.

3.3.7. Determination of copy number of split-marker constructs

3.3.7.1. Preparation of DIG-labelled probe

The *hyg*^{R} probe was generated using the PCR DIG Probe Synthesis Kit (Roche Diagnostics, Germany). The template DNA was the pTA-Hyg plasmid. The optimised PCR reaction conditions mentioned for the *hyg*^{R} primer sets were used for the amplification of the probe using the internal *hyg*^{R} primer set (HY-N + YG-N). The 25 µl reaction volume for preparation of the Digoxigenin-11-dUTP (DIG) labelled hygromycin (hyg) experimental probe was set up using 1 x PCR buffer with added $MgCl_2$, 1x PCR DIG mix, 0.5 µM of each primer and 0.053 U/µl Enzyme Mix (Expand High Fidelity). A 1x dNTP mix solution replaced the 1x PCR DIG mix in the unlabelled control probe and negative water control. The thermal cycler conditions of the BioRAD S100™ for the primer sets were as follow: 95°C for two minutes, and 30 cycles of 95°C for 30 seconds, 62°C for 30 seconds, and 72°C for 40 seconds, which was followed by a final extension step of 72°C for five minutes. The synthesis of the labelled probe was analysed on a 1.5 % agarose gel alongside the unlabelled and negative controls.

3.3.7.2. Quantification of DIG-labelled probe

The yield of the DIG-labelled probe was estimated in a spot test with a DIG-labelled control (PCR DIG Probe synthesis kit) as outlined in the DIG Application Manual for filter hybridisation (Roche Diagnostics, Germany). The DIG-labelled probe was purified by filtration through a 20 µm receiver column containing Sephadex® G50 resin. A serial dilution was made (1:10) of the 1 ng/µl DIG-labelled control DNA and the DIG-labelled probe. The final concentrations of the control DNA were 100 pg/µl, 10 pg/µl, 1 pg/µl, 0.1 pg/µl and 0.01 pg/µl. The dilutions were spotted (1 µl) in two rows onto a piece of nylon membrane (Hybond N^+, Amersham) for the control and experimental probe respectively.

The nucleic acids were fixed to the membrane by cross-linking with a five minute incubation under UV light after which the membrane was briefly rinsed in Washing buffer (DIG Wash and Block Buffer set, Roche Diagnostics, Germany). The membrane was then incubated at room temperature for 30 minutes in the blocking solution (DIG Wash and Block Buffer set, Roche Diagnostics, Germany) followed by incubation in a diluted (1:5000) Anti-DIG-alkaline phosphatase antibody (Roche Diagnostics, Germany) solution at room temperature for 30 minutes. The membrane was washed twice with the washing buffer for fifteen minutes per wash at room temperature, which was followed by incubation in the detection buffer (DIG Wash and Block Buffer set, Roche Diagnostics, Germany) for two minutes. The colour substrate solution (45 µl NBT and 35 µl BCIP in detection buffer) was added to the membrane and allowed to develop in the dark overnight. The reaction was stopped by washing the membrane with TE buffer. The concentration of the probe was estimated by comparing the intensities of the experimental probe spots to that of the control.

3.3.7.3. Digestion of genomic DNA

Genomic DNA was isolated from five day old wild type and putative *Δcrp1* knock-out strains as described in the 'Isolation of genomic DNA' section using the ZR Fungal/Bacterial DNA Midi™ kit. The restriction digest was set up in a 60 µl reaction. The reaction was composed of the following components: 1x Buffer O (50 mM Tris-HCl, 10 mM $MgCl_2$, 100 mM NaCl and 0.1 mg/µl BSA), and six units of the restriction enzyme BglII (ThermoFisher Scientific, Waltham, USA) together with 6 µg genomic DNA. The restriction digest reactions were incubated at 37°C

for five hours after which 200 ng of digested DNA was analysed on a 0.8 % agarose gel to determine degree of genomic DNA digestion. The complete genomic DNA digest was separated on an EtBr stained 0.8 % agarose gel at 55 V for 2.5 hours. The DIG-labelled molecular weight marker II (Roche Diagnostics, Germany) was loaded onto the gel together with the FastRuler™ Middle Range ruler (ThermoFisher Scientific, Waltham, USA).

The digested genomic DNA separated by agarose gel electrophoresis was depurinated by incubating the gel, with gentle shaking, twice in 0.25 M HCl for 15 minutes, after which the gel was rinsed with sterile double distilled water. The gel was then incubated in a Neutralisation solution (0.4 NaOH) for 15 minutes at room temperature followed by equilibrating the gel in 20 x SSC for ten minutes. The DNA was capillary transferred with 0.4 M NaOH from the agarose gel onto nylon membrane (Hybond N^+, Amersham).

The nylon membrane containing the digested *C. zeina* genomic DNA was placed in a hybridisation tube containing preheated (42°C) Pre-hybridisation solution (50% Formamide, 5 x SSC, 0.1% N-lauroylsarcosine, 0.02% SDS and 2% blocking solution) and incubated at 42°C for 30 minutes. The solution was replaced with Hybridisation solution containing 10 ng/ml of the DIG labelled *hyg* probe, which was denatured in boiling water for five minutes in a microcentrifuged tube containing 50 µl distilled water. A total of 25 ml of the hybridisation solution was used to replace the pre-hybridisation solution, and incubated at 42°C overnight. Thereafter a low stringency wash (2 x SSC containing 0.1% SDS) was performed at room temperature for five minutes with gentle shaking and then repeated. Immediately afterwards two high stringency washes (0.5 x SSC containing 0.1% SDS) were performed by adding preheated wash solution and incubating at 68°C for 15 min. Hybridisation signals were detected via chemiluminesence using the CSP-Star™ (Roche Diagnostics, Germany) as a substrate. The semi-dry membrane was placed in a plastic bag and exposed to X-ray film in a container for various exposure times to detect different signal strengths.

3.3.8. Expression of endogenous *Cercospora zeina crp1* gene

Total RNA was extracted from wild type and putative *Δcrp1* knock-out *C. zeina* strains. The fungal strains were cultivated on cellophane sheets placed on V8® media plates for five days in constant darkness at room temperature. The RNA extractions were performed using the RNeasy® Plant Mini kit (Qiagen, Venlo, Netherlands) according to the manufacturer's specifications. Approximately 100 mg flash frozen fungal tissue was ground under liquid nitrogen and added to a microcentrifuge tube containing the guanidine hydrochloride lysis buffer (Buffer RLC). Contaminating genomic DNA was removed from the resulting RNA samples following the on-column DNase digestion with the RNase-Free DNase set according to the manufacturer's guidelines (Qiagen, Venlo, Netherlands). Following on-column digestion the RNA was eluted in 30 µl RNase-free water. The eluate was subjected to an additional incubation (five minutes at room temperature) and centrifugation step through the RNeasy® spin column in order to increase the final RNA concentration. The concentration and purity of the RNA samples were determined using the Thermo Scientific Nanodrop™ 2000 spectrophotometer (ThermoFisher Scientific, Waltham, USA). The integrity of RNA was checked on a 0.8% agarose gel stained with EtBr, where the respective ribosomal RNAs should appear as sharp bands. A smear instead of sharp bands is a clear indication of degradation during the RNA isolation process.

Purified RNA samples were used for the synthesis of cDNA using the Maxima H Minus First Strand cDNA Synthesis Kit (ThermoFisher Scientific, Waltham, USA) according to the manufacturer's specifications. A total of 3 µg of each RNA sample was used for the synthesis of cDNA using the random hexamer primer set. A RT-minus negative control (reaction contains no Maxima H Minus enzyme mix) was included in the experiment to detect the presence of contaminating genomic DNA.

The primer set was manually designed to span the 3' intron of the endogenous *crp1* gene *C. zeina* as shown in Figure 2 and Table 1. The primer set compatibility, dimer and hairpin formation, and the stability of the 3' regions of the primer sets tested on NETprimer (http://premierbiosoft.com/netprimer/). The PCR reactions were set up in a total volume of

10 µl, which consisted of: 1 x KAPA2G Robust HotStart ReadyMix (KapaBiosystems, Wilmington, Massachusetts) and 0.5 µm of each primer. The amount of the template DNA added to the PCR reaction was 10 ng. The thermal cycler conditions of the BioRAD S100™ for the two primer sets were as follow: 95°C for five minutes, and 35 cycles of 95°C for 20 seconds, 60°C for 30 seconds, and 72°C for 40 seconds, which was followed by a final extension step of 72°C for five minutes. A control reaction containing genomic DNA (50 ng) isolated from wild type *C. zeina* was added to indicate the presence of genomic DNA in the other samples. A second no-template negative control was added, which provided an indication of contamination in the reagents. The PCR amplicons were separated on a 2.0% agarose gel stained with EtBr and visualised. The optical density of the bands were analysed with ImageJ (http://imagej.nih.gov/ij). The relative expression of the *crp1* gene and that of the *hyg*^{R} gene at the logarithmic phase were calculated by dividing each of the optical densities generated by the *Δcrp1* knock-outs and the wild type strains with that of the reference gene (elongation factor 1 α) (Langenhoven, 2015).

3.3.9. Phenotypic characterisation of putative *Δcrp1* knock-outs

3.3.9.1. *Cercospora zeina* conidial light assay

Conidia were harvested from both the wild type and the putative *Δcrp1* knock-out *C. zeina* strains. The spores were scraped from five day old plates using double distilled water. The amount of spores were counted using a Neubauer cell counting chamber. The formula used to count the spores across four squares was:

Total cells/ml = (Cells counted) x (Dilution factor/Squares counted) x 10 000

The spore concentration of all strains were diluted to 2 x10^{5} cell/ml and used to inoculate V8® media plates in triplicate for each strain. The cultures were incubated at room temperature at two different light conditions, which included constant light and constant darkness. The conidia from all the cultures were harvested and counted as above. Comparison of the individual putative *Δcrp1* knock-out and wild type *C. zeina* strains cultured under either constant light or darkness were performed by one-way ANOVA with Dunnett's multiple comparison post-test using GraphPad Prism 5 (San Diego, California, USA). Two-way ANOVA

with Bonferroni's multiple comparison test was performed to compare the individual strains cultured under the two light conditions to each other.

3.3.9.2. Melanin production in constant light and darkness

Fungal cultures were grown in triplicate for seven days at room temperature either in constant light or constant darkness. The fungal strains were inoculated with equal amounts ($2x10^5$ cell/ml) of spores on V8® media plates. A melanin isolation protocol was developed and optimised based on the methods proposed by Bashyal et al. (2010) and Lingappa et al. (1963). In brief, five gram of mycelial tissue was scraped from seven day old plates and boiled in ten millilitre distilled water for five minutes. The mycelial solution was centrifuged at 5000 x g for five minutes after which the mycelial pellet was washed with distilled water. The pigment was extracted by autoclaving the mycelial pellet in three millilitre 1 N NaOH for 20 minutes at 120°C. The pigment solution was centrifuged at 2000 rpm and the supernatant transferred to a new conical tube. The alkaline pigment was precipitated through acidification (pH 2) with HCl and incubated at -20°C overnight. The precipitated pigment was then centrifuged at 5000 x g for ten minutes to pellet the pigment, which was washed three times with distilled water. The resulting pigment pellet was dried overnight in dehumidified conditions. The melanin concentration was determined through a spectrophotometric assay. A melanin standard curve was generated by preparing 0 – 20 µg/ml concentration of the standard with each concentration having three technical replicates. The dried melanin samples (and melanin standard) were solubilised in one millilitre 1 N NaOH for two hours at 80°C and centrifuged at 12 000 x g for ten minutes. The supernatant was transferred to new microcentrifuge tubes and the absorbance measured at 405 nm. All three biological replicates had three technical replicates for the spectrophotometric assay. A 1:5 dilution was prepared from the unknown samples (melanin extracted from the putative *Δcrp1* knock-out and wild type strains). Comparison of the individual putative *Δcrp1* knock-out to the wild type strains cultured under either constant light or darkness was performed by analysis of variance tests using GraphPad Prism 5 (San Diego, California, USA) as above.

3.3.9.3. Pathogenesis of putative *Cercospora zeina Δcrp1* knock-outs

The GLS sensitive maize inbred line B73 was used in this study and grown in a phytotron with the layout seen in Figure 3. The phytotron is registered as a type one containment unit (for the period: 21 December 2013 – 21 December 2015) with the Department of Agriculture, Forestry and Fisheries of the Republic of South Africa in terms of regulation four of the Genetically Modified Act, 1997 (Act no. 15 of 1997) (registration number: 39.2/University of Pretoria – 12/091).

A drip irrigation system was designed in this study so that each plant received the same amount of water and nutrients. The maize plants were grown in a 1:1 ratio of river sand to potting soil. The conidia from seven day old *C. zeina* cultures were harvested using a 0.01% Tween 20 solution. Five week old maize plants were infected with $2x10^5$ spores/ml wild type and putative *Δcrp1* knock-out strains in triplicate for an early (6 dpi), mid (13 dpi) and late (25 dpi) time point. Four leaves of each maize plant were inoculated using the paint brush method, the spore suspension was mixed after every application to ensure equal distribution of the spores. The infected plants were grown in the dark for 48 hours at approximately 100% humidity at 34°C to aid the infection process after which a 16 hour light/8 hour dark cycle was followed. The temperature and humidity reading were monitored using the HOBO® Pro v2, whereas light intensity was logged using the HOBO Pendant 64K (Onset®, Bourne, MA, USA).

Stomatal interactions were counted and compared across the putative *Δcrp1* knock-out and wild type strains. Leaves were collected from each of the three biological replicates and stained in a 1% Congo red solution, which stains the fungal hyphae (Slifkin and Cumbie, 1988). The stained leaf pieces were visualised under a Zeiss LSM 510 Meta confocal microscope (Zeiss, Oberkocchen, Germany) at the University of Pretoria's Laboratory for Microscopy and Microanalysis. The three different types of stomatal interactions observed included hyphae growing across, over or around the stomatal opening. In total 50 interactions were counted per fungal strain per biological replicate and recorded. Stomatal interactions observed for the individual putative *Δcrp1* knock-out strains were compared to the wild type strain performed by one-way ANOVA as above.

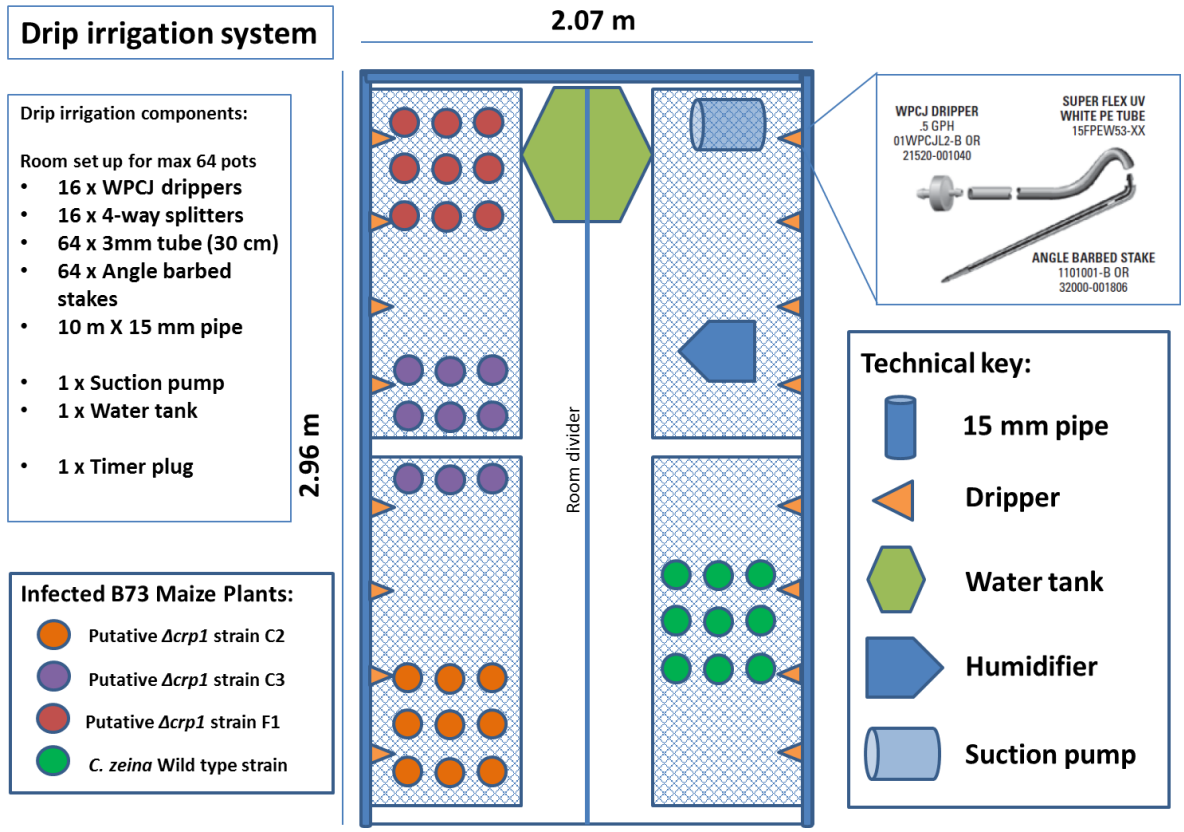

Figure 3. Experimental layout of maize plants for infection with *Cercospora zeina* wild type and *Δcrp1* knock-out strains. The drip irrigation system designed for the phytotron is composed of WPC-CJ drippers that delivers 2L of water per hour connected to angle barbed stakes, which are placed into the soil. The closed circular system is connected to a CRI 0.37 kW suction pump that drives the water from the tank through the system. The irrigation system is connected to a standard programmable timer plug. An additional humidifier was placed in the room. In total nine B73 maize plants were inoculated per *Δcrp1* knock-out and wild type strain separated by a room divider. The uninfected control B73 maize plants were grown in a separate phytotron under the same growth conditions to avoid cross infection.

3.4. Results

3.4.1. Verification of split-marker construct sequences

The overall aim of this experiment was to confirm that the generated *C. zeina* fungal protoplasts were transformed with split marker constructs of expected sequence. The putative *Δcrp1* knock-outs were generated by transforming *C. zeina* protoplasts with the 5' and 3'-constructs. Prior to the experiment, the predicted sequences of the 5'- and 3'-constructs were assembled *in silico* based on the *crp1* flanking regions and the *hyg*-cassette sequence. The *hyg*-cassette contained in the pTA-hyg plasmid was sequenced in the forward and reverse direction using the M13 primer set in order to obtain the full length sequence. The size of the *hyg*-cassette is 1549 bp with an open reading frame of 1026 bp encoding the hygromycin B phosphotransferase enzyme (Figure B1 in the Appendix B). The identity of the hyg^R gene was verified by performing a BLASTn using the open reading frame sequence, which aligned to the *Fusarium graminearum* hygromycin resistance gene (DQ384628.1).

The 5'- and 3'-split marker constructs were cloned into the pJet1.2 vector using the CloneJet™ kit and transformed into competent DH5α *E.coli* cells. A colony PCR using the pJet primer set confirmed the presence of a 1 500 bp insert (data not shown). The colony PCR revealed two different size insertions in the 5'-construct colonies differing by 50 bp (data not shown). Restriction enzyme analysis was used to identify the correct 5'-construct (see below).

The *in silico* restriction maps of the 5'- and 3'-constructs are shown in Figure 4A. The two 5-construct colonies were designated 5'_1 and 5'_7, and a single 3'-construct colony, 3'_1, was selected. Restriction digests of the pJet1.2 vectors containing the 5-construct as an insert were performed using one single and four double digestions. The single digest with BglII (Figure 4 B, lanes 3 and 9) cuts on either side of the insert and is expected to result in 2974 bp (vector) and 1486 bp (insert) bands. The double digest using BglII + EcoRI (lanes 4 and 10) and BglII + BamHI (lanes 7 and 13) release the insert (2974 bp vector) and cut once inside the insert generating a 1083 bp and 550 bp band as seen in Figure 4B. The other two double digest using SalI + EcoRI (lanes 5 and 11) and SalI + BamHI (lanes 6 and 12) cut twice in the insert and are expected to produce a band of 410 and 4055 bp. The 5'_1 plasmid did not produce the

550 bp with the BglII + EcoRI and BglII + BamHI double digests, and the 400 bp band from the SalI + EcoRI and SalI + BamHI double digests. This construct therefore had a deletion and all further analyses were performed with 5'_7. The 3'_1 plasmid was digested with BglII (Figure 14 B, lane 15) and BglII + XbaI (lane 16). The single digest resulted in a 1350 bp insert and 2974 bp vector band. The double digest resulted in three bands, XbaI cuts within the plasmid and in the vector. Based on the restriction digest results the 5'_7 and 3'_1 plasmids were sequenced to obtain the sequences of the split-marker constructs.

Sequencing of the constructs using the pJet primer sets resulted in truncated sequences based on their insert length. Therefore the 5'_7 plasmid was sequenced using the following primers: F5N, F2, M13-F, HYG-F, YG-N and HY-N. The 3'_1 plasmid was sequenced using YG-N, HY-N, HYG-R, M13-R, F3 and F6N. The resulting overlapping sequences were assembled to generate the complete 5' and 3'- constructs and the overlapping knock-out construct was generated *in silico* (Figure 4C).

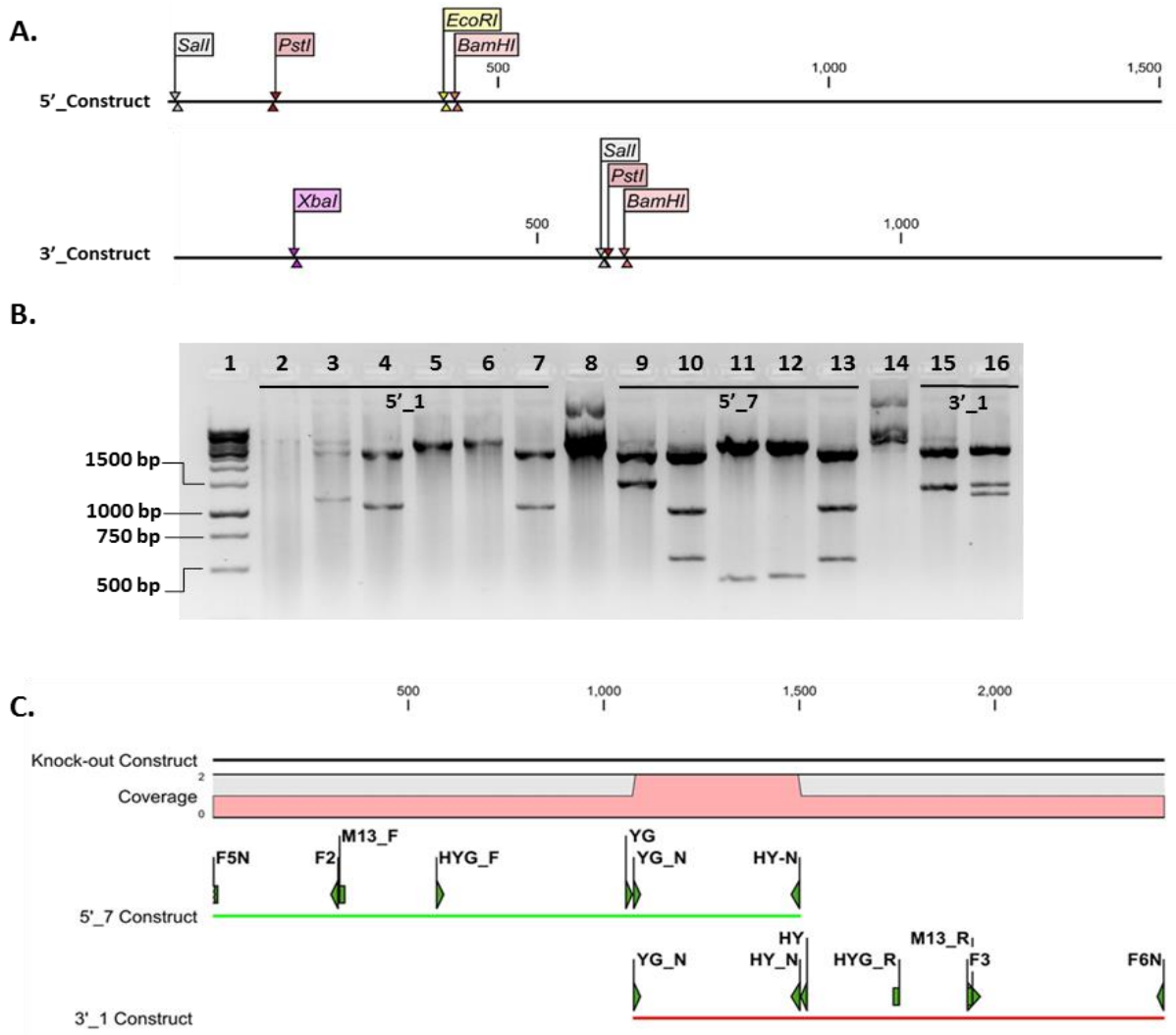

Figure 4. Verification of the split marker constructs' sequences. (A) *In silico* assembly of the 5'- and 3' constructs indicating the restriction sites present in the respective constructs. (B) The restriction digests of the pJet1.2 vectors containing the putative 5'_1 and 5'_7 and 3'_1 constructs as insert flanked by BglII restriction cut sites. The 5'- construct containing vectors were digested with BglII (lanes 3 and 9), BglII + EcoRI (lanes 4 and 10), SalI + EcoRI (lanes 5 and 11), SalI + BamHI (lanes 6 and 12) and BglII + BamHI (lanes 7 and 13). The 3'-construct containing vector was digested with BglII (lane 15) and BglII + XbaI (lane 16). Lanes 2, 8 and 14 represents the undigested plasmid. Lane 1 is the GeneRuler 1 kb DNA ladder. (C) The 5'_7 and 3'_1 constructs sequences were confirmed and the primer binding sites annotated on the sequences. The construct sequences were assembled to represent the recombined *hyg* knock-out construct to confirm the internal hyg^R regions overlap.

3.4.2. Initial large scale transformant screen

The putative *Δcrp1* knock-out and the wild type *C. zeina* strains were cultured on V8® media supplemented with 90µg/ml hygromycin B. DNA was extracted from all 64 putative *Δcrp1* knock-out and the wild type strains. The rapid DNA extraction method developed in this study yielded DNA of a good quality, based on the amplification of the histone H3 fragment (data not shown). The 64 putative *Δcrp1* knock-outs were subjected to screening for the presence

of the entire *hyg*^{R} gene using the M13 primer set that flanks the *hyg*-cassette. Since previous amplification attempts proved to be difficult the reaction was optimised through adding PCR enhancers. Dimethyl sulfoxide (DMSO) and Bovine Serum Albumin (BSA) was added at 9% and 0.8 µg/µl respectively. The DMSO disrupts DNA base-pairing, which results in denaturing of secondary structures, whereas BSA interacts competitively to DNA polymerase inhibitors. In total only nine of the 64 putative *Δcrp1* knock-outs showed positive amplification of the 1549 bp *hyg*-cassette. The nine putative *Δcrp1* knock-outs were A11, B7, B8, C1, C2, C3, C6, E5 and F1 as indicated in Figure 5.

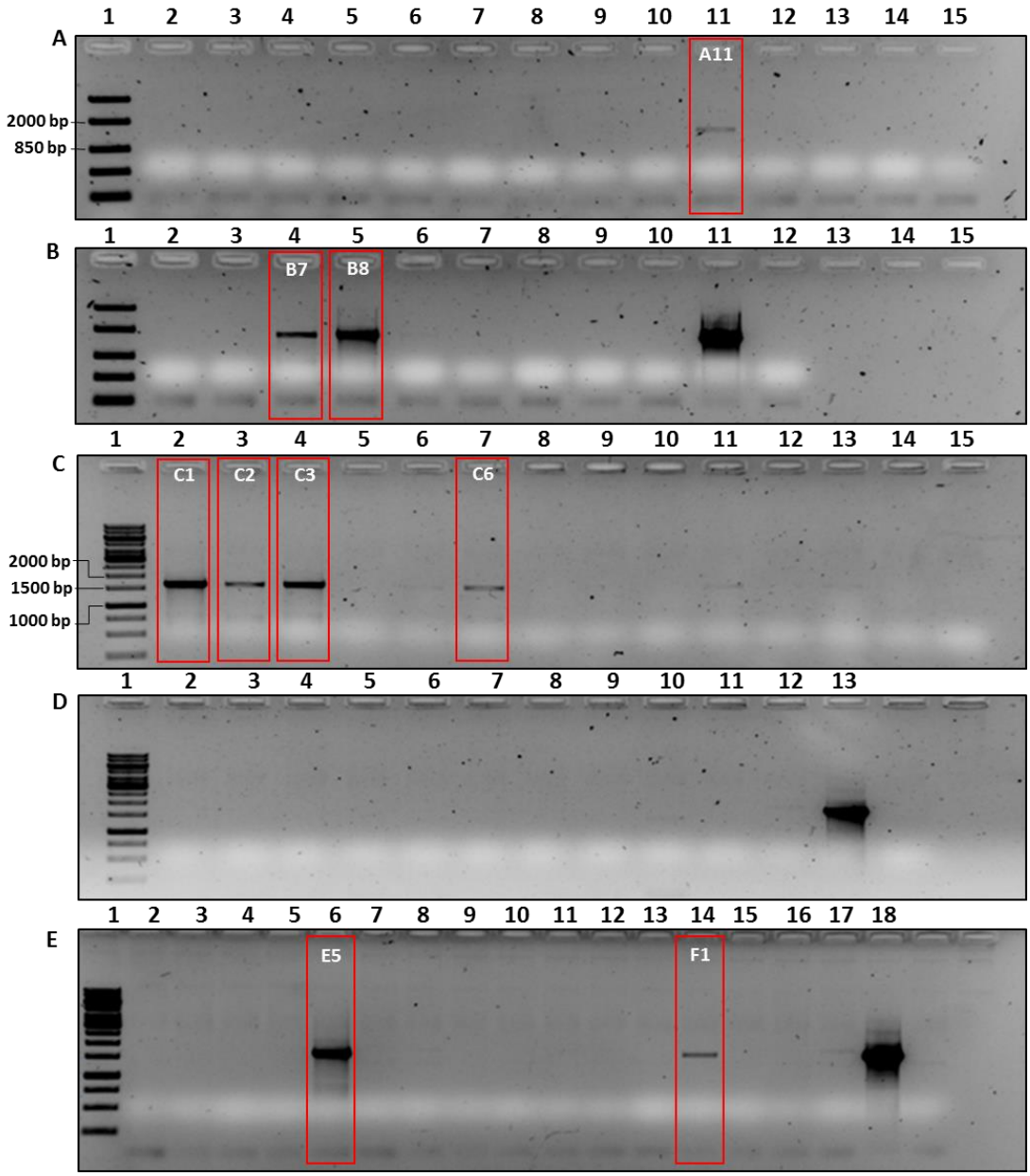

Figure 5. Amplification of hygromycin resistance gene from putative *Cercospora zeina Δcrp1* strains. The presence of the complete *hyg*^{R} gene in the putative *Δcrp1* knock-outs was screened for using the M13 primer set. In total 64 putative *Δcrp1* knock-outs were screened with DNA extracted using the rapid DNA extraction method. The positive control, pTA-HYG, is indicated in B.11, D.13, E.18, with a size of 1549 bp. In total nine putative Δ*crp1* knock-outs screened positive for the presence of the *hyg*^{R} gene, which are indicated by the red boxes, with their respective annotations.

3.4.3. Genotypic screen of putative *Δcrp1* knock-outs

3.4.3.1. Screen for Hygromycin resistance gene (*hyg*^{R})

The nine hygromycin positive *Δcrp1* knock-out strains were cultured on V8® media in the dark at room temperature for five generations (successive sub-culturing) to achieve a high density culture for genomic DNA isolations. Four of the nine putative *Δcrp1* knock-outs were selected to perform genotypic characterisation of the transformants. The selected putative transformants were C2, C3, E5 and F1, based on their ability to grow on the V8® media supplemented with 90 µg/ml hygromycin. The DNA was isolated using the ZR Fungal/Bacterial DNA Midi™ isolation kit. The putative transformants were confirmed to be *C. zeina* following the species specific histone H3 gene amplification (Figure 6A) which is used to differentiate between *C. zeina* and *C. zeae-mayids* (Crous et al., 2006). In order to confirm the presence of the *hyg*^{R} gene, putative transformants were subjected to two separate PCR amplifications, the first using the M13 primer set (as in section 3.4.2) and the second using an internal *hyg*^{R} primer set as shown in Figure 6B. The M13 test (Figure 6C) showed that all four (C2, C3, E5, and F1) contains the entire *hyg*^{R} gene. The internal *hyg*^{R} amplification was designed to confirm the results obtained from the M13 screen and revealed that only C2, C3 and F1 contained the entire selectable marker gene and that E5 did not (Figure 6D). The putative *Δcrp1*_C2, *Δcrp1*_C3 and *Δcrp1*_F1 knock-out strains were selected to be further characterised.

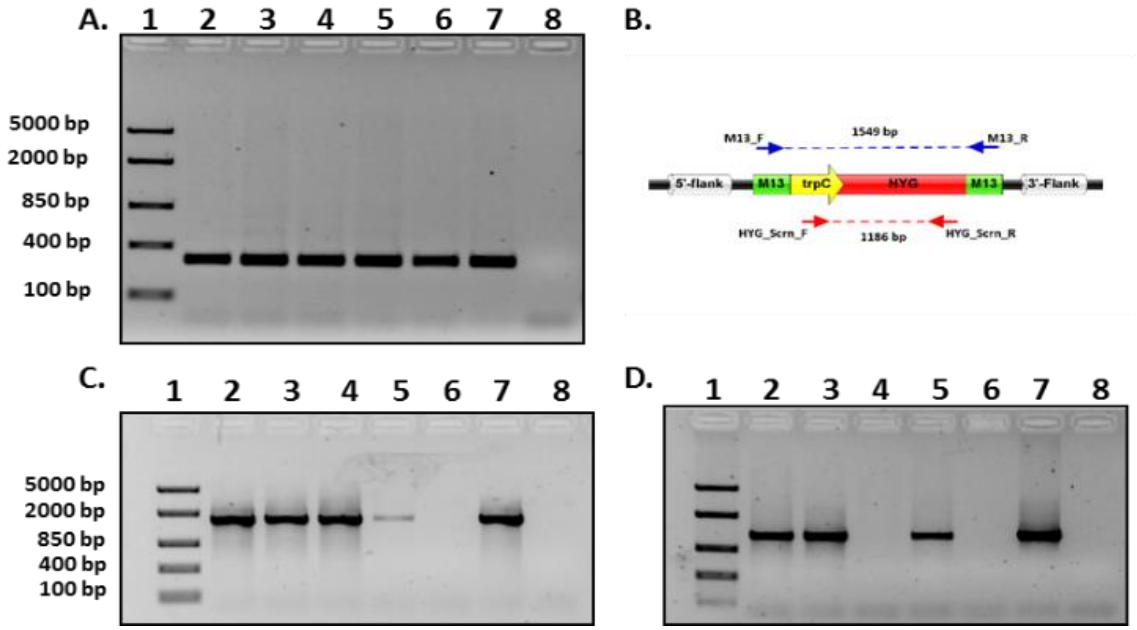

Figure 6. Screen of putative *Δcrp1* knock-outs for the presence of the *hyg*-cassette. (A) Histone PCR screen to verify the strains are *C. zeina* and test the quality of the DNA. (B) The primer sets used to screen for the presence of the *hyg*^{R} gene. The M13 (blue) and the HYG_Screen (red) primer set, which binds to the *trpC* promoter and the 3'-end of the inserted antibiotic selectable marker. (C) The M13 primer set showed positive amplification of *Δcrp1*_C2 (lane 2), *Δcrp1*_C3 (lane3), *Δcrp1*_E5 (lane 4), *Δcrp1*_F1 (lane5) and the pTA-Hyg control (lane 7) with a band size of 1549 bp. No amplification was observed in the wild type (lane 6) and negative control (lane 8). (D) The HYG_Screen amplification, which indicated that *Δcrp1*_C2 (lane 2), *Δcrp1*_C3 (lane 3), *Δcrp1*_F1 (lane 5) and the pTA-Hyg control amplified a band of 1186 bp (lane 7). Lane 4, *Δcrp1*_E5 and lane 6 (Wild type) showed no amplification. The negative water control is represented by lane 8.

3.4.3.2. Confirm correct genomic location of inserted *hyg*^{R} gene

The split-marker constructs used to transform the fungal protoplast are only able to form a functional *hyg*^{R} gene when homologous recombination occurs between the 5'- and 3-flanking regions of the *C. zeina* genomic DNA and between the two overlapping *hyg*^{R} regions. However, the knock-out constructs may also insert ectopically in other places of the genome. Primer sets were designed to regions upstream and downstream of the 5'- and 3'-flank and internal to the *hyg*^{R} gene as shown in Figure 7A. The 5'–external primer set (Ext5_crp1 + Ext5_HY) was expected to produce a product size of 888 bp, whereas the 3'-external primer set (Ext3_YG + Ext3_crp1) was expected to produce a product size of 1052 bp. All three the putative *Δcrp1* knock-outs, *Δcrp1*_C2, *Δcrp1*_C3 and *Δcrp1*_F1 showed positive amplification of the 5'- and 3'-external products (Figure 7B). No amplification took place in the wild type strain, which is the negative control in this experiment. Based on this external primer screen

all three putative *Δcrp1* knock-outs were shown to be positive for the insertion of the *hyg*^{R} gene into the endogenous *crp1* gene region of *C. zeina*.

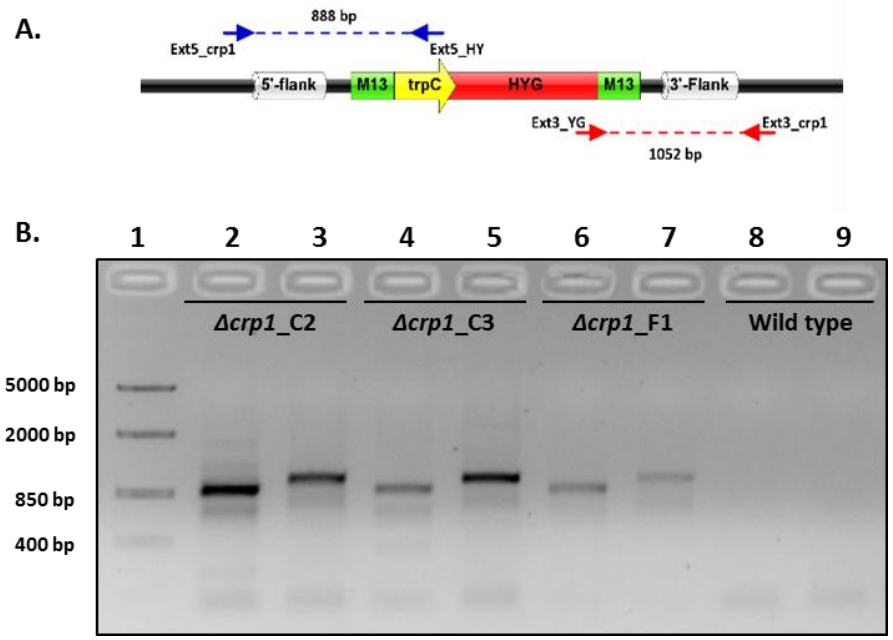

Figure 7. External primer screen of putative *Cercospora zeina Δcrp1* knock-outs. (A) Two primer sets were designed to screen whether or not the 5'- and 3' construct inserted into the correct genomic location. The Ext5_crp1 primer binds outside of the inserted region upstream of the *crp1* gene, whereas the Ext5-HY primer binds on the opposite strand on the 5' region of the inserted *hyg*^{R} gene. The Ext3_crp1 primer binds outside of the inserted region downstream of the *crp1* gene, whereas the Ext3-HY primer binds on the opposite strand on the 3' region of the inserted *hyg*^{R} gene. (B) The amplification of the external products. Lanes 2, 4, 6 and 8 represents the 5'-external screen. Lanes 3, 5, 7 and 9 represents the 3'-external screen. Positive amplification of 888 bp for the 5'-external region is shown for *Δcrp1*_C2, *Δcrp1*_C3 and *Δcrp1*_F1. The 3'-external screen was positive for *Δcrp1*_C2, *Δcrp1*_C3 and *Δcrp1*_F1, which is 1052 bp in length. The wild type strain showed no amplification for the 5'- (lane 8) and 3'-external (lane 9) screen.

3.4.3.3. Determination of copy number of the inserted *hyg*^{R} gene

The number of *hyg*^{R} insertion events in the putative *Δcrp1* knock-outs, *Δcrp1*_C2, *Δcrp1*_C3 and *Δcrp1*_F1 was tested through a Southern blot (Brown, 2001). The DIG-labelled internal *hyg*^{R} probe shows a slight increase in size on the agarose gel shown in Figure 8A due to the incorporation of larger DIG dNTPs compared to the unlabelled dNTP control of 428 bp. The primer binding sites of HY-N and YG-N and the region to which the probe will hybridise to are shown in Figure 8B. The concentration of the DIG labelled probe was determined through a spot test with a serial dilution (10^{-1}, 10^{-2}, 10^{-3}, 10^{-4} and 10^{-5}) of the DIG-labelled control and the *hyg* experimental probe. The concentration of the probe was determined to be 10 pg/µl and added to 25 ml hybridisation buffer at 10 ng/ml. The putative *Δcrp1* knock-out and wild

type strains were cultured on cellophane sheets placed on V8® media, with the knock-out strains' media supplemented with 90 µg/ml hygromycin B. A total of six microgram of genomic DNA from the putative *Δcrp1* knock-out and wild type strains were digested with BglII for five hours as seen in Figure 8C. Complete digestion is observed for the wild type (lane 3), *Δcrp1*_C3 (lane 5) and *Δcrp1*_F1 (lane 6), whereas the incomplete digestion took place of *Δcrp1*_C2 genomic DNA.

Following hybridisation, binding of the probe to the genomic DNA was visualised by exposure to X-ray film. The X-ray film exposed for 30 minutes is shown in Figure 8D. No hybridisation signal is present for the wild type strain as expected. A single hybridisation signal is present for *Δcrp1*_C3 (lane 5) and *Δcrp1*_F1 (lane 6), which was confirmed by longer exposure times. Longer exposure times were tested to confirm no faint signals are present, which could indicate ectopic insertions of the *hyg*-cassette. A very faint single hybridisation signal is present for *Δcrp1*_C2 (lane 4) after a five hour exposure period. The expected size of the signal, based on *in silico* restriction site prediction, is 15 021 bp. The sizes of the hybridisation signals for *Δcrp1*_C3 and *Δcrp1*_F1 is approximately 6550 bp and 4500 bp respectively. The very faint hybridisation signal for *Δcrp1*_C2 (lane 4) is approximately 20 000 bp.

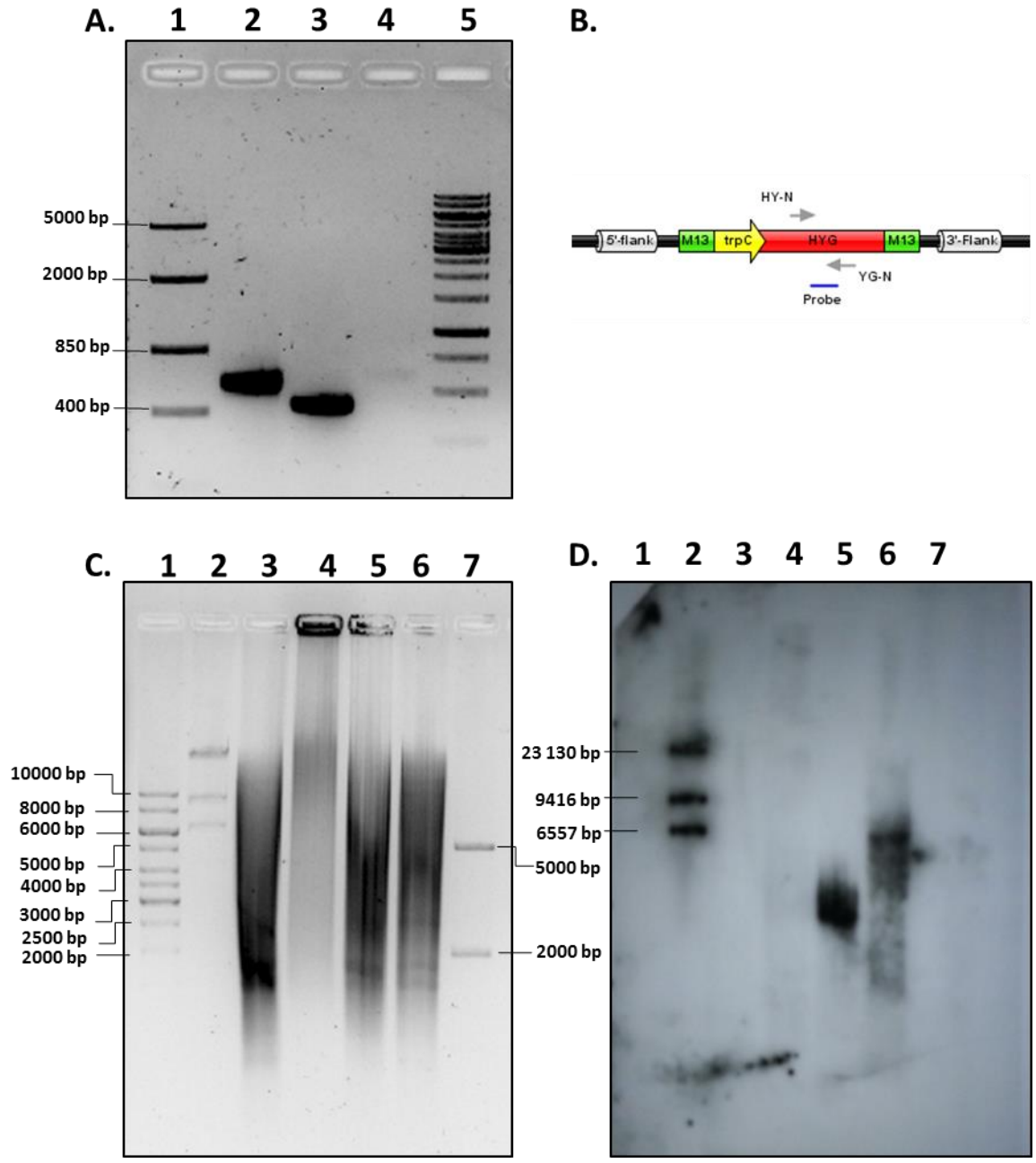

Figure 8. Inserted hygromycin resistance gene copy number analysis of the putative *Δcrp1* knock-outs. (A) Amplification of the DIG-labelled probe (lane 2) and the unlabelled control (lane 3), which is 428 bp in length. (B) The internal *hyg*^{R} gene primer set, HY-N + YG-N, used to amplify the DIG-labelled probe. (C) The genomic DNA restriction digest using BglII for the wild type (lane 3), *Δcrp1*_C2 (lane 4), *Δcrp1*_C3 (lane 5) and *Δcrp1*_F1 (lane 6). The GeneRuler™ 1kb DNA ladder (lane 1), DNA molecular weight marker II (DIG-labelled) (Lane 2) and the FastRuler™ Middle range DNA ladder (lane 7). (D) The Southern blot using the internal HYG region as a probe, with the x-ray film developed for 30 minutes. Lane 2 represents the DIG-labelled DNA molecular weight marker II. Lane 3 represents the wild type strain, which showed no *hyg*^{R} gene insertions. The *Δcrp1*_C2 (lane 4), *Δcrp1*_C3 (lane 5) and *Δcrp1*_F1 (lane 6) showed single insertion events. The knock-out strains *Δcrp1*_C2 showed a weak hybridisation signal which was only visible after 5 hour exposure.

3.4.3.4. Expression of endogenous *crp1* gene

Total RNA was extracted from the putative *Δcrp1* knock-out and wild type strains cultured in constant darkness for seven days on V8® media plates using the RNeasy® Plant Mini kit. The three technical replicates of each strain were pooled prior to the RNA extraction. The two ribosomal RNA subunits, 28S and 18S, are visible as sharp band on the agarose gel in Figure 9A, showing minimal degradation of the RNA samples. The RNA concentrations ranged from 778.3 ng/µl for *Δcrp1*_C2 to 1146.5 ng/µl for the wild type strain. The purity (A260/A280) of the isolated RNA was between 2.1 – 2.2, which is an indication that the sample is not contaminated with protein.

Primers were designed to span the fourth intron of the *crp1* gene as shown in Figure 9B. The primer set spans the 3'-terminal intron, amplifying a 207 bp fragment in genomic DNA and 134 bp fragment in cDNA. The *crp1* gene is expressed in the putative *Δcrp1* knock-out and the wild type strain as seen in the semi-quantitative PCR Figure 9 C lane 2 - 13. The genomic DNA control is shown in lane 14, whereas the negative water control (no DNA template) is shown in lane 15. The non-template water control shows no sign of contamination of the PCR reaction. A slight difference in the expression of the endogenous *crp1* gene is seen at cycle 27 (Figure 9C, lanes 3, 6, 9 and 12). The expression of the *C. zeina* reference gene, Elongation factor 1-alpha (Langenhoven, 2015) is seen in Figure 9D based on a semi-quantitative PCR performed at 15, 18 and 21 cycles.

The inserted hygromycin resistance gene is only expressed in the putative *Δcrp1* knock-out strains and not in the wild type as seen in Figure 9D. The internal overlapping fragment between the two split marker constructs were amplified to produce a product size of 428 bp for the hyg^R gene. No expression of the hyg^R gene is observed in the wild type strain as seen in Figure 9E, lanes 11 -13.

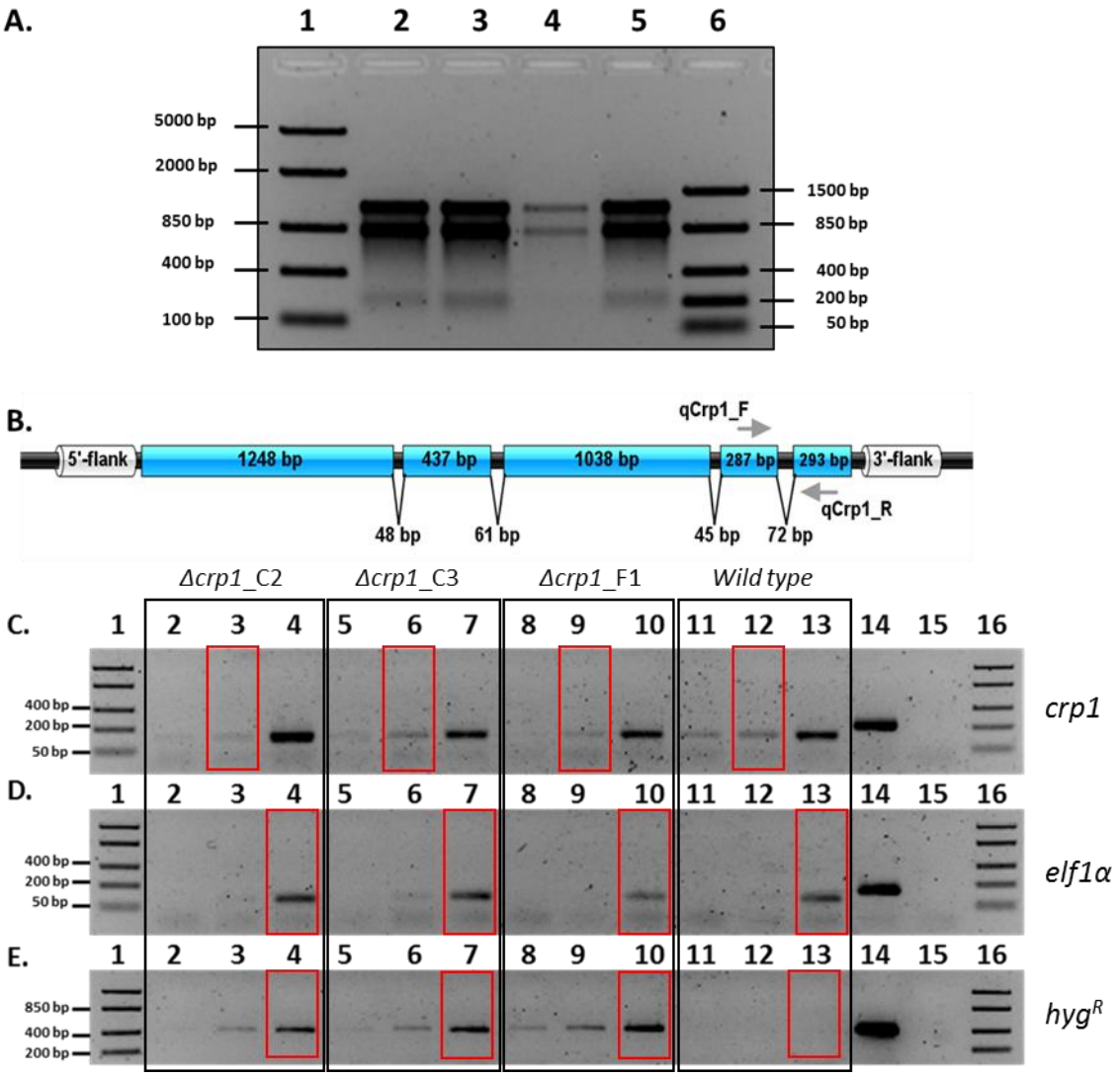

Figure 9. Semi-quantitative RT-PCR of the endogenous *crp1* gene in *Cercospora zeina* wild type and *Δcrp1* knock-out strains. (A) Total RNA extraction for the putative *Δcrp1* knock-out strains, *Δcrp1*_C2 (lane 2), *Δcrp1*_C3 (lane 3) and *Δcrp1*_F1 (lane 4) and the wild type strain (lane 5). (B) The *C. zeina crp1* gene with the five exon and four intron region indicated. The *crp1* expression primer set was designed to span the last intron region of 72 bp. (C) Expression of the *crp1* gene. Lanes 2 to 13 represents positive amplification of the *crp1* gene (134 bp) for the *Δcrp1* knock-out strains, *Δcrp1*_C2, *Δcrp1*_C3 and *Δcrp1*_F1 and the wild type strain, respectively. Lane 14 represents the wild type genomic DNA control of 207 bp. Lane 15 represent the negative no-template control. (D) Amplification of the reference gene, Elongation factor 1-alpha. Amplification of the putative *Δcrp1* knock-out strains and the wild type strains are represented by lanes 2 to 13. *C. zeina* wild type strain genomic control is represented in lane 14 (154 bp). Lane 15 represent the negative non-template control. (E) Amplification of the inserted *hyg*^{R} gene. Lanes 2 to 13 represent positive amplification of the *hyg*^{R} gene (428 bp) for the *Δcrp1* knock-out strains, *Δcrp1*_C2, *Δcrp1*_C3 and *Δcrp1*_F and the wild type strain, respectively. Lane 14 represents the pTA-Hyg plasmid DNA control of 428 bp. Lane 15 represent the negative no-template control. Cycles for the endogenous *crp1* gene and the inserted *hyg*^{R} gene were performed at 25, 27, and 29, whereas for the reference gene 15, 18 and 21 cycles were used. The red boxes indicate the selected logarithmic stages for the respective genes and *C. zeina* strains used to calculated relative expression of the genes.

The amplified *crp1* gene fragment from both the *C. zeina* wild type and the *Δcrp1* knock-out strains was sequenced using the cDNA (Figure 10) and the genomic DNA (Figure B5 in Appendix B) as a template. Sequencing was performed in the forward and reverse direction using the *crp1*_frag_F and *crp1*_frag_R primers respectively (Table 1). The sequences between the wild type and the *Δcrp1* knock-out strains were identical. As a confirmation, the LOV domain of the *crp1* gene was also sequenced from cDNA (Figure 11) and genomic DNA (Figure B6 in Appendix B) from both the wild type and *Δcrp1* knock-out strains using the LOV primer set (Table 1). These LOV domain sequences from both the wild type and *crp1* knock-out strains were also identical.

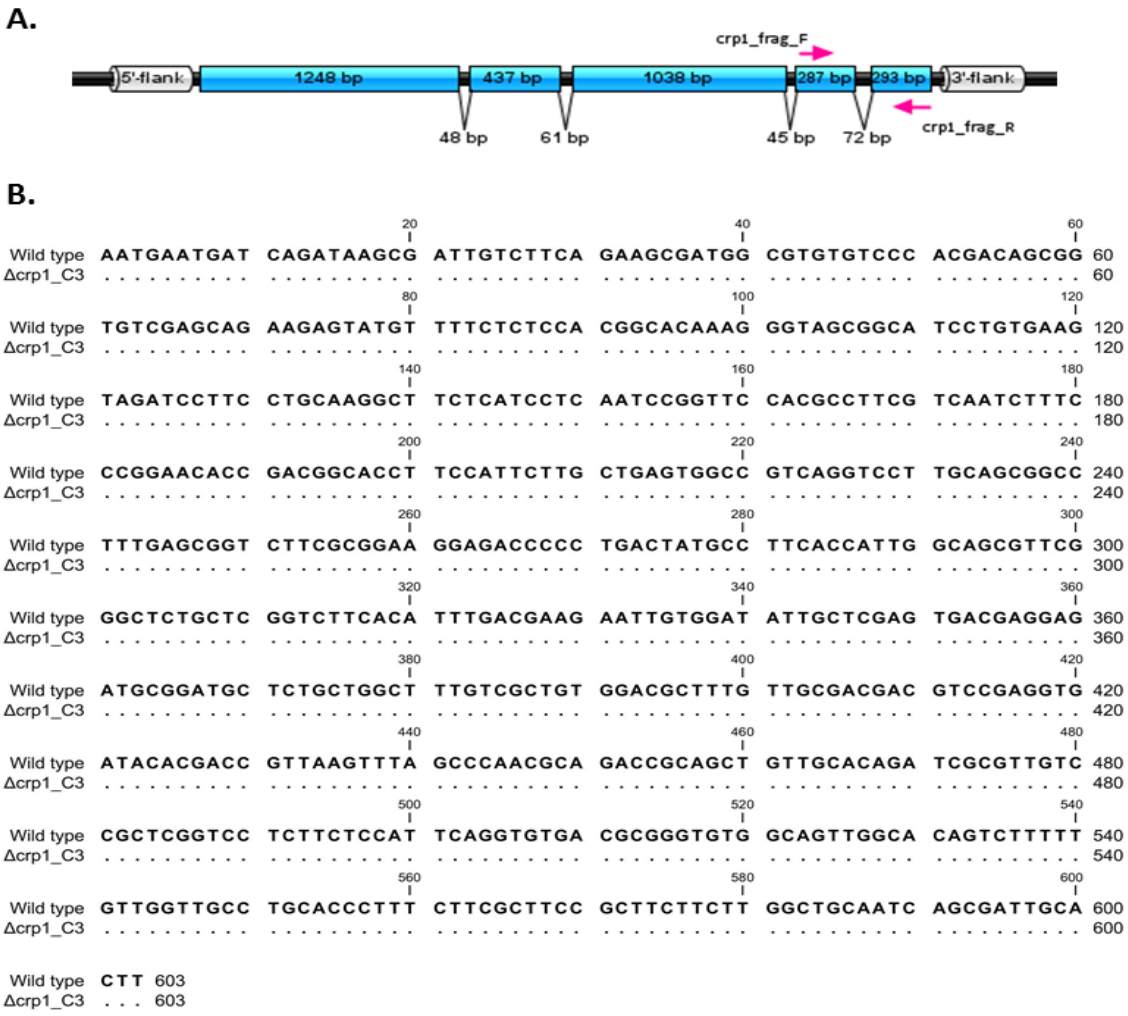

Figure 10. Terminal *crp1* fragment sequence alignment from cDNA. (A) Graphical representation of the crp1_frag_F and crp1_R primer binding sites in the *crp1* gene in pink. (B) The terminal fragment

cDNA sequence alignment from the putative *Δcrp1*_C3 knock-out and wild type strains. The sequences were obtained using the *crp1*_frag primer set. The dots represents identical residues.

A.

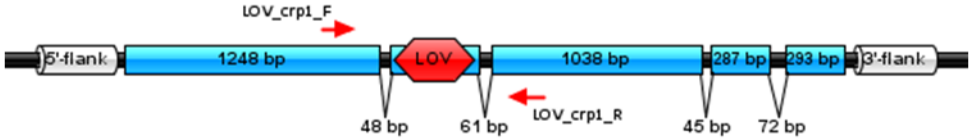

B.

```
                    20                  40                  60
Wild type  CGTTCATGAC GTAGCGCGGC ATGGTCATGC CACGTTGATA GTTGATAGAG TACGAACCAT 60
Δcrp1_C3   .......... .......... .......... .......... .......... .......... 60

                    80                 100                 120
Wild type  CGGGATTCTT GTTCGTCACC GCATTCGGCT GCTCTACCAG ATCGACCTGG AATCCGACAA 120
Δcrp1_C3   .......... .......... .......... .......... .......... .......... 120

                   140                 160                 180
Wild type  AGAACTTCAC CTGATCAGAG TCCCACGAGA TGGGTATCAT GGTTAGCAAG TTCATGAAGG 180
Δcrp1_C3   .......... .......... .......... .......... .......... .......... 180

                   200                 220                 240
Wild type  GCTGGCCTCC TCGTCGATAA TTGATCAGCG ATATCTGGGC TTCCCTCCGA AGGTTGATCA 240
Δcrp1_C3   .......... .......... .......... .......... .......... .......... 240

                   260                 280                 300
Wild type  TGTTCTTCAA GTAGAGCACC GAGTCATCAT CGACGTATTT TCGCCTTATG CCAGGCGCGA 300
Δcrp1_C3   .......... .......... .......... .......... .......... .......... 300

                   320                 340                 360
Wild type  CGTTCCCGTC TGGTGATTGC AGGAACCGAC AGTTGCGGCC AAGGATCATG TGTTTCGTGT 360
Δcrp1_C3   .......... .......... .......... .......... .......... .......... 360

                   380                 400                 420
Wild type  AACCTGTCAG CCTCTCAAAA TTCTCCGAGC AGTACACGAT GGGAAAATCG TCCTTCTCCG 420
Δcrp1_C3   .......... .......... .......... .......... .......... .......... 420

                   440                 460                 480
Wild type  CGTCACACAC GACAAAGGCG CAAGACAGGT CCACGGATCC AATGTTGATC TCTGGATCAG 480
Δcrp1_C3   .......... .......... .......... .......... .......... .......... 480

                   500                 520                 540
Wild type  GTCTTGTAGC GACCCGCATA AGCACGCCAA GCATGTCAAA TCCAGTCGAA GAGTAAGCAT 540
Δcrp1_C3   .......... .......... .......... .......... .......... .......... 540

                   560
Wild type  TCTTGTACAC GGACTGCATA TGAGGCTTG 569
Δcrp1_C3   .......... .......... ......... 569
```

Figure 11. *Cercospora zeina* wild type and putative *Δcrp1*_C3 LOV sequence alignment from cDNA. (A) Graphical representation of the LOV_crp1_F and LOV_crp1_R primer binding sites in the *crp1* gene in red. (B) The alignment of cDNA sequences from the putative *Δcrp1*_C3 knock-out and wild type strains generated using the LOV_*crp1*_F and LOV_*crp1*_R primer set. The dots represents identical residues.

The relative expression of the *crp1* gene and the *hyg*^{R} gene between the *Δcrp1* knock-out and wild type strains were determined as shown in Figure 12. The logarithmic phase for the *crp1*, *elf1α* and *hyg*^{R} expression was determined to be at 27, 21 and 29 cycles respectively. This

semi-quantitative approach based on optical densities is only a crude method to estimate relative gene expression (normalised against the *elf1α* reference gene) and should be confirmed with quantitative RT-PCR. No change in relative expression of the endogenous *crp1* gene was observed in the *Δcrp1*_C3 and *Δcrp1*_F1 knock-out strains, whereas *Δcrp1*_C2 showed a 2.6-fold change in expression. As mentioned, the expression of the *hyg*^{R} gene is only present in the *Δcrp1* knock-out strains and not in the *C. zeina* wild type (Figure 12).

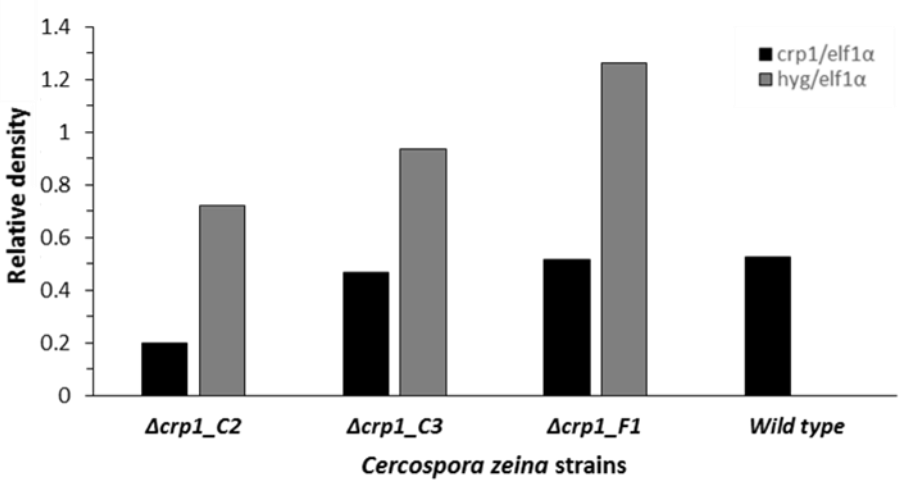

Figure 12. Relative expression of endogenous *crp1* gene and the inserted *hyg*^{R} gene in *Cercospora zeina* strains. The relative expression of the *crp1* gene to the elongation factor 1-α (represented by the black bars) of the *Δcrp1*_C3 and *Δcrp1*_F1 knock-out strains indicated no significant change compared to the wild type, whereas *Δcrp1*_C2 showed a 2.6-fold change to the wild type. Only the *Δcrp1* knock-out strains express the *hyg*^{R} gene as represented by the grey bars (relative expression of the *hyg*^{R} gene to the elongation factor α-1 reference gene), and not the *C. zeina* wild type.

3.4.4. Phenotypic screen of putative *Cercospora zeina Δcrp1* knock-outs

3.4.4.1. Assessment of asexual spore production in *Cercopora zeina* in light

Cercospora zeina wild type strains produce significantly more spores ($P < 0.0001$) when grown in constant darkness compared to constant light as seen in Figure 13. The *C. zeina* wild type conidia concentration is thus reduced four-fold when grown in constant light compared to constant darkness. We set out to see what effect the disruption of the *crp1* (*wc-1* orthologue) will have on the pathogen's ability to produce conidia. The strains were cultured in triplicate per light condition, which were constant darkness and constant light. The putative *Δcrp1*

knock-outs showed a severe reduction in spore formation (2.9, 3.5 and 1.6 fold-change for *Δcrp1*_C2, *Δcrp1*_C3 and *Δcrp1*_F1 respectively) when cultured in constant light compared to constant darkness, but to a lesser degree when compared to the wild type. The one-way ANOVA test based on the Dunnett's multiple comparison test revealed that there is a significant difference with a 2.2 fold-change between the spore formation of *Δcrp1*_C2 and *Δcrp1*_F1 compared to the wild type cultures grown in constant light (Figure 13).

The de-repression of conidia production in light by the disruption of the CRP1 protein in *C. zeae-maydis* revealed that the blue light photoreceptor plays a role in light-dependent repression of conidia (Kim et al., 2011). Here we showed that disruption of the CRP1 protein in *C. zeina* also resulted in de-repression of conidia production in the *Δcrp1*_C2 and *Δcrp1*_F1 knock-out strains (Figure 13).

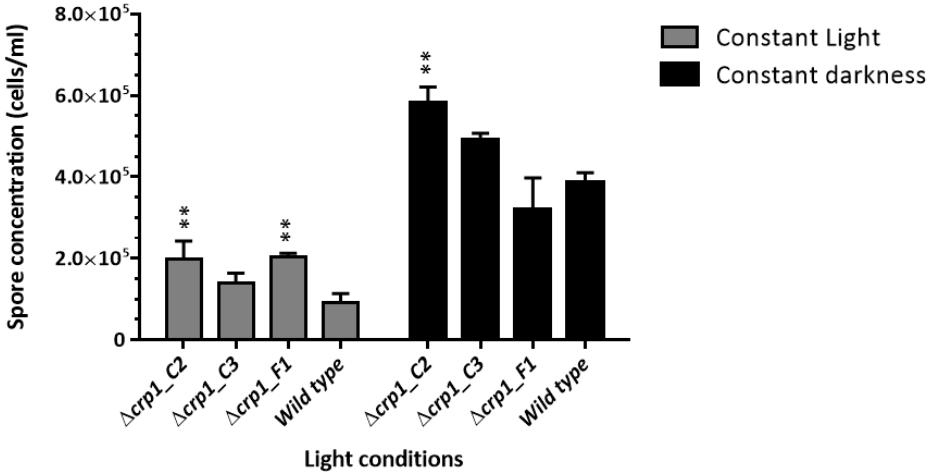

Figure 13. The effect of light on *Cercopora zeina Δcrp1* and wild type spore production. The wild type produced significantly less spores when cultured in constant light compared to darkness ($P < 0.0001$). The putative *Δcrp1* knock-out strains, C2 and F1, produced significantly more spores than the wild type cultured in constant light ($P < 0.01$). When cultured in constant darkness the putative *Δcrp1* knock-out strain, C2, produced significantly more spores compared to the wild type strain ($P < 0.01$). Error bars indicate 95% CI (confidence interval) based on the mean. The asterisk (*) indicates significant differences of the putative *Δcrp1* knock-out strains compared to the wild type for the respective light conditions.

3.4.4.2. Melanin assay

The putative *Δcrp1* knock-out strains produced visually darker cultures when grown on V8® media compared to the wild type with black droplets forming in the mycelial surface. These putative knock-out strains became darker cultures with successive sub-culturing. This led us to speculate that the darker cultures were due to an increased in melanin production between the putative *Δcrp1* knock-out and the wild type strains. Melanin production is known to be induced in response to high light intensities and UV exposure as a photo protective pigment. To test if more melanin is produced in *Δcrp1* knock-outs, all cultures were grown in triplicate in constant darkness and constant light in order to determine if light plays a role in the melanin production of the putative *Δcrp1* knock-out strains. A melanin standard curve was generated ranging from 0 – 100 µg/ml as seen in Figure B2 in Appendix B, which represents a total of nine readings per melanin concentration. This graph was used to determine the melanin concentration of the putative *Δcrp1* knock-out and the wild type strains. The pigment extracted from the putative *Δcrp1* knock-out and wild type strains was confirmed to be melanin based on the diagnostic tests proposed by Thomas (1955). In this regard, the extracted pigment was insoluble in water, dark brown in colour, soluble in 1 N NaOH and precipitated at a low pH in the presence of hydrochloric acid. Another test routinely used to characterise the pigment as melanin is that the log absorbance of melanin when plotted against the wavelength gives a linear curve with a negative slope. This was observed for the pigment extracted from cultures in this experiment (Figure B3 in Appendix B)

A clear difference was observed between the phenotypes of the strains cultured in constant light and constant darkness. The strains grown in constant light produced darker mycelia whereas in constant darkness, a light grey phenotype was observed (Figure 14). The putative *Δcrp1* knock-out strains produced a slightly darker phenotype when grown in constant darkness with black droplets forming on top of the mycelial surface (Figure B4 in Appendix B).

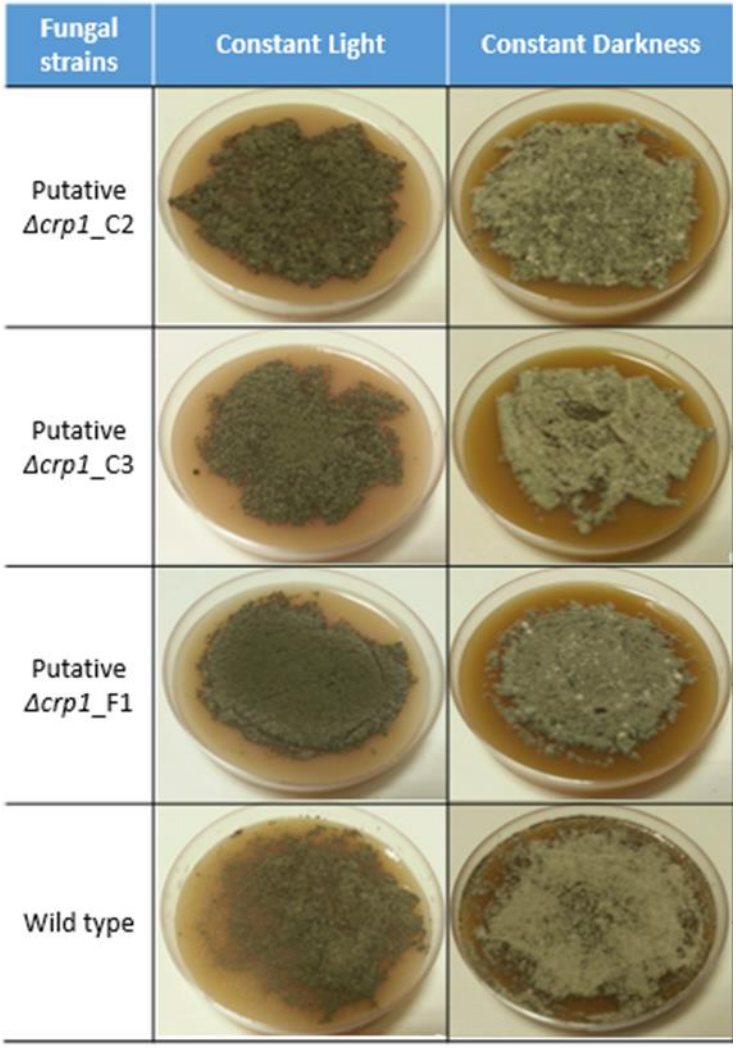

Figure 14. The effect of light on *Cercospora zeina* phenotype. The putative *Δcrp1* knock-out and the wild type strains were cultured in constant light and darkness for seven days. The cultures grown in constant light were darker, melanised cultures, whereas the cultures grown in constant darkness were light grey in colour.

Melanin concentrations of the putative *Δcrp1* knock-out and wild type strains, across the three biological replicates, were determined based on the melanin standard curve as seen in Figure B2 in Appendix B. Comparison of melanin concentrations between individual strains in constant light and darkness did not indicate any significant differences in melanin production. However, putative *Δcrp1* knock-out strains produced significantly higher concentrations of melanin when cultured in constant light and constant darkness compared to the wild type strain as seen in Figure 15.

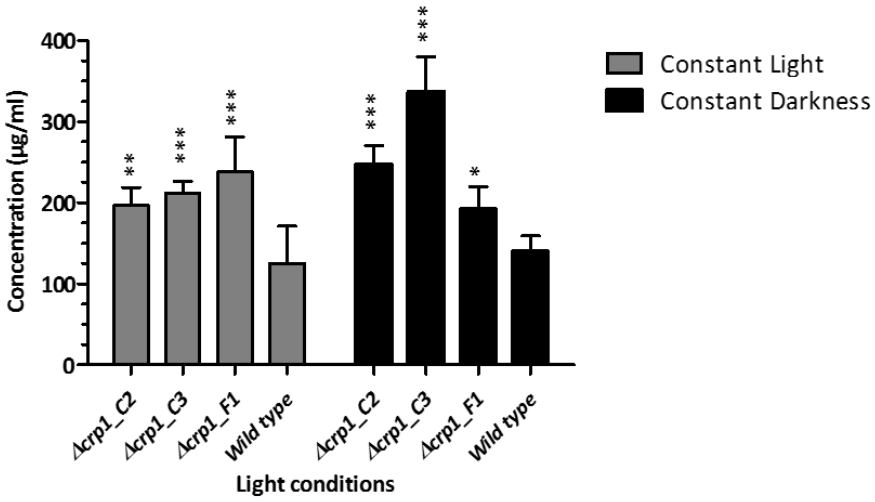

Figure 15. *Cercospora zeina* melanin production under light and dark conditions. The concentration of melanin produced between the wild type and the putative Δ*crp1* knock-out strains cultured in constant light and darkness. The putative *Δcrp1* knock-out strains produced significantly more melanin compared to the wild type when cultured in constant light and in constant darkness. The comparison between constant light and darkness of the individual strains did not show significant differences. The asterisk (*) indicates significant P-values at $P \leq 0.05$, $P \leq 0.01$, $P \leq 0.001$ for one, two and three asterisks, respectively Error bars indicate 95% CI (confidence interval) based on the mean.

3.4.4.3. Pathogenicity of putative *Cercospora zeina Δcrp1* knock-outs on maize

The maize inbred line B73, which is susceptible to *C. zeina* infection, was germinated in a phytotron at 34°C and high relative humidity. A drip irrigation system was designed, which delivers the same amount of water to each pot as seen in Figure 16 A and B. The first two maize infection trials resulted in yellowing of the plants two weeks after germination, which is an indication of a nitrogen deficiency, eventhough the plants were fertilised with a low concentration of soluble fertiliser (Nutrifeed, Starke Ayres, Bredell, Johannesburg) daily through the drip irrigation system. The yellowing of the leaves was reversed by fertilising the plants weekly with a concentrated NPK (nitrogen, phosphorous and potassium) granule fertiliser (Leaf and Lawn, Wonder™, Efekto™, Johannesburg) with the nitrogen concentration being higher than that of phosphorous and potassium in a 2:1 ratio.

The plants were infected five weeks after germination at the L7 stage with 2 x 10^5 cells/ml *C. zeina* wild type and knock-out strains. A room barrier was setup (as outlined in Figure 3) to separate the plants inoculated with the three putative *Δcrp1* knock-out strains and the wild type strains as seen in Figure 16 C. The uninfected control plants were grown in a separate phytotron under the same conditions.

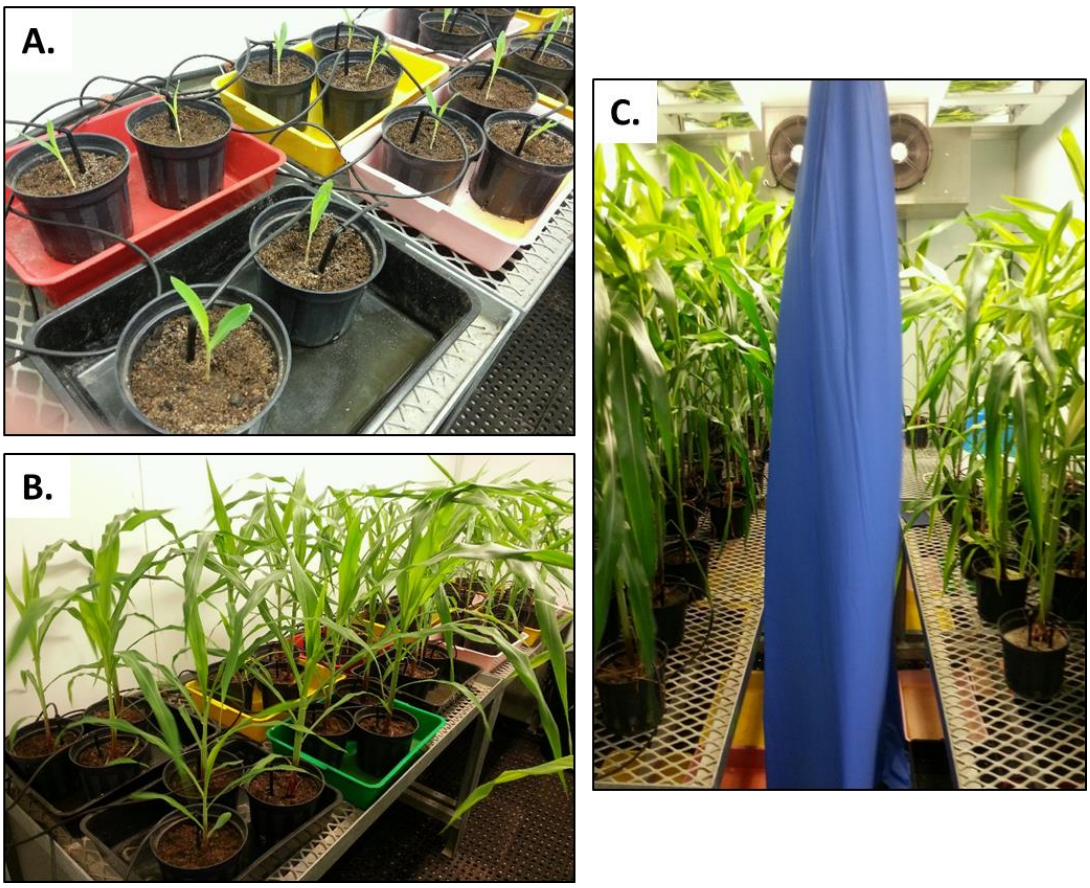

Figure 16. Infection of maize line B73 in a contained phytotron. (A) The maize inbred B73 line's seed germinated within one week after planting. (B) The plants at two weeks old. (C) The plants at seven weeks, after infection. The blue is the room divider, separating the plants infected with the putative *Δcrp1* knock-out strains on the left from the maize plants infected with the wild type strain on the right.

Infection of maize plants with *C. zeina* generally results in the formation of chlorotic spots within six days and lesions within thirteen days (Liversage, observation from glasshouse infections). In three consecutive maize infection trials none of the typical symptoms were observed on the infected leaves. Conditions were ideal for infection including high temperature and relative humidity. Lesions similar to GLS were observed on some of the

infected maize plants as seen in Figure 17 A- C, spots on the leaf surface, which over time forms lesions confined by the leaf margins. These lesion, however are light yellow/cream in colour and turn translucent over time, whereas the GLS lesions (Figure 17 D) are tan in colour with a grey centre where conidia are produced on conidiophores.

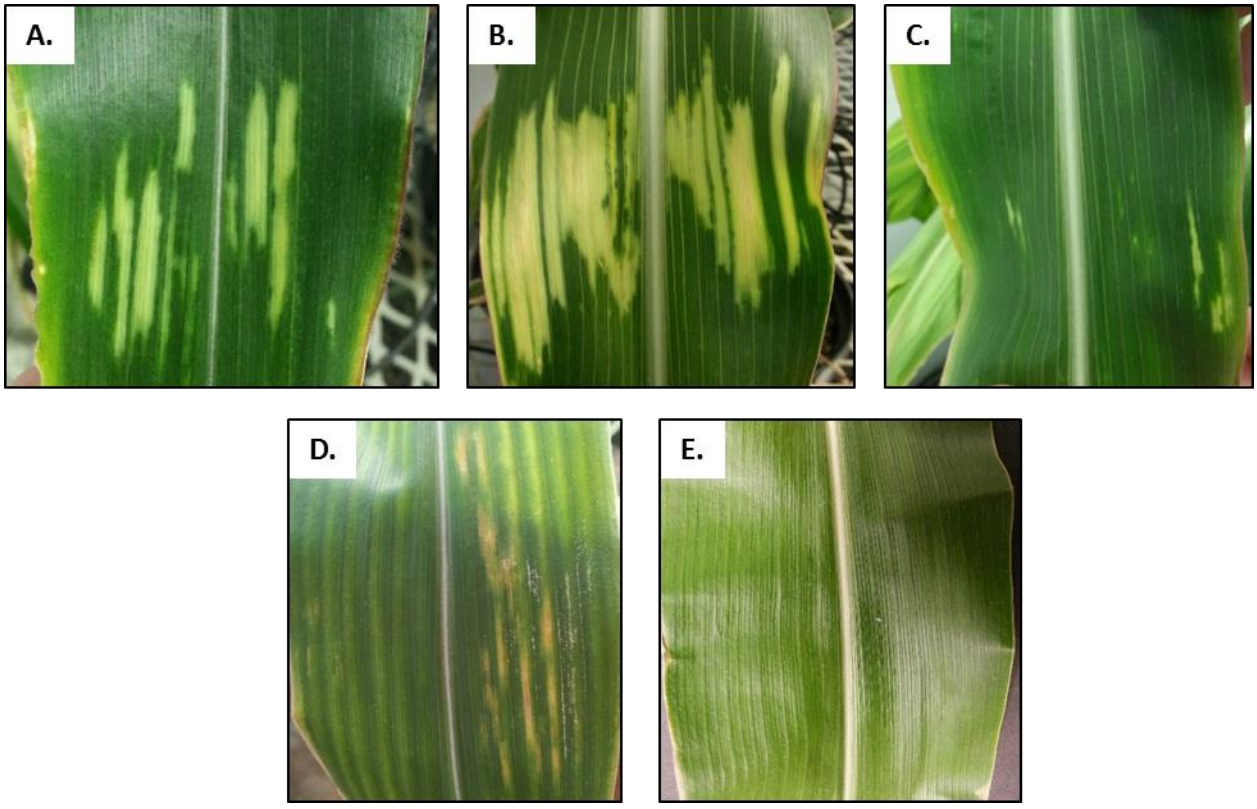

Figure 17. Grey leaf spot symptom development on infected maize B73 lines. The lesion type discolouration of the leaves infected (grown in a phytotron) with the putative *Δcrp1*_C2 (A), *Δcrp1*_C3 (B) knock-out and the wild types (C) strains have similarities to lesion formed in the glasshouse (D) when plants are infected with the wild type strain of *C. zeina*. (E) Maize inbred B73 uninfected controlled plant.

Since no visible signs of infection could be obtained, and the transgenic fungal strains had to be used within the confines of a contained phytotron, an alternative method was used to investigate the pathogenicity of the putative *Δcrp1* knock-out strains. The maize leaves were harvested at an early (six dpi), mid (13 dpi) and late time point (25 dpi) across the three biological replicates of each strain. The inoculated leaf pieces were stained in a 1% Congo red solution which stains the fungal hyphae (Slifkin and Cumbie, 1988). Confocal microscopy was performed on the leaves inoculated with wild type strain as seen in Figure 18. The stomata

on the leaf surface were evenly spaced in a 'stitching' pattern. The red auto fluorescence emitted by the leaf was transformed to black and white in order to better visualise the red fluorescence of the stained fungal hyphae. The stained maize leaves inoculated with *C. zeina* wild type strain indicated a branched hyphal network forming over the stomata, which is believed to be appresoria formation (Kim et al., 2011).

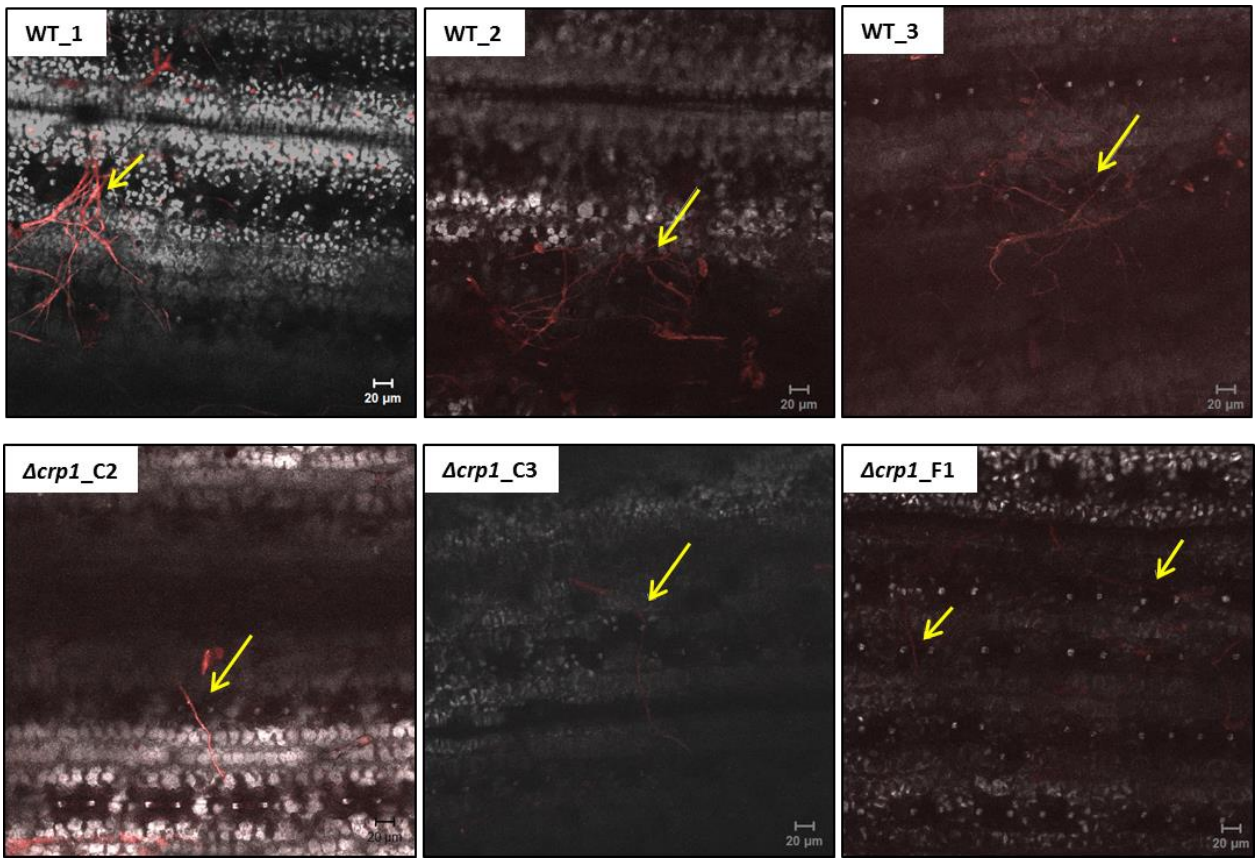

Figure 18. Confocal microscopy of maize inoculated leaf with *Cercospora zeina* wild type and *Δcrp1* knock-out strains. The rows of stomata can be clearly seen in the images forming a characteristic stitching pattern of monocot leaves. The fungal hyphae (stained red) forms a branching network over the stomata in the wild type across all the images indicated by yellow arrows to aid in the identification of the interaction. The ability of the fungal hyphae (stained in red) to branch out and form a network over the stomata is present at low frequencies in the putative *Δcrp1* knock-out strains. The putative *Δcrp1*_C2 shows a single, unbranched hyphae growing over the stomata. The putative *Δcrp1*_C3 shows a single, unbranched hyphae growing around the stomata. The putative *Δcrp1*_F1 shows a single, unbranched hyphae growing over the stomata.

Maize leaves inoculated with the *Δcrp1* knock-out strains showed a drastic reduction in the formation of a hyphal network over the stomata. In Figure 18 the predominant types of stomatal interactions are shown for the putative *Δcrp1* knock-out strains. Additional confocal images can be seen in in Figure B8 in the Appendix B. Sub-optimal image resolution was obtained, however the red stained fungal hyphae are still visible. The Congo red solution is light sensitive as are the stained samples, and the longer the samples were exposed to light the more reduced the fluorescent signal was. Single unbranched hyphae were observed on the maize leaves inoculated with the putative *Δcrp1* knock-out strains. The unbranched hyphae either grew either over the stomata or around it in close proximity.

The potential level of pathogenicity of the putative *Δcrp1* knock-out strains was determined by counting the type of stomatal interactions across the three biological replicates. The assumption made was that the pathogen has a high level of potential pathogenicity if there is formation of a branched hyphal network over the stomata (Kim et al., 2011). The potential level of pathogenicity is reduced when the type of stomatal interaction is single, unbranched hyphae growing either across or around the stomata. The percentage of each of the three types of stomatal interactions across the strains is shown in Figure 19 A and a graphical representation of the interactions in Figure 19 B. The *Δcrp1* knock-out strains showed a significant reduction ($P \leq 0.001$) in the formation of a branched hyphal network over the stomata, indicating that the *Δcrp1* knock-out strains have a reduced potential level of pathogenicity. The three *Δcrp1* knock-out strains showed a 6.2, 3.0 and 3.3 fold-change in network formation compared to the wild type strain for *Δcrp1*_C2, *Δcrp1*_C3 and *Δcrp1*_F1 respectively. The wild type showed significantly less single unbranched hyphae growing either around or over the stomata compared to the putative *Δcrp1* knock-out strains.

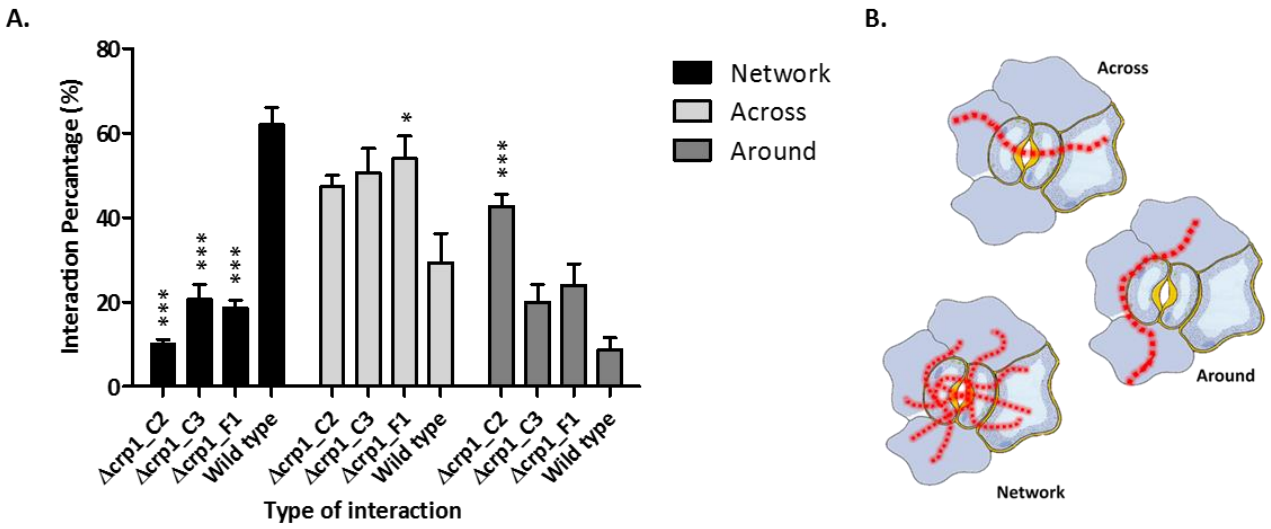

Figure 19. Stomatal interactions of *Cercospora zeina* wild type and *Δcrp1* knock-out strains on maize leaves. (A) The percentage of the type of stomatal interactions observed across three biological replicates and three technical replicates (preparation and staining of the leaves) for 50 random interactions counted per replicate. The putative *Δcrp1* knock-out strains, C2, C3 and F1 showed a significant reduction in network formation compared to the wild type strain. The asterisk (*) indicates significant P-values at $P \leq 0.05$ and $P \leq 0.001$ for one and three asterisks, respectively. Error bars indicate 95% CI (confidence interval) based on the mean. (B) Graphical representation of the three types of stomatal interactions observed under the confocal microscope.

3.5. Discussion

This study was the first successful gene disruption performed in *Cercospora zeina* using the split marker approach. The *crp1* gene, which is homologous to the *wc-1* gene characterised in *N. crassa,* is present in the genome sequence of *C. zeina* (Liversage, 2012). In this study the *crp1* gene, encoding a blue light photoreceptor, was functionally characterised and its potential role in pathogenicity shown.

3.5.1. Genotypic characterisation of the putative *Δcrp1* knock-out strains

A rapid DNA extraction method was developed for the screening of a large number of putative *Δcrp1* knock-out samples. Initial attempts to isolate genomic DNA using rapid protocols failed to deliver reliable results (Cenis, 1992; Griffin et al., 2002). The putative *Δcrp1* knock-out cultures were darker and more melanised, which might interfere with the isolation of pure, inhibitor free DNA and could affect downstream reactions (Eckhart et al., 2000). In order to improve the quality of isolated DNA, the lysis buffer was modified to include urea that aids to solubilise melanin, which is known to co-precipitate with DNA during an extraction (Eckhart et al., 2000). Furthermore, an additional phenol:chloroform step was added to denature and separate any protein contamination from the DNA samples. The developed protocol delivered reproducible results for all the samples, as determined by the effective amplification of the histone H3 gene from all 64 samples (data not shown).

The initial screens using the genomic DNA isolated using the rapid DNA extraction method were performed using the M13 primer set that flanks the *hyg*-cassette. This primer set screened for the presence of the complete *hyg*-cassette. A total of nine putative *Δcrp1* knock-outs were identified during the initial screen. A genomic DNA extraction method yielding high concentrations of DNA for subsequent screening was unsuccessful. An attempt to modify the CTAB protocol by adding urea to the lysis buffer and an additional phenol:chloroform step proved insufficient to remove inhibitors, as the efficiency of the PCR reactions declined after a few days. Melanin contains a large number of free carboxylic acid residues that are able to bind to charged molecules, such as DNA polymerase, and subsequently inactivates the

enzyme (Eckhart et al., 2000). The ZR Fungal/Bacterial DNA Midi™ isolation kit (Zymo Research) was therefore used and yielded good quality DNA but lower concentrations as compared to the CTAB method. In addition, PCR reactions were optimised by adding DMSO and BSA, which prevent the formation of secondary structures and binding of inhibitors to the DNA polymerase, respectively (Farell and Alexandre, 2012).

The M13 primer results were verified using another *hyg*-cassette screen primer set designed to the *trpC* promoter and 3'-end of the open reading frame of the hyg^R gene (Velushka Swart, personal communication). The external primer screen showed that the entire *hyg*-cassette is inserted into the correct genomic locations in the putative *Δcrp1* knock-out strains. This screen however does not eliminate the possibility of ectopic insertions, and for this a Southern hybridisation was performed using an internal hyg^R gene region as a probe.

The Southern hybridisation showed that a single integration event took place in all three of the putative *Δcrp1* cultures. However, the expected size of the hyg^R fragments, as calculated from the *C. zeina* genome sequence was not obtained. There are four possible scenarios that could be used to explain the size differences generated. The first, and most likely possibility, is that the laboratory strains of *C. zeina* accumulated spontaneous mutations as a result of successive sub-culturing, which can result in changes within the genome sequence and thus the restriction sites (Ronald et al., 2006). It is important to keep generating glycerol stocks of the cultures after every few generations of sub-culturing to ensure that one can go back to the original cultures should a result such as this be generated. Secondly, there could be an error in the draft genome sequence of *C. zeina* used in this study, which resulted in some BglII restriction sites not being predicted. The third scenario relates to the restriction digest of the genomic DNA. Whenever a restriction digest is performed using genomic DNA, one must first perform a digest using a dilution series of the enzyme digested for varying periods. This will allow one to see whether or not complete digestion occurred, and circumvent the possibility of star activity, which results in other random sites being cut other than the specific restriction site. It is also be important to perform restriction digests using two different restriction enzymes, which will allow one to confirm the results. However, in this project we were unable

to perform another restriction digest since isolation of genomic DNA from the *Δcrp1* knock-out strains proved to be difficult and yielded low amounts of DNA. The fourth and less likely possibility is that during homologous recombination new restriction sites could have been introduced at the site of integration.

The *crp1* gene expression data indicated that the *crp1* gene was still being expressed in the putative *Δcrp1* knock-out strains. Possible scenarios were developed in an attempt to explain the results. Firstly, there could be more than one copy of the *crp1* gene present in the genome sequence of *C. zeina*. However, sequencing results based on the fragments produced in RT-PCR proved that there are no nucleotide differences in the 3' terminal *crp1* nor the LOV domain sequence, which makes this scenario less likely (Figure 10 and 11). In order to confirm that there is only a single copy of the *crp1* gene present in the wild type *C. zeina,* we will need to perform a Southern hybridisation using a *crp1* gene specific probe. Secondly, it is possible that the putative *Δcrp1* knock-out cultures could be contaminated with spores from the wild type strain resulting in a mixed culture. Even though the knock-out strains were cultivated on media supplemented with the antibiotic hygromycin, the wild type mycelia would be protected by the *Δcrp1* hygromycin resistant mycelial matt formed by sub-culturing. A way to prevent this from happening is that one should generate single spore cultures after every few generations to ensure that pure cultures are being worked with.

The most likely scenario for the *crp1* gene being expressed in knock-outs, however is the tendency of heterokaryon formation during protoplast generation. This phenomena is apparently common in transformation techniques using protoplasts, and have been observed before in *Cercospora nicotiana* and other species such as *Alternaria alternata* and *Sclerotinia sclerotiorum* (Choquer et al., 2007; Pruss et al., 2014; Veluchamy and Rollins, 2008). Protoplasts are the cytosolic content of fungal cells, which are released during cell wall lysis. All the intracellular organelles are contained within the protoplast, including the nuclei. During protoplast regeneration, after being transformed with the two split marker constructs, protoplasts containing transformed and un-transformed nuclei can fuse together (Muralidhar and Panda, 2000). Fusion of protoplasts result in the formation of a heterokaryon that might

display a hybrid gene expression between the wild type and the *Δcrp1* knock-out strains (Muralidhar and Panda, 2000). The solution to this problem is to generate protoplasts (to split the heterokaryons) from the putative *Δcrp1* knock-out strains and to then isolate single spores (Pruss et al., 2014). Based on the observation that endogenous *crp1* gene is expressed (to a lesser extent as seen in Figure 12) in the putative *Δcrp1* knock-out strains, the phenotypic characterisation observed for *Δcrp1* knock-out strains is not an indication of the complete absence of the *crp1* gene, but is more similar to a knock-down approach.

3.5.2. Phenotypic characterisation of putative *Δcrp1* knock-out strains

The phenotypic screens identified a possible role for CRP1 protein in the growth and development of *C. zeina*. It may be argued that since expression of the *crp1* gene is detected in the *Δcrp1* knock-out strains, one cannot deduce the function of the gene. However, we observed clear phenotypic differences between the *Δcrp1* knock-out and the wild type strains in this project, which leads to reason that even at a reduced expression (especially *Δcrp1*_C2 knock-out strain) we are able to functionally characterise the role of the *crp1* gene in the growth and development of *C. zeina*. The conidia light assay showed that spore formation in the wild type is severely reduced by culturing the fungus in constant light compared to constant darkness (Figure 13). This result is similar to what Kim et al. (2011) observed in *C. zeae-maydis*, but to a lesser extent, as the *C. zeae-maydis* wild type strain was unable to produce spores in constant light. The CRP1 protein is thus believed to repress the production of spores in constant light as the knock-outs were able to produce more spores.

The melanin assay showed that there are only slight differences in the melanin concentrations being produced by the individual wild type and putative *Δcrp1* knock-out strains cultured in constant light and darkness, although there is a clear phenotypic difference (Figure 14). However, comparing the putative knock-out strains to the wild type cultured in constant light showed significantly more melanin is produced by the *Δcrp1* knock-out strains compared to the wild type strains (Figure 15).

The putative *Δcrp1* knock-out strains showed a distinct phenotypic difference to the wild type strains in terms of melanin production. The knock-out strains produced black droplets on top of the mycelial matt when grown in constant darkness and light (Figure B4 in Appendix B). Furthermore, based on visual observation, the putative *Δcrp1* knock-out strains excreted more melanin into the growth media, than the wild type cultures. These two observations argue that there might be a difference in the way melanin is deposited between wild type and knock-out strains, and that light influences the way melanin is produced and stored in the fungus.

Melanin is deposited in the fungal wall as granules that cross-links to polysaccharides, in particular, chitin. The granules can be deposited into the innermost cell wall (Nosanchuk and Casadevall, 2003), in the middle of the cell wall (Walker et al., 2010) or the outer cell wall (Caesor-Tanthat et al., 1995). The way melanin is deposited between the putative *Δcrp1* knock-out and the wild type strains could be detected in future work using the copper sulphide-silver method developed by Butler et al. (2005). This acts as a melanin probe that can be detected using light or electron microscopy. Applying this method will enable us to conclusively say that blue light plays a role in the melanin production pathway.

The possibility also exists that the “melanin” droplets seen on the putative *Δcrp1* knock-out cultures are due to water condensation, which means that the cell wall of the knock-out strains could have a higher hydrophobicity compared to the wild type. The porosity of the cell wall is influenced by the amount of melanin granules deposited into the cell wall. The difference in porosity can be tested through generating a size exclusion column made from SDS-boiled cell walls (Jacobson and Ikeda, 2005). The elution rate of dextran through the cell wall formed columns can be compared between the wild type and the *Δcrp1* knock-out strains. The more melanin deposited into the outer cell wall the smaller the pore size will be, which results in the cell wall being more hydrophobic (Jacobson and Ikeda, 2005).

A maize infection trail using the susceptible maize inbred line, B73, was setup in a phytotron, which provides an artificial controlled growth environment (Figure 2). An infection trial could not be conducted in the green house since a genetically modified strain, *Δcrp1*, was used to inoculate the maize plants. Temperature and relative humidity are important factors to consider when conducting infection trials using *C. zeina*. Thorson and Martinson (1993) showed that RH greater than 95 % is needed for optimal infection to take place. The level of moisture on the leaf surface encourages spore germination and spore survival (Beckman and Payne, 1983). The level of RH in the phytotron fluctuated between 57 – 100 % (Figure B7). The pseudo GLS lesions we observed on the maize plants grown in the phytotron (Figure 17 A and B) was possibly due to high light intensities (Felix Middleton, personal communication). Since no GLS symptoms could be produced during the infection trials in the phytotron, a stomatal interaction observation was applied to quantify the level of potential pathogenicity of the *Δcrp1* knock-out strains compared to the wild type.

The different stomatal interactions observed between the putative *Δcrp1* knock-out and wild type strains were counted and compared (Figure 19). The wild type strain generated a high level of network formation over the stomata. Since we could not clearly observe the formation of appressoria, network formation was used as an indication of high potential level of pathogenicity. Kim *et al.* (2011) showed that the wild type *C. zeae-maydis* hyphae re-orientated its growth towards the stomata and is able to form a hyphal network and infiltrate the plants. Only chlorotic spots were observed on the maize leaves infected with the *C. zeae-maydis Δcrp1* knock-out strains. The *C. zeina* putative *Δcrp1* knock-out strains in this study, showed a reduced level of potential pathogenicity since a lower percentage of network formation over the stomata was observed. The *Δcrp1*_C2 knock-out strain, which showed a 2.6-fold reduction in *crp1* expression compared to the wild type revealed a 6.2-fold reduction in the ability in network formation.

3.5.3. Concluding remarks

In conclusion, the split marker approach proved to be successful in single gene displacement in *Cercospora zeina*. We hypothesise that expression of the endogenous *crp1* gene detected in the *Δcrp1* knock-outs is due to a heterokaryon formation. However, clear phenotypic differences between the wild type and the *Δcrp1* knock-out strains, and the reduced expression of *crp1* in at least one of the knock-out strains (*Δcrp1*_C2) indicates that the *crp1* disrupted strains may represent a *crp1* knock-down from which some insight into the role of CRP1 can be determined. The *crp1* gene was found to be involved in the regulation of light dependent repression of conidia formation. Furthermore, the CRP1 protein is believed to play a role in the way melanin is deposited in the fungal cell wall. The potential pathogenicity of *C. zeina* is regulated by blue light. The early stage of infection is dependent on the ability of the fungus to perceive the opening of the stomata and the reorientation of its hyphal growth towards the stomata. To complete Falkow's molecular version of Koch's postulates (Falkow, 1988) complementation of the *Δcrp1* knock-out strains with the endogenous *crp1* gene is required to verify that the observed phenotype is due to the disruption of the *crp1* gene.

3.6. References

Beckman, P., Payne, G., 1983. Cultural techniques and conditions influencing growth and sporulation of *Cercospora zeae-maydis* and lesion development in corn. *Phytopathology*. **73**, 286-89.

Bhatia, A., Munkvold, G.P., 2002. Relationships of environmental and cultural factors with severity of gray leaf spot in maize. *Plant Disease.* **86**, 1127-33.

Bluhm, B.H., Dunkle, L.D., 2008. PHL1 of *Cercospora zeae-maydis* encodes a member of the photolyase/cryptochrome family involved in UV protection and fungal development. *Fungal Genet. Biol.* **45**, 1364–72.

Butler, M.J., Gardiner, R.B., Day, A.W., 2005. Fungal melanin detection by the use of copper sulfide-silver. *Mycologia*. **97**, 312-19.

Cenis, J.L., 1992. Rapid extraction of fungal DNA for PCR amplification. *Nucleic Acids Res.* **20**, 2380.

Chen, H., Lee, M.H., Daub, M.E., Chung, K.-R., 2007. Molecular analysis of the cercosporin biosynthetic gene cluster in *Cercospora nicotianae*. *Mol. Microbiol.* **64**, 755–70.

Choquer, M., Lee, M., Bau, H., Chung, K., 2007. Deletion of a MFS transporter-like gene in *Cercospora nicotianae* reduces cercosporin toxin accumulation and fungal virulence. *FEBS Lett*. **581**, 489-94.

Christensen, A., Quail, P., 1996. Ubiquitin promoter-based vectors for high-level expression of selectable and/or screenable marker genes in monocotyledonous plants. *Transgenic Res.* **5**, 213-18.

Crous, P.W., Groenewald, J.Z., Groenewald, M., Caldwell, P., Braun, U., Harrington, T.C., 2006. Species of *Cercospora* associated with grey leaf spot of maize. *Stud. Mycol.* **55**, 189–97.

Eckhart, L., Bach, J., Ban, J., Tschachler, E., 2000. Melanin binds reversibly to thermostable DNA polymerase and inhibits its activity. *Biochem. Biophys. Res. Commun.* **271**, 726–30.

Fairhead, C., Llorente, B., Denis, F., Soler, M., Dujon, B., 1996. New vectors for combinatorial deletions in yeast chromosomes and for gap-repair cloning using “split-marker”recombination. *Yeast*. **12**, 1439-57.

Falkow, S., 1988. Molecular Koch’s postulates applied to microbial pathogenicity. *Rev. Infect. Dis*. **10**, 274-76.

Farell, E.M., Alexandre, G., 2012. Bovine serum albumin further enhances the effects of organic solvents on increased yield of polymerase chain reaction of GC-rich templates. *BMC Res. Notes.* **5**, 257.

Fu, J., Hettler, E., Wickes, B., 2006. Split marker transformation increases homologous integration frequency in *Cryptococcus neoformans. Fungal Genet. Biol.* **43**, 200-12.

Griffin, D.W., Kellogg, C.A., Peak, K.K., Shinn, E.A., 2002. A rapid and efficient assay for extracting DNA from fungi. *Lett. Appl. Microbiol.* **34**, 210–14.

Jacobson, E.S., Ikeda, R., 2005. Effect of melanization upon porosity of the cryptococcal cell wall. *Med. Mycol.* **43**, 327–33.

Kim, H., Ridenour, J.B., Dunkle, L.D., Bluhm, B.H., 2011. Regulation of stomatal tropism and infection by light in *Cercospora zeae-maydis*: evidence for coordinated host/pathogen responses to photoperiod. *PLoS Pathog.* **7**, e1002113.

Kück, U., Hoff, B., 2010. New tools for the genetic manipulation of filamentous fungi. *Appl. Microbiol. Biotechnol.* **86**, 54-62.

Langenhoven, B. (2015). Insight into three putative *Cercospora zeina* effector genes and the role they play in virulence. MSc. University of Pretoria.

Latterell, F.M., Rossi, A.E., 1983. Gray leaf spot of corn: a disease on the move. *Plant Dis*. **67**, 842–47.

Lingappa, Y., Sussman, A.S., Bernstein, I.A., 1963. Effect of light and media upon growth and melanin formation in *Aureobasidium pullulans* (de By.)Arn. (=p*ullularia pullulans*). *Mycopathol. Mycol. Appl.* **20**, 109–28.

Liversage, J., 2012. Functional characterisation of the *Cercospora zeina crp1* gene as a putative pathogensis regulation factor. Unpublished BSc (Hons) Dissertation, University of Pretoria.

Möller, E., Bahnweg, G., 1992. A simple and efficient protocol for isolation of high molecular weight DNA from filamentous fungi, fruit bodies, and infected plant tissues. *Nucleic Acids*. **20**, 6115-6.

Munkvold, G.P., Martinson, C. a, Shriver, J.M., Dixon, P.M., 2001. Probabilities for profitable fungicide use against gray leaf spot in hybrid maize. *Phytopathology.* **91**, 477–84.

Muralidhar, R. V., Panda, T., 2000. Fungal protoplast fusion – a revisit. *Bioprocess Eng.* **22**, 429–31.

Nelson, R., Pryor, B., Lodge, J., 2003. Sequence length required for homologous recombination in *Cryptococcus neoformans*. *Fungal Genet. Biol.* **38**, 1-9.

Pratt, R., Aramayo, R., 2002. Improving the efficiency of gene replacements in *Neurospora crassa*: a first step towards a large-scale functional genomics project. *Fungal Genet. Biol.* **37**, 56-71.

Pruss, S., Fetzner, R., Seither, K., Herr, A., Pfeiffer, E., Metzler, M., Lawrence, C.B., Fischer, R., 2014. Role of the *Alternaria alternata* blue-light receptor LreA (white-collar 1) in spore formation and secondary metabolism. *Appl. Environ. Microbiol.* **80**, 2582–91.

Ronald, J., Tang, H., Brem, R.B., 2006. Genomewide evolutionary rates in laboratory and wild yeast. *Genetics.* **174**, 541–4.

Sen, D., Joshi, A.K., Prasad, L.C., 2010. Association of melanin content with conidiogenesis in *Bipolaris Sorokiniana* of barley (*Hordeum vulgare L.*). *World J. Microbiol. Biotechnol.* **26***,* 309–16.

Shim, W., Dunkle, L.D., 2003. CZK3 , a MAP kinase kinase kinase homolog in *Cercospora zeae-maydis*, regulates cercosporin biosynthesis, fungal development, and pathogenesis. *MPMI.* **16**, 760–8.

Taylor, R., Walker, D., McInnes, R., 1993. *E. coli* host strains significantly affect the quality of small scale plasmid DNA preparations used for sequencing. *Nucleic Acids Res.* **21**, 1677-8.

Thorson, P., Martinson, C., 1993. Development and survival of *Cercospora zeae-maydis* germlings in different relative-humidity environments. *Phytopathology*. **83**, 153-57.

Upchurch, R., Walker, D., 1991. Mutants of *Cercospora kikuchii* altered in cercosporin synthesis and pathogenicity. *ASM*. **57**, 2940-5.

Veluchamy, S., Rollins, J.A., 2008. A CRY-DASH-type photolyase/cryptochrome from *Sclerotinia sclerotiorum* mediates minor UV-A-specific effects on development. *Fungal Genet. Biol.* **45**, 1265–76.

Walker, C. a, Gómez, B.L., Mora-Montes, H.M., Mackenzie, K.S., Munro, C. a, Brown, A.J.P., Gow, N. a R., Kibbler, C.C., Odds, F.C., 2010. Melanin externalization in *Candida albicans* depends on cell wall chitin structures. *Eukaryot. Cell*. **9**, 1329–42.

Ward, J., Stromberg, E., 1999. Gray leaf spot: a disease of global importance in maize production. *Plant Disease.* **83**, 884-95.

You, B.J., Lee, M.-H., Chung, K.-R., 2009. Gene-specific disruption in the filamentous fungus *Cercospora nicotianae* using a split-marker approach. *Arch. Microbiol.* **191**, 615–22.

General Discussion

Chapter 4

Blue light perception in host-pathogen interactions – Insights and future prospects into molecular infection strategies of *Cercospora zeina*

4.1. Introduction

Maize (*Zea mays*) is the most important grain crop in Southern Africa, and is the main staple food crop in South Africa, especially in the rural areas. Furthermore, maize forms the base for animal grain feed. Currently, crop production in South Africa is not keeping up with population growth. Food production in South Africa increases at an annual rate of about 2%, while the population grows at an average rate of 3% (Tittonell and Giller, 2013). In addition, South Africa depends on maize exports to neighbouring countries for economic growth, and thus to show a profit, annual crop production rates of 4 -7% are required (Breman and Debrah, 2003).

Agricultural intensification, which is increasing maize production per unit area, is the preferred solution for expanding the current production area in order to increase annual crop production rates (Mueller et al., 2012; Ruffo and Gentry, 2014). To keep up with the increasing food demands of the growing population, we need to increase the yield of the crop and close yield gaps. The difference between the actual yield of a farmer and the potential yield is referred to as the yield gap (Cassman et al., 2003). The yield of a crop, when grown in favourable environments with optimal water and nutrient supply, and effective pest and disease control, is referred to as yield potential (Evans and Fischer, 1999). In general, maize yields do not exceed 70% of the potential yield of a harvest (Dobermann et al., 2003). Thus to increase profits and ensure food security, we need to minimise yield gaps by understanding the factors that reduce and or limit crop yield potential.

4.2. Factors affecting crop yield potential.

Factors that influence crop yield potential are abiotic and biotic factors. Drought and nutrient deficiencies are the two most common abiotic stresses and yield-limiting factors for maize production (Mueller et al., 2012). In 2014, South Africa produced 14.9 million tonnes of maize, which was 20% higher than previous years (GIEWS, 2015). The drought experienced in the 2014/2015 growing season however, resulted in a 35% decrease in maize production, which increased the yield-gap during this season. South Africa only produced around 10 million tonnes in the 2014/2015 growing season, and as a result, had to import maize from neighbouring countries, specifically Zambia, to stabilise national demands (GIEWS, 2015).

The major biotic stresses responsible for yield-reduction are weed competition, insect damage and diseases (Ruffo and Gentry, 2014). Various hybrid maize varieties (insect and herbicide resistant cultivars) are susceptible to fungal foliar diseases (Ruffo and Gentry, 2014), two of which are of particular importance in South Africa namely grey leaf spot (causal agent: *Cercospora zeina*) and northern corn leaf blight (causal agent: *Exserohilum turcicum*). Grey leaf spot can cause yield losses that range between 50 – 65%, depending on the level of resistance of the maize hybrid (Ward et al., 1999). Maize yields are lowered due to a decrease in the photosynthetic area of the plants, which in turn decreases the strength and stability of the stalk resulting in lodging and a reduction in the amount of grain harvested (Dodd, 1980).

4.3. Current management of GLS in the field. Conventional approaches to control grey leaf spot are limited and not sustainable. Management factors that increase the risk of grey leaf spot are planting susceptible hybrids, no crop rotation, using no- or minimum tillage practices, irrigation, planting maize late in the season and planting at higher densities that will increase the spread of the disease (Wise and Mueller, 2011). Systemic foliar fungicides, in particular with the active compounds picoxystrobin (strobilurin) and cyproconazole (triazole), have been shown to be effective against a broad-spectrum of fungal pathogens (Grossmann and Retzlaff, 1997). Fungicides are effective in controlling grey leaf spot in the field and result in higher yields when applied at the correct time and frequency (Ward et al., 1996). However, increases in fungicide treatment concentration and the number of applications during the season depends on whether or not the expected income from the treated fields exceeds the additional cost of the fungicide (Ward et al., 1997). The use of fungicides to control GLS in the field is not only an economical risk to the farmer but is also not sustainable as fungicidal resistance builds up over time (Ward et al., 1997). Furthermore, ergosterol inhibitors such as azole in fungicides pose a health risk and are being considered for tighter regulation by the European Commission (EU) due to the increase in human hormone-related diseases (Jones, 2014).

4.4. Infection strategy of *Cercospora zeina*. Successful control of grey leaf spot in the field is dependent on understanding the molecular strategies *Cercospora zeina* uses in order to evade and manipulate the maize host plant's immune system. The early stage of infection is of particular importance to understand how the fungus perceives the stomatal opening and infiltrates the plant to cause disease (Kim et al., 2011). Entry into the host plant by *C. zeina* through the stomata was shown to be similar to that of *C. zeae-maydis* based on confocal microscopy using a green fluorescently tagged strain of *C. zeina* (A.E. Visser, personal communication).

The ability of the fungus to perceive the stomatal opening has been shown in *C. zeae-maydis* to be regulated by the CRP1 orthologue of the White Collar-1 protein first characterised in *Neurospora crassa* (Ballario et al., 1996; Kim et al., 2011). In our study we showed that the level of potential pathogenesis of the *C. zeina* is reduced following the knock-out of the white collar-1 gene.

4.5. Functional characterisation of genes in *Cercospora zeina*. The split marker approach proved to be a feasible option for knocking out a gene of interest and determining its function in *Cercospora zeina*. However, various steps in the generation of knock-outs had to be optimised since this was the first attempt at disrupting a gene in this fungus. Based on results obtained and obstacles encountered in this project I would like to suggest a work flow (as indicated by the bracketed steps in paragraphs below) for the generation of future gene knock-out experiments in *C. zeina*.

The first step will be to determine the copy number of the gene of interest (step 1) in order to select an appropriate gene disruption approach. The expression of single copy genes can be disrupted using either a knock-in (inserting a piece of foreign DNA into the gene of interest) or a knock-out strategy where the gene of interest is replaced with an antibiotic selectable marker (Kück and Hoff, 2010). RNA interference will be more appropriate if more than one copy of the gene is present in the genome of the organism (Kück and Hoff, 2010).

Generation of the split marker constructs (step 2) proved to be a difficult task due to the GC rich sequence in the 5'-region flanking the *crp1* in *C. zeina*. Combining the gene flanking regions with the *hyg* fragments showed to be more efficient using single overlap extension PCR (SOEing PCR) (Horton, 1993) than a fusion PCR approach. The sequences of the individual constructs should then be cloned and the sequences verified before transformation of the fungal protoplasts.

Initial screening of the knock-outs (step 3) should first be performed with gene specific primers (presence or absence of the endogenous gene) followed by hyg^R specific primers (presence or absence of the inserted hyg^R gene), and lastly the genomic location primers (confirm that hyg^R gene inserted into correct location). Addition of 9% DMSO and 0.8 µg/µl BSA to the PCR reactions assisted in minimising the effect of any inhibitors produced by the knock-out strains (Farell and Alexandre, 2012). Once all three PCR amplifications have yielded desirable results one can proceed with screening for ectopic insertions (step 4) using a hyg^R specific probe in a Southern hybridisation experiment before characterising the function of the gene. Restriction digest of the genomic DNA should be performed using at least two different enzymes in order to verify the copy number of the inserted hygromycin resistance gene. If however, amplification of the endogenous gene is observed and the amplification of the hyg^R screens are positive then a heterokaryon has formed and the transformed cultured should be subjected to another cell wall lysis step to produce protoplasts in order to split the two nuclei or alternatively repeat the transformation step with the split marker constructs (Pruss et al., 2014).

The verified knock-out strains can then be phenotypically characterised (step 5) and its effect on pathogenicity determined (step 6). In this study we have shown that the current phytotron setup is not efficient for maize infection trials with *C. zeina*. Conducting a maize infection trial with seedlings covered in bags to increase the humidity could be a possible solution to the problem (M.B.L. Malefo, personal communication). Maize infection trials using the knock-out strains in comparison to the *C. zeina* wild type will reveal the extent the gene of interest plays

in pathogenesis. Quantification of the *in planta* fungal load can be determined and compared at each time point for both the knock-out and wild type strains using a real time PCR approach developed for *C. zeina* maize infections (Korsman et al., 2011). Confocal microscopy using the 1% Congo red stain can be done concurrently with the fungal quantification at each time point to visually assess differences in infection structures between the wild type and knock-out strains. Finally, complementation of the knock-out strains with the endogenous gene will enable one to complete Falkow's molecular version of Koch's postulates (Falkow, 1988), and confirm that phenotype observed is due to the disrupted gene.

4.6. Regulation of pathogenesis by blue light in *Cercospora zeina*. The ability to perceive blue light through the functioning of the White Collar-1 protein has been shown to be essential to the survival of *Botrytis cinerea*. Briefly, Canessa et al. (2013) has shown that in order for the fungus to successfully colonise the host plant tissue the WC-1 protein is required to detoxify reactive oxygen species (ROS) produced by the host during an immune response. The White Collar-1 protein is required not only to protect the fungus against plant derived ROS, but also endogenous phytotoxins such as cercosporin produced by *C. zeae-maydis* (Kim et al., 2011; Kuratani et al., 2010). Although not experimentally shown, sensitivity to ROS produced by the host could be a reason why the disease did not progress in leaves infected with *C. zeae-maydis Δcrp1* knock-out strain.

The White Collar-1 protein has been shown to be responsible for regulating blue light dependent growth and development processes in various fungi. However, many of the processes in the White Collar-1 knock-out strains were only delayed as was the case for cercosporin production in *C. zeae-maydis* and secondary metabolite production in *Fusarium* species as well as photomorphogenesis in *Coprinus cinereus* (Estrada and Avalos, 2008; Kim et al., 2013, 2011; Terashima et al., 2005). These papers suggested that another unidentified blue light photoreceptor might be responsible for regulating blue light dependent processes either in sync with White Collar-1 or independently. In this study we identified a putative blue light cryptochrome (CRY-DASH) photoreceptor in the genome sequences of *C. zeina* and *C. zeae-maydis*. It would be interesting to see what blue light dependent process are affected

by disrupting this *cry-dash* gene in *C. zeina* and to examine the expression profiles of light dependent genes (discussed in Chapter 1) in double mutants of both the *crp1* and the *cry-dash* gene.

4.7. Proposed management of grey leaf spot disease in the field. RNA interference (RNAi) is an emerging strategy to control fungal pathogens through inhibiting the expression of genes vital to the survival of the pathogen (Nunes and Dean, 2012; Rajam, 2012). Host induced gene silencing (HIGS) is based on the down regulation of important gene(s) that are required for the fungal growth and development through the uptake of double stranded (dsRNA) or small interfering RNA (siRNA) produced by transgenic plants (Duan et al., 2012). The host plant is transformed with a binary vector expressing hair-pin RNA specific to a fungal gene or gene family, which will result in reduced transcript numbers of the target gene and ultimately the function of that gene.

Over the last few years more reports have shown the positive effect of HIGS incorporated in food crops in response to in biotrophic, necrotrophic and hemibiotropic fungi. *Fusarium* wilt (caused by *Fusarium oxysporum*) can be controlled in transgenic banana lines expressing siRNA targeting *Fusarium* transcription factor 1 (*ftf1*) and the velvet protein both involved in growth and development of the fungus (Ghag et al., 2014). Furthermore, the hemobiotroph, *Fusarium graminearum* was effectively managed in barely and *Arabidopsis thaliana* plants, both expressing dsDNA targeting transcripts of the fungal cytochrome P450 lanasterol C-14α-dimethylase (CYP51) (Koch et al., 2013). The biotrophic oomycete, *Bremia lactucae*, which causes downy mildew of lettuce, can be inhibited through host induced gene silencing in traingenic plants expressing inverted repeats of fragments of the cellulose synthase (CES1) gene (Govindarajulu et al., 2014).

Incorporating HIGS as a durable and sustainable genetic disease resistance strategy requires careful consideration of which fungal gene(s) to target that will result in reduced pathogenesis. Targeting effector genes, especially the genes involved in the gene-for-gene

concept, called avirulence genes (*Avr*), would not be a feasible option for a HIGS strategy since the genes are constantly evolving in order to evade recognition by the corresponding host resistance (R) gene (Stukenbrock and McDonald, 2009). Genes that are involved in the growth and development of the fungus, which play a role in determining the virulence or the development of disease in the host plant could be possible targets to consider (Nunes and Dean, 2012).

The White Collar-1 protein is well conserved across the fungal kingdom, as shown in this study (Chapter 2), and will possibly make a good target for host induced silencing resulting in a broad host resistance. In theory, targeting the N-terminal PAS domain, the light-oxygen-voltage (LOV) domain, of *C. zeina* will not alter the expression of the host endogenous plant blue light perception proteins due to the low sequence similarity. Results obtained in this study (Chapter 3) suggest reduced expression of the *crp1* gene in *C. zeina* had a significant effect on the pathogen's ability to produce infection structures and thus its ability to cause disease.

Understanding the infection strategy of *C. zeina* is important if one wants to control the disease in the field. In *C. zeae-maydis* the *Δcrp1* knock-out strains were able to infect the maize plants, but the disease progression was halted at the formation of chlorotic spots (Kim et al., 2011). The disease could not progress and thus mature lesions were not able to form. Using a proteomic approach one can identify the effector proteins that are under the control of blue light by comparing the protein profiles between maize plants infected with either the *Δcrp1* knock-out or the wild type strains. A method to extract apoplastic fluid from infected maize leaves has been developed by the Cereal Foliar Pathogen Research (CFPRG) group, which can be used to extract secreted effector proteins from the infected leaves (Liversage, unpublished).

4.8. Concluding remarks. In conclusion, this study represented the first split marker approach applied to *Cercospora zeina* to study gene function. We managed to successfully replace the

crp1 gene with a hygromycin resistance gene, even though the endogenous gene was still expressed at a reduced level. In this chapter a work flow for future knock-out experiments in *C. zeina* has been proposed in order to avoid obstacles experienced in this project. However, despite this, we managed to show that the *crp1* gene plays a key role in early infection of maize plants. The conservation of this gene makes it attractive for host induced silencing experiments, which will possibly result in a durable resistance strategy to manage grey leaf spot disease in the field. It is expected that maize plants harbouring the RNAi construct will show broad host resistance due to the conservation, of the LOV domain in the WC-1 gene in fungi. A durable genetic disease management strategy such as HIGS stably introduced into maize lines could provide us with an environmentally friendly sustainably strategy to close the yield-gap, and thus ensure an increase in annual maize production rates in the future.

4.9. References

Ballario, P., Vittorioso, P., Magrelli, A., Talora, C., Cabibbo, A., Macino, G., Sapienza, L., 1996. White collar-1 , a central regulator of blue light responses in *Neurospora* , is a zinc finger protein. *EMBO J.* **15**, 1650–57.

Breman, H., Debrah, S., 2003. Improving African Food Security. *SAIS Rev.* **23**, 153–70.

Canessa, P., Schumacher, J., Hevia, M. a, Tudzynski, P., Larrondo, L.F., 2013. Assessing the effects of light on differentiation and virulence of the plant pathogen *Botrytis cinerea*: characterization of the White Collar Complex. *PLoS One.* **8**, e84223.

Cassman, K., 2003. Meeting cereal demand while protecting natural resources and improving environmental quality. *Annu. Rev.* **28**, 315-58.

Dobermann, A., Arkebauer, T., Cassman, K., Drijber, R., Lindquist, J., Specht, J., Walters, D., Yang, H., Miller, D., Binder, D., Teichmeier, G., Ferguson, R., Wortmann, C., 2003. Understanding corn yield potential in different environments. *Agron. Hortic. Fac. Publ.* **542**, 1 - 6.

Dodd, J., 1980. The photosynthetic stress-translocation balance concept of sorghum stalk-rot. Proc. Int. Work. Sorghum diseases, a world review. Proc Intl Wkshp on Sorghum Diseases, sponsored jointly by Texas A & M university (USA) and ICRISAT, Patancheru, AP, 502324, India, pp 300–305.

Duan, C., Wang, C., Guo, H., 2012. Application of RNA silencing to plant disease. *Silence*. **3**, 1-8.

Estrada, A.F., Avalos, J., 2008. The White Collar protein WcoA of *Fusarium fujikuroi* is not essential for photocarotenogenesis, but is involved in the regulation of secondary metabolism and conidiation. *Fungal Genet. Biol.* **45**, 705–18.

Evans, L.T., Fischer, R.A., 1999. Yield Potential. *Crop Sci.* **39**, 1544.

Farell, E.M., Alexandre, G., 2012. Bovine serum albumin further enhances the effects of organic solvents on increased yield of polymerase chain reaction of GC-rich templates. *BMC Res. Notes.* **5**, 257.

Ghag, S., Shekhawat, U.K.S., Ganapathi, T.R., 2014. Host-induced post-transcriptional hairpin RNA-mediated gene silencing of vital fungal genes confers efficient resistance against *Fusarium* wilt in banana. *Plant Biotechnol*. **12**, 541-53.

GIEWS, (2015). Expected sharp fall in Southern African maize production raises food security concerns. [online] Available at: http://www.fao.org/news/story/en/item/284839/icode/ [Accessed 29 Apr. 2015].

Govindarajulu, M., Epstein, L., Wroblewski, T., Michelmore, R.W., 2014. Host-induced gene silencing inhibits the biotrophic pathogen causing downy mildew of lettuce. *Plant Biotechnol*.

Grossmann, K., Retzlaff, G., 1997. Bioregulatory effects of the fungicidal strobilurin kresoxim-methyl in wheat (*Triticum aestivum*). *Pestic. Sci.* **50**, 11-20.

Korsman, J., Meisel, B., Kloppers, F.J., Crampton, B.G., Berger, D.K., 2011. Quantitative phenotyping of grey leaf spot disease in maize using real-time PCR. *Eur. J. Plant Pathol.* **133**, 461–71.

Kim, H., Ridenour, J.B., Dunkle, L.D., Bluhm, B.H., 2011. Regulation of stomatal tropism and infection by light in *Cercospora zeae-maydis*: evidence for coordinated host/pathogen responses to photoperiod? *PLoS Pathog*. **7**, e1002113.

Kim, H., Son, H., Lee, Y.-W., 2013. Effects of light on secondary metabolism and fungal development of *Fusarium graminearum*. *J. Appl. Microbiol*. doi:10.1111/jam.12381

Koch, A., Kumar, N., Weber, L., 2013. Host-induced gene silencing of cytochrome P450 lanosterol C14α-demethylase–encoding genes confers strong resistance to *Fusarium* species. *Proc. Natl. Acad. Sci. U.S.A.* **110**, 19324-29.

Kück, U., Hoff, B., 2010. New tools for the genetic manipulation of filamentous fungi. *Appl. Microbiol. Biotechnol.* **86**, 54-62.

Kuratani, M., Tanaka, K., Terashima, K., Muraguchi, H., Nakazawa, T., Nakahori, K., Kamada, T., 2010. The dst2 gene essential for photomorphogenesis of *Coprinopsis cinerea* encodes a protein with a putative FAD-binding-4 domain. *Fungal Genet. Biol.* **47**, 152–8.

Mueller, N., Gerber, J., Johnston, M., 2012. Closing yield gaps through nutrient and water management. *Nature*. **490**, 254-57.

Nunes, C., Dean, R., 2012. Host-induced gene silencing: a tool for understanding fungal host interaction and for developing novel disease control strategies. *Mol. Plant Pathol.* **13**, 519-29.

Pruss, S., Fetzner, R., Seither, K., Herr, A., Pfeiffer, E., Metzler, M., Lawrence, C.B., Fischer, R., 2014. Role of the *Alternaria alternata* blue-light receptor LreA (white-collar 1) in spore formation and secondary metabolism. *Appl. Environ. Microbiol*. **80**, 2582–91.

Rajam, M., 2012. Host induced silencing of fungal pathogen genes: An emerging strategy for disease control in crop plants. *Cell Dev. Biol*. **1**, 118.

Ruffo, M., Gentry, L., 2014. Evaluating management factor contributions to reduce corn yield gaps. *Agron. 107*, 495-505.

Stukenbrock, E., McDonald, B., 2009. Population genetics of fungal and oomycete effectors involved in gene-for-gene interactions. *Mol. Plant-Microbe Interact*. **22**, 371-380.

Terashima, K., Yuki, K., Muraguchi, H., Akiyama, M., Kamada, T., 2005. The *dst1* gene involved in mushroom photomorphogenesis of *Coprinus cinereus* encodes a putative photoreceptor for blue light. *Genetics.* **171**, 101–8.

Tittonell, P., Giller, K.E., 2013. When yield gaps are poverty traps: The paradigm of ecological intensification in African smallholder agriculture. *F. Crop. Res.* **143**, 76–90.

Ward, J.M.J., Agricultural, C., X, P.B., Af-, S., Laing, M.D., Rijkenberg, F.H.J., Pathology, P., 1996. Frequency and timing of fungicide applications for the control of gray leaf spot in maize. *Am. Phytopath. Soc.* **81**, 41-48.

Ward, J.M.J., Darroch, M.D.,Laing, M.D., Cairns, L.P., Dicks, H.M., 1997. The economic benefits of fungicide treatment of maize for the control of grey leaf spot (*Cercospora zeae-maydis*) in KwaZulu-Natal. *S.A. J. Plant and Soil.* **14**, 43–48.

Ward, J.M.J., Stromberg, E.L., Nowell, D.C., 1999. Gray leaf spot: A disease of global importance in maize production. *Plant Disease.* **83**, 884-95.

Wise, K., Mueller, D., 2011. Are fungicides no longer just for fungi? An analysis of foliar fungicide use in corn. *APSnet Featur.* doi:10.1094/APSnetFeature-2011-0531.

Research Summary

Title:	Functional characterisation of the *Cercospora zeina crp1* gene in pathogenesis
Student:	Johan Liversage
Supervisor:	Dr. B.G. Crampton
Co-supervisor:	Prof. D.K. Berger

Blue light and the perception thereof plays a fundamental role in the survival of all organisms in changing environments. *Cercospora zeina*, is the causal agent of grey leaf spot (GLS) disease of maize plants in Southern Africa. The disease is of great economic importance as annual yield losses of up to 65% are experienced by South African farmers. The White Collar-1 protein (WC-1) has been characterised in *Neurospora crassa* and found to entrain the fungal circadian clock and regulate growth and development of the pathogen. In this study we set out to identify the orthologue of the WC-1 protein in *C. zeina,* and determine to what level blue light plays a role in the development of GLS in maize. The infection strategy followed by *C. zeina* is understudied at a molecular level, and therefore in order to effectively control the disease in the field, we need to understand the mechanisms used by the pathogen to infect and colonise the host.

The orthologue of the WC-1 protein was identified in the draft genome sequence of *C. zeina* and compared to WC-1 from other fungi. Blue light photoreceptors homologous to the WC-1 protein all contain a modified PAS domain, light-oxygen-voltage (LOV) domain to which the FAD chromophore binds to activate the protein. Phylogenetic relationships of WC-1 homologues from three fungal phyla (Ascomycota, Basidiomycota and Zygomycota) were inferred using a maximum likelihood approach. The results indicated that the Basidiomycota WC-1 homologues underwent independent evolution compared to the other two phyla. The orthologues of the other four circadian clock proteins, WC-2, FRQ, FWD-1 and FRH were identified in the genome sequences of *C. zeina* and *C. zeae-maydis*. Furthermore, a previously unidentified putative blue light photoreceptor of the cryptochome family, CRY-DASH, was identified in *C. zeina* and *C. zeae-maydis* that might also regulate blue light responses in the pathogens.

We functionally characterised the CRP1 protein in *C. zeina* using a split marker approach, which replaces the gene if interest with a hygromycin resistance gene (hyg^R). Putative *Δcrp1* knock-outs were generated and cultured on V8® media supplemented with hygromycin. Putative knock-outs were screened for the presence of the complete hygromycin resistance gene followed by verification that the hyg^R gene inserted into the correct genomic location.

Southern hybridisation using an internal *hyg*^{R} fragment revealed only a single copy of the inserted gene with no ectopic insertions. Although the genetic screens clearly showed that the endogenous *crp1* gene was replaced by the *hyg*^{R} gene, expression of the gene was still detected in *Δcrp1* knock-outs, although at reduced levels compared with the wild type *C. zeina* possibly due to the formation of a heterokaryon. The reduced expression of the *crp1* gene in the knock-out lines still showed clear phenotypic differences compared to the wild type fungus. Phenotypic characterisation of the putative *Δcrp1* knock-outs indicated that the *crp1* gene plays a role in light dependent repression of conidia formation. The *crp1* gene is also believed to play a role in the way melanin is deposited (i.e. to which cell layer the melanin granules are transported) and in the production of melanin in constant light. Furthermore, the potential level of pathogenesis of the *Δcrp1* knock-outs was decreased based on the significant reduction in the formation of a hyphal network over the stomata used to infiltrate the host plant.

In conclusion, all the components of the fungal circadian clock are conserved within *C. zeina*. We successfully disrupted the *C. zeina crp1* the homologue of WC-1, the limiting component of the circadian clock in fungi using a split marker approach. The *crp1* gene was found, even at reduced expression levels, to play a role in light dependent spore production, secondary metabolism of melanin and the pathogenesis through reduced stomatal tropism.

Appendix A.

Table A1. White Collar-1 orthologues in the Ascomycete phylum. Sequences retrieved from Uniprot (www.uniprot.org). Accession numbers are shown as well as the literature citations for each sequence.

Name	Accession number	Phylum	*Species*	Size (bp)	Reference
AcLreA	A1CJ49	Ascomycota	*Aspergillus clavatus*	872	Fedorova et al., 2008
AnLreA	Q5B7P4		*Aspergillus nidulans*	836	Galagan et al., 2005
AoWc1	EGX47394		*Arthrobotrys oligospora*	908	Yang et al., 2011
BfWc1	EDN19381		*Botryotinia fuckeliana*	1159	Blanco-Ulate et al., 2013
BoBlr1	BAF35570		*Bipolaris oryzae*	1054	Kihara et al., 2007
CgWc1	Q2HHB2		*Chaetomium globosum*	993	Birren et al., 2005
CgrWc1	EFQ30482		*Colletotrichum graminicola*	1031	O'Connell et al., 2012
CzCrp1	Not Available		*Cercospora zeina*	1100	Liversage, 2012
CzmCrp1	AEH41590		*Cercospora zeae-maydis*	1101	Kim et al., 2011
CmWc1	EGX96523		*Cordyceps militaris*	963	Zheng et al., 2011
EdLreA	EHY58306		*Exophiala dermatitidis*	1045	Chen et al., 2014
FfWcoA	AM778551		*Fusarium fujikuroi*	1024	Estrada & Avalos, 2007
FgWc1	FGSG_07941		*Fusarium graminearum*	1035	Cuomo et al., 2007
FoWc1	ABY47609		*Fusarium oxysporum*	1020	Ruiz-Roldan et al., 2007
FvWc1	HM045019		*Fusarium verticillioides*	1023	Stubnya et al., 2010
GcWc1	EFW99773		*Grosmannia clavigera*	1185	DiGuistini et al., 2011
HjWc1	AAV80185		*Hypocrea jecorina*	1040	Schmoll et al., 2005
LmWc1	CBX98033		*Leptosphaeria maculans*	1153	Rouxel et al., 2011
MaWc1	EFY99524		*Metarhizium anisopliae*	1040	Gao et al., 2011
MgWc1	L7IVP8		*Magnaporthe grisea*	1070	Xue et al., 2012
MgraWc1	EGP83257		*Mycosphaerella graminicola*	1068	Goodwin et al., 2011
MoMgwc1	EHA50060		*Magnaporthe oryzae*	1101	Kim et al., 2011
MtWc1	G2QI59		*Myceliophthora thermophila*	1033	Berka et al., 2011
NcWc1	Q01371		*Neurospora crassa*	1167	Ballario et al., 1996
NhWc1	C7ZLV6		*Nectria haematococca*	1025	Coleman et al., 2009
OsWc1a	CGMCC3.16320		*Ophiocordyceps sinensis*	1104	Yang et al., 2014
Oswc1b	CGMCC3.16319		*Ophiocordyceps sinensis*	1105	Yang et al., 2014
PaWc1	Q86ZJ6		*Podospora anserina*	1042	Anonymous, 2006
PmLreA	B6QTG4		*Penicillium marneffei*	963	Fedorova et al., 2007
PnWc1	EAT80456		*Phaeosphaeria nodorum*	1079	Hane et al., 2007
PtrWc1	B2VXI8		*Pyrenophora tritici-repentis*	936	Manning et al., 2013
SsWc1	A7F3V7		*Sclerotinia sclerotiorum*	941	Amselem et al., 2011
TaBlr1	AAU14171		*Trichoderma atroviride*	1020	Casas-Flores et al., 2004
TbWc1	CAE01390		*Tuber borchii*	956	Ambra et al., 2004
TtWc1	G2R6R5		*Thielavia terrestris*	1033	Berka et al., 2011
VaWc1	C9SRC0		*Verticillium alfalfae*	986	Klosterman et al., 2011
VdWc1	EGY20305		*Verticillium dahliae*	1112	Klosterman et al., 2011

Table A2. White Collar-1 orthologues in the Basidiomycota and Zygomycota phylum. Sequences retrieved from Uniprot (www.uniprot.org). Accession numbers are shown as well as the literature citations for each sequence. AtPhot (*Arabidopsis thaliana* phototropin) used as an outgroup in WC-1 phylogenetic study.

Name	Accession number	Phylum	*Species*	Size (bp)	Reference
AbWc1	K9I2M0	Basidiomycota	*Agaricus bisporus*	880	Morin et al., 2012
CcDst1	AB195817		*Coprinopsis cinerea*	1175	Terashima et al., 2005
CgatWc1	E6R5V0		*Cryptococcus gattii WM276*	1096	D'Souza et al., 2011
CnBwc1	AAT73612		*Cryptococcus neoformans*	1141	Lu et al., 2005
GfWc1	BAO20282.1		*Grifola frondosa*	881	Kurahashi et al., 2014
LePhrA	BAF56991		*Lentinula edodes*	924	Sano et al., 2007
PhWc1	R9P1WO		*Pseudozyma hubeiensis*	1064	Konishi et al., 2013
UhWc1	I2FY83		*Ustilago hordei*	1093	Laurie et al., 2012
UmWc1	XP_759327		*Ustilago maydis*	1085	Kamper et al., 2006
RsWc1	L8WYM9		*Rhizoctonia solani*	872	Zheng et al., 2013
ScWc1	D8QDZ3		*Schizophyllum commune H4-8*	843	Ohm et al., 2010
PbMadA	ABB77846	Zygomycota	*Phycomyces blakeleeanus*	660	Idnurm et al., 2006
PbWcoA	ABB77844		*Phycomyces blakeleeanus*	624	Idnurm et al., 2006
PcMadA1	B8YIE3		*Pilobolus crystallinus*	622	Kubo, 2009
PcMadA2	B8YIE4		*Pilobolus crystallinus*	616	Kubo, 2009
PcMadA3	B8YIE5		*Pilobolus crystallinus*	638	Kubo, 2009
McWc1a	CAJ13843		*Mucor circinelloides*	649	Silva et al., 2006
McWc1b	CAJ13844		*Mucor circinelloides*	697	Silva et al., 2006
McWc1c	CAJ13845		*Mucor circinelloides*	596	Silva et al., 2006
RoWc1a	Contig 16338		*Rhizopus oryzae* 16338	647	Idnurm et al., 2006
RoWc1b	Contig 09997		*Rhizopus oryzae* 09997	726	Idnurm et al., 2006
RoWc1c	Contig 14273		*Rhizopus oryzae* 14273	532	Idnurm et al., 2006
AtPhot	AAC01753	**Plantae**	*Arabidopsis thaliana*	996	Kubo, 2009

Table A3. Identification of functional domains in White Collar-1 orthologues of Ascomycete phylum. Domain architecture was identified using the SMART domain analysis (www.SMART.com). Coiled-coil domains (CC) and Zinc-Finger (Znf).

Name	PAS-A bp region	Size (bp)	PAS-B bp region	Size (bp)	PAS-C bp region	Size (bp)	ZnF bp region	Size (bp)	CC
AcLreA	292 - 420	129	485 - 597	113	603 – 669	67	825 - 870	46	Y
AnLreA	228 - 354	127	419 - 526	108	537 – 602	66	781 - 833	53	Y
AoWc1	248 - 376	129	441 - 554	114	560 – 626	67	790 - 842	53	Y
BfWc1	356 - 496	141	562 - 675	114	681 – 747	67	932 - 984	53	Y
BoBlr1	364 - 493	130	560 - 673	114	674 – 745	72	928 - 981	54	Y
CgWc1	352 - 480	129	548 - 662	115	665 – 737	73	N/A	N/A	Y
CgrWc1	366 - 495	130	563 - 676	114	682 – 748	67	903 - 955	53	Y
CzCrp1	425 - 553	129	619 - 732	114	738 – 804	67	966 - 1017	52	Y
CzmCrp1	424 - 552	129	618 - 731	114	734 – 803	70	965 - 1016	52	Y
CmWc1	315 - 443	129	510 - 623	114	624 – 695	72	835 - 887	53	Y
EdLreA	360 - 488	129	555 - 668	114	671 – 740	70	911 - 969	59	Y
FfWcoA	342 - 470	129	538 - 651	114	652 – 723	72	873 - 925	53	Y
FgWc1	352 - 480	129	548 - 661	114	662 – 733	72	884 - 936	53	Y
FoWc1	338 - 466	129	534 - 647	114	648 – 719	72	869 - 921	53	Y
FvWc1	341 - 469	129	537 - 650	114	651 – 722	72	872 - 924	53	Y
GcWc1	426 - 556	131	649 - 762	114	768 – 834	67	1001 - 1053	53	Y
HjWc1	361 - 489	129	556 - 669	114	670 – 741	72	894 - 946	53	Y
LmWc1	460 - 589	130	656 - 769	114	770 – 841	72	1023 - 1075	53	Y
MaWc1	353 - 481	129	548 - 661	114	662 – 733	72	887 - 939	53	Y
MgWc1	386 - 514	129	587 - 706	120	712 – 778	67	924 - 976	53	Y
MgraWc1	391 - 519	129	585 - 698	114	701 – 770	70	940 - 992	53	Y
MoMgwc1	386 - 514	129	587 - 706	120	712 – 778	67	955 - 1007	53	Y
MtWc1	347 - 475	129	542 - 656	115	669 – 735	67	914 - 968	55	Y
NcWc1	380 - 508	129	576 - 689	114	695 – 761	67	928 - 980	53	Y
NhWc1	344 - 472	129	540 - 653	114	654 – 725	72	874 - 926	53	Y
OsWc1a	415 - 543	129	610 - 723	114	724 – 795	72	949 - 1000	52	Y
Oswc1b	416 - 544	129	611 - 724	114	725 – 796	72	950 - 1001	52	Y
PaWc1	323 - 452	130	520 - 633	114	639 – 705	67	864 - 920	57	Y
PmLreA	323 - 451	129	515 - 628	114	630 – 700	71	886 - 938	53	Y
PnWc1	387 - 516	130	582 - 695	114	696 – 767	72	950 - 1002	53	Y
PtrWc1	233 - 362	130	429 - 542	114	543 – 614	72	800 - 852	53	Y
SsWc1	310 - 444	135	511 - 624	114	630 – 696	67	879 - 931	53	Y
TaBlr1	341 - 469	129	536 - 649	114	650 – 721	72	869 - 921	53	Y
TbWc1	286 - 414	129	484 - 597	114	603 – 669	67	824 - 879	56	Y
TtWc1	316 - 444	129	511 - 624	114	625 – 699	75	882 - 932	51	Y
VaWc1	317 - 446	130	514 - 627	114	628 – 699	72	856 - 908	53	Y
VdWc1	488 - 617	130	634 - 753	120	754 – 825	72	982 - 1034	53	Y

Table A4. Identification of functional domains in White Collar-1 orthologues of Basidiomycete and Zygomycete phylum. Domain architecture was identified using the SMART domain analysis (www.SMART.com). Coiled-coil domains (CC) and Zinc-Finger (Znf). AtPhot (*Arabidopsis thaliana* phototropin) used as an outgroup in WC-1 phylogenetic study.

Name	PAS-A bp region	Size (bp)	PAS-B bp region	Size (bp)	PAS-C bp region	Size (bp)	ZnF bp region	Size (bp)	CC
AbWc1	186 - 323	138	423 - 567	145	N/A	N/A	N/A	N/A	Y
CcDst1	301 - 437	137	531 - 674	144	N/A	N/A	N/A	N/A	Y
CgatWc1	508-639	132	704-826	123	N/A	N/A	N/A	N/A	Y
CnBwc1	552 - 683	132	748 - 868	121	870 - 919	50	N/A	N/A	Y
GfWc1	191-328	138	424-576	153	597-663	67	N/A	N/A	Y
LePhrA	165 - 300	136	419 - 558	140	588 - 654	67	N/A	N/A	Y
PhWc1	379 - 510	132	576 - 718	143	724 - 790	67	N/A	N/A	Y
UhWc1	409 - 540	132	606 - 748	143	754 - 820	67	N/A	N/A	Y
UmWc1	401 - 531	131	597 - 739	143	745 - 811	67	N/A	N/A	Y
RsWc1	319 - 449	131	489 - 615	127	617 - 688	72	N/A	N/A	Y
ScWc1	205-342	138	436-562	127	N/A	N/A	N/A	N/A	Y
PbMadA	95 - 223	129	299 - 414	116	421 - 487	67	618 - 653	36	Y
PbWcoA	70 - 198	129	279 - 396	118	398 - 467	70	582 - 617	36	Y
PcMadA1	57 - 185	129	260 - 375	116	377 - 448	72	575 - 609	35	Y
PcMadA2	79 - 207	129	282 - 397	116	411 - 477	67	N/A	N/A	Y
PcMadA3	81 - 209	129	285 - 400	116	410 - 476	67	601 - 635	35	Y
McWc1a	77 - 205	129	280 - 395	116	400 - 468	69	589 - 641	53	Y
McWc1b	60 - 189	130	306 - 421	116	437 - 505	69	N/A	N/A	Y
McWc1c	29 - 157	129	243 - 358	116	380 - 433	54	560 - 593	34	Y
RoWc1a	76 - 204	129	284 - 399	116	401 - 472	72	597 - 647	51	Y
RoWc1b	123 - 251	129	347 - 462	116	483 - 549	67	N/A	N/A	Y
RoWc1c	5 - 136	132	194 - 307	114	321 - 378	58	488 - 532	45	Y
AtPhot	186 - 303	118	464 - 581	118	N/A	N/A	N/A	N/A	Y

Table A5. The identification of LOV domains in plant phototropins.

Species	Size (bp)	Name	LOV1 bp region	Size (bp)	Name	LOV2 bp region	Size (bp)
Prunus persica	1000	PpeLOV1	183 – 300	118	PpeLOV2	465 – 582	118
Setaria italica	899	SiLOV1	102 – 219	118	SiLOV2	369 – 486	118
Solanum lycopersicum	1017	SlLOV1	191 – 308	118	SlLOV2	486 – 603	118
Brassica rapa subsp. Pekinensis	881	BrLOV1	118 – 235	118	BrLOV2	374 – 491	118
Physcomitrella patens	1133	PpaLOV1	303 – 420	118	PpaLOV2	594 – 711	118
Capsella rubella	995	CrLOV1	185 – 302	118	CrLOV2	463 – 580	118
Arabidopsis thaliana	996	AtLOV1	186 – 303	118	AtLOV2	464 – 581	118
Medicago truncatula	1053	MtLOV1	146 – 263	118	MtLOV2	429 – 546	118
Ricinus communis	1006	RcLOV1	196 – 313	118	RcLOV2	482 – 599	118
Glycine max	977	GmLOV1	166 – 283	118	GmLOV2	447 – 564	118
Brachypodium distachyon	909	BdLOV1	105 – 222	118	BdLOV2	382 – 499	118
Oryza sativa Japonica Group	921	OsLOV1	125 – 242	118	OsLOV2	402 – 519	118
Selaginella moellendorffii	930	SmLOV1	138 – 255	118	SmLOV2	399 – 516	118
Sorghum bicolor	890	SbLOV1	92 – 209	118	SbLOV2	360 – 477	118
Eutrema halophilum	997	EhLOV1	185 – 302	118	EhLOV2	463 – 580	118
Zea mays	703	ZmLOV1	103 – 220	118	ZmLOV2	377 – 494	118

Table A6. The identification of LOV domains in plant ZTL (Adagio protein).

Name	Species	Size (bp)	LOV bp region	Size (bp)
PpeLOV	*Prunus persica*	626	46 - 172	131
SiLOV	*Setaria italica*	625	49 - 174	126
SlLOV	*Solanum lycopersicum*	607	56 - 181	126
BrLOV	*Brassica rapa subsp. pekinensis*	616	27 - 155	129
CrLOV	*Capsella rubella*	624	50 - 173	124
AtLOV	*Arabidopsis thaliana*	619	45 - 168	124
MtLOV	*Medicago truncatula*	635	55 - 176	122
RcLOV	*Ricinus communis*	630	51 - 176	126
GmLOV	*Glycine max*	620	41 - 163	123
BdLOV	*Brachypodium distachyon*	621	47 - 172	126
OsLOV	*Oryza sativa Japonica Group*	630	54 - 179	126
SmLOV	*Selaginella moellendorffii*	587	3 - 119	117
SbLOV	*Sorghum bicolor*	619	43 - 168	126
EhLOV	*Eutrema halophilum*	623	55 - 174	120
ZmLOV	*Zea mays*	609	32 - 157	126

Table A7. Bacterial LOV domains. The LOV domain sequences were extracted from bacterial sensory proteins.

Name	Accession number	Species	Sequence description	Protein size (bp)	LOV domain	Size (Bp)
Proteobacteria						
AgrovitLOV	WP_012653887.1	Agrobacterium_vitis	PAS_sensor_protein	411	68 - 185	118
CaulospLOV	WP_018061565.1	Caulobacter_sp.	PAS_sensor_protein	373	22 - 139	118
AgroalbLOV	WP_006728201.1	Agrobacterium_albertimagni	PAS_sensor_protein	375	26 - 143	118
MetexLOV	WP_015823468.1	Methylobacterium_extorquens	PAS_sensor_protein	354	23 - 140	118
CaulvibLOV	WP_010918174.1	Caulobacter_vibrioides	PAS_sensor_protein	368	22 - 139	118
AurmanLOV	WP_009210920.1	Aurantimonas_manganoxydans	PAS_sensor_protein	389	37 - 154	118
MesciLOV	WP_013531003.1	Mesorhizobium_ciceri	PAS_sensor_protein	382	27 - 144	118
MetpopLOV	WP_012455344.1	Methylobacterium_populi	PAS_sensor_protein	354	23 - 140	118
MesorspLOV	ESY34200.1	Mesorhizobium_sp.	PAS_sensor_protein	368	13 - 130	118
Cyanobacteria						
CcLOV	WP_006098397.1	Coleofasciculus_chthonoplastes	PAS_fold_family	776	28 - 145	118
MvLOV	WP_006631032.1	Microcoleus_vaginatus	PAS_sensor_protein	1102	9 - 126	118
OnLOV	WP_015175561.1	Oscillatoria_nigro-viridis	PAS_sensor_protein	1102	9 - 126	118
LaLOV	WP_023069313.1	Lyngbya_aestuarii	sensory_box_protein	1212	347 - 464	118
NsLOV	WP_015141307.1	Nostoc_sp._PCC_7524	PAS_domain_S-box	1019	202 - 319	118
GsLOV	WP_015172542.1	Geitlerinema_sp._PCC_7407	PAS_Sensor_Protein	1135	426 - 543	118
SsLOV	WP_015126290.1	Synechococcus_sp._PCC_6312	PAS_sensor_protein	1154	317 - 434	118
Gs2LOV	WP_006530862.1	Gloeocapsa_sp.	PAS_domain_S-box	1137	196 - 313	118

Appendix B.

>Partial pTA-Hyg
GGGGCGAATTGGGCCCGACGTCGCATGCTCCCGGCCGCCATGGCCGCGGGATTAAGAATTCGGCCGGCCGCT
GGATCCAGTGGAGGTCAACAATGAATGCCTATTTTGGTTTAGTCGTCCAGGCGGTGAGCACAAAATTTGTGTC
GTTTGACAAGATGGTTCATTTAGGCAACTGGTCAGATCAGCCCCACTTGTAGCAGTAGCGGCGGCGCTCGAA
GTGTGACTCTTATTAGCAGACAGGAACGAGGACATTATTATCATCTGCTGCTTGGTGCACGATAACTTGGTGC
GTTTGTCAAGCAAGGTAAGTGGACGACCCGGTCATACCTTCTTAAGTTCGCCCTTCCTCCCTTTATTTCAGATTC
AATCTGACTTACCTATTCTACCCAAGCATCCAAATGAAAAAGCCTGAACTCACCGCGACGTCTGTCGAGAAGTT
TCTGATCGAAAAGTTCGACAGCGTCTCCGACCTGATGCAGCTCTCGGAGGGCGAAGAATCTCGTGCTTTCAGC
TTCGATGTAGGAGGGCGTGGATATGTCCTGCGGGTAAATAGCTGCGCCGATGGTTTCTACAAAGATCGTTAT
GTTTATCGGCACTTTGCATCGGCCGCGCTCCCGATTCCGGAAGTGCTTGACATTGGGGAGTTCAGCGAGAGCC
TGACCTATTGCATCTCCCGCCGTGCACAGGGTGTCACGTTGCAAGACCTGCCTGAAACCGAACTGCCCGCTGT
TCTCCAGCCGGTCGCGGAGGCCATGGATGCGATCGCTGCGGCCGATCTTAGCCAGACGAGCGGGTTCGGCCC
ATTCGGACCGCAAGGAATCGGTCAATACACTACATGGCGTGATTTCATATGCGCGATTGCTGATCCCCATGTG
TATCACTGGCAAACTGTGATGGACGACACCGTCAGTGCGTCCGTCGCGCAGGCTCTCGATGAGCTGATGCTTT
GGGCCGAGGACTGCCCCGAAGTCCGGCACCTCGTGCATGCGGATTTCGGCTCCAACAATGTCCTGACGGACA
ATGGCCGCATAACAGCGGTCATTGACTGGAGCGAGGCGATGTTCGGGGATTCCCAATACGAGGTCGCCAACA
TCCTCTTCTGGAGGCCGTGGTTGGCTTGTATGGAGCAGCAGACGCGCTACTTCGAGCGGAGGCATCCGGAGC
TTGCAGGATCGCCGCGCCTCCGGGCGTATATGCTCCGCATTGGTCTTGACCAACTCTATCAGAGCTTGGTTGA
CGGCAATTTCGATGATGCAGCTTGGGCGCAGGGTCGATGCGACGCAATCGTCCGATCCGGAGCCGGGACTGT
CGGGCGTACACAAATCGCCCGCAGAAGCGCGGCCGTCTGGACCGATGGCTGTGTAGAAGTACTCGCCGATAG
TGGAAACCGACGCCCCAGCACTCGTCCGAGGGCAAAGGAATAGAGTAGATGCCGACCGGGCGCGCCGGATC
CAAAATCACTAGTGCGGCCGCCTGCAGGTCGACCATATGGGAGAGCTCCCAACGCGTTGGATGCATAGCTTG
AGTATTCCTATAGTGTCACCTAAAT

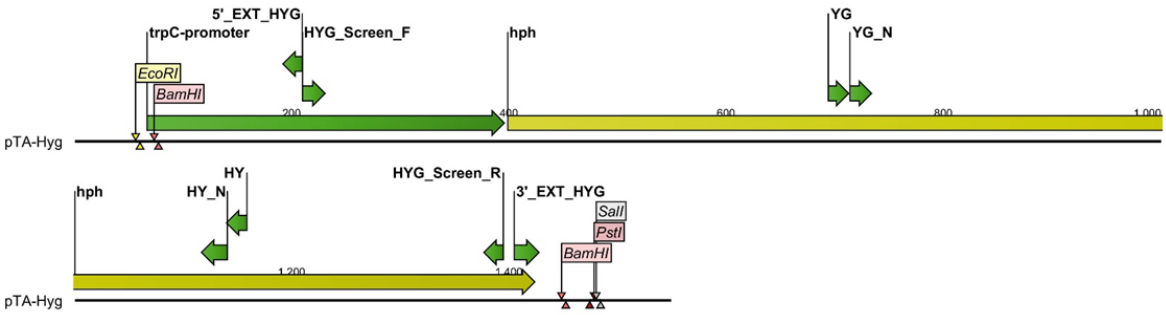

Figure B1. **Partial *hyg*-cassette sequence**. The sequence length is 1 549 bp. The open reading frame (ORF) is shown by the yellow arrow - the size is 1026 bp. The HYG-primers used to construct the split-markers are, YG, YG-N, HY and HY-N indicated on the figure by green arrows at 694, 714, 1140 and 1117 bp respectively. The screening primers are HYG_Screen_F and HYG_Screen_R binding to the *trpC* promoter and the 3'-end of the *Hyg*^{R} open reading frame.

>3'_Splitmarker_Construct
TCGCATCCGCGCTGGAATCTTTACTCCCTGTGGCCCGGAATGCTGCGACAGTTCGTGCCTCTTCAGATTGTCCT
CTCTCGCGGTGGAGAATTTGCACCAATCGTACCGGCATCGACGACCATCAGTGCTGTTGTGCTTTGCTTCGAG
ATGACGTTCGAGGCTCCTCTAGAGCTTGTACTCCTTCGTACAGCCTGCAATGGAGCACACGAACTTCGCAGTG
TGAGGCTGTCGAAGGTGTCCACCATGCCGCGCATGCGCATGTTCTCTGAGATCGCCTGCATCAATGATAAGAC
TTGTACATCCTGGCTAAGGACACGTCCACTTTTTGCCAGAGCGCATGGCGACTATCTCGGTGAAGTCCGTCTC
GCAAATGAATGATCAGATAAGCGATTGTCTTCGGAAGCGATGGCGTGTGTCCCACGACAGCGGTGTCGAGCA
GAAGAGTATGTTTTCTCTCCACGGCACAAAGGGTAGCGGCATCCTGTGAAGCAGGAAACAGCTATGACTATG
ATTACGCCAAGCTATTTAGGTGACACTATAGAATACTCAAGCTATGCATCCAACGCGTTGGGAGCTCTCCCATA
TGGTCGACCTGCAGGCGGCCGCACTAGTGATTTTGGATCCGGCGCGCCCGGTCGGCATCTACTCTATTCCTTT
GCCCTCGGACGAGTGCTGGGGCGTCGGTTTCCACTATCGGCGAGTACTTCTACACAGCCATCGGTCCAGACGG
CCGCGCTTCTGCGGGCGATTTGTGTACGCCCGACAGTCCCGGCTCCGGATCGGACGATTGCGTCGCATCGACC
CTGCGCCCAAGCTGCATCATCGAAATTGCCGTCAACCAAGCTCTGATAGAGTTGGTCAAGACCAATGCGGAGC
ATATACGCCCGGAGGCGCGGCGATCCTGCAAGCTCCGGATGCCTCCGCTCGAAGTAGCGCGTCTGCTGCTCCA
TACAAGCCAACCACGGCCTCCAGAAGAGGATGTTGGCGACCTCGTATTGGGAATCCCCGAACATCGCCTCGCT
CCAGTCAATGACCGCTGTTATGCGGCCATTGTCCGTCAGGACATTGTTGGAGCCGAAATCCGCATGCACGAGG
TGCCGGACTTCGGGGCAGTCCTCGGCCCAAAGCATCAGCTCATCGAGAGCCTGCGCGACGGACGCACTGACG
GTGTCGTCCATCACAGTTTGCCAGTGATACACATGGGGATCAGCAATCGCGCATATGAAATCACGCCATGTAG
TGTATTGACCGATTCCTTGCGGTCCGAATGGGCCGAACCCGCTCGTCTGGCTAAGATCGGCCGCAGCGATCGC
ATCCATGGCCTCCGCGACCGGCTGGAGAACAGCGGGCAGTTCGGT

>5'_7_Splitmarker_Construct
CCTGCTGCCTGTCGACTGGCTGCCTGGCCGAGAGCCTTCTGCGCTGCACAGCTTCCCGCCCGCGAGCAACCAC
GCACTCGCCTCACCACCGCGCCGTGGCTCACTCCGCCGACTCCCACGCCCGCCCGCCGCCACCTGCACCTCCGC
TCCACCGCGGGCTGCAGCGCACAGCACGCCGAACGCCCCGTCCGGTGCATTGGAAGCGCCGCCAGCGCCGCC
GCCGTGTCAGCTTACCCATATCTCTCGTCACCGAGCGGAGCGCAGCCCGTGTTGCTCGCTTCTGCACGTCCCGA
TCTCTGGGTTACACCACCACCGCAGCTTCGTAAAACGACGGCCAGTAAATTGTAATACGACTCACTATAGGGC
GAATTGGGCCCGACGTCGCATGCTCCCGGCCGCCATGGCCGCGGGATTAAGAATTCGGCCGGCCGCTGGATC
CAGTGGAGGTCAACAATGAATGCCTATTTTGGTTTAGTCGTCCAGGCGGTGAGCACAAAATTTGTGTCGTTTG
ACAAGATGGTTCATTTAGGCAACTGGTCAGATCAGCCCCACTTGTAGCAGTAGCGGCGGCGCTCGAAGTGCG
ACTCTTATTAGCAGACAGGAACGAGGACATTATTATCATCTGCTGCTTGGTGCACGATAACTTGGTGCGTTTGT
CAAGCAAGGTAAGTGGACGACCCGGTCATACCTTCTTAAGTTCGCCCTTCCTCCCTTTATTTCAGATTCAATCTG
ACTTACCTATTCTACCCAAGCATCCAAATGAAAAAGCCTGAACTCACCGCGACGTCTGTCGAGAAGTTTCTGAT
CGAAAAGTTCGACAGCGTCTCCGACCTGATGCAGCTCTCGGAGGGCGAAGAATCTCGTGCTTTCAGCTTCGAT
GTAGGAGGGCGTGGATATGTCCTGCGGGTAAATAGCTGCGCCGATGGTTTCTACAAAGATCGTTATGTTTATC
GGCACTTTGCATCGGCCGCGCTCCCGATTCCGGAAGTGCTTGACATTGGGGAGTTCAGCGAGAGCCTGACCTA
TTGCATCTCCCGCCGTGCACAGGGTGTCACGTTGCAAGACCTGCCTGAAACCGAACTGCCCGCTGTTCTCCAG
CCGGTCGCGGAGGCCATGGATGCGATCGCTGCGGCCGATCTTAGCCAGACGAGCGGGTTCGGCCCATTCGGA
CCGCAAGGAATCGGTCAATACACTACATGGCGTGATTTCATATGCGCGATTGCTGATCCCCATGTGTATCACTG
GCAAACTGTGATGGACGACACCGTCAGTGCGTCCGTCGCGCAGGCTCTCGATGAGCTGATGCTTTGGGCCGA
GGACTGCCCCGAAGTCCGGCACCTCGTGCATGCGGATTTCGGCTCCAACAATGTCCTGACGGACAATGGCCGC
ATAACAGCGGTCATAGACTGGAGCGAGGCGATGTTCGGGGATTCCCAATACGAGGTCGCCAACATCCTCTTCT
GGAGGCCGTGGTTGGCTTGTAGTGGAGCAGCAGACGCGCTA

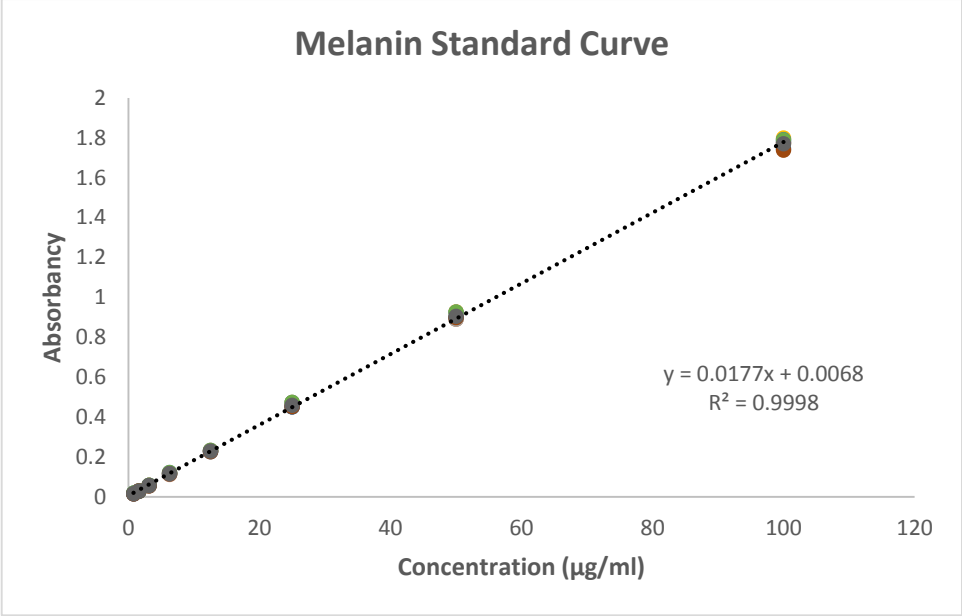

Figure B2. Melanin standard curve. A melanin standard curve was generated with the concentration ranging from 0 – 100 µg/ml. The graph represents nine replications (3 x technical replication for every one of the three technical preparations per concentration) per absorbency reading for each melanin concentration. The formula for the trend line, going through all nine data series, is shown on the graph, with the R^2 value being 0.9998.

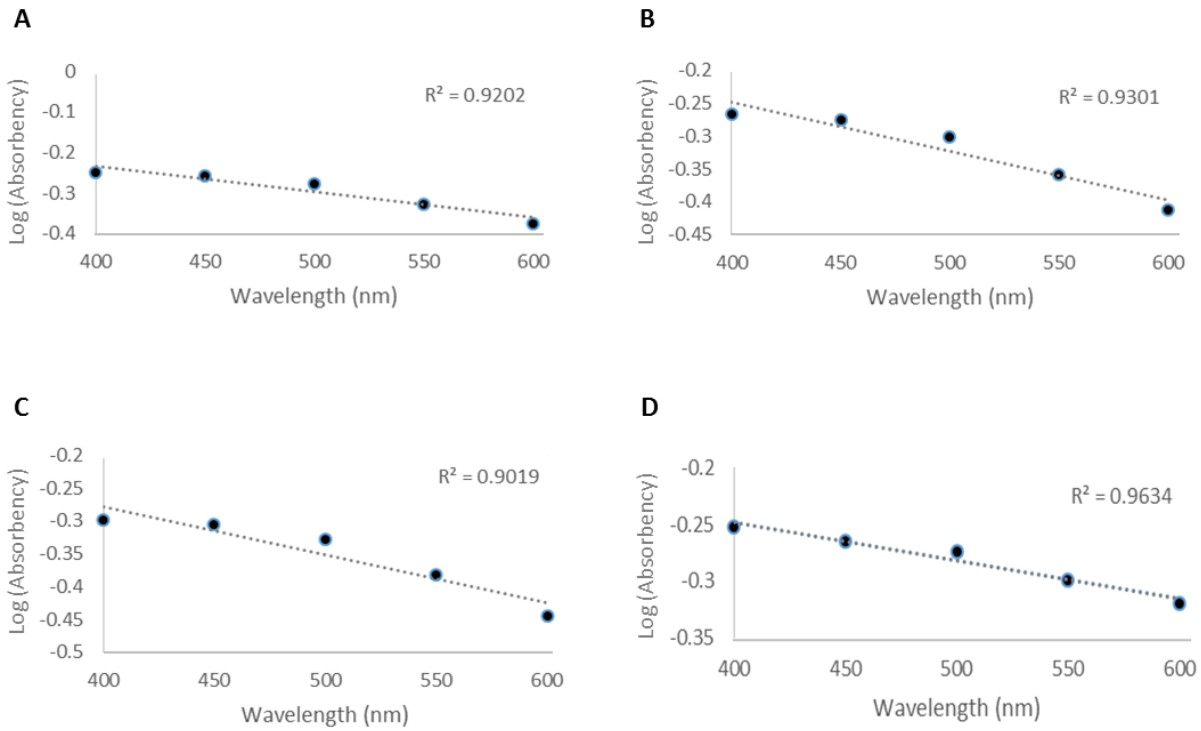

Figure B3. Melanin absorbency curve. Linear plot with negative slope obtained from extracted melanin from the putative *Δcrp1*_C2 (A), *Δcrp1*_C3 (B), *Δcrp1*_F1 (C) knock-out and wild type (D) strain.

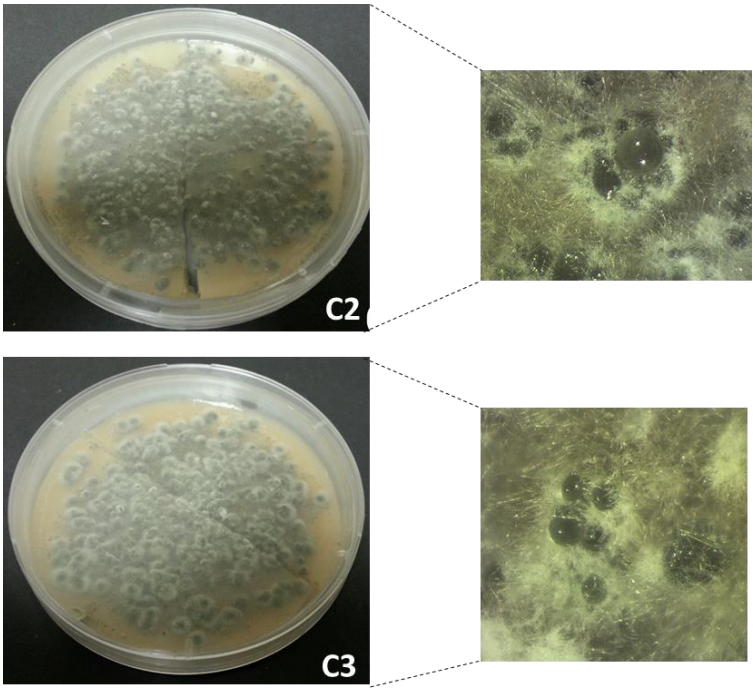

Figure B4. Droplet formation on putative *Δcrp1* knock-out cultures. The heavily melanised putative *Δcrp1*_C2 and *Δcrp1*_C3 *Cercospora zeina* knock-out strains grown on V8® media. The black droplet formation on top of the colonies is clearly visible under a light microscope.

```
                                20                  40                  60
                                |                   |                   |
Wild type GTGCAGGCAA CCAACAAAAA GACTGTGCCA ACTGCCACAC CCGCGTCACA CCTGAATGGA 60
Δcrp1_C3  .......... .......... .......... .......... .......... .......... 60
                                80                  100                 120
                                |                   |                   |
Wild type GAAGAGGACC GAGCGGACAA CGCGATCTGT GCAACAGCTG CGGTCTGCGT TGGGCTAAAC 120
Δcrp1_C3  .......... .......... .......... .......... .......... .......... 120
                                140                 160                 180
                                |                   |                   |
Wild type TTGTAAGTTT GTGAACCCTG ATTGTCGTTC CCGTCTCGTG GCCTTACTTC CTGGACAAAC 180
Δcrp1_C3  .......... .......... .......... .......... .......... .......... 180
                                200                 220                 240
                                |                   |                   |
Wild type ACTGACAAGT GCACGAGCAG AACGGTCGTG TATCACCTCG GACGTCGTCG CAACAAAGCG 240
Δcrp1_C3  .......... .......... .......... .......... .......... .......... 240
                                260                 280                 300
                                |                   |                   |
Wild type TCCACAGCGA CAAAGCCAGC AGAGCATCCG CATCTCCTCG TCACTCGAGC AATATCCACA 300
Δcrp1_C3  .......... .......... .......... .......... .......... .......... 300
                                320                 340                 360
                                |                   |                   |
Wild type ATTCTTCGTC AAATGTGAAG ACCGAGCAGA GCCCGAACGC TGCCAATGGT GAAGGCATAG 360
Δcrp1_C3  .......... .......... .......... .......... .......... .......... 360
                                380                 400                 420
                                |                   |                   |
Wild type TCAGGGGGTC TCCTTCCGCG AAGACCGCTC AAAGGCCGCT GCAAGGACCT GACGGCCACT 420
Δcrp1_C3  .......... .......... .......... .......... .......... .......... 420
                                440                 460                 480
                                |                   |                   |
Wild type CAGCAAGAAT GGAAGGTGCC GTCGGTGTTC CGGGAAAGAT TGACGAAGGC GTGGAACCGG 480
Δcrp1_C3  .......... .......... .......... .......... .......... .......... 480
                                500                 520                 540
                                |                   |                   |
Wild type ATTGAGGATG AGAAGCCTTG CAGGAAGGAT CTACTTCACA GGATGCCGCT ACCCTTTGTG 540
Δcrp1_C3  .......... .......... .......... .......... .......... .......... 540
                                560                 580                 600
                                |                   |                   |
Wild type CCGTGGAGAG AAAACATACT CTTCTGCTCG ACACCGCTGT CGTGGGACAC ACGCCATCGC 600
Δcrp1_C3  .......... .......... .......... .......... .......... .......... 600
                                620
                                |
Wild type TTCTGAAGAC AATCGCTTAT CTGATCATTC ATT 633
Δcrp1_C3  .......... .......... .......... ... 633
```

Figure B5. *Cercospora zeina crp1* terminal fragment sequence alignment. The alignment of genomic DNA sequences from the putative *Δcrp1*_C3 knock-out and wild type strains using the crp1_frag_F and crp1_frag_R primer set. The dots represent identical residues.

Figure B6. *Cercospora zeina* genomic DNA *crp1* LOV domain sequence alignment. The LOV domain sequence alignment from genomic DNA of the putative *Δcrp1*_C3 knock-out and wild type strains using the LOV_crp1_F and LOV_crp1_R primer set. The dots represent identical residues.

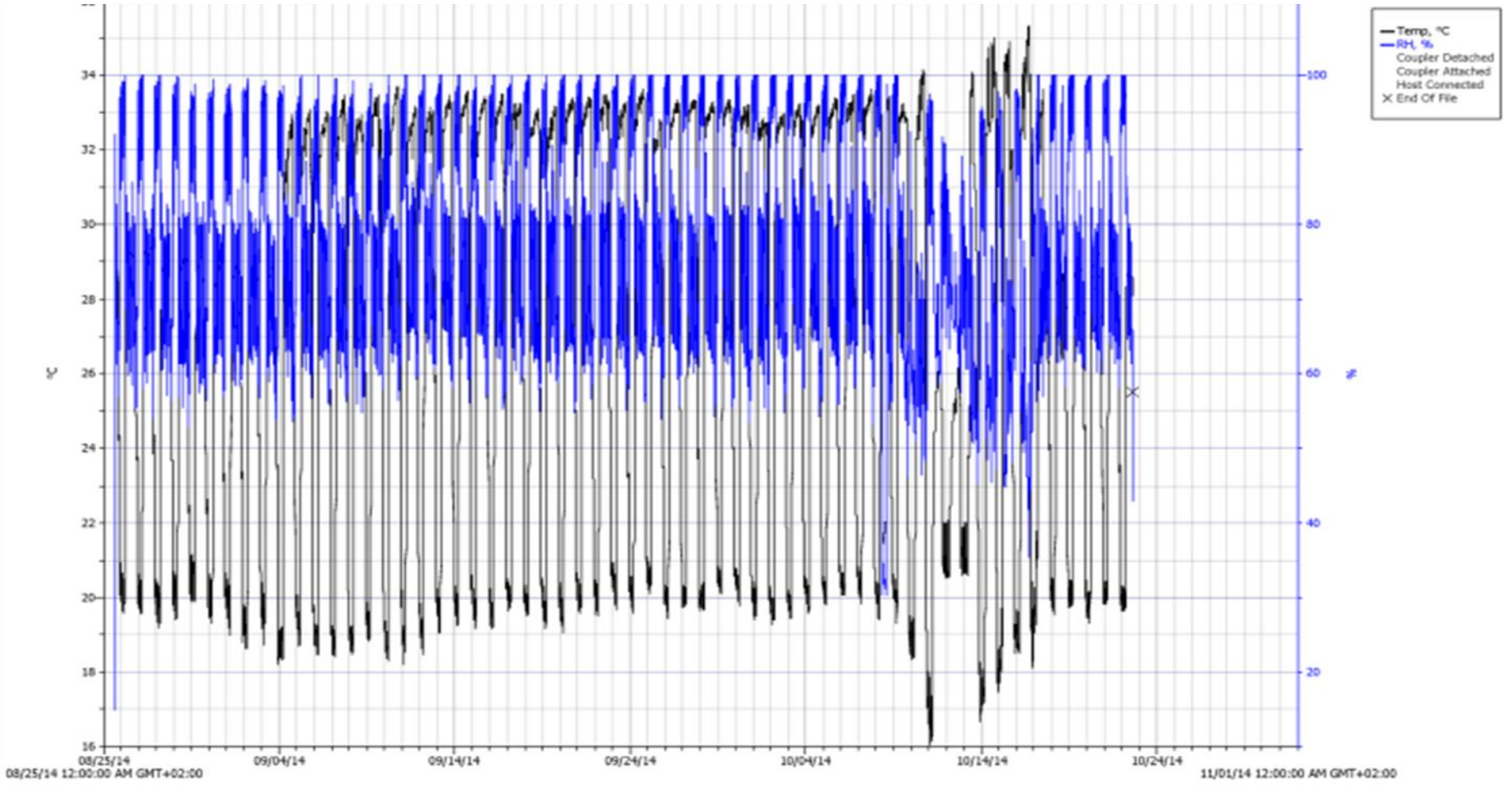

Figure B7. Temperature and relative humidity readings of the phytotron during *Cercospora zeina* infection of maize.

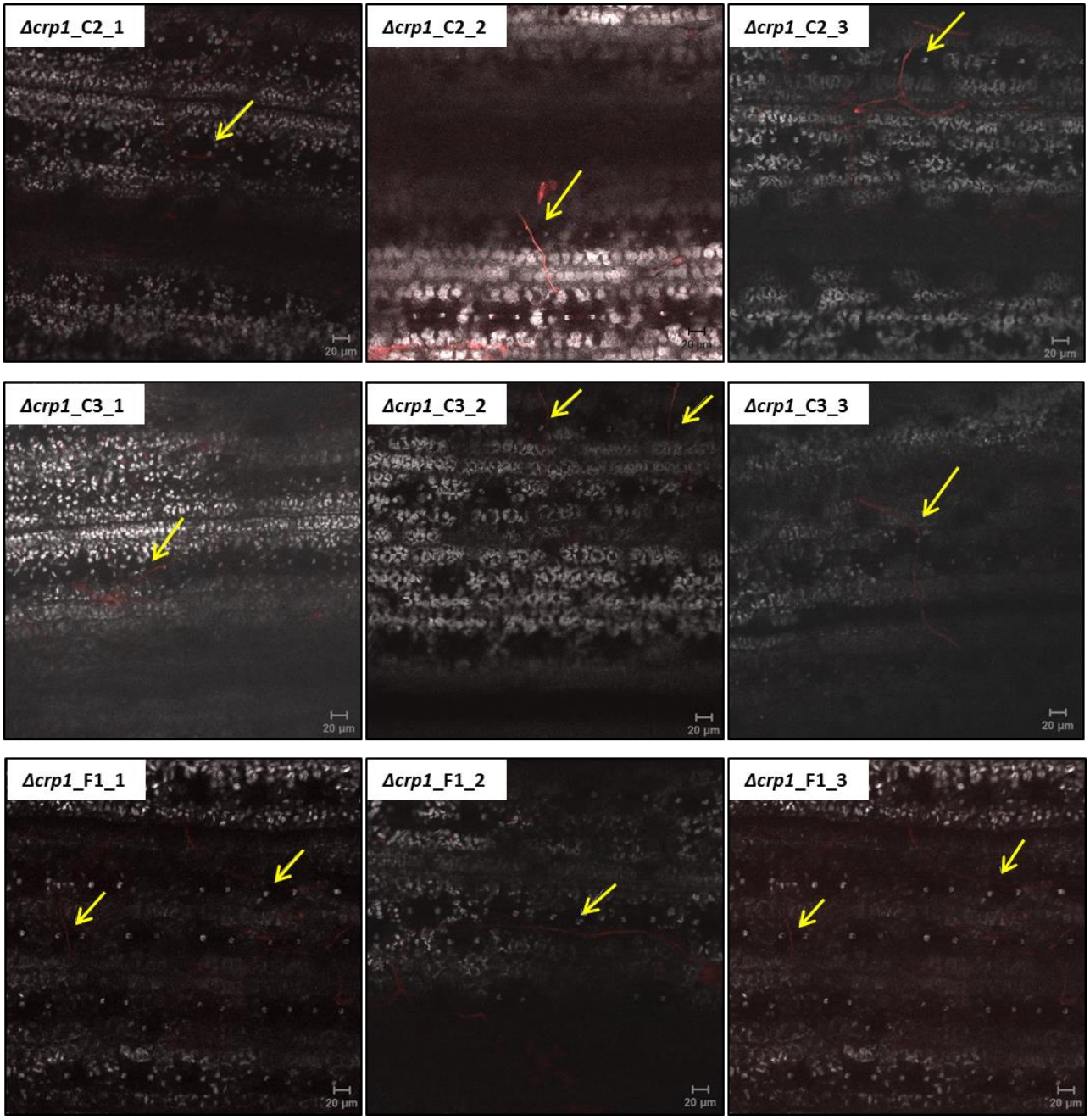

Figure B8. Additional confocal microscopy images of maize inoculated leaves with putative *Δcrp1* knock-out strains. The stomatal interactions are indicated by the yellow arrows.